Wright State University

CORE Scholar

Browse all Theses and Dissertations | Theses and Dissertations

2014

# Peroxisome Proliferator-Activated Receptor Alpha: Insight into the Structure, Function and Energy Homeostasis

Dhawal P. Oswal
*Wright State University*

Follow this and additional works at: https://corescholar.libraries.wright.edu/etd_all

 Part of the Biomedical Engineering and Bioengineering Commons

## Repository Citation

Oswal, Dhawal P., "Peroxisome Proliferator-Activated Receptor Alpha: Insight into the Structure, Function and Energy Homeostasis" (2014). *Browse all Theses and Dissertations*. 1361.
https://corescholar.libraries.wright.edu/etd_all/1361

This Dissertation is brought to you for free and open access by the Theses and Dissertations at CORE Scholar. It has been accepted for inclusion in Browse all Theses and Dissertations by an authorized administrator of CORE Scholar. For more information, please contact library-corescholar@wright.edu.

# PEROXISOME PROLIFERATOR-ACTIVATED RECEPTOR ALPHA: INSIGHT INTO THE STRUCTURE, FUNCTION AND ENERGY HOMEOSTASIS

A dissertation submitted in partial fulfillment of the
requirements for the degree of
Doctor of Philosophy

By

Dhawal P. Oswal
B.Pharm., Pune University, 2007
M.S., Wright State University, 2009

---

2014
Wright State University

COPYRIGHTS BY

DHAWAL P. OSWAL

2014

WRIGHT STATE UNIVERSITY
GRADUATE SCHOOL

9th May, 2014

I HEREBY RECOMMEND THAT THE DISSERTATION PREPARED UNDER MY SUPERVISION BY Dhawal P. Oswal ENTITLED Peroxisome proliferator-activated receptor alpha: Insight into the structure, function and energy homeostasis BE ACCEPTED IN PARTIAL FULFILLMENT OF THE REQUIREMENTS FOR THE DEGREE OF Doctor of Philosophy.

_____
Heather A. Hostetler, Ph.D.
Dissertation Director

_____
Mill W. Miller, Phd
Director,
Biomedical Sciences Ph.D. Program

_____
Robert E. W. Fyffe, Ph.D.
Vice President for Research and
Dean of the Graduate School

Committee on Final Examination

_____
Heather A. Hostetler, Ph.D.

_____
Lawrence J. Prochaska, Ph.D.

_____
David R. Cool, Ph.D.

_____
Steven J. Berberich, Ph.D.

_____
Khalid M. Elased, Pharm.D., Ph.D.

# ABSTRACT

Oswal, Pravin Dhawal Ph.D., Biomedical Sciences Ph.D. program, Department of Biochemistry and Molecular Biology, Wright State University, 2014. Peroxisome proliferator-activated receptor alpha: Insight into the structure, function and energy homeostasis

Peroxisome proliferator-activated receptor alpha (PPARα) belongs to the family of ligand-activated nuclear transcription factors and serves as a lipid sensor to regulate nutrient metabolism and energy homeostasis. The transcriptional activity of PPARα is thought to be regulated by the binding of exogenous ligands (example, fenofibrate, TriCor®), as well as endogenous ligands including fatty acids and their derivatives. Although long-chain fatty acids (LCFA) and their thioesters (long-chain fatty acyl-CoA; LCFA-CoA) have been shown to activate PPARα of several species, the true identity of high-affinity endogenous ligands for human PPARα (hPPARα) has been more elusive. This two part dissertation is a structural and functional evaluation of human and mouse PPARα binding to LCFA and LCFA-CoA using biophysical and biochemical approaches of spectrofluorometry, circular dichroism spectroscopy, mutagenesis, molecular modelling and transactivation assays.

The first goal of this dissertation was to determine whether LCFA and LCFA-CoA constitute high-affinity endogenous ligands for full-length hPPARα. Data from spectrofluorometry suggests that LCFA and LCFA-CoA serve as physiologically relevant endogenous ligands of hPPARα. These ligands bind hPPARα and induce strong secondary structural changes in the circular dichroic spectra, consistent with the binding

of ligand to nuclear receptors. Ligand binding is also associated with activation of hPPARα, as observed in transactivation assays. The second goal of this dissertation was to determine whether there exist species differences for ligand specificity and affinity between hPPARα and mouse PPARα (mPPARα). This is important because despite high amino acid sequence identity (>90%), marked differences in PPARα ligand binding, activation and gene regulation have been noted across species.

Similar to previous observations with synthetic agonists, we reported differences in ligand affinities and extent of activation between hPPARα and mPPARα in response to saturated long chain fatty acids. In order to determine if structural alterations between the two proteins could account for these differences, we performed *in silico* molecular modeling and docking simulations. Modeling suggested that polymorphisms at amino acid position 272 and 279 are likely to be responsible for differences in saturated LCFA binding to hPPARα and mPPARα. To confirm these results experimentally, spectrofluorometry based-binding assays, circular dichroism, and transactivation studies were performed using a F272I mutant form of mPPARα. Experimental data correlated with *in silico* docking simulations, further confirming the importance of amino acid 272 in LCFA binding. Although the driving force for evolution of species differences at this position are yet unidentified, this study enhances our understanding of ligand-induced regulation by PPARα.

Apart from demonstrating significant structure activity relationships explaining species differences in ligand binding, data in this dissertation identifies endogenous ligands for hPPARα which will further help delineate the role of PPARα as a nutrient sensor in regulating energy homeostasis.

## TABLE OF CONTENTS

**INTRODUCTION.....1**

Peroxisome proliferator-activated receptors (PPAR).....2

PPARα: Structure .....4

The A/B region .....6

DNA binding domain (DBD) or C domain .....7

Hinge region or D domain .....11

Ligand binding domain or E/F domain .....11

PPARα: Mode of action .....14

Conformational changes .....14

Coactivators and corepressors .....18

Cellular localization and chain of events .....21

PPARα: Ligands, physiological role and knockout mice phenotype .....25

Ligands .....25

Physiological role of PPARα in lipid metabolism .....27

Physiological role of PPARα in lipoprotein metabolism .....30

## TABLE OF CONTENTS (Continued)

Physiological role of PPARα in inflammation .....30

PPARα knockout mice model.....31

**HYPOTHESIS.....32**

Development of Hypothesis .....32

Hypothesis .....35

**CHAPTER I .....37**

Abstract .....38

Introduction .....39

Materials and Methods .....41

Chemicals .....41

Purification of Recombinant PPARα protein .....41

Direct Fluorescent Ligand Binding Assays .....42

Displacement of Bound Fluorescent BODIPY C16-CoA by Non-fluorescent Ligands:.....43

Quenching of PPARα Aromatic Amino Acid Residues by Non-fluorescent Ligands .....43

**TABLE OF CONTENTS (Continued)**

Secondary Structure Determination Effect of ligand binding on PPARα Circular Dichroism .....44

Mammalian Expression Plasmids .....45

Cell culture and Transactivation assays .....45

Statistical Analysis.....46

Results .....47

Full-length hPPARα and mPPARα protein purification .....47

Binding of fluorescent fatty acid and fatty acyl-CoA to PPARα .....49

Binding of endogenous LCFA and LCFA-CoA to hPPARα – Displacement of bound BODIPY C16-CoA .....54

Binding of endogenous LCFA and LCFA-CoA to mPPARα – Displacement of bound BODIPY C16-CoA .....59

Binding of endogenous LCFA and LCFA-CoA to hPPARα – Quenching of intrinsic aromatic amino acid fluorescence .....63

Binding of endogenous LCFA and LCFA-CoA to mPPARα – Quenching of intrinsic aromatic amino acid fluorescence .....69

**TABLE OF CONTENTS (Continued)**

Effect of endogenous fatty acids and fatty acyl-CoAs on hPPARα secondary structure .....75

Effect of endogenous fatty acids and fatty acyl-CoAs on mPPARα secondary structure .....81

Effect of fatty acids and fatty acyl-CoA on transactivation of human and mouse PPARα-RXRα heterodimers .....87

Discussion .....91

**CHAPTER II .....95**

Abstract .....96

Introduction .....97

Materials and Methods .....100

Molecular modeling simulations.....100

Molecular docking simulations .....100

Chemicals .....102

Purification of Recombinant F272I mutant mPPARα protein .....102

Fluorescence based Ligand Binding Assays .....102

**TABLE OF CONTENTS (Continued)**

Secondary Structure Determination: Effect of ligand binding on F272I mPPARα circular dichroism .....103

Mammalian Expression Plasmids .....103

Cell culture and Transactivation assays .....104

Statistical Analysis.....105

Results and Discussion.....106

Molecular modeling simulations of hPPARα-LBD and mPPARα-LBD .....106

Molecular docking simulations with hPPARα-LBD and mPPARα-LBD.....110

Purification of full-length recombinant F272I mPPARα.....128

Binding of fluorescent fatty acids and fatty acyl-CoAs to F272I mPPARα.....130

Binding of endogenous LCFA and LCFA-CoA to F272I mPPARα .....132

Effect of endogenous fatty acids and fatty acyl-CoAs on F272I mPPARα secondary structure .....141

Effect of fatty acids on transactivation of PPARα-RXRα heterodimers .....147

**TABLE OF CONTENTS (Continued)**

**SUMMARY AND CONCLUSIONS** ..... **152**

**BIBLIOGRAPHY/REFERENCES** ..... **164**

**APPENDIX** ..... **199**

Abstract ..... 200

Introduction ..... 201

Development of hypothesis ..... 208

Materials and Methods ..... 212

Chemicals ..... 212

Electrophoretic mobility shift assays (EMSA) ..... 212

Cell culture and treatments: ..... 213

RNA isolation and qRT-PCR ..... 213

Western Blotting Analysis ..... 214

Plasmids ..... 215

Transactivation assays ..... 216

Results and Discussion ..... 218

**TABLE OF CONTENTS (Continued)**

Electrophoretic mobility shift assays (EMSA) .....218

Adiponectin expression in HepG2 cells and its regulation by hPPARα ligands 224

Transactivation assays .....229

Future directions .....237

**BIBLIOGRAPHY/REFERENCES .....239**

**LIST OF ABBREVIATIONS .....261**

## LIST OF FIGURES

### INTRODUCTION

1. Pre-messenger RNA and domain structure of PPARα ..... 5
2. Illustration of PPAR-RXR heterodimer binding to DNA ..... 10
3. Illustration of "mousetrap" model for PPARα activation ..... 17
4. PPAR mechanism of action ..... 24
5. Genes regulated by PPARα and their role in lipid metabolism ..... 29

### CHAPTER I

6. SDS-PAGE and Coomassie blue staining of recombinant hPPARα and mPPARα proteins ..... 48
7. Binding of fluorescent fatty acid and fatty acyl-CoA to hPPARα ..... 51
8. Binding of fluorescent fatty acid and fatty acyl-CoA to mPPARα ..... 53
9. Binding of endogenous LCFA and LCFA-CoA to hPPARα: Displacement of bound BODIPY C16-CoA ..... 55
10. Binding of endogenous LCFA and LCFA-CoA to mPPARα – Displacement of bound BODIPY C16-CoA ..... 60

## LIST OF FIGURES (Continued)

11. Binding of endogenous LCFA and LCFA-CoA to hPPARα – Quenching of intrinsic aromatic amino acid fluorescence ..... 64

12. Binding of endogenous LCFA and LCFA-CoA to mPPARα – Quenching of intrinsic aromatic amino acid fluorescence ..... 71

13. Effect of endogenous fatty acids and fatty acyl-CoAs on hPPARα secondary structure ..... 77

14. Effect of endogenous fatty acids and fatty acyl-CoAs on mPPARα secondary structure ..... 83

15. Effect of fatty acids and fatty acyl-CoA on transactivation of human and mouse PPARα-RXRα heterodimers ..... 89

**CHAPTER II**

16. Comparison of primary amino acid sequence of human and mouse PPARα ..... 107

17. An overlay of the energy minimized structures of hPPARα-LBD and mPPARα-LBD ..... 109

18. Validation of molecular docking simulations ..... 111

19. Comparison of molecular docking simulations of C16:0 complexed with hPPARα-LBD, mPPARα-LBD and F272I mPPARα-LBD ..... 115

20. Energy minimized structures of hPPARα-LBD in complex with palmitoleic acid, stearic acid and docosahexaenoic acid ..... 117

## LIST OF FIGURES (Continued)

21. Energy minimized structures of mPPARα-LBD in complex with palmitoleic acid, stearic acid and docosahexaenoic acid .....120

22. Energy minimized structures of F272I mPPARα-LBD in complex with palmitoleic acid, stearic acid and docosahexaenoic acid .....123

23. Illustration of saturated LCFA binding to human and mouse PPARα – Importance of amino acid residues at position 272 and 279 .....125

24. Ligand binding pocket volumes for hPPARα-LBD, mPPARα-LBD, F272I mPPARα-LBD and F272I, M279T mPPARα-LBD.....127

25. SDS-PAGE and Coomassie blue staining of purified recombinant mPPARα and F272I mPPARα.....129

26. Binding of fluorescent fatty acid and fatty acyl-CoA to F272I mPPARα .....131

27. Binding of endogenous LCFA and LCFA-CoA to F272I mPPARα – Displacement of bound BODIPY C16-CoA.....133

28. Binding of endogenous LCFA and LCFA-CoA to F272I mPPARα – Quenching of intrinsic aromatic amino acid fluorescence.....137

29. An overlay of the far UV circular dichroic spectra of hPPARα, mPPARα and F272I mPPARα .....142

30. Effect of endogenous fatty acids and fatty acyl-CoAs on F272I mPPARα secondary structure .....144

## LIST OF FIGURES (Continued)

31. Effect of fatty acids and fatty acyl-CoA on transactivation of human, mouse and F272I mouse PPARα-RXRα heterodimers ..... 149

**APPENDIX**

32. Primary structure of adiponectin ..... 203

33. Electrophoretic mobility shift assays (EMSA) ..... 222

34. Adiponectin expression in HepG2 cells and its regulation by hPPARα ligands 228

35. The transactivation of adiponectin promoter in COS-7 cells ..... 231

36. Effect of PPARα ligands on the transactivation of adiponectin promoter ..... 233

## LIST OF TABLES

### CHAPTER I

I. Affinity of hPPARα for non-fluorescent ligands determined by quenching of hPPARα aromatic amino acid fluorescence and by displacement of hPPARα-bound BODIPY C16-CoA ..... 68

II. Affinity of mPPARα for non-fluorescent ligands determined by quenching of PPARα aromatic amino acid fluorescence and by displacement of mPPARα-bound BODIPY C16-CoA ..... 74

III. Effect of ligands on the relative proportion of hPPARα secondary structure determined by circular dichroism spectroscopy ..... 80

IV. Effect of ligands on the relative proportion of mPPARα secondary structure determined by circular dichroism spectroscopy ..... 86

### CHAPTER II

V. Comparison of binding energies for mouse and human PPARα LBD complexed with LCFA ligands ..... 118

VI. Affinity of F272I mPPARα for non-fluorescent ligands determined by quenching of PPARα aromatic amino acid fluorescence and by displacement of F272I mPPARα-bound BODIPY C16-CoA ..... 140

## LIST OF TABLES (Continued)

VII. Effect of ligands on the relative proportion of F272I mPPARα secondary structure determined by circular dichroism spectroscopy.....146

ACKNOWLEDGEMENTS

I would like to thank my advisor Dr. Heather A. Hostetler for the opportunity to work in her lab, for the disciplined training enviorment and for her guidance and patience throughout my dissertation research. I would also like to thank my committee members Drs. Berberich, Cool, Elased and Prochaska for their time and their invaluable input over all these years. My sincere thanks to Dr. Alter for helpful suggestions and incredible guidance in a large portion of this dissertation work.

Thanks to Dr. Rider for not only his scientific input, but also for helping me get started in a biochemistry and molecular biology lab. To all the past and present members of the Hostetler lab, thank you for your friendship and for all your assistance over the years. I would also like to extend my gratitude to my BMS colleagues for all of their support and willingness to help out whenever needed. Thanks to all the people associated with the Biomedical Sciences Ph.D. program and the Department of Biochemistry and Molecular Biology at Wright State University for all their encouragement and support.

I would especially like to thank to all my friends in the United States, who I first met at Wright State University, for all your encouragement and support. They have been my family and my support system away from home. Since I don't say this often (and will probably not in future!!) – Thank you. Graduate School was much more enjoyable with all of you around. I would also like to thank my family and friends back home for all their patience, encouragement and constant support throughout my graduate school years.

Lastly, a special thanks to my brothers, sisters and my lovely wife for their unconditional love and support. This dissertation would not have been possible without your enthusiastic support of my ambitions.

# DEDICATION

This dissertation research endeavor is dedicated to the loving memory of:

My beloved mother Maya Oswal

My grandparents Pukhraj Gandhi and Navuben Gandhi

My sister Charu Raigandhi

Whose love for me knew no bounds and whose memories will always keep me going

# INTRODUCTION

The relationship between obesity and metabolic disturbances, including increased lipids and glucose, cardiovascular disease (CVD), hypertension and diabetes, has been known and described for decades. A syndrome linking obesity to metabolic abnormalities, CVD and diabetes was described in 1988 by Dr. Reaven in his Banting lecture as 'syndrome X' (*1*). Today, this syndrome is referred to as the metabolic syndrome (named by the World Health Organization; WHO) and has a WHO diagnostic code of ICD9. The metabolic syndrome includes a group of risk factors that increase the risk for cardiovascular morbidities and diabetes (*2, 3*). Obesity, which tops the list in the metabolic syndrome, affects more than one-third of adults (35.7%) and approximately 17% (or 12.5 million) of children in the US alone (*4, 5*). It is a major risk factor for coronary heart disease, hypertension, atherosclerosis, dyslipidemia and diabetes and the estimated 2012 annual direct medical cost of obesity in the United States (for data from 2000-2005) is $190.2 billion (*6*). The exact molecular mechanisms underlying these associations are still not clear.

Obesity is a medical condition defined as an increased mass of adipose tissue and has often been related to dysregulated lipid homeostasis. It is an illeness where the health of an individual (and hence life expectancy) is adversely affected by excess body fat. Under normal energy homeostasis, dietary long chain fatty acids (LCFA) not only serve as major metabolic fuels and important components of biological membranes, but they

also play a significant role as gene regulators and signaling molecules that regulate metabolic pathways governing fuel utilization, storage, transport and mobilization. Dysregulated LCFA alter this energy homeostasis and thus have been implicated in various metabolic, endocrine and cardiovascular complications. One of the plausible explanations of such regulation and mis-regulation includes their interactions with the nutrient sensing family of transcription factors called the peroxisome proliferator-activated receptors (PPAR).

**Peroxisome proliferator-activated receptors (PPAR)**

PPARs belong to the nuclear hormone receptor superfamily of ligand-activated transcription factors which play important regulatory roles in numerous cellular processes related to fatty acid metabolism, glucose metabolism, inflammation, differentiation and proliferation (*7-10*). PPARs form the group C of subfamily 1 of the superfamily of nuclear hormone receptors (NR1). There are three members of this subfamily of nuclear receptors: PPARα (NR1C1), PPARβ/δ (NR1C2) and PPARγ (NR1C3) (*9*). The founding member of the family (PPARα) was identified because a structurally diverse group of chemicals including fibric acid derivatives, phthalate plasticizers and certain herbicides resulted in massive proliferation of peroxisomes in rodents (*11-13*). Reddy *et. al.* (1987) used these chemicals as affinity ligands to identify and purify the receptor/protein responsible for such effects from the cytosolic fraction of rat livers (*14*). This protein/receptor was indicative of being isolated as a dimer and was termed as peroxisome proliferator-binding protein (PPbP) (*14*). The exact identity of the true

peroxisome proliferator binding protein (in the dimeric complex) remained elusive until 1990.

Isseman and Green (1990) were the first to clone the receptor activated by peroxisome proliferators which became named as peroxisome proliferator-activated receptor alpha (*15*). Since the discovery of PPARα, two other PPAR subtypes, PPARβ/δ and PPARγ were identified (*16, 17*). They are encoded by distinct single copy genes located on human chromosomes 22 (PPARα), 6 (PPARβ/δ) and 3 (PPARγ) (*18-20*). While the splice variants of PPARγ (γ1 and γ2) are generated as a result of alternate promoter usage and splicing (*21*), the PPARα splice variant transcript lacks 200 bp around exon 6 (9.7kb compared to 9.9kb) and gives rise to a premature stop codon resulting in truncated protein that lacks a large part of the ligand binding region (174 amino acids as compared to 468 in wild-type; Fig. 1) (*22*). This truncated protein is present widely in human tissues and when compared to the wild-type PPARα its ratio varies among individuals (from 1:1 to 1:4 - based on the two subjects tested in a previous study) (*22*). The truncated PPARα protein is believed to have a repressive activity on the wild-type form of the protein (by competing with cofactors that bind the N-terminal portion of the protein) (*22*).

The three PPAR subtypes display distinct patterns of tissue distribution (*16*). PPARα is expressed in tissues mainly with high metabolism rates such as liver, heart, muscle, kidney and brown fat where it serves as a potent activator of genes involved in lipid catabolism. In fact, synthetic agonists of PPARα (example, fenofibrate, TriCor®; fenofibric acid, TriLipix®; gemfibrozil, Lopid®) have been used as therapeutic agents in the treatment of hyperlipidemia (*7-10*). PPARβ/δ is broadly expressed with highest levels

found in intestines and keratinocytes. Apart from exerting metabolic effects similar to PPARα in gut, skin and brain, it is also involved in neuronal development, inflammation, keratinocyte differentiation and wound healing (*7-10*). PPARβ/δ agonists (example, GW501516 and MBX-2085) have been under clinical investigations (in clinical trials) (*23, 24*) but are yet to be seen on the market. PPARγ on the other hand is predominantly expressed in adipocytes and macrophages where it activates genes involved in lipogenesis and adipocyte differentiation (*7-10*). While thiazolidinediones such as pioglitazone (Actos®) are potent PPARγ agonist used in management of diabetes, others such as rosiglitazone (Avandia®) have either been taken off the market in some countries (mainly Europe) or prescribed with caution (U.S.A.), owing to side effects such as weight gain and increased risks of heart attacks.

**PPARα: Structure**

The human PPARα gene spans ~93.2 kb on chromosome 22 and gives rise to a 9.9 kb transcript in humans (8.5 kb in mouse). This transcript encodes a 468 amino acid and 52 kDa protein (*18*). Like other members of the nuclear hormone receptors, the PPARα protein structure also consists of distinct functional domains – the N terminal A/B domain, the DNA binding domain (DBD) or C domain, hinge region or D domain and the ligand binding domain (LBD) or E/F domain (Fig. 1). The PPAR transcript reveals common structural organization with the translated region composed of 8-9 coding exons depending on the transcript variant in question (*18, 25*).

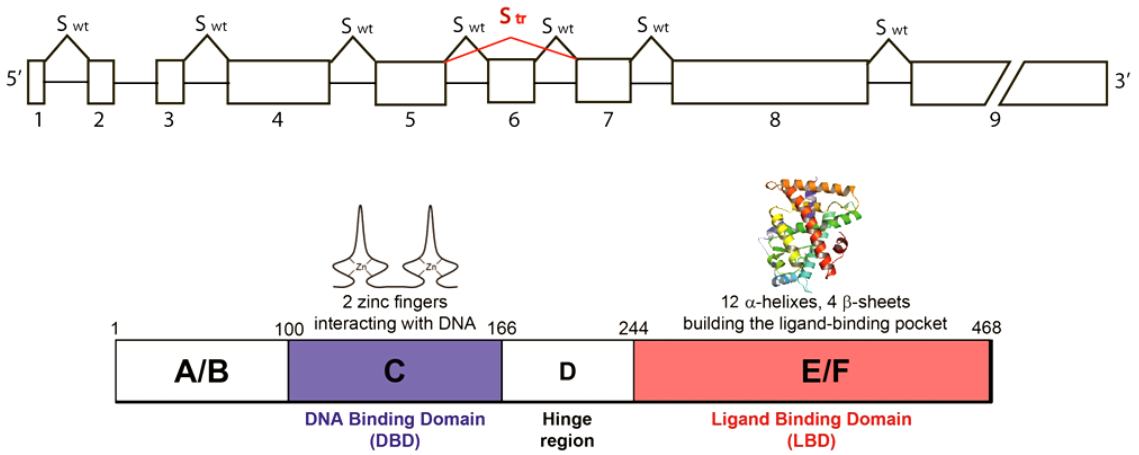


**Fig. 1.** Pre-messenger RNA and domain structure of PPARα. *Top panel:* The pre-messenger RNA for human PPARα demonstrating splicing events, $S_{wt}$ and $S_{tr,}$ that generate wild-type PPARα (9.9 kb) and truncated PPARα transcripts (9.7 kb; with premature stop codon in exon 7). *Bottom panel:* Domain structure of PPARα protein (wild-type), left to right: the N-terminus A /B domain, the C domain or DNA binding domain containing two zinc-finger motifs that bind the DNA in the regulatory region of target genes, the D domain or hinge region that allows for conformational changes upon ligand binding and the - the E/F domain or the ligand-binding domain (LBD) containing the ligand-dependent transactivation function (AF-2). The hPPARα ribbon structure is adopted from PDB code 1K7L (*26*)

*The A/B region*: The N-terminal A/B domain amongst most nuclear hormone receptors displays the weakest evolutionary conservation and is highly variable, both in sequence and length. These domains are also poorly structured, and this has been confirmed using deuterium exchange mass spectrometry, circular dichroism spectroscopy and NMR spectroscopy (*27-29*). For this reason, the X-ray crystal structure of the A/B domain has not been resolved till date. The length of the N-terminal A/B domain in PPARα is 100 amino acids (Fig. 1), and it harbors a ligand-independent transactivation function (AF-1) that is responsible for low-level transactivation activity of the receptor (tested in GAL4-fusion proteins) (*30*). Although the A/B domain in PPARα has poor structural organization, it has been suggested that secondary structure formation in this domain is an important step towards AF1 mediated transactivation (*30*). This was demonstrated by two observations 1) AF-1 domain adopts α-helical characteristic in the presence of a strong α-helix stabilization agent such as trifluoroethanol and 2) mutation of hydrophobic amino acids in the AF-1 domain (possibly involved in α-helix formation) impacted the transcriptional activity of the protein (*30*).

The importance of the A/B domain in PPARα is highlighted by the fact that deletion of the A/B domain results in a gene-dependent alteration in PPARα transcriptional activity. For example, deletion of the A/B domain disrupts the PPARα-mediated transactivation of the acyl-CoA oxidase promoter, but it does not affect the transactivation of cytochrome P450 4A6 promoter (*30, 31*). In addition, the A/B domain of PPAR is suggested to contribute towards maintaining subtype specificity amongst the PPAR subtypes. For example, addition of the PPARα A/B domain to PPARγΔAB (A/B domain truncated) enhances its ability to activate PPARα specific target genes (*32*) and

the addition of PPARγ A/B domain to non-adipogenic PPARβ/δΔAB (A/B domain truncated) imparts adipogenic potential to the resulting PPARβ/δ protein (*33*). As far as its relation/association with other domains in the protein is concerned, a recent research article demonstrates that mutation of residues in the A/B domain (S112) altered ligand binding and activity (function of E/F domain) of PPARγ (*34*). These findings suggest that studies carried out using individual nuclear receptor domains or truncated forms of nuclear receptors must be interpreted with caution.

*DNA binding domain (DBD) or C domain:* The DNA binding domain is the most conserved domain within the nuclear hormone receptor superfamily (*9*). The DBD of nuclear hormone receptors recognizes a 6 nulceotide core motif in the DNA and binds to two copies of such a motif (constituting a hormone responsive element) as a dimer. Factors such as the 5' flanking extension of the core motifs, spacing of the two core motifs and their relative orientation (direct repeats, inverted repeats or everted repeats) determine which nuclear receptor dimer binds the hormone response element (*35*). Amongst the PPAR subtypes, the DBD bears about 78-86 % amino acid identity and it encompasses amino acids 101-166 in PPARα (Fig. 1) (*8, 36*). The PPAR-DBD consists of two zinc finger motifs and in each motif four cysteine residues coordinate and chelate one $Zn^{2+}$ ion. The alpha helical components of the two zinc finger motifs lie perpendicular to each other. The amino acids that are responsible for registering contacts with specific nucleotides in the DNA are present towards the C terminus of the first zinc finger in a region termed as the "P box." Hydrogen bonding contacts are made between amino acid residues in this region and the major groove of the DNA. Similarly, the region

towards the N terminus of the second zinc finger is referred to as the “D box” and amino acids present in this region are involved in heterodimerization. (*25, 29, 37, 38*)

PPARα binds DNA as obligate heterodimers with other nuclear receptors, mainly the retinoid X receptors (RXR). The PPAR-RXR heterodimer recognizes and binds to a consensus sequence on the DNA, termed the peroxisome proliferator response element (PPRE). While these PPRE were first characterized using synthetic oligonucleotides (*39*), the first natural PPRE was found in the regulatory region (promoter) of the acyl-CoA oxidase (ACOX) gene (*17, 40*). In addition, recent genome-wide profiling of PPARα binding sites has revealed about 46% of PPAR-RXR binding sites within the intronic regions (*41*). The PPRE belongs to the direct repeat 1 (DR1) category and consists of two AGG(A/T)CA half sites separated by one nucleotide (Fig. 2). The binding to the PPRE occurs in a manner such that PPAR is oriented towards the 5’ end and RXR is oriented to the 3’end. This is in contrast to other nuclear receptor heterodimers such as the vitamin D receptor-retinoid X receptor heterodimer (VDR-RXR) or thyroid receptor-retinoid X receptor heterodimer (TR-RXR) where RXR is oriented towards the 5’end (*38, 42*).

Detailed analysis of PPRE sequences from PPAR target genes has helped to define additional PPRE determinants (*43*). These PPRE determinants impart subtype specificity as well as DNA binding polarity to the PPAR-RXR heterodimer and include the spacing nucleotide as well as the COOH-terminal extension (CTE) of the DBD (*31, 42-44*). The amino acid residues present in the CTE of the PPARs play a significant role in the recognition of the PPRE and form significant interactions with the 5’ flanking sequence of the PPRE (Fig. 2) (*29, 43*). While PPAR binds DNA only as a heterodimer (and not as a monomer), deletion of its N-terminal A/B domain allows the truncated

protein to non-specifically bind DNA as a monomer in *in vitro* assays (*31*). While the physiological significance of such binding is unclear, it serves as evidence of interdomain communication and the importance of full-length nuclear receptors. The DBD of a nuclear receptor such as PPAR, forms an interface with its own LBD as well as the LBD of its heterodimeric partner – thereby influencing ligand binding (*29*). These data point to two important conclusions; 1) since PPARs bind to DNA only as a heterodimer it reflects the evolution and divergence of PPARs from its monomeric nuclear receptor cousins and 2) since the DBD can influence ligand binding, it emphasizes on the importance of conducting ligand-binding studies with full-length forms of nuclear receptors.


**Fig. 2.** Illustration of PPAR-RXR heterodimer binding to DNA. X-ray crystallized complex of PPARγ (magenta) and RXRα (green) bound to a PPRE containing AGGTCA direct repeat separated by one nucleotide (DR1) (Source PBD code 3DZY (*29*)).

*Hinge region or D domain:* Adjacent to the DNA binding domain is the D domain or the hinge region. As the name suggests the D domain serves as a 'hinge' between the highly structured C and E/F domains (Fig. 1). The hinge region is not well conserved amongst PPAR subtypes or amongst nuclear receptors in general (*45*). It allows for conformational changes in protein structure upon ligand binding. The D domain also contains the CTE of the DBD which renders polarity and subtype specificity for binding to the PPRE (*31, 42-44*). For example, the CTE of the DBD (contained in the hinge region) interacts with nucleotides in the 5' flank of the PPRE (*29*) and conservation of this 5' flanking sequence of the PPRE is essential for PPARα binding - thus imparts subtype specificity (*43*) This region is also thought to harbor the nuclear localization signals and contain sites for protein-protein interaction (*45*).

*Ligand binding domain or E/F domain:* The C-terminal ligand binding domain (LBD) or E/F domain for the PPARs is highly structured and contains ligand-dependent activation function (AF-2). Compared to the DNA binding domain, the LBD bears less amino acid identity (63-71 %) amongst the PPAR isotypes (*9, 36*). The X-ray crystal structures of all the PPAR-LBD isotypes have been resolved and studied in great detail. Before going in depths of the PPARα structure, it is necessary to clarify some terminology issues, particularly with the E and F domains. In addition to the A/B, C and D domains, researchers in the nuclear receptor field often classify receptors as having only an E domain (*46*), both E and F domains (*46, 47*) or an E/F domain (*8, 10*). It is thus important to clarify these differences in terminology. Classically, the nuclear receptor LBD is defined as the domain between the beginning of helix 1 through the end of helix 12 (AF-2) (*46*). Any region beyond helix 12 (seen in the progesterone, estrogen and

retinoic acid receptors) is referred to as the 'F domain' (*46*). Since the PPARα-LBD is composed of 12 α-helices, with only four amino acids at the C-terminus, for the sake of simplicity herein the LBD is referred to as the E/F domain.

The human PPARα-LBD extends from amino acids 280-468 (Fig. 1) and contains a ligand-dependent transactivation function (AF-2), a major dimerization interface and sites for interaction with coactivator and corepressor proteins (*8-10*). Recently, it has also been demonstrated that the PPAR-LBD may have additional interfaces for interaction with its own DBD as well as the DBD of its heterodimeric partner (*29*). Structurally the PPARα-LBD is folded in a three-layered helical sandwich formed by 12 α-helices (designated H1-H12) and a four stranded β-sheet (*26*). The central core of this helical sandwich is packed in way to create a 1400 $Å^3$ cavity, the ligand binding pocket (*26*). The volume of the PPARα-LBD pocket is quite comparable to other PPAR isotypes but is substantially larger than some other nuclear receptors such as thyroid receptor (600 $Å^3$) and retinoid X receptor (RXR; ~500 $Å^3$) (*9, 26, 48-50*).

X-ray crystal structures of the PPARs in complex with agonist-bound ligands and the understanding of nuclear receptor activation has helped in the design of specific agonists, partial agonists as well as antagonists. The crystal structure of the PPARα-LBD in complex with GW409544 agonist reveals that the carboxylic acid group of the agonist forms hydrogen bonds with Y464 on helix 12 and Y314 on helix 5 (Fig. 3) (*26*). The rest of the GW409544 ligand is largely lipophilic and is stabilized by hydrophobic interactions with the amino acids lining the pocket of the PPARα-LBD. These interactions stabilize the receptor in an "active" conformation. Based on this information, Xu *et al.* elegantly designed a potent PPARα antagonist in which the carboxylic acid

group of the GW409544 agonist was substituted by an ethyl amide such that it would disrupt the hydrogen bonding with Y464 (*51*). As a result of this substitution, the antagonist blocks the helix 12 from adopting the "active" conformation.

The ligand binding pocket of human PPARα assumes a Y-shape and spans between the C-terminal helix 12 and the 4 stranded β-sheet, splitting into roughly two arms along helix 3. Compared to the PPARα-LBD structure, the ligand binding pocket of agonist bound PPARγ-LBD and PPARβ/δ-LBD are 'T' and 'Y' shaped respectively (*49, 50*). The amino acids lining their ligand binding pocket bear several conserved and nonconserved amino acid changes that dictate the shape and volume of the pocket and thereby impart ligand specificity to the isotypes. For example, H323 in the human PPARγ-LBD corresponds to Y314 in the human PPARα-LBD and imparts ~1000-fold greater selectivity for the binding of farglitazar (thiazolidinediones) to PPARγ (*26*). Also, a single methionine to valine substitution at 417 (M417V) in human and/or chick PPARβ/δ imparts fibrate (PPARα specific agonist) binding characteristic to the protein (*52*).

Several hydrophilic residues lining the PPARγ or PPARβ/δ pocket are converted to hydrophobic residues in PPARα – rendering the PPARα pocket much more hydrophobic as compared to either PPARγ or PPARβ/δ (*26*). In the ligand bound (agonist) conformation the human PPARα pocket is lined by a mix of largely hydrophobic residues (I241, L247, L254, I272, F273, I317, F318, L321, M330, V332, I339, L344, L347, F351, I354, M355, V444, L456, L460), a few polar residues (S280, T279, E251, C275, C276, Y314, H440) and is capped by Y464 from the AF-2 helix (*26*). However, irrespective of the amino acid changes or the distinct ligand binding

specificities amongst all PPAR isotypes, they all contain a similar network of hydrogen bond forming amino acid residues (near the AF-2) that are involved in receptor activation upon ligand binding (*26*). PPARα binds to the PPRE in its target genes only as an obligate heterodimer with RXR (*38, 39, 47*). The heterodimerization interface is mainly formed by helices 9 and 10. This was confirmed in studies involving deletion of helix 10-12 as well as a L433R mutation in PPARα which caused impaired heterodimerization with RXR (*53, 54*).

**PPARα: Mode of Action**

*Conformational changes:* Ligand binding induced conformational changes are hallmarks of nuclear receptor action (*53*). The human genome contains 48 nuclear receptors and notably many of their LBD have been crystallized in the holo or liganded state. This is because the binding of a ligand stabilizes the conformation of a nuclear receptor, making it convenient to crystallize (*26, 49, 50, 55, 56*). Nonetheless, a few nuclear receptors have been crystallized in the unliganded state; including, apo-RXRα-LBD and apo-PPARγ-LBD (*49, 57*). Based on comparison of the apo and holo state of nuclear receptors, a "mousetrap" model/mechanism of nuclear receptor activation has been proposed (*58*).

The "mousetrap" model was first proposed on the basis of x-ray crystal structures of the apo-RXR-LBD (*57*) and the holo-retinoic acid receptor LBD (RAR-LBD) (*59*) and later extended to other nuclear receptors using apo/holo-state structures of the RXRα-LBD and PPARγ-LBD (*49, 57*). According to this model, in the unliganded nuclear receptor, the helix 12 (AF-2) is angled away from the body of the LBD. The binding of a

ligand causes conformational changes and concomitant swinging of helix 12 (AF-2; moves closer to the LBD) such that it "traps" the ligand and prevents its exit (Fig. 3) (*58*). Hydrophobic and electrostatic interactions between the ligand and amino acids lining the pocket and helix 12 (Y464 in PPARα; (*26*)) stabilize and reposition helix 12. In some nuclear receptors, including the PPARs, the AF-2 is stabilized by specific interactions between the ligand and the amino acids of helix 12 (*58*), but in others the helix 12 is stabilized indirectly by other intervening residues (*55, 56, 58*) (Fig. 3).

While the "mousetrap" model is widely accepted for nuclear receptor activation (including that for PPARα), recently a "dynamic stabilization" model has also been proposed to account for the plasticity of the nuclear receptor ligand binding pocket and to explain the appearance of helix 12 proximal to the LBD, even in absence of ligands (*56, 60, 61*). According to this model, the AF-2 along with other regions of the LBD are rather mobile in an unliganded nuclear receptor. The binding of ligand stabilizes overall conformational dynamics of the receptor along with repositioning of helix 12 via specific interactions with the ligand (Y464 in PPARα) (*60*). However, if the helix 12 is stabilized proximal to the LBD in an unliganded state, then according to this model that nuclear receptor is likely to show constitutive activity (*55, 56, 61*). For example, the constitutive activity of nuclear receptor related protein 1 (NURR1) (*62*) is explained by this model. This model helps explain the dynamic/plastic nature of most nuclear receptors including the PPARs (*56*) and has been well supported by various solution based biophysical studies. For example, NMR studies (*63*), proteolytic sensitivity studies (*64, 65*), fluorescence studies (*66*) as well as secondary structure melting studies (*67*) have all

demonstrated that the relatively unstable apo-state nuclear receptor LBD switches to a more rigid and stable conformation upon ligand binding (*60, 61*).

Regardless of the "mousetrap" mechanism or the "dynamic stabilization" model, the helix 12 (AF-2) switches from a rather mobile conformation to a more stable position proximal to the ligand binding pocket. This results in exposure of a new surface on the receptor that recruits transcriptional activators and other components of the transcription machinery, resulting in enhanced/repressed transcription of a specific set of target genes (*68, 69*). This phenomenon, mediated by ligand binding, is crucial for receptor activation.

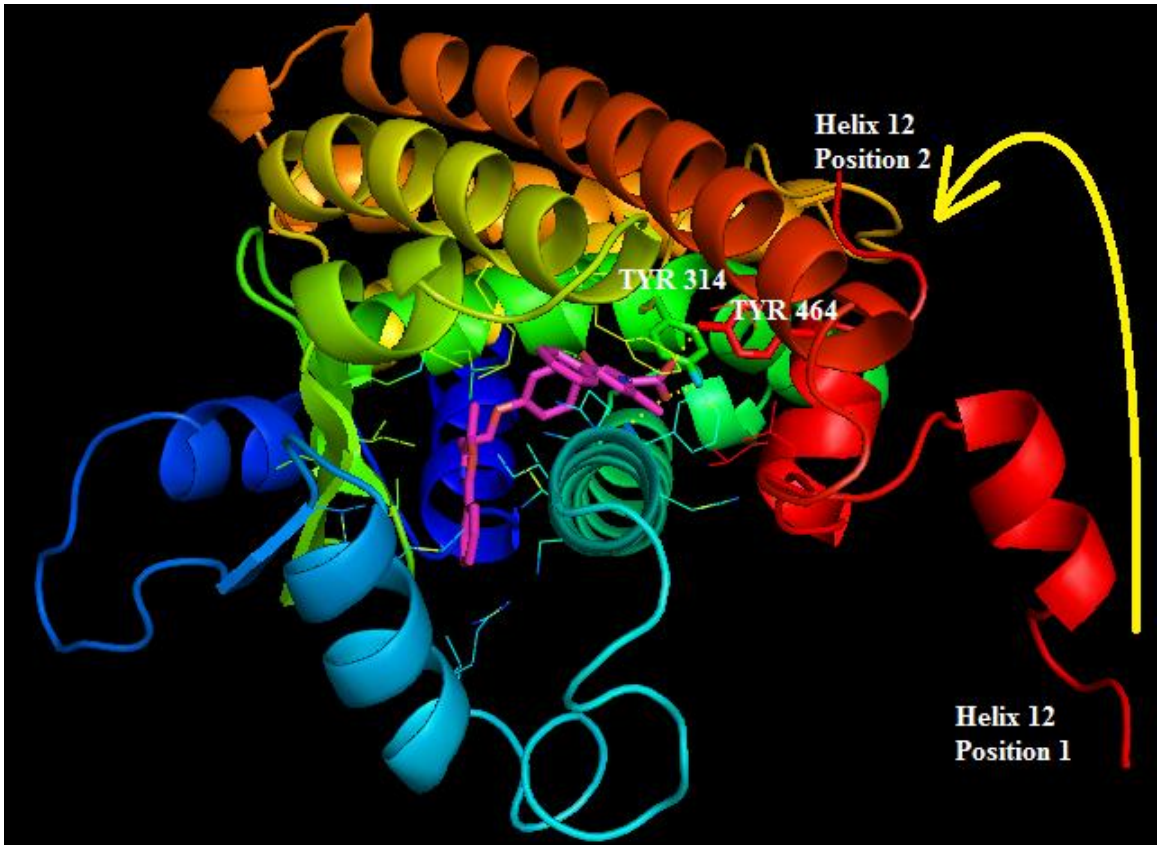


**Fig. 3.** Illustration of "mousetrap" model for PPARα activation. In the unliganded state the helix 12 (AF-2; red) is away from the LBD of PPARα (position 1). Upon ligand binding the AF-2 is stabilized proximal to the ligand binding pocket (position 2) by specific interactions between the ligand and amino acids residing in helix 12 (example Tyr-464). (PDB file (1K7L) adapted from (*26*))

*Coactivators and Corepressors:* Nuclear receptor mediated transcriptional regulation of genes is a complex process and also involves two classes of transcriptional cofactors/coregulators (corepressors and coactivators) (*68, 69*). The development of squelching experiments and yeast two hybrid have marked the discovery and identification of a large number of coactivators and corepressors that transmit the nuclear receptor signals to the transcriptional machinery (*70, 71*). In the simplest form, corepressors bind to the PPAR-RXR heterodimer in an unliganded state and render it inactive. Ligand binding induces specific conformational changes that result in the release of corepressors and the recruitment of coactivator proteins. Coactivators or corepressors respectively bring about transcriptional activation or repression of the target genes by mechanisms including chromatin modification (via intrinsic histone acetyltransferase activity (HAT) or histone deacetylase activity (HDAC)) and physical interactions with the transcriptional initiation machinery (*68, 69*).

The first class of nuclear receptor coregulators includes the coactivators. Binding of an agonist ligand results in repositioning of helix 12 together with other structural changes that lead to the creation of a distinct surface on the protein. These novel surfaces allow for recruitment of coactivator proteins with a conserved LXXLL motifs or (L, leucine and X, any amino acid; also called 'NR box') such as the steroid receptor coactivator (SRC-1) (*68, 69, 72*). SRC-1 was the first nuclear receptor coactivator to be discovered (*72*), and its interaction with LXXLL motifs were first seen in the crystal structure of the PPARγ-LBD (*49*). In addition to interacting with LXXLL motifs in the LBD of nuclear receptors, coactivator proteins may also interact with the A/B domain of nuclear receptors. For example, SRC-1 and coactivators belonging to the transcriptional

mediators/intermediary factor 2 (TIF-2) family also interact with the A/B domain of nuclear receptors such as the estrogen and androgen receptors (*73, 74*) . It is thus possible that the N-terminal A/B domain (AF-1) and the LBD (AF-2) may not always function independently but may rather serve as a single common recruiting surface for such coactivators. The molecular mechanism of action of coactivators results from their ability to reorganize/remodel chromatin. While coactivators such as SRC-1 possess intrinsic HAT activity that aid in chromatin remodeling, others such as TIF-2 function by physically recruiting histone acetyltransferases (*70, 73, 74*). Decondensation of chromatin is then followed by recruitment of basal transcriptional machinery to the target gene promoters including TATA binding protein (TBP) and RNA polymerase II (*75*).

The observation that certain nuclear receptors such as the thyroid receptor (TR) and retinoic acid receptor (RAR) repress transcription even in the liganded state led to the discovery of a second class of nuclear receptor coregulators called the corepressors (*76*). Examples of corepressor proteins that bind the PPAR-RXR heterodimer in an unliganded state include nuclear receptor corepressor (NCoR) and silencing mediator of retinoid and thyroid hormone receptors (SMRT) (*76, 77*). These corepressors bind to a LXXXIXXXL motif (also termed as the 'CoRNR box') on the surface of the protein that does not involve helix 12 (*78*). Although the CoRNR box is similar to the LXXXL coactivator motif, the three extra amino acids in the CoRNR box cannot be accommodated in the ligand bound nuclear receptor conformation (with the repositioned helix 12) (*78, 79*). In contrast to the mechanism of action for coactivators, corepressors bring about transcriptional repression through intrinsic or recruited histone deacytylase activity (*70, 75, 76*), and the phenomenon of coactivator recruitment is accompanied by corepressor

release. For example, release of NCoR upon binding of Wy-14,643 (agonist) to PPARα (*77*).

Since the discovery and cloning of SRC-1 (*72*) and NCoR (*76, 77*), more than 300 transcriptional cofactors have been identified that associate with nuclear receptors such as the PPAR (*8, 80*). These cofactors allow for the interaction of the PPAR-RXR complex with other proteins/complexes associated with the basal transcription machinery, resulting in enhanced/repressed transcription of a specific set of target genes (Fig. 4) (*68, 69*). However such diversity of 300 or more cofactors not only enhances the multiplicity of nuclear receptor activation, but also adds complexity in our understanding of nuclear receptor mediated transcriptional regulation. For example: why are there multiple coregulators with the same HAT/HDAC activity? Do they bind nuclear receptors in a sequential or combinatorial manner? Does there exist competition for these coregulators? How do tissue-restricted distribution and/or regulation of cofactors affect nuclear receptor action? While many of these questions are still under extensive investigations, some of the outcomes are presented below.

Tissue restricted distribution and physiological regulation of these cofactors could be a means of finer regulation of nuclear receptor action. For example, 1) PPARγ can activate the transcription of uncoupling protein 1 (UCP1) in brown fat but not fibroblasts. This was because PPARγ coactivator-1 (PGC-1), which serves as a coactivator for PPARγ, is expressed primarily in brown fat and skeletal muscles (*81*). Further PGC-1 expression is also regulated physiologically by body temperature. Thus exposure of mice to cold temperatures increases the activity of PGC-1 and thereby increases the transcriptional activity of PPARγ (*81*). Similarly tissue restricted

distribution of other cofactors such as SRC-1 may further modulate the transcriptional activity of nuclear receptors (*82*).

Irrespective of the vast scope of research in understanding the downstream molecular mechanism of cofactors, the phenomenon of coactivator-recruitment upon ligand binding has resulted in the development of coactivator-dependent receptor ligand binding assays (CARLA) (*83*, *84*). Although these assays have provided valuable information on the identity of ligands for orphan receptors, many of these assays were conducted with truncated forms of nuclear receptors (only the LBD). Since coactivators such as SRC-1 has been demonstrated to interact with the A/B domain of nuclear receptors (in addition to LXXLL motifs in the LBD) (*74*), the significance of these findings are not clear. These data further emphasize the need to conduct such ligand binding studies with full-length forms of nuclear receptors.

*Cellular localization and chain of events:* The cellular localization of nuclear hormone receptors is a result of equilibrium between the nucleus and the cytoplasm (*85*). According to the widely accepted dogma, nuclear receptors are predominantly localized in the nucleus at equilibrium (even in absence of ligand) (*46*). However, in contrast to this, unliganded steroid hormone receptors are primarily localized in the cytoplasm where they are bound/chaperoned to heat-shock protein 90 (HSP90) (*86*, *87*). They translocate to the nucleus to perform their transcription regulatory function upon ligand binding (*86, 87*). As far as PPARα is concerned, it is generally agreed that it is predominantly localized in the nucleus (*88-92*). However, recent studies demonstrate some evidence for dynamic shuttling of PPARα between the cytosol and the nucleus (*89, 93-95*). Umemoto *et al.* further demonstrated that the nuclear transport of PPARα is accelerated by the

addition of ligands (*93*). These findings suggest that extracellular signals (ligands) could dissect the PPARα dynamics into discrete nuclear-cytoplasmic shuttling steps.

In addition to this, there is also controversy regarding the chain of events – particularly heterodimerization and DNA binding. Based on the definition of a "domain" and information from individual crystal structures of nuclear receptor LBD or DBD, it was thought that each functions independently (*55*). However, the intact structure of the PPAR-RXR heterodimer bound to a PPRE revealed three heterodimerization interfaces (*29*). Two of these were already known and included the LBD-LBD interface and the DNA dependent DBD-DBD interface. What was not known was this third interface (also DNA dependent) formed between the PPAR-LBD and the RXR-DBD (*29*). This interface suggests that PPAR ligands could influence DNA binding through the PPAR-LBD. This led to the idea that ligands could themselves target a specific subset of genes (*55*). In contrast, the fact that the PPAR-RXR complex had two DNA dependent interfaces, suggests that DNA motifs could allosterically regulate heterodimerization and receptor activation (*29*, *55*).

Although these finding do not give a clear picture on the chain of events, they do add to our understanding of the dynamic nature of nuclear receptor activation. The static model for transcription factor action assumes that upon activation the transcription factor is either: 1) bound (for a fairly long length of time), or 2) not bound to the DNA (*96-98*). However recent studies with chromatin immunoprecipitation and sequencing (ChIP-seq), fluorescence recovery after photobleaching (FRAP) and fluorescence correlation spectroscopy (FCS) have given light to the dynamic properties of nuclear receptors (*96*, *98*). These studies gave rise to a dynamic or "hit and run" model of transcription factor

action where there is a rapid cycling of DNA binding-unbinding with ligand-dependent cycle/binding time and receptor mobility (*96, 98*). For example, RXR agonist treatment largely affected the occupancy time of genomic regions to which RXR bound (*96-98*). It is anticipated that other nuclear receptors such as PPARα also follow a similar trend where they rapidly bind and unbind DNA in the absence of ligands. However, addition of ligands results in slowing down of such shuttling such that the residence time on the DNA is significantly increased.

To summarize, PPARα binds to a PPRE in its target genes as a permissive heterodimer with RXR (PPARα-RXR) (Fig. 4). Ligand binding and recruitment of cofactors (coactivators or corepressors) mediates the ability of PPARα to regulate transcription of its target genes. Like mentioned earlier, irrespective of high structural homology, identical PPRE sequences and shared cofactors, a number of factors determine isotype specificity among the PPARs. These include: amino acids lining the ligand binding pocket (*26*), the 5' flanking extension (to the DR1), spacing nucleotide (in PPRE) (*31, 42-44*), tissue restricted expression of each isoform (*7-10, 16*), availability of ligands, competition for mutual dimerization partners (such as RXR), availability and recruitment of cofactors (*8, 9, 81, 82*).

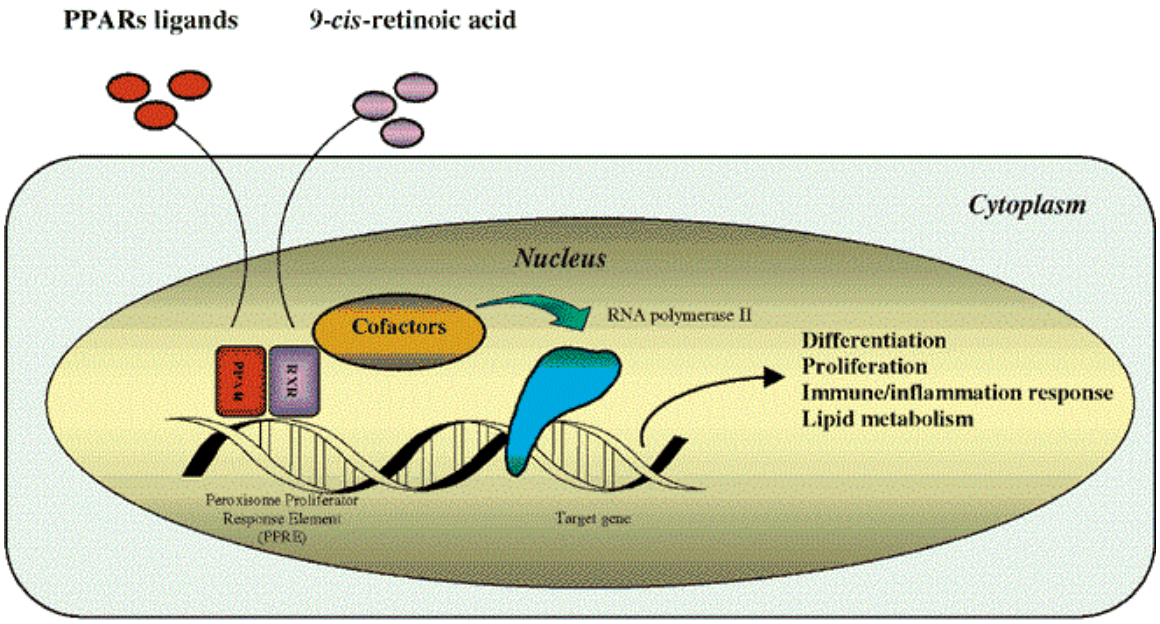


**Fig. 4.** PPAR mechanism of action. PPARs form heterodimers with retinoid X receptors (RXR) and bind to DNA sequences called peroxisome proliferator response element (PPRE) in the promoter region of target genes. Recruitment of cofactors (coactivators or corepressors) mediates the ability of PPAR's to stimulate or repress the transcription of target genes involved in difference cellular functions (modified from (*99*)).

**PPARα: Ligands, physiological role and knockout mice phenotype**

*Ligands:* Even before the discovery and cloning of the PPARα gene, a vast array of structurally diverse chemicals were known to lower serum lipids and cause massive peroxisomal proliferation in mice. These chemicals included fibric acid and its derivatives, nafenopin, methyl clofenapate, industrial phthalate-monoester plasticizers such as, di-(2-ethylhexyl)-phthalate (DEHP; used as a solvent/softner in manufacture of PVC plastics), certain herbicides, pesticides and industrial solvents (*7-13*). A mechanistic search on how these chemicals act lead to the discovery of a protein dimer which was aptly named peroxisome proliferator-binding protein (PPbP) (*14*). However, since the cloning of the receptor responsible for binding to peroxisome proliferators it was designated as Peroxisome Proliferator-Activated Receptor alpha (PPARα) (*15*). Today the ligands of PPARα have been classified into two main categories: endogenous ligands and exogenous (synthetic) ligands.

Synthetic ligands of PPARα include agonists such as clofibrate, fenofibrate (TriCor®), fenofibric acid (TriLipix®), gemfibrozil (Lopid®), ciprofibrate, Wy-14,643 and chemicals such as certain industrial plasticizers (DEHP, di-(2-ethylhexyl)-adipate (DEHA)), herbicides (phenoxyacetic acid) and pesticides (diclofop-methyl and pyrethrin family) (*7-13*). While, short-term administration of synthetic PPARα ligands in mice or rats leads to transactivation of genes involved in lipid catabolism, chronic administration leads to peroxisomal proliferation and hepatic carcinomas (*7-13*). The chronic effects of PPARα agonists are not seen in non-rodent species like guinea pig, dog, rhesus monkeys, nonhuman primates or humans (*100-104*) where they serve as potent hypolipidemic agents to lower plasma VLDL and triglyceride levels and increase high density

lipoprotein (HDL) levels. For this reason PPARα agonists have continued to be an attractive drug target for the pharmaceutical industry and are used in the treatment of dyslipidemia. In conjunction with statins, they are also prescribed in the treatment of hypercholesterolemia (high cholesterol) (*8-10, 105-107*). Other chemicals, particularly plasticizers (example DEHP - used in the manufacturing of plastics) and herbicides that activate PPARα are potential environmental toxins that contaminate ground water. While their acute impact in human health is unclear, they do raise long-term or lifetime health concerns.

A quest for natural endogenous ligands revealed that PPARα was not an orphan receptor. Pioneering studies using different reporter assays (GAL4, chloramphenicol acetyltransferase or CAT assay, luciferase), CARLA assays and competition assays (radioactive) demonstrated that a variety of fatty acids and their derivatives are able to interact with, and transactivate PPARα (*83, 84, 108-113*). These include fatty acid derivatives obtained via lipoxygenase (leukotriene $B_4$ or LTB4, hydroxyeicosatetraenoic acid or HETE) or cycloxygenase (prostaglandins) pathways (*111, 112*), branched chain fatty acids (phytanic acid) (*114*) and long chain dietary fatty acids (*115-117*). As such, fatty acids and their metabolites that interact with PPARα can be derived from the diet or obtained via *de novo* synthesis. Alternatively, it has been proposed that fatty acids and their derivatives are presented to PPARα in the nucleus by specific intracellular proteins such as fatty acid binding protein (FABP) or acyl-CoA binding protein (ACBP) (*118, 119*). This hypothesis is supported by data demonstrating interaction of FABP with fatty acids and their ability to translocate across to the nucleus to interact with PPARα (*88, 89, 95, 120*).

Evidence suggests that PPARα has evolved to primarily sense endogenous lipids and/or lipid metabolites as ligands and regulate the expression of target genes involved in their metabolism (*111, 114, 121*). The first set of evidence for this came from studies involved the use of fatty acyl CoA oxidase 1 (ACOX1) knockout mice (*121*). ACOX is the first and rate limiting enzyme involved in the fatty acid β-oxidation pathway and is regulated by PPARα. Disruption of ACOX1 caused accumulation of long chain fatty acyl-CoA and profound activation of PPARα (owing to accumulation of PPARα ligands) (*121*). Another study that highlighted the role of PPARα as a lipid sensor was done utilizing PPARα knockout mice (PPARα-/-). LBT4 is an inflammatory eicosanoid derived from arachidonic acid that activates PPARα and induces genes that would neutralize or degrade LBT4 itself (*111*). Exposure of PPARα-/- mice to LBT4 (or its precursors) leads to a prolonged inflammatory response (compared to wild-type mice) because genes involved in neutralizing the inflammatory response are not induced (*111*).

Today it is established that PPARα plays a crucial role not only in the transport and β-oxidation (break-down) of fatty acids but also in the inhibition of *de novo* fatty acid synthesis (*8-10*). Since altered levels of fatty acids are associated with the development of diabetes, obesity, hypertension, cardiovascular diseases and atherosclerosis, mis-regulation of PPARα activity and/or metabolic pathways may contribute to the pathology of these disease states. Alternately PPARα activation by pharmacological or dietary intervention may help combat obesity and its co-morbities.

*Physiological role of PPARα in lipid metabolism:* Lipid metabolism orchestrated in the liver primarily involves fatty acid oxidation and lipogenesis. Fatty acid oxidation primarily occurs in three main subcellular organelles: mitochondria, peroxisomes (β-

oxidation) and microsomes (ω-oxidation). Some of the key enzymes involved in these processes possess PPRE motifs in their promoters and are under direct control of PPARα. These include 1) proteins involved in the transport of fatty acids into the cell such as fatty acid transport protein (FATP), fatty acid translocase (FAT/CD36) (*122, 123*), fatty acid binding protein (FABP) (*124*) and carnitine palmitoyl transferase I (CPT I) (*125*) (Fig. 5), 2) the enzyme that esterifies free fatty acids into fatty acyl coenzyme A – acyl CoA synthase (*126*), 3) enzymes involved in the process of peroxisomal, mitochondrial and microsomal fatty acid oxidation such as ACOX (*17, 40, 127*), medium chain acyl CoA dehydrogenase (MCAD) (*128*) and cytochrome P450 (*129, 130*) amongst others (Fig. 5) (*25*).

As far as lipogenesis is concerned, PPARα downregulates enzymes involved in *de novo* lipid synthesis such as acetyl CoA carboxylase (ACC) and fatty acid synthase (FAS) (Fig. 5) (*25*). While this effect appears paradoxical to its well established function in fat catabolism, it is believed to be an indirect effect brought about by regulation of other transcription factors such as sterol regulatory element-binding protein (SREBP-1c) and liver X receptor α (LXRα) (*8, 9, 131, 132*). SREBP-1c is a transcription factor that plays crucial role in the regulation of lipogenic genes such as FAS and stearoyl CoA desaturase (*133*). In humans, its role in lipogenesis is under direct regulation of PPARα and LXRα - brought via two LXR response elements (LXRE) and one PPRE in the SREBP-1c gene (*132*). Interestingly, LXRα is an 'oxysterol sensor,' whose role in cholesterol homeostasis and lipogenesis (via SREBP-1c) is under direct regulation of PPARα via an active PPRE found in its regulatory region (*134*). Thus PPARα regulates lipogenesis in a dual manner – directly via SREBP-1c and indirectly via LXRα.

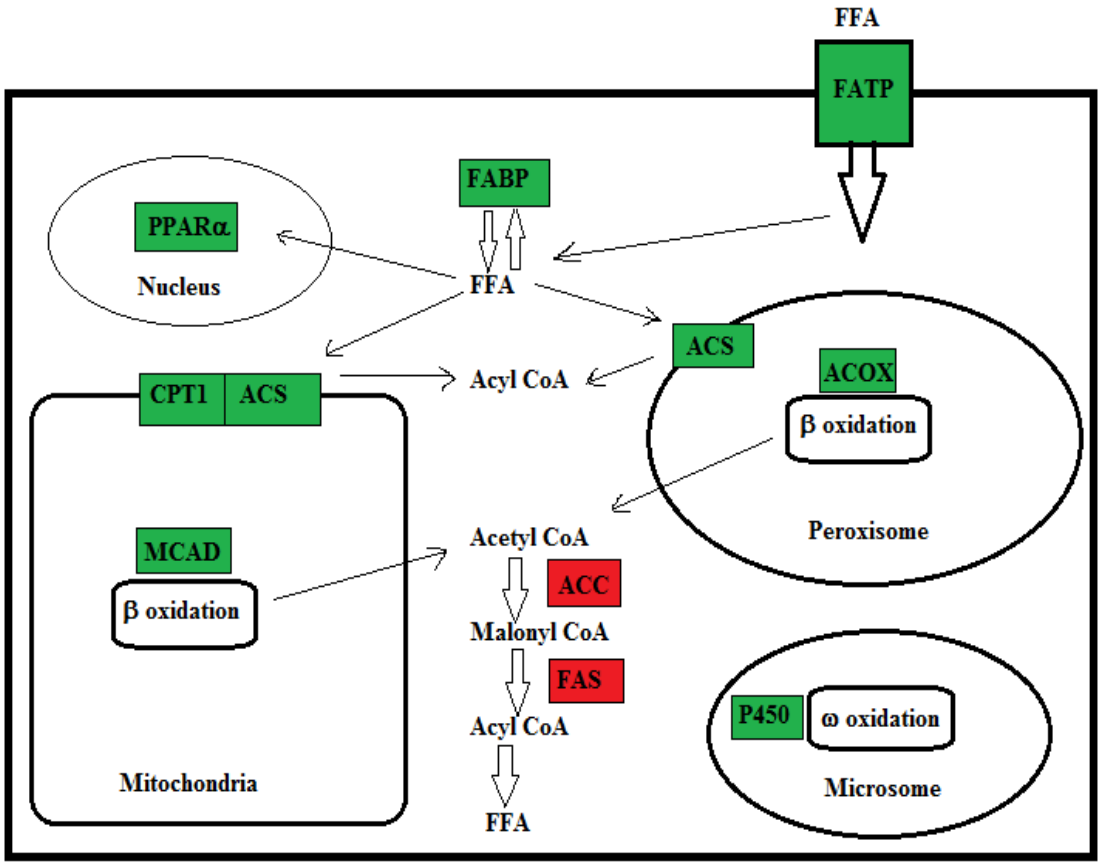


**Fig. 5.** Example of some genes regulated by PPARα and their role in lipid metabolism. Upregulated genes are shown in green and include FATP – fatty acid transport protein, FABP – fatty acid binding protein, MCAD – medium chain acyl CoA dehydrogenase, P450 – cytochrome P450 fatty acid ω-hydroxylase, ACOX – acyl CoA oxidase, CPTI – carnitine palmitoyl transferase I and ACC – acetyl CoA carboxylase. Downregulated genes are shown in red and include FAS – fatty acid synthase and ACS – acyl CoA synthetase. FFA – free fatty acids.

*Physiological role of PPARα in lipoprotein metabolism:* Owing to enhanced β-oxidation caused by PPARα agonists, triglyceride-rich lipoprotein particles are subjected to catabolism - resulting in decreased secretion of very low density lipoproteins (VLDL) by the liver (*8*). PPARα agonists also induce lipoprotein lipase (LPL) activity resulting in increased triglyceride hydrolysis. This effect is brought about in a dual manner: 1) they induce the LPL promoter (containing a PPRE) (*135*) and 2) they reduce the activity/levels of apolipoprotein (Apo) C-III (ApoC-III) which is an inhibitor of LPL (*136, 137*). The expression of human ApoA-I and ApoA-II is also under direct control of PPARα and such regulation is not seen in rodents (*138, 139*). ApoA-I and ApoA-II are major component of HDL that help clear cholesterol (*138, 139*). Therefore in humans, PPARα agonists increase the formation and secretion of HDL, and aid in transport (reverse cholesterol transport) and excretion of cholesterol (anti-atherosclerotic) (*8, 138, 139*). In addition to these effects, PPARα agonists also bring about cholesterol homeostasis indirectly through LXRα-mediated regulation/induction of ATP-cassette transporter A1 (ABCA1) and cholesterol 7α-hydroxylase (CYP7A) – resulting in an efflux and excretion of cholesterol into bile (*140, 141*).

*Physiological role of PPARα in inflammation:* PPARα brings about anti-inflammatory actions by two means. First, PPARα directly binds inflammatory fatty acid derivatives like LBT4 and promotes their breakdown/metabolism by inducing genes involved in such pathways (*111*). Second, PPARα agonists decrease/inhibit inflammatory cytokines (IL-1, IL-6), tumor necrosis factor α (TNFα), inducible nitric acid synthase (iNOS) and cyclooxygenase-2 (COX-2) indirectly via negative crosstalk with the nuclear factor-kappa beta (NfκB) (*142, 143*). In chronic hyperlipidemia and/or early atherosclerosis

macrophages engulf oxidized LDL (generated via free oxygen radicals), giving rise to macrophage foam cells. When these foam cells accumulate at particular foci within the intima of a blood vessel, it begins the formation of a necrotic, inflammatory atherosclerotic lesion (*144*). Owing to the beneficial role played by PPARα in reducing inflammation (preventing formation of oxidized LDL) and promoting reverse cholesterol transport (described above), PPARα agonists prevent the formation of macrophage foam cells and also have anti atherosclerotic effects (*8, 138-141*).

*PPARα knockout mice model:* Gonzalez et al. generated the first PPARα knockout mouse by targeted disruption of the PPARα ligand binding domain coding region (*145*). These mice are viable, fertile and display no detectable gross phenotype. However, under condition of fasting these mice exhibit severe hypoglycemia and hypothermia (*145*). While such fasting would normally result in PPARα activation and induction of fatty acid oxidation, in PPARα knockout mice, fatty acid oxidation is largely impaired, resulting in enhanced accumulation of fat droplets in the liver (*145*). The role of PPARα in lipid homeostatis is further highlighted by the fact that PPARα knockout mice exhibit reduced capacity to metabolize long chain fatty acids and develop dyslipidemia and steatosis (*146-148*). These findings therefore augment the role of PPARα as a lipid sensor in the regulation of lipid metabolism.

Although PPARα knockout mice display normal basal levels of peroxisomal β-oxidation enzymes in the liver, administration of synthetic PPARα agonists fails to induce PPARα responsive genes such as ACOX (*145*). In contrast to the normal basal levels of peroxisomal β-oxidation enzymes in the liver, PPARα knockout mice display lower levels of mitochondrial fatty acid oxidation enzymes (*146*). PPARα knockout mice

also do not display the 'classical' peroxisome proliferator response and fail to develop hepatic cancers when chronically treated with PPARα agonists such as clofibrate or WY14,643 (*145*). Further, transgenic PPARα knockout mice that express human PPARα in the liver also do not exhibit any liver tumors when chronically exposed to PPARα agonists such as WY14,643 (*149, 150*) - suggesting that there exist some species variation in the structure/function of PPARα. All these findings with PPARα knockout mice have during the past 18 years have further highlighted the role of PPARα in energy homeostasis and inflammation.

**Development of hypothesis**

Although a plethora of exogenous ligands have been shown to activate PPARα, the identity of high-affinity endogenous ligands has been more elusive. In the last two decades, an overwhelming amount of data indicate that PPARα is not an orphan receptor, and that fatty acids and its derivatives are able to regulate PPARα transcriptional activity. The first endogenous ligands (fatty acids) able to activate PPARα were identified in transactivation assays that used the glucocorticoid response element or estrogen response element containing reporters and chimeric receptor constructs of glucocorticoid receptor DBD and PPARα-LBD or estrogen receptor DBD and PPARα-LBD (*109, 110*). However, since such transactivation could result from multiple indirect pathways, the direct interaction of fatty acids with PPARα had to be tested.

Owing to its important role in regulating metabolism and energy homeostasis, a number of assays have been developed to study the interaction of fatty acids and their derivatives with recombinant forms of mouse and xenopous PPARα. These include: 1)

Radioligand binding assays – these are competition assays based on displacement of bound radioligand by the ligand of interest (*108, 111*), 2) Scintillation proximity assays – uses scintillation to measure the binding of a receptor-bound radioligand to another molecule localized to a microsphere (*151*), 3) Limited proteolysis assays – based on the protease sensitivity of the receptor in presence and absence of ligand (*53*), 4) Ligand induced complex (LIC) assays – based on the ligand dependent binding of PPAR-RXR heterodimer to a PPRE (*113*), and 5) Co-activator recruitment assays – based on the ligand dependent recruitment of co-activators (*83*). A combination of all of these studies have indicated that fatty acids and their metabolites (fatty acyl-coenzyme A) interact with this class of nuclear receptors (*83, 84, 108-113*). These studies utilized the recombinant LBD of mouse, rat, or xenopous PPARα protein and reported binding affinities ($K_d$) in the micromolar ranges (*83, 84, 108-113*). Although these studies provide a wealth of information, particularly on the possible endogenous ligands for PPARα, they have certain limitations. These include limitations in the techniques used, the use of truncated and tagged form of PPARα-LBD and the lack of consideration of the possible species differences in the activity and function of the PPARα protein.

In order to be classified as a ligand for a nuclear receptor, mere *in vitro* physical interaction is not sufficient. The ligand must also be present within the cell/nucleus in sufficient amounts (*46, 118*). The nuclear concentration of fatty acids and their metabolites have been determined to be in the nanomolar ranges (*88, 95, 117, 118, 120, 152*) – making these micromolar binding affinities (for FA and FA-CoA) physiologically irrelevant. Many of the assays described above involve the physical separation of bound vs. unbound fraction which often disturbs the equilibrium. Therefore dissociation

constants ($K_d$) derived by such means often underestimate the binding affinity (*115, 117, 118*). The binding affinities reported for FA and their derivatives from these studies are in the micromolar ranges (*88, 95, 117, 118, 120, 152*) and it is doubtful that local FA concentrations will ever reach such high levels *in vivo* (*118*). Thus the significance of such findings are not clear.

Pioneering studies by Ellinghaus *et al.*, Lin *et al.* and Hostetler *et al.* using fluorescence based binding assays circumvented this problem and reported binding affinities for FA and their derivatives in the physiological ranges (*114, 115, 117*). However, these studies were again carried out with truncated forms of the mouse protein which may give rise to anomalous results that may not be representative of the human PPARα (*153, 154*). While such studies with truncated/tagged forms of mouse or xenopous PPARα have led to accumulation of valuable information particularly on ligand discovery, they also did not account for the A/B domain effects or the likelihood of interdomain communication.

Classically it was believed that nuclear receptor domains are like individual beads on a string, such that each domain could function independently. However, an increasing number of solution based biophysical studies, some of which are listed below, have suggested that nuclear receptor domains are integrated together such that information or changes in one part of a domain are transmitted to another (*55*). For example, 1) Deletion or mutation in the N-terminal A/B domain of PPARs affects DNA binding (*31*), ligand binding (*34*) and ligand-mediated transcriptional activation, depending on the target gene (*30, 31*) and 2) The DBD of nuclear receptors such as androgen receptor, glucocorticoid receptor and PPARs has been demonstrated to communicate with their respective LBD

such that the DBD impacts the receptor structure and activity at the LBD (*155-157*). These findings emphasize the need to carry out binding studies using putative endogenous ligands for PPARα and full-length forms of the protein.

While FA and FA-CoA have been demonstrated to serve as ligands for mouse, rat and xenopous forms of PPARα (*16, 108, 110, 113, 115-117*) no such studies have been conducted using the full-length human PPARα (hPPARα). This is an important gap in research that needs to be addressed, because, based on the type of assays used, these same studies also demonstrate species differences for ligand specificity and affinity (*16, 84, 108, 110, 113, 115-117*). For example the xenopus PPARα seems to have a weaker affinity for fatty acids than hPPARα (*84, 108*), but higher affinity than rat PPARα (*83, 110*). Similar differences in the binding and activation of PPARα has also been seen in response to synthetic agonists (*158-160*). While a strong divergence in the pattern of PPARα regulated genes has been seen in humans vs. rodents, differences in the extent of transcriptional activation of human and mouse PPARα proteins have also been observed in response to certain hypolipidemic agents and pthalate monoesters (*161-163*). Since a single amino acid change in the mouse PPARα-LBD (E282) resulted in altered activity of the protein (*164*) and alteration of a single amino acid in human PPARα (V444M) produced PPARδ ligand binding characteristics (*52*), it is possible that amino acid differences affect ligand binding.

Considering the crucial role of PPARα in lipid homeostasis, it is essential to elucidate its endogenous ligands of full length forms of the protein using an assay whose functional read-out is not just physiologically relevant, but also sensitive enough to determine species differences in such binding between the human and mouse forms of the

protein. *Therefore, we hypothesize that long chain fatty acids (LCFA) and/or their thioesters (LCFA-CoA) constitute high affinity endogenous ligands for full-length hPPARα and there exist significant differences in such affinity between hPPARα and mPPARα.* Studies that would ascertain the identity of true endogenous ligands of human PPARα would aid in a deeper understanding of energy metabolism and possible therapeutic dietary interventions.

The goals of this dissertation are 1) to investigate whether LCFA and LCFA-CoA constitute high-affinity endogenous ligands for full-length hPPARα. These data will be important to understand the molecular role of dietary nutrients in hPPARα mediated regulation of energy homeostasis. 2) To determine if there exist differences in affinity for ligands between hPPARα and mPPARα and further explore the possible mechanisms for such differences. This is important because the rodent model has been used as a classical model to study PPARα. Such differences in ligand binding specificity and affinity between mouse and human PPARα will call for careful interpretation of data using mouse as a model for studying this protein. Further, knowledge about the mechanisms of species differences may help develop better drugs and dietary regimens with greater specificity for human versus rodent PPARα for combating obesity and its related disorders.

# CHAPTER I

# DIVERGENCE BETWEEN HUMAN AND MURINE PEROXISOME PROLIFERATOR-ACTIVATED RECEPTOR ALPHA LIGAND SPECIFICITIES

## 1. Abstract

Peroxisome proliferator-activated receptor alpha (PPARα) belongs to the family of ligand-dependent nuclear transcription factors which regulate energy metabolism. Although there exists remarkable overlap in the activities of PPARα across species, studies utilizing exogenous PPARα ligands suggest species differences in binding, activation, and physiological effects. While unsaturated long-chain fatty acids (LCFA) and their thioesters (long-chain fatty acyl-CoA; LCFA-CoA) function as ligands for recombinant mouse PPARα (mPPARα), no such studies have been conducted with full-length human PPARα (hPPARα). The objective of the current study was to determine whether LCFA and LCFA-CoA constitute high-affinity endogenous ligands for hPPARα or whether there exist species differences for ligand specificity and affinity. Both hPPARα and mPPARα bound with high affinity to LCFA-CoA; however, differences were noted in LCFA affinities. A fluorescent LCFA analogue was bound strongly only by mPPARα and naturally-occurring saturated LCFA were bound stronger by hPPARα than mPPARα. Similarly, unsaturated LCFA induced transactivation of both hPPARα and mPPARα, while saturated LCFA induced transactivation only in hPPARα expressing cells. These data identified LCFA and LCFA-CoA as endogenous ligands of hPPARα, demonstrated species differences in binding specificity and activity, and may help delineate the role of PPARα as a nutrient sensor in metabolic regulation (*165*).

## 2. Introduction

Whole body energy homeostasis is regulated in part by nutrient-sensing members of the nuclear hormone receptor superfamily of ligand-dependent transcription factors, such as the peroxisome proliferator-activated receptor alpha (PPARα). Like other nuclear hormone receptors, the PPARα protein is comprised of several distinct domains, including a highly conserved DNA binding domain (DBD) and a less conserved C-terminal ligand binding domain (LBD). In highly metabolic tissues such as liver and heart, PPARα heterodimerizes with the retinoid X receptor alpha (RXRα, and this heterodimer potently activates genes involved in fatty acid oxidation (*39, 110, 166*). At a cellular level PPARα regulates fatty acid metabolism, glucose metabolism, inflammation, differentiation, and proliferation (*167-169*).

Although a multitude of exogenous ligands have been shown to activate both human and mouse PPARα (*17, 39, 162, 170*), the identity of high-affinity endogenous ligands has been more elusive. Studies utilizing recombinant PPARα proteins have largely focused on the ligand binding domain of mouse PPARα (mPPARα). These studies suggest that long-chain fatty acids (LCFA) and their activated metabolites (long-chain acyl-CoAs, LCFA-CoA) may function as endogenous PPARα ligands (*114-117*). Such ligand binding has been shown to induce PPARα conformational changes and increase transactivation, consistent with expectations for an endogenous ligand of a nuclear receptor.

While LCFA and LCFA-CoA have been studied as putative ligands for mouse PPARα (mPPARα), no such studies have been conducted with the full-length mPPARα or human PPARα (hPPARα). Although there exists remarkable overlap in the activities

of PPARα across species, human and mouse PPARα proteins promote transcription to a different extent in response to certain hypolipidemic agents and pthalate monoesters (*161-163*), suggesting species difference may exist. Administration of PPARα agonists (e.g. Wy-14,643) to rodents results in peroxisome proliferation and hepatic cancer – effects not observed in humans (*102*). Even though human and mouse PPARα proteins share 91% identity (*18*), the observed physiological responses to exogenous activators suggest that minor sequence differences may be important to PPARα function.

The objective of the current study was to elucidate whether LCFA and/or LCFA-CoA constitute high-affinity endogenous ligands for full-length hPPARα and to determine if species differences affect ligand specificity. Since elevated LCFA are associated with metabolic, endocrine, and cardiovascular complications, these data are important for understanding the molecular role of dietary nutrients in PPARα mediated energy homeostasis. As putative ligands of PPARα, LCFA and/or LCFA-CoA may control their own metabolism by binding PPARα and inducing PPARα regulated genes important for fatty acid uptake, transport, and oxidation. Thus, dysregulated LCFA could alter the transcriptional activity of PPARα leading to hyper- or hypo- activation of these genes and further contributing to the metabolic imbalance.

## 3. Materials and Methods

*Chemicals:* Fluorescent fatty acid (BODIPY-C12, BODIPY-C16, NBD stearate) were purchased from Molecular Probes, Inc. (Eugene, OR). Eicosapentaenoyl-CoA, docosapentaenoyl-CoA, docosahexaenoyl-CoA, BODIPY C12-CoA BODIPY C16-CoA were synthesized by Ms. Alagammai Kaliappan (Hostetler lab) and purified by HPLC as previously described (*117*, *171*), and found to be >99% unhydrolyzed. All other fatty acid ligands and clofibrate were from Sigma-Aldrich (St. Louis, MO). Rosiglitazone (LKT labs) was a kind gift from Dr Khalid Elased and bovine serum albumin (lipid-free) was obtained from Gemini Bioproducts (Sacramento, CA).

*Purification of Recombinant PPARα protein:* Full-length hPPARα (amino acids 1-468) and full-length mPPARα (amino acids 1-468) were used for all experiments presented herein. Bacterial expression plasmids for full-length hPPARα (6xhis-GST-hPPARα) and full-length mPPARα (6xhis-GST-mPPARα) were produced by Dr. S. Dean Rider, Jr. (Wright State University). Protein expression, purification, and optimization of hPPARα protein was conducted by Ms. Madhumitha Balanarasimha (*172*). Mouse PPARα was purified using the protocol designed by Ms. Balanarasimha (*172*). Briefly, 6xhis-GST-PPARα fusions were expressed in Rosetta™2 cells (Novagen, Gibbstown, NJ) and purified by GST affinity chromatography. Eluted proteins were concentrated, dialyzed, and tested for purity by SDS-PAGE with Coomassie blue staining and immunoblotting as previously described (*116*, *117*). Protein concentrations were estimated by Bradford Assay (Bio-Rad Laboratories, Hercules, CA) and by absorbance spectroscopy using the molar extinction coefficient for the protein.

*Direct Fluorescent Ligand Binding Assays:* Fluorescent ligand (BODIPY C16 or BODIPY C16-CoA) binding measurements were performed as described earlier (*117, 173*). Briefly, 0.1 µM hPPARα or mPPARα was titrated with increasing concentrations of fluorescent ligand. This concentration of PPARα protein was chosen, because it gave the maximal signal to noise ratio, while allowing saturable binding of most of the examined ligands to be reached at concentrations below their critical micellular concentrations. The CMC for fatty acids and fatty acyl-CoA tested herein ranges from 1-200 µM (*174*). It decreases with chain length and is highly dependent on temperature, pressure and presence of electrolytes (*175, 176*).

Fluorescence emission spectra (excitation, 465 nm; emission, 490-550 nm) were obtained at 24°C with a PC1 photon counting spectrofluorometer (ISS Inc., Champaign, IL) and corrected for background (protein only and fluorescent ligand only). The dissociation constant ($K_d$) was calculated from a single site saturation plot of fluorescence intensity ($F_i$) versus concentration ($C$) according to equation 1 as previously described (*117, 177, 178*).

$$y = \frac{B_{\max} \times x}{K_d + x} \qquad \text{(Eq. 1)}$$

where $B_{\max}$ represents the maximal fluorescence ($F_{max}$) and $y$ is the fluorescence intensity at a given concentration of ligand, $x$. The saturation curves were also fitted to a Hill plot according to equation 2 as described previously (*116, 117*) to determine the number of binding sites ($n$) (*117*).

$$y = \frac{ax^b}{c^b + x^b} \qquad \text{(Eq. 2)}$$

where, *a* is the maximal fluorescence ($F_{max}$), *b* is the number of binding sites (*n*), and *c* is the $K_d$. A double reciprocal plot of $1/(1-F_i/F_{max})$ and $C/(F_i/F_{max})$ was also used to confirm the dissociation constant ($K_d$) equal to the number of binding sites (*n*). The slope of the line resulting from such a plot was equal to $1/K_d$ and the number of linear lines is equal to the number of binding sites (n) (*116*, *117*).

*Displacement of Bound Fluorescent BODIPY C16-CoA by Non-fluorescent Ligands:* Based on the binding affinities obtained with the direct fluorescent ligand binding assays for BODIPY C16-CoA, 0.1 μM PPARα was mixed with BODIPY C16-CoA at the concentration where maximal fluorescence intensity first occurred (75nM for hPPARα and 130nM for mPPARα). The maximal fluorescence intensity was measured, and the effect of increasing concentrations of naturally-occurring ligands was measured as a decrease in fluorescence (*115-117*, *173*). Emission spectra were obtained and corrected for background as described above for BODIPY. The inhibition constant ($K_i$) value for each ligand was estimated according to equation 3 (*115-117*, *173*).

$$\frac{EC_{50ligand}}{[BODIPY\ C16-CoA]_{total}} = \frac{K_{i,ligand}}{K_{d,BODIPY\ C16-CoA}} \qquad \text{(Eq. 3)}$$

where, $EC_{50ligand}$ represents the concentration of naturally-occurring ligands required for displacing half of the fluorescent BODIPY-C16-CoA from the protein, $K_{i,ligand}$ is the efficiency of the ligand to displace BODIPY C16-CoA, and $K_{d,BODIPY\ C16\text{-}CoA}$ is the binding affinity of BODIPY C16-CoA obtained as described above.

*Quenching of PPARα Aromatic Amino Acid Residues by Non-fluorescent Ligands:* The direct binding of hPPARα or mPPARα to non-fluorescent ligands was

determined by quenching of intrinsic PPARα aromatic amino acid fluorescence as described (*116, 117*). Briefly, hPPARα or mPPARα (0.1 μM) was titrated with increasing concentrations of ligand. Emission spectra from 300-400 nm were obtained at 24°C upon excitation at 280 nm with a PC1 photon counting spectrofluorometer (ISS Inc., Champaign, IL). Data were corrected for background and inner filter effects, and a single site saturation plot of the change in fluorescence intensity ($F_o$-$F_i$) versus concentration ($C$) was used to determine the inhibition constant ($K_d$) as per equation 1 (*117*). In this case, $B_{max}$ represents the maximal change in fluorescence ($F_o$-$F_{min}$) and $y$ is the change in fluorescence intensity ($F_o$-$F$) at a given concentration of ligand, $x$ (*116, 117*). The number of binding sites (n) was determined using a hill plot generated as per equation 2 where, $a$ is the maximal change in fluorescence ($F_{max}$), $b$ is the number of binding sites ($n$), and $c$ is the $K_d$ (*116, 117, 173*). A double reciprocal plot of $1/(1-F_i/F_{max})$ and $C/(F_i/F_{max})$ was further used to confirm the number of binding sites ($n$) as described above. However, in this case $F_i$ represents the change in fluorescence ($F_o$-$F$) and $F_{max}$ represents the maximal change in fluorescence.

*Secondary Structure Determination Effect of ligand binding on PPARα Circular Dichroism*: Circular dichroic spectra of hPPARα or mPPARα (0.6 μM in 600 μM HEPES pH 8.0, 24 μM dithiothreitol, 6 μM EDTA, 6 mM KCl and 0.6 % glycerol) were taken in the presence and absence of LCFA and LCFA-CoA (0.6 μM) with a J-815 spectropolarimeter (Jasco Inc., Easton, MD) as previously described (*116, 117*). Spectra was recorded from 260 to 187 nm with a bandwidth of 2.0 nm, sensitivity of 10 millidegrees, scan rate of 50 nm/min and a time constant of 1 s. Ten scans were averaged for percent compositions of α-helices, β-strands, turns and unordered

structures with the CONTIN/LL program of the software package CDpro (*116, 117, 179*).

*Mammalian Expression Plasmids:* Mammalian expression plasmids pSG5-hPPARα, pSG5-mPPARα, pSG5-hRXRα, and pSG5-mRXRα were produced by Dr. S. Dean Rider, Jr. (Wright State University). The reporter construct, PPRE×3 TK LUC was a kind gift of Dr. Bruce Spiegelman (Addgene plasmid # 1015) and contained three copies of the acyl-CoA oxidase (ACOX) peroxisome proliferator response element (PPRE) (*180*).

*Cell culture and Transactivation assays:* COS-7 cells (ATCC, Manassas, VA) were grown in DMEM supplemented with 10 % fetal bovine serum (Invitrogen, Grand Island, NY) at 37°C with 5% $CO_2$ in a humidified chamber. Cells were seeded onto 24-well culture plates and transfected with Lipofectamine™ 2000 (Invitrogen, Grand Island, NY) and 0.4 µg of each full-length mammalian expression vector (pSG5-hPPARα, pSG5-hRXRα, pSG5-mPPARα, pSG5-mRXRα) or empty plasmid (pSG5), 0.4 µg of the PPRE×3 TK LUC reporter construct, and 0.04 µg of the internal transfection control plasmid pRL-CMV (Promega Corp., Dinosaur, WI) as previously described (*117, 173*). Following transfection incubation, medium was replaced with serum-free medium for 2 h, ligands (1µM) were added, and the cells were grown for an additional 20 h. Fatty acids were added as a complex with bovine serum albumin (BSA) as described (*181*). Firefly luciferase activity, normalized to Renilla luciferase (for transfection efficiency), was determined with the dual luciferase reporter assays system (Promega, Madison, WI) and measured with a SAFIRE$^2$ microtiter plate reader (Tecan Systems, Inc. San Jose, CA). Clofibrate treated samples overexpressing both

PPARα and RXRα were arbitrarily set to 1.

*Statistical Analysis:* Data were analyzed by SigmaPlot™ (Systat Software, San Jose, CA) and a one-way ANOVA was used to evaluate overall significance. A Fisher Least Significant difference (LSD) post-hoc test was used to identify individual group differences. The results are presented as mean ± SEM. The confidence limit of $p < 0.05$ was considered statistically significant.

## 4. Results

*Full-length hPPARα and mPPARα protein purification:* Based on recent demonstrations that truncation of a nuclear transcription factor can significantly affect ligand binding affinity, specificity, and consequently receptor activity (*153, 154*), full-length hPPARα and mPPARα were used for all experiments. SDS-PAGE and Coomassie blue staining indicated predominant bands of 52 kDa corresponding to the expected size of full-length hPPARα and mPPARα, for which densitometry indicated greater than 85% purity (Fig. 6A). Western blotting confirmed that the predominant protein bands were PPARα (Fig. 6B).

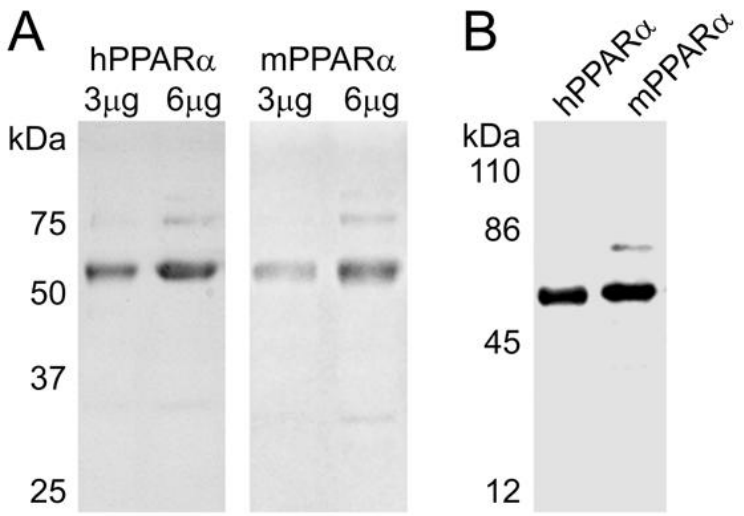


**Fig. 6.** (A) SDS-PAGE and Coomassie blue staining of 3 μg and 6 μg purified recombinant hPPARα (left) and mPPARα (right) showing relative purity of the protein. The prominent band at 52 kDa is full-length, untagged recombinant PPARα. (B) Western blot of 1 μg purified recombinant hPPARα (left) and mPPARα (right) confirming the 52 kDa band is untagged, full-length PPARα.

*Binding of fluorescent fatty acid and fatty acyl-CoA to PPARα:* The sensitivity of the BODIPY fluorophore to environmental hydrophobicity is useful for determining if binding represents a direct molecular interaction within the hydrophobic ligand binding pocket of PPARα. In aqueous buffer without protein, BODIPY fluorescence was low for each of the examined fluorophores. Titration of hPPARα with BODIPY C16-CoA resulted in increased fluorescence with an emission maximum near 515 nm (Fig. 7A). This increased fluorescence was saturable near 100 nM (Fig. 7B, circles), indicating high affinity binding ($K_d$ = 25 ± 4 nM). These data transformed into a linear double reciprocal plot (Fig. 7B, inset), consistent with a single binding site ($R^2$ > 0.95). In contrast, a smaller, non-saturable increase in fluorescence was seen upon titration of hPPARα with BODIPY C16 fatty acid (Fig. 7C), indicating only weak or non-specific binding. Binding of hPPARα to BODIPY C12 fatty acid (Fig. 7D, triangles), BODIPY C12-CoA (Fig. 7D, filled circles) or NBD stearate (Fig. 7E) resulted in non-saturable changes in fluorescence ($K_d$ > 450 nM).

Titration of mPPARα with BODIPY C16-CoA resulted in a similar increase in BODIPY C16-CoA fluorescence (Fig. 8A) as noted for hPPARα, with the exception that slightly higher BODIPY C16-CoA concentrations were required to reach saturation (Fig. 8B). This resulted in a lower binding affinity ($K_d$ = 65 ± 9 nM), but was still consistent with a single binding site (Fig. 8B, and inset). While hPPARα binding to BODIPY C16 fatty acid was non-saturable, mPPARα binding to BODIPY C16 fatty acid resulted in strong fluorescence changes with saturation near 50 nM (Fig. 8C), suggesting high affinity binding ($K_d$ = 19 ± 4 nM). Although these data were consistent with previous data suggesting that a truncated mPPARα protein can bind to both

BODIPY C16 fatty acid derivative and BODIPY C16-CoA with high affinity (*173*), these data also suggested that species differences exist in ligand binding specificity.

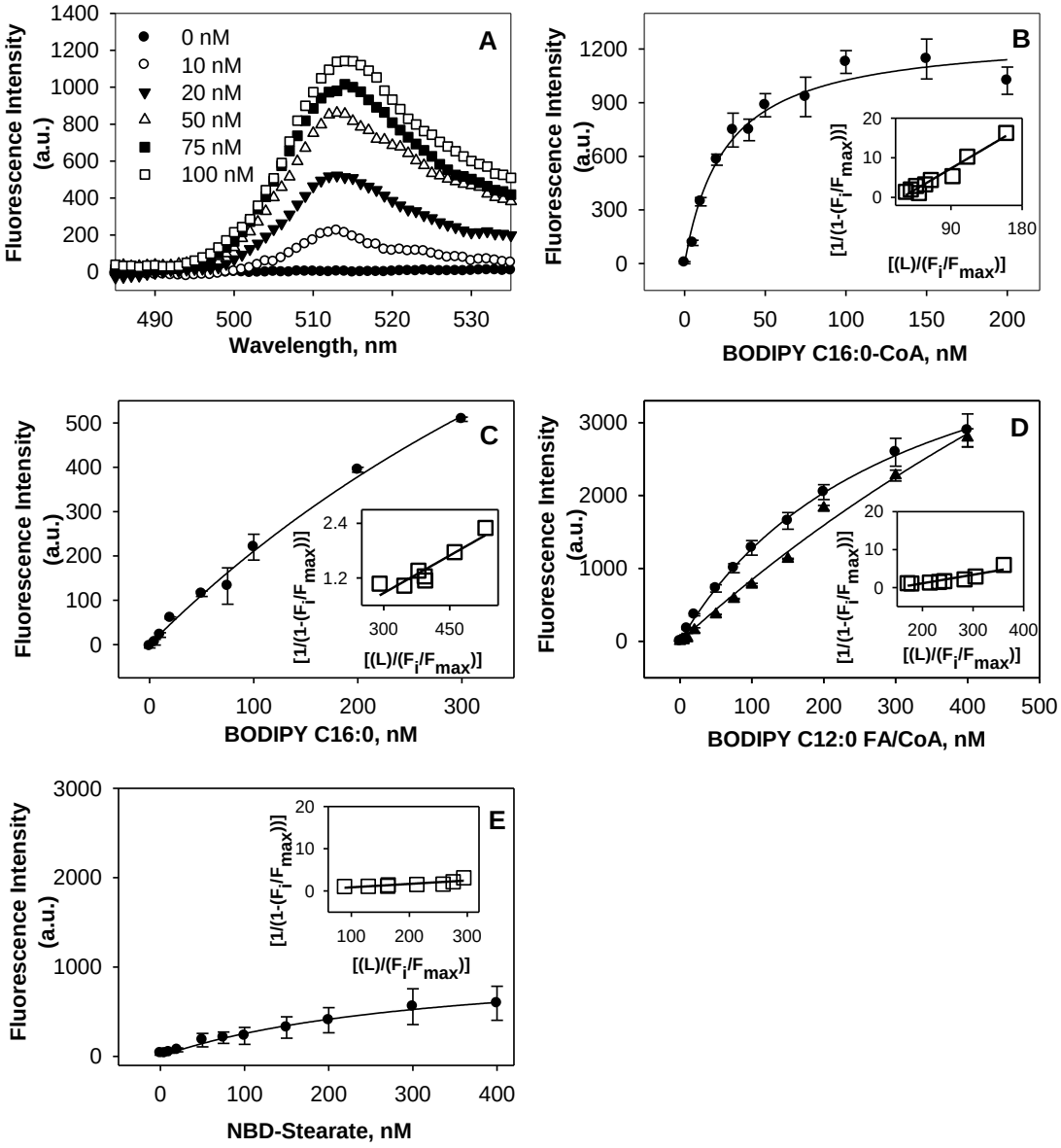
A
0 nM
10 nM
20 nM
50 nM
75 nM
100 nM
Fluorescence Intensity (a.u.)
Wavelength, nm
B
BODIPY C16:0-CoA, nM
C
BODIPY C16:0, nM
D
BODIPY C12:0 FA/CoA, nM
E
NBD-Stearate, nM
[1/(1-(F_i/F_max))]
[(L)/(F_i/F_max)]

**Fig. 7.** (A) Corrected fluorescence emission spectra of 0.1 μM hPPARα titrated with 0 (filled circles), 10 (open circles), 20 (filled triangles), 50 (open triangles), 75 (filled squares) and 100 nM (open squares) of BODIPY C16-CoA upon excitation at 465 nm, demonstrating increased fluorescence intensity upon binding to hPPARα. Plot of hPPARα maximal fluorescence emission as a function of BODIPY C16:0-CoA (B) and BODIPY C16:0 FA (C). Plot of the maximal hPPARα fluorescence emission as a function of BODIPY C12:0 FA (D, triangles), BODIPY C12:0-CoA (D, filled circles) and NBD stearate (E, filled circles) concentration. Insets reperesent linear plots of the binding curves for BODIPY C16-CoA (B), BODIPY C16 FA (C) BODIPY C12-CoA (D) and NBD stearate (E). All values represent the mean ± S.E., $n \geq 3$.

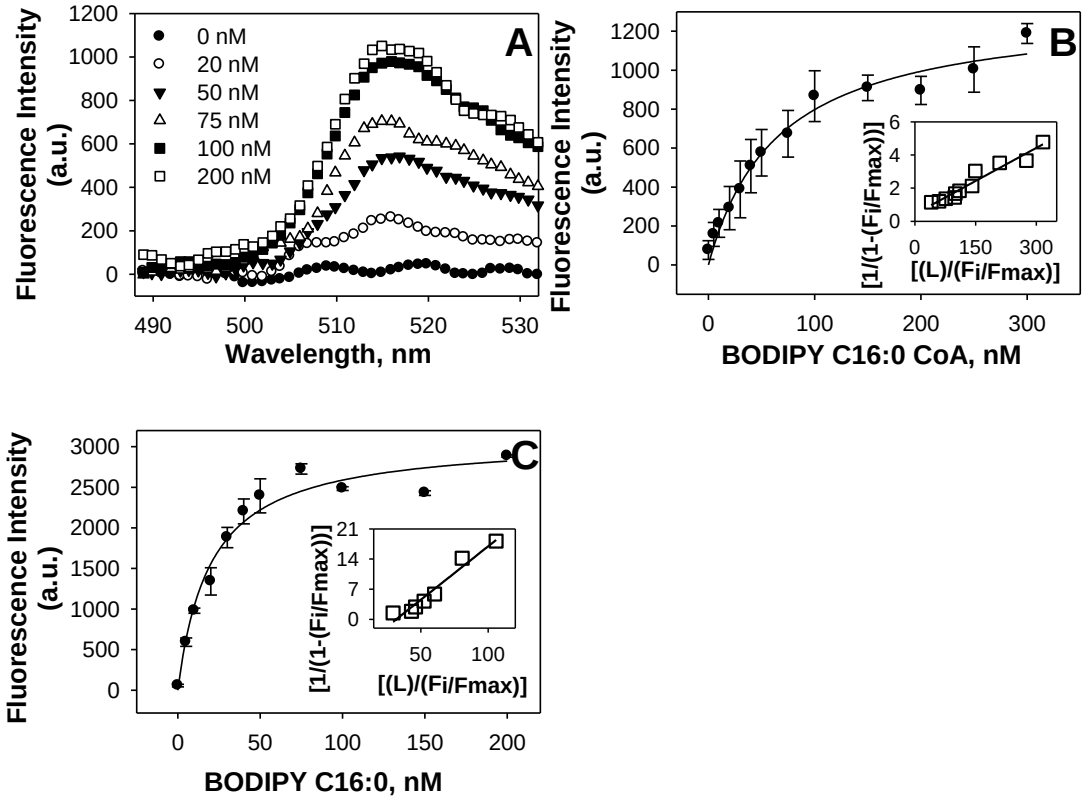


**Fig. 8.** (A) Corrected fluorescence emission spectra of 0.1 μM mPPARα titrated with 0 (filled circles), 20 (open circles), 50 (filled triangles), 75 (open triangles), 100 (filled squares) and 200 nM (open squares) of BODIPY C16-CoA upon excitation at 465 nm, demonstrating increased fluorescence intensity upon binding to mPPARα. Plot of mPPARα maximal fluorescence emission as a function of BODIPY C16:0-CoA (B) and BODIPY C16:0 FA (C). Insets represent linear plots of the binding curve from each panel. All values represent the mean ± S.E., n ≥ 3.

*bound BODIPY C16-CoA:* To determine the ligand specificity of hPPARα for naturally-occurring, endogenous fatty acids, LCFA and LCFA-CoA were examined for their ability to displace BODIPY C16-CoA from the hPPARα ligand binding pocket, which was observed as decreased BODIPY fluorescence. With the exception of lauric acid and lauryl-CoA (Fig. 9U, Fig. 9V), titration with fatty acids and fatty acyl-CoAs resulted in significantly decreased BODIPY fluorescence (Fig. 9A-R). Quantitative analyses of these data suggested strong affinity binding ($K_i$ = 10-40 nM, Table I). By comparison, the synthetic PPARα agonist clofibrate showed slightly weaker affinity (Fig. 9S; $K_i$ = 48 nM), while the synthetic PPARγ agonist rosiglitazone showed no displacement (Fig. 9T; Table I). These data revealed that both LCFA and LCFA-CoA are capable of displacing a fluorescent fatty acyl-CoA, suggesting that both LCFA and LCFA-CoA could be endogenous ligands of hPPARα. These data are in contrast with displacement studies conducted with a truncated form of mPPARα, which showed that only unsaturated LCFA, but not saturated LCFA, could displace a bound fluorescent fatty acid (*115*), and suggest that important differences may exist between hPPARα and mPPARα.

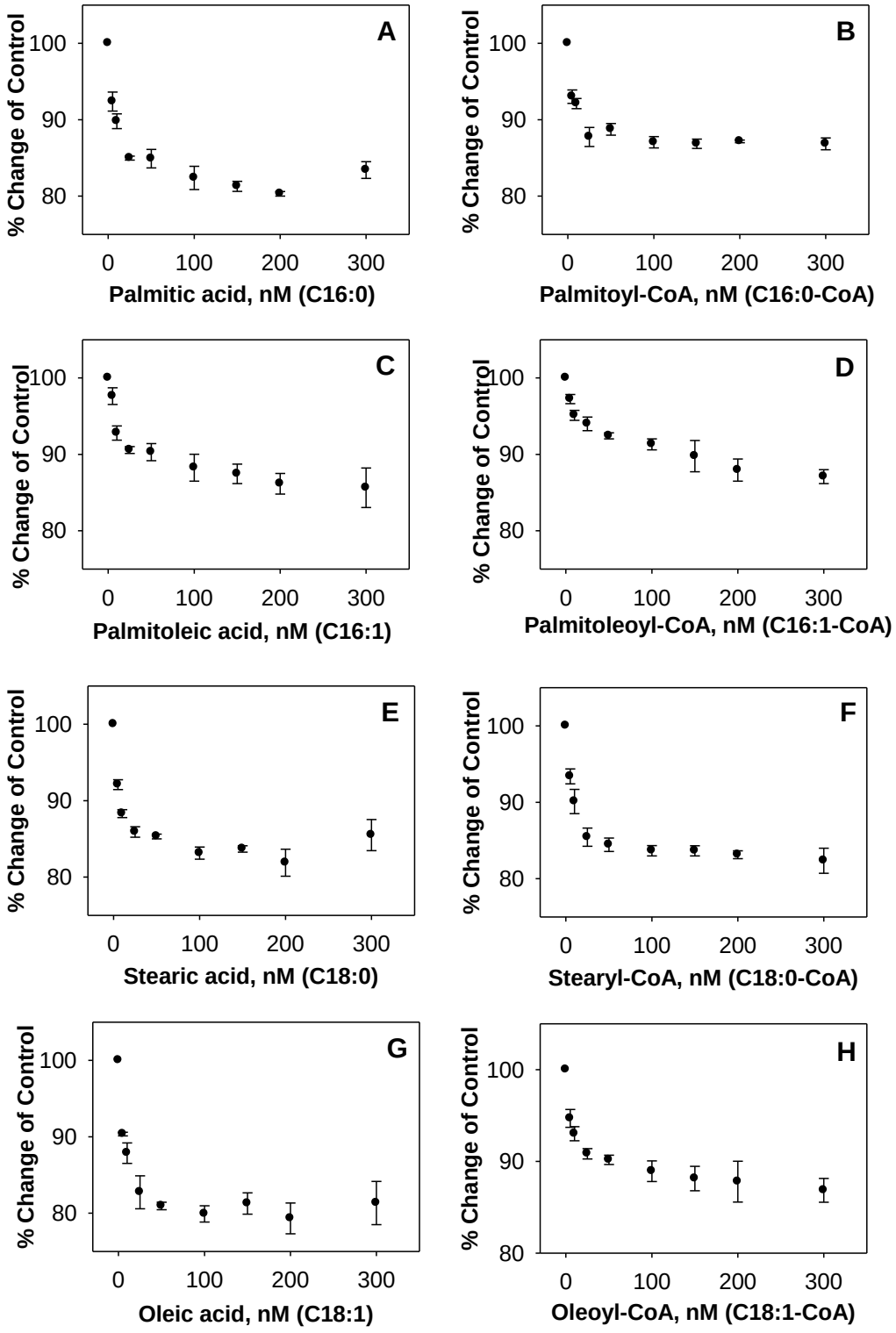
A
% Change of Control
100
90
80
0
100
200
300
Palmitic acid, nM (C16:0)
B
% Change of Control
100
90
80
0
100
200
300
Palmitoyl-CoA, nM (C16:0-CoA)
C
% Change of Control
100
90
80
0
100
200
300
Palmitoleic acid, nM (C16:1)
D
% Change of Control
100
90
80
0
100
200
300
Palmitoleoyl-CoA, nM (C16:1-CoA)
E
% Change of Control
100
90
80
0
100
200
300
Stearic acid, nM (C18:0)
F
% Change of Control
100
90
80
0
100
200
300
Stearyl-CoA, nM (C18:0-CoA)
G
% Change of Control
100
90
80
0
100
200
300
Oleic acid, nM (C18:1)
H
% Change of Control
100
90
80
0
100
200
300
Oleoyl-CoA, nM (C18:1-CoA)

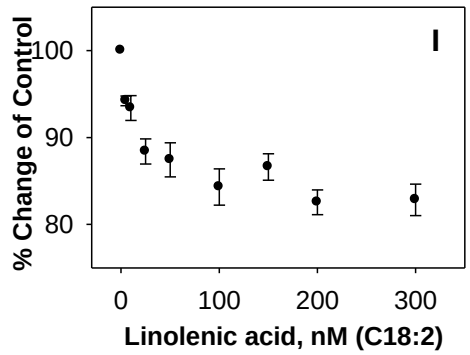
I
% Change of Control
100
90
80
0
100
200
300
Linolenic acid, nM (C18:2)

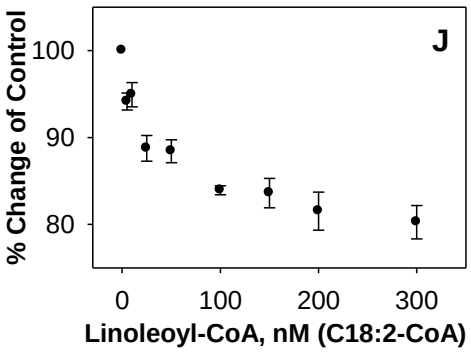
J
% Change of Control
100
90
80
0
100
200
300
Linoleoyl-CoA, nM (C18:2-CoA)

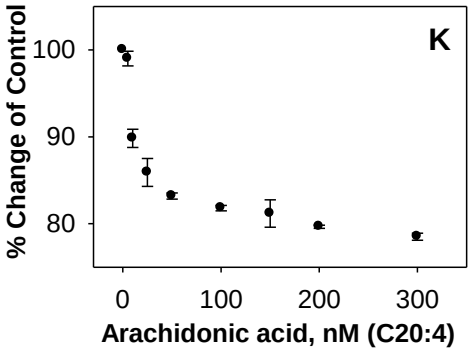
K
% Change of Control
100
90
80
0
100
200
300
Arachidonic acid, nM (C20:4)

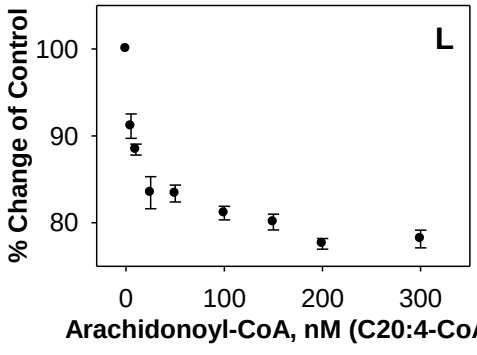
L
% Change of Control
100
90
80
0
100
200
300
Arachidonoyl-CoA, nM (C20:4-CoA)

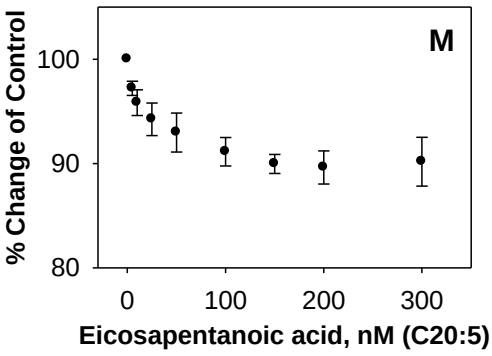
M
% Change of Control
100
90
80
0
100
200
300
Eicosapentanoic acid, nM (C20:5)

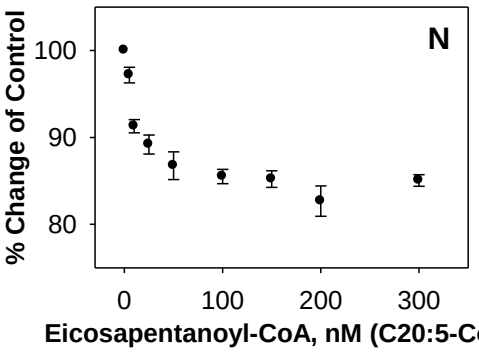
N
% Change of Control
100
90
80
0
100
200
300
Eicosapentanoyl-CoA, nM (C20:5-CoA)

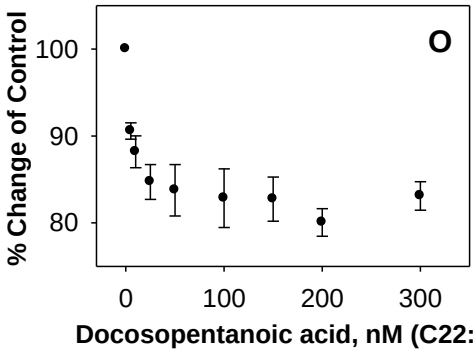
O
% Change of Control
100
90
80
0
100
200
300
Docosopentanoic acid, nM (C22:5)

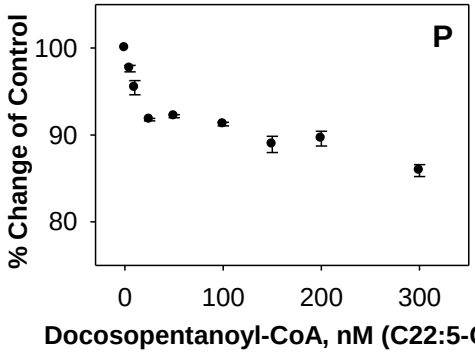
P
% Change of Control
100
90
80
0
100
200
300
Docosopentanoyl-CoA, nM (C22:5-CoA)

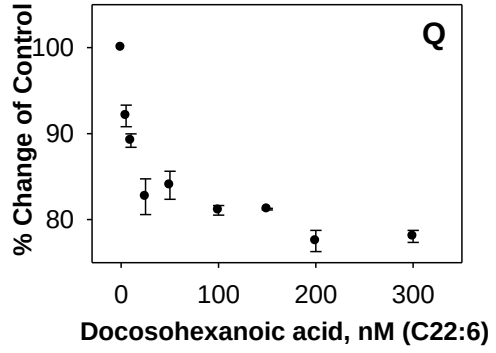
Q
% Change of Control
100
90
80
0
100
200
300
Docosohexanoic acid, nM (C22:6)

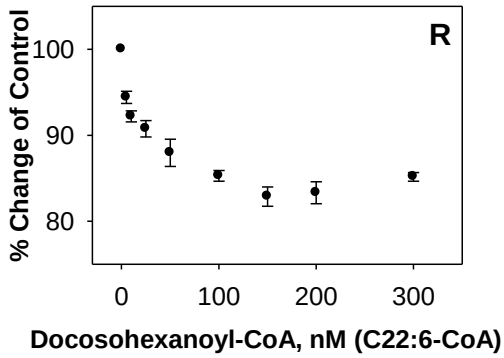
R
% Change of Control
100
90
80
0
100
200
300
Docosohexanoyl-CoA, nM (C22:6-CoA)

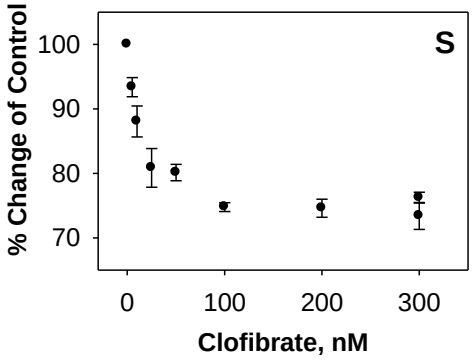
S
% Change of Control
100
90
80
70
0
100
200
300
Clofibrate, nM

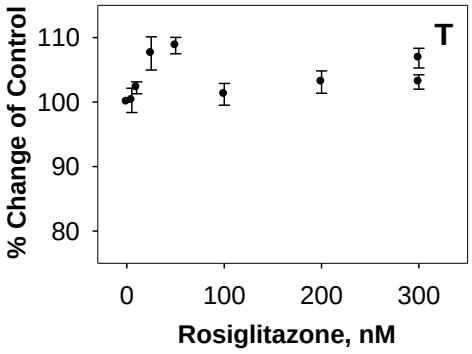
T
% Change of Control
110
100
90
80
0
100
200
300
Rosiglitazone, nM

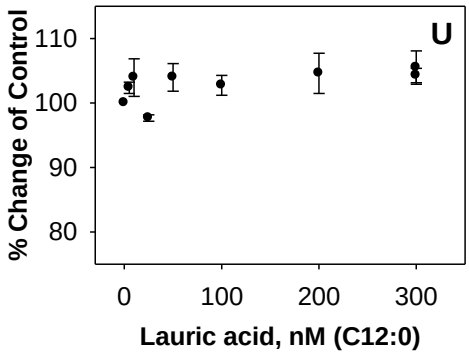
U
% Change of Control
110
100
90
80
0
100
200
300
Lauric acid, nM (C12:0)

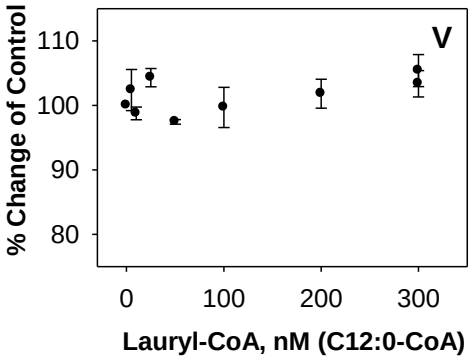
V
% Change of Control
110
100
90
80
0
100
200
300
Lauryl-CoA, nM (C12:0-CoA)

**Fig. 9.** Interaction of naturally occurring fatty acids and fatty acyl-CoA with hPPARα based on displacement of hPPARα-bound BODIPY C16-CoA. hPPARα complexed with BODIPY C16-CoA at mole ratio corresponding to the number of binding sites was titrated with the following ligands: (A) palmitic acid, (B) palmitoyl-CoA, (C) palmitoleic acid, (D) palmitoleoyl-CoA (E) stearic acid (F) stearoyl-CoA, (G) oleic acid, (H) oleoyl-CoA, (I) linoleic acid, (J) linoleoyl-CoA (K) arachidonic acid, (L) arachidonoyl-CoA (M) eicosapentaenoic acid, (N) eicosapentaenoyl-CoA, (O) docosapentanoic acid, (P) docosapentanoyl-CoA, (Q) docosahexanoic acid, (R) docosahexanoyl-CoA, (S) clofibrate, (T) rosiglitazone, (U) lauric acid and (V) lauryl-CoA. The maximal fluorescence emission of BODIPY C16-CoA was measured at 515 nm (excitation at 465 nm). Data are presented as percent change of initial fluorescence plotted as a function of ligand concentration. All values represent mean ± S.E., $n \geq 3$.

*Binding of endogenous LCFA and LCFA-CoA to mPPARα – Displacement of bound BODIPY C16-CoA:* To compare the ability of naturally-occurring LCFA and LCFA-CoA to displace BODIPY C16-CoA from the binding pocket of mPPARα (versus hPPARα), we first mixed mPPARα with a saturating concentration of BODIPY C16-CoA. Since the BODIPY C16-CoA binding affinity for mPPARα is much weaker than for hPPARα, a higher concentration of BODIPY C16-CoA is needed to reach saturation and ensure BODIPY C16-CoA-bound mPPARα (130 nM). This was followed by titration with naturally occurring LCFA and LCFA-CoA. Displacement of bound BODIPY C16-CoA was observed as a decrease in BODIPY fluorescence. With the exception of lauric acid and lauryl-CoA (Fig 10O, 10P), titration with fatty acids and fatty acyl-CoA resulted in significantly decreased BODIPY fluorescence (Fig. 10A-L). Quantitative analyses of these data suggested that, with the exception of the saturated LCFA (palmitic acid, $K_i$ = 135 nM and stearic acid, $K_i$ = 134 nM), most LCFA and LCFA-CoA demonstrated strong affinity binding ($K_i$ = 13-38 nM, Table II) for mPPARα. The mPPARα showed similar displacement and affinity for the synthetic PPARα agonist clofibrate (Fig 10M; $K_i$ = 46 nM, Table II) as compared hPPARα (Table I), and the synthetic PPARγ agonist rosiglitazone showed no displacement (Fig. 10N; Table II). These data show that LCFA and LCFA-CoA are both capable of displacing a fluorescent fatty acyl-CoA, suggesting that both LCFA and LCFA-CoA could be endogenous ligands of mPPARα. When compared to binding data from hPPARα (Table I), these data also suggest differences in the ligand binding specificity between hPPARα and mPPARα, particularly for saturated LCFA.

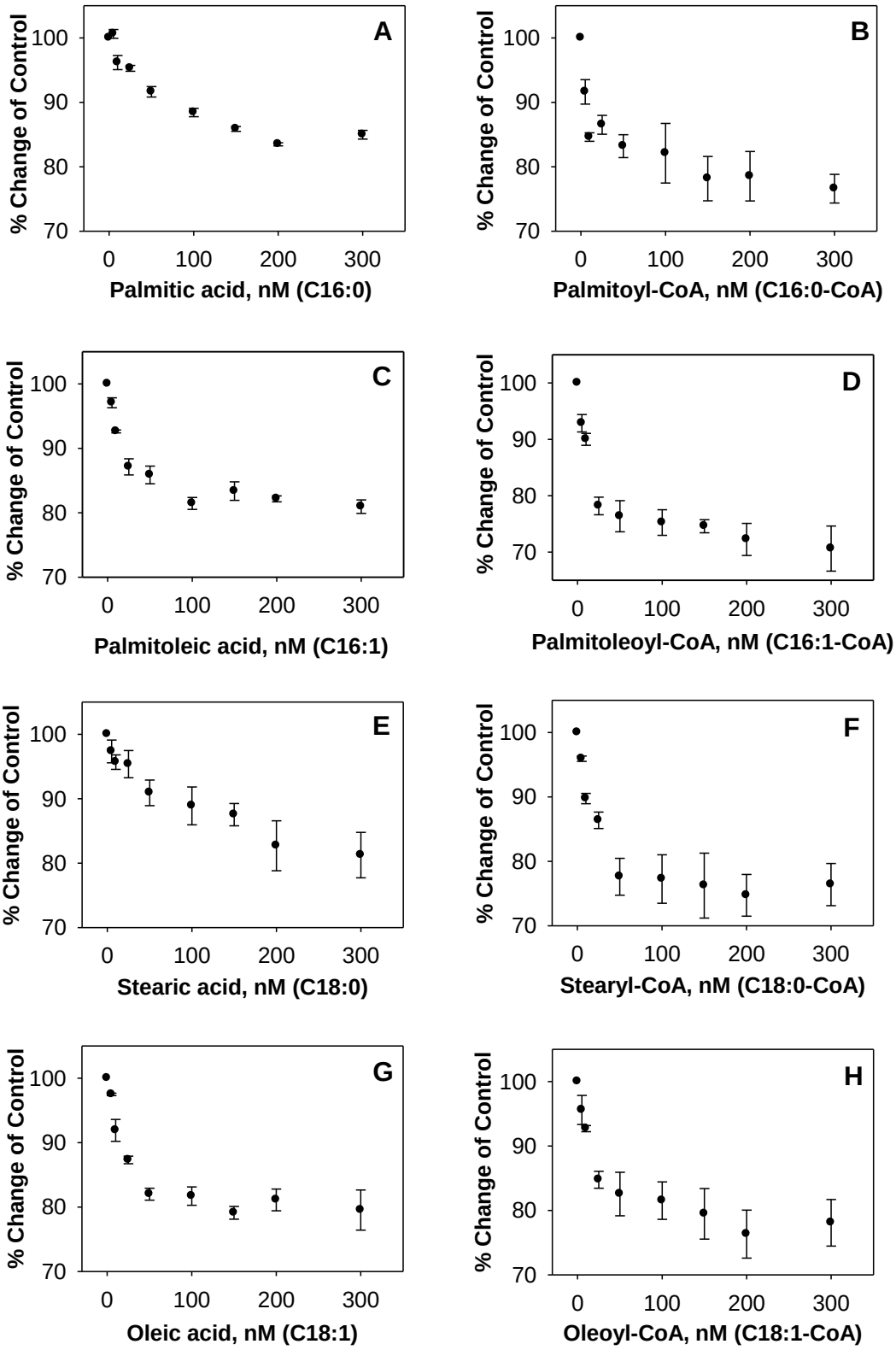
A
% Change of Control
100
90
80
70
0
100
200
300
Palmitic acid, nM (C16:0)
B
% Change of Control
100
90
80
70
0
100
200
300
Palmitoyl-CoA, nM (C16:0-CoA)
C
% Change of Control
100
90
80
70
0
100
200
300
Palmitoleic acid, nM (C16:1)
D
% Change of Control
100
90
80
70
0
100
200
300
Palmitoleoyl-CoA, nM (C16:1-CoA)
E
% Change of Control
100
90
80
70
0
100
200
300
Stearic acid, nM (C18:0)
F
% Change of Control
100
90
80
70
0
100
200
300
Stearyl-CoA, nM (C18:0-CoA)
G
% Change of Control
100
90
80
70
0
100
200
300
Oleic acid, nM (C18:1)
H
% Change of Control
100
90
80
70
0
100
200
300
Oleoyl-CoA, nM (C18:1-CoA)

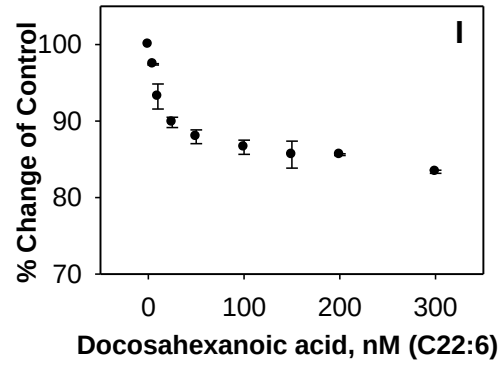
I
% Change of Control
100
90
80
70
0
100
200
300
Docosahexanoic acid, nM (C22:6)

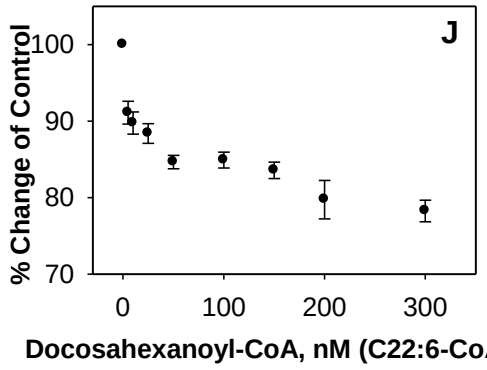
J
% Change of Control
100
90
80
70
0
100
200
300
Docosahexanoyl-CoA, nM (C22:6-CoA)

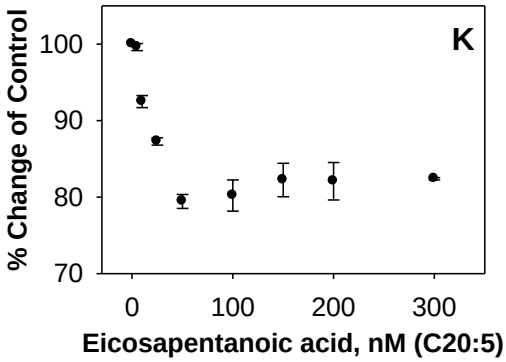
K
% Change of Control
100
90
80
70
0
100
200
300
Eicosapentanoic acid, nM (C20:5)

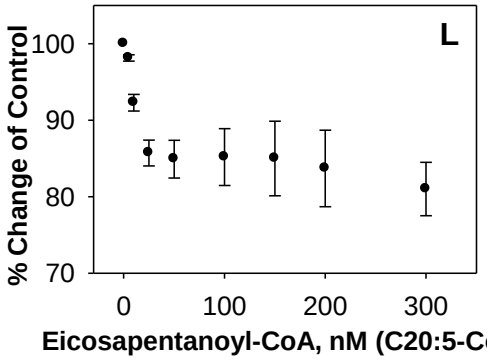
L
% Change of Control
100
90
80
70
0
100
200
300
Eicosapentanoyl-CoA, nM (C20:5-CoA)

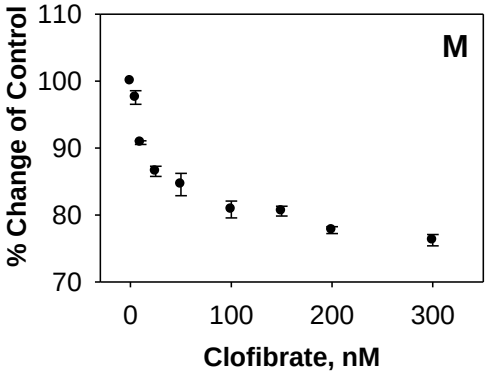
M
% Change of Control
110
100
90
80
70
0
100
200
300
Clofibrate, nM

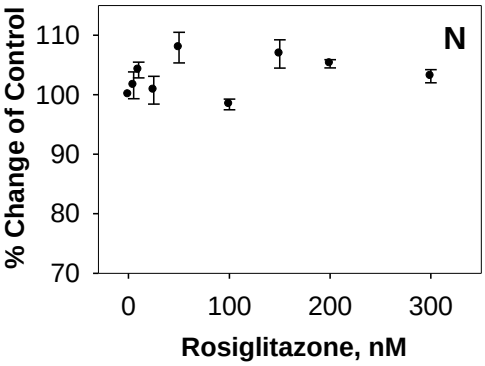
N
% Change of Control
110
100
90
80
70
0
100
200
300
Rosiglitazone, nM

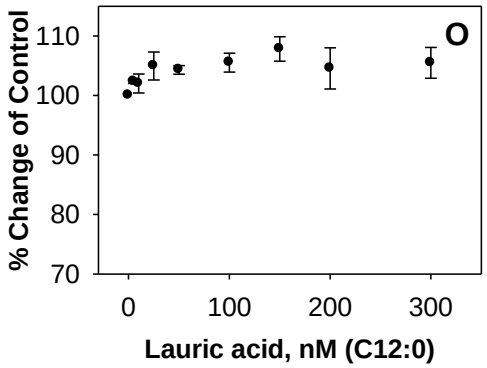
O
% Change of Control
110
100
90
80
70
0
100
200
300
Lauric acid, nM (C12:0)

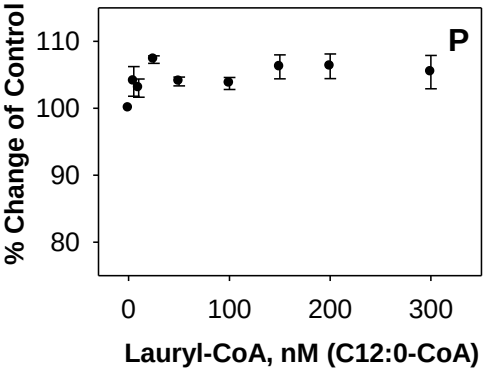
P
% Change of Control
110
100
90
80
0
100
200
300
Lauryl-CoA, nM (C12:0-CoA)

**Fig. 10.** Interaction of naturally occurring fatty acids and fatty acyl-CoA with mPPARα based on displacement of mPPARα-bound BODIPY-C16 CoA. mPPARα complexed with BODIPY C16-CoA at mole ratio corresponding to the number of binding sites was titrated with the following ligands: (A) palmitic acid, (B) palmitoyl-CoA, (C) palmitoleic acid, (D) palmitoleoyl-CoA (E) stearic acid (F) stearoyl-CoA, (G) oleic acid, (H) oleoyl-CoA, (I) eicosapentaenoic acid, (J) eicosapentaenoyl-CoA, (K) docosahexanoic acid (L) docosahexanoyl-CoA, (M) clofibrate, (N) rosiglitazone (O) lauric acid and (P) lauryl-CoA. The maximal fluorescence emission of BODIPY C16-CoA was measured at 515 nm (excitation at 465 nm). Data are presented as percent change of initial fluorescence plotted as a function of ligand concentration. All values represent mean ± S.E., $n \geq 3$.

*Binding of endogenous LCFA and LCFA-CoA to hPPARα – Quenching of intrinsic aromatic amino acid fluorescence:* Since previous data has suggested that fluorescent fatty acid analogues are not always bound the same as endogenous fatty acids due to bulky side chains altering the energy minimized state of the molecule (*117, 173*), the binding of LCFA and LCFA-CoA to hPPARα was also measured directly by spectroscopically monitoring the quenching of hPPARα aromatic amino acid emission. Titration of hPPARα with the saturated LCFA palmitic acid (Fig. 11A) and stearic acid (Fig. 11E) yielded sharp saturation curves with maximal fluorescence changes at 100 nM, and both transformed into linear reciprocal plots (insets), indicating high affinity binding at a single binding site ($R^2 > 0.9$). Similar results were obtained for all examined LCFA and LCFA-CoA (Fig. 11A-R), with single site binding affinities in the 10-30 nM range (Table I), similar to affinities determined by displacement assays. Titration with lauric acid (Fig. 11U) and lauryl-CoA (Fig. 11V) did not significantly alter hPPARα fluorescence, and no binding was detected (Table I). The PPARα agonist clofibrate strongly quenched hPPARα fluorescence (Fig. 11S), but displayed weaker affinity than the LCFA (Table I), while the PPARα agonist rosiglitazone showed no binding (Fig. 11T), further confirming that hPPARα bound saturated, monounsaturated, and polyunsaturated LCFA and LCFA-CoA with high affinity.

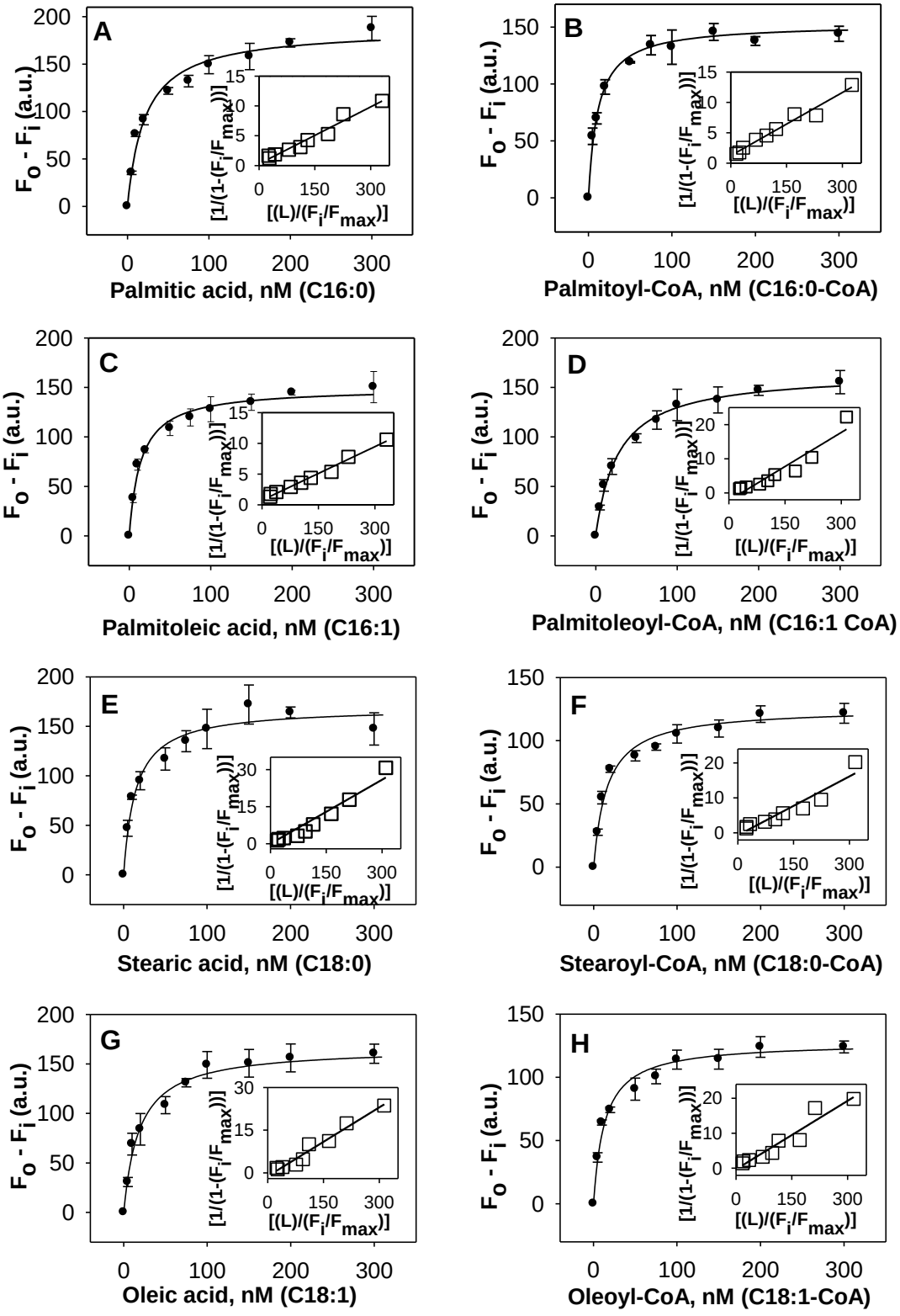
A
B
C
D
E
F
G
H
$F_o - F_i$ (a.u.)
Palmitic acid, nM (C16:0)
Palmitoyl-CoA, nM (C16:0-CoA)
Palmitoleic acid, nM (C16:1)
Palmitoleoyl-CoA, nM (C16:1 CoA)
Stearic acid, nM (C18:0)
Stearoyl-CoA, nM (C18:0-CoA)
Oleic acid, nM (C18:1)
Oleoyl-CoA, nM (C18:1-CoA)
$[1/(1-(F_i/F_{max}))]$
$[(L)/(F_i/F_{max})]$

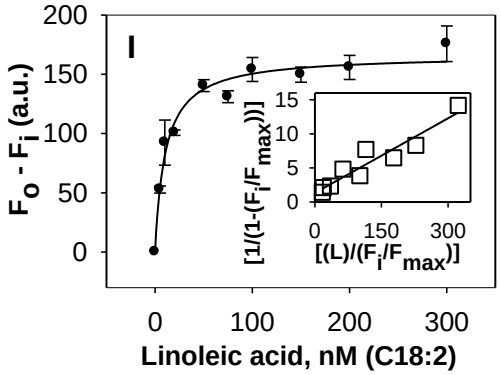


Linoleic acid, nM (C18:2)

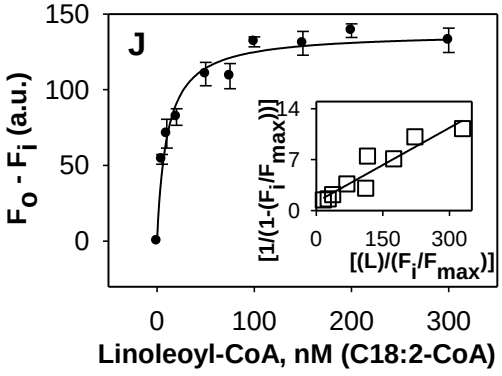


Linoleoyl-CoA, nM (C18:2-CoA)

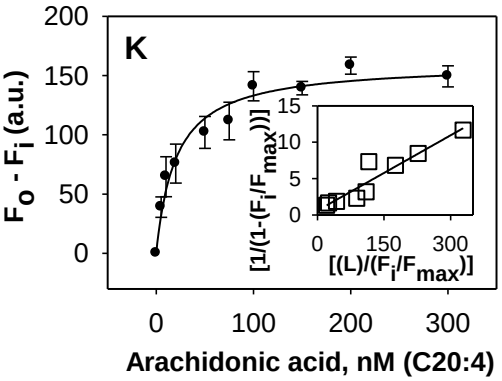


Arachidonic acid, nM (C20:4)

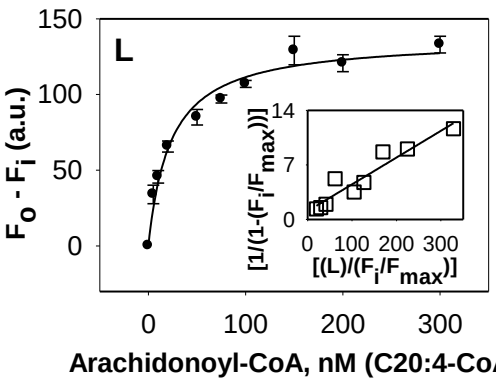


Arachidonoyl-CoA, nM (C20:4-CoA)

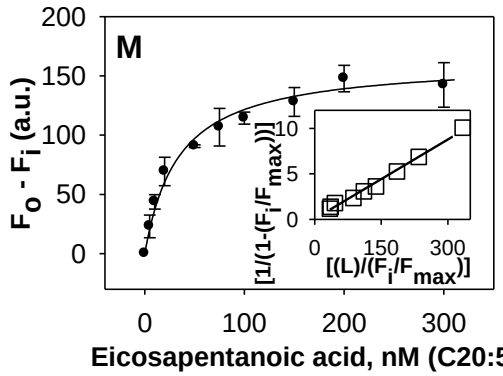


Eicosapentanoic acid, nM (C20:5)

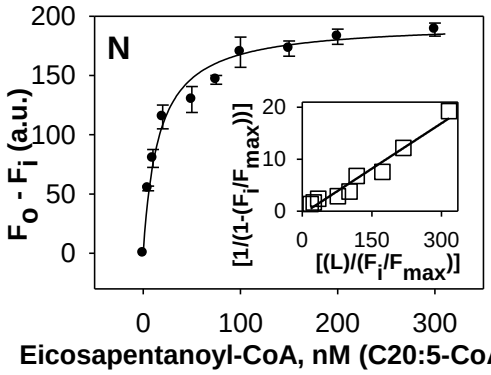


Eicosapentanoyl-CoA, nM (C20:5-CoA)

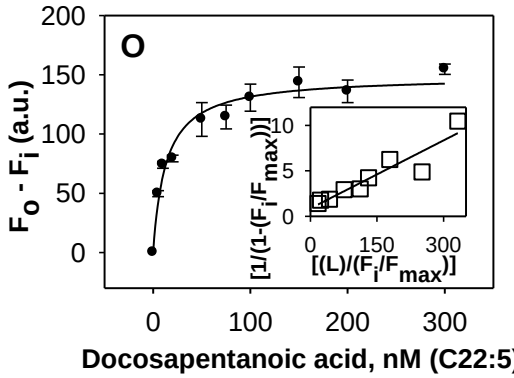


Docosapentanoic acid, nM (C22:5)

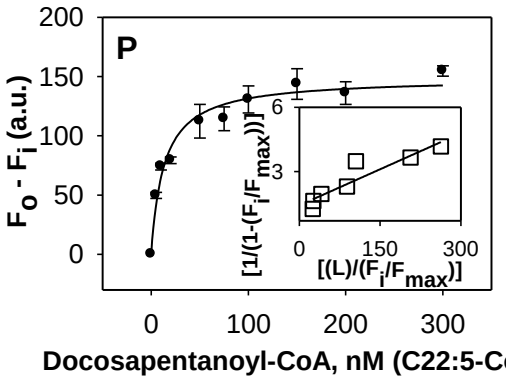


Docosapentanoyl-CoA, nM (C22:5-CoA)

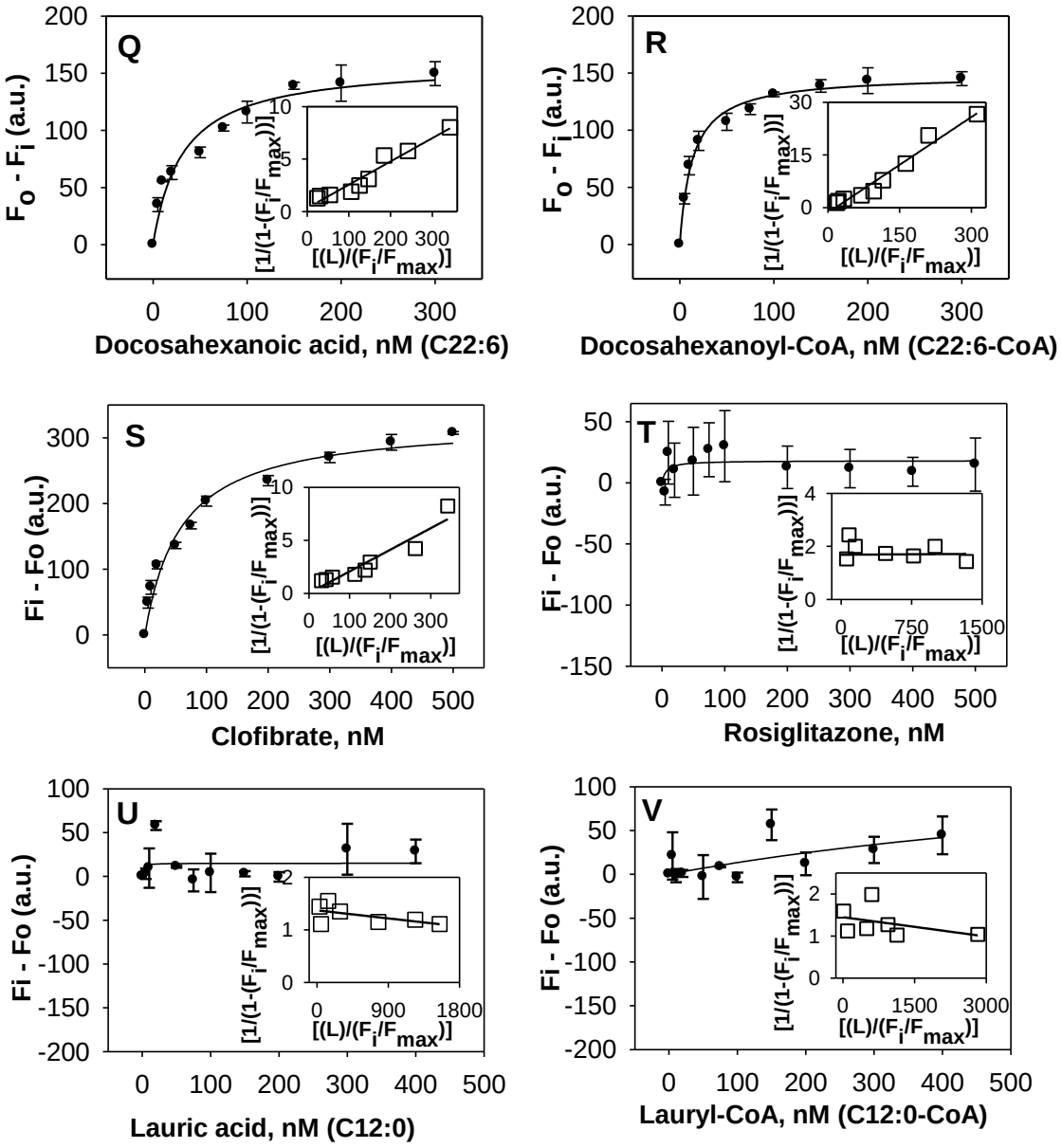
Q
$F_o - F_i$ (a.u.)
Docosahexanoic acid, nM (C22:6)
$[1/(1-(F_i/F_{max}))]$
$[(L)/(F_i/F_{max})]$
R
$F_o - F_i$ (a.u.)
Docosahexanoyl-CoA, nM (C22:6-CoA)
$[1/(1-(F_i/F_{max}))]$
$[(L)/(F_i/F_{max})]$
S
Fi - Fo (a.u.)
Clofibrate, nM
$[1/(1-(F_i/F_{max}))]$
$[(L)/(F_i/F_{max})]$
T
Fi - Fo (a.u.)
Rosiglitazone, nM
$[1/(1-(F_i/F_{max}))]$
$[(L)/(F_i/F_{max})]$
U
Fi - Fo (a.u.)
Lauric acid, nM (C12:0)
$[1/(1-(F_i/F_{max}))]$
$[(L)/(F_i/F_{max})]$
V
Fi - Fo (a.u.)
Lauryl-CoA, nM (C12:0-CoA)
$[1/(1-(F_i/F_{max}))]$
$[(L)/(F_i/F_{max})]$

**Fig. 11.** Interaction of naturally-occurring fatty acids and fatty acyl-CoA with hPPARα. Direct binding assay based on quenching of hPPARα aromatic amino acid fluorescence emission when titrated with the following ligands: (A) palmitic acid, (B) palmitoyl-CoA, (C) palmitoleic acid, (D) palmitoleoyl-CoA (E) stearic acid (F) stearoyl-CoA, (G) oleic acid, (H) oleoyl-CoA, (I) linoleic acid, (J) linoleoyl-CoA (K) arachidonic acid, (L) arachidonoyl-CoA (M) eicosapentaenoic acid, (N) eicosapentaenoyl-CoA, (O) docosapentanoic acid, (P) docosapentanoyl-CoA, (Q) docosahexanoic acid, (R) docosahexanoyl-CoA, (S) clofibrate, (T) rosiglitazone, (U) lauric acid and (V) lauryl-CoA. Data are presented as the change in fluorescence intensity ($F_0$- $F_i$) plotted as a function of ligand concentration. Insets represent linear plots of the binding curve from each panel. All values represent mean ± S.E., $n \geq 3$.

**Table I**. Affinity of hPPARα for non-fluorescent ligands determined by quenching of hPPARα aromatic amino acid fluorescence and by displacement of hPPARα-bound BODIPY C16-CoA.

| Ligand | Chain length: double bonds (position) | $K_d$ (nM) Fatty acid | $K_d$ (nM) Fatty acyl-CoA | $K_i$ (nM) Fatty acid | *Ki* (nM) Fatty acyl-CoA |
|---|---|---|---|---|---|
| Lauric acid/CoA | C12:0 | ND | ND | ND | ND |
| Palmitic acid/CoA | C16:0 | 22±3 | 11±1 | 16±2 | 10±2 |
| Palmitoleic acid/CoA | C16:1 (n-7) | 16±2 | 29±4 | 26±6 | 46±8 |
| Stearic acid/CoA | C18:0 | 14±2 | 16±2 | 13±3 | 15±2 |
| Oleic acid/CoA | C18:1 (n-9) | 19±3 | 13±1 | 13±2 | 16±3 |
| Linoleic acid/CoA | C18:2 (n-6) | 12±1 | 12±2 | 26±6 | 40±8 |
| Arachidonic acid/CoA | C20:4 (n-6) | 24±5 | 23±3 | 24±3 | 17±2 |
| Eicosapentanoic acid/CoA | C20:5 (n-3) | 34±4 | 16±2 | 38±5 | 26±5 |
| Docosapentanoic acid/CoA | C22:5 (n-3) | 13±2 | 18±4 | 10±2 | 30±6 |
| Docosahexanoic acid/CoA | C22:6 (n-3) | 30±5 | 14±1 | 18±3 | 28±5 |
| Clofibrate | | 58±6 | | 48±6 | |
| Rosiglitazone | | ND | | ND | |

Values represent the mean ± S.E. ($n \geq 3$). ND, not determined.

*Binding of endogenous LCFA and LCFA-CoA to mPPARα – Quenching of intrinsic aromatic amino acid fluorescence:* Binding of full-length mPPARα to LCFA and LCFA-CoA was also measured by spectroscopically monitoring the quenching of mPPARα aromatic amino acid emission. Although titration with the saturated LCFA palmitic acid (Fig. 12A) and stearic acid (Fig. 12E) resulted in decreased mPPARα fluorescence, the slopes of these curves were much shallower than that of hPPARα with palmitic acid (Fig. 11A) or stearic acid (Fig. 11E), with the change in fluorescence intensity plateauing off at approximately 300 nM. Transformation of these data into double reciprocal plots yielded single lines (Fig. 12A, Fig. 12E, insets), indicating single binding sites for both. However, multiple replicates yielded much weaker binding affinities for mPPARα ($K_d$ = 92 nM for palmitic acid and 81 nM for stearic acid, Table II) than hPPARα (Table I). Titration of mPPARα with the other examined LCFA and LCFA-CoA yielded sharp saturation curves with the maximal change in fluorescence intensity noted at approximately 100 nM (Fig. 12A-L) indicating high affinity binding ($K_d$ = 14-37 nM, Table II). These data transformed into linear reciprocal plots (insets), indicating binding at a single binding site ($R^2 > 0.9$). Similar to hPPARα, no significant mPPARα binding was noted for lauric acid (Fig. 7O), lauryl-CoA (Fig. 12P), or rosiglitazone (Fig. 12N), while clofibrate binding resulted in the strongest fluorescence changes (Fig. 12M). Although the weak binding of palmitic acid and stearic acid to full-length mPPARα was consistent with previous data using mPPARΔAB (*115-117*), it was significantly different from the binding of hPPARα with the same ligand (Table I). On the other hand, while mPPARΔAB demonstrated weak binding towards polyunsaturated fatty acids (PUFA), such as eicosapentanoic

acid and docosahexaenoic acid, our data employing full-length mPPARα and hPPARα demonstrated high-affinity binding for both these PUFA (Table I and Table II). These findings suggest two important conclusions. There exist species dependent differences in the ligand binding specificity and affinity between human and mouse PPARα, and the N-terminal domain of PPARα plays an unexpected, but important, role in the ligand binding function of the protein.

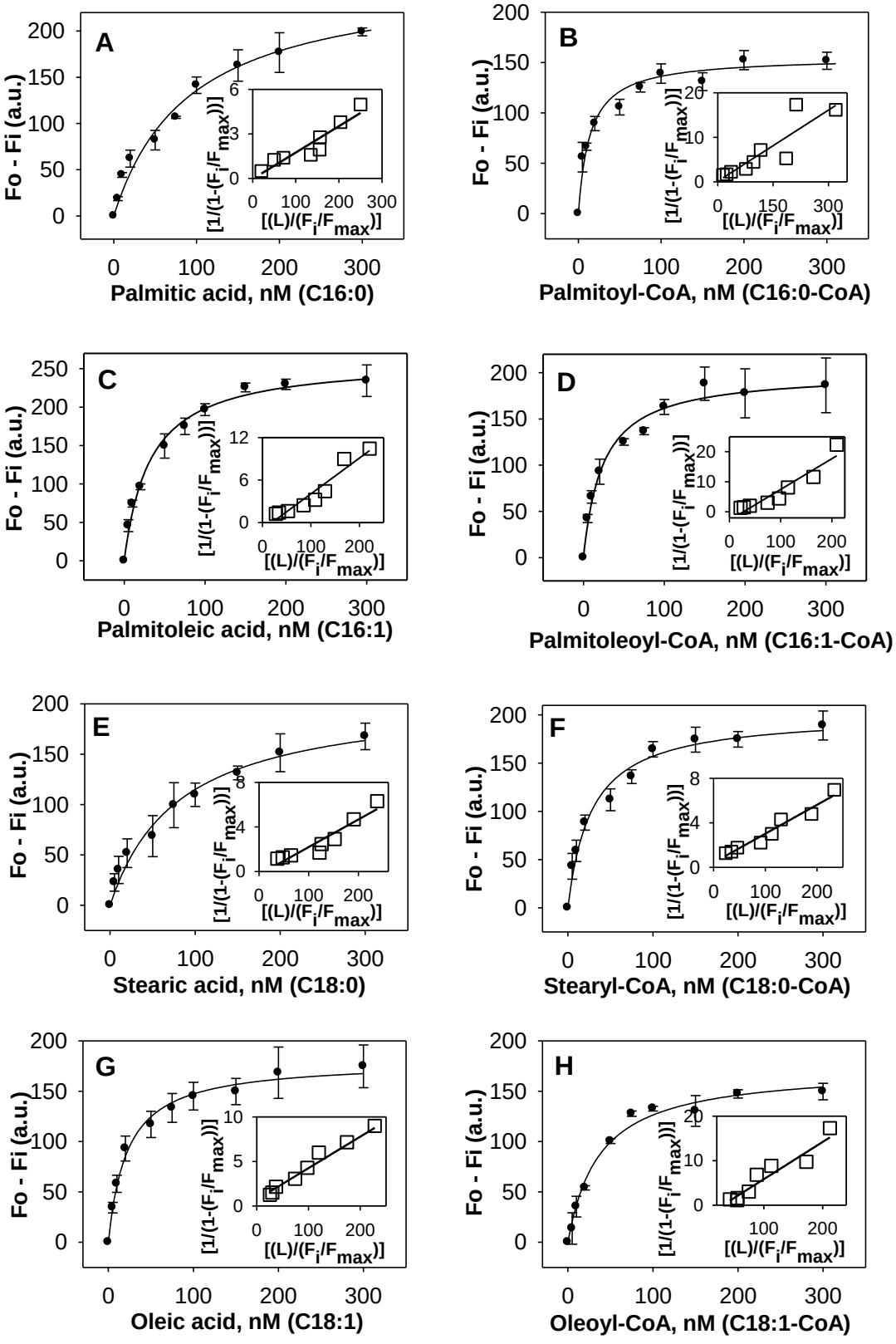
A
Fo - Fi (a.u.)
Palmitic acid, nM (C16:0)
[1/(1-(Fi/Fmax))]
[(L)/(Fi/Fmax)]
B
Palmitoyl-CoA, nM (C16:0-CoA)
C
Palmitoleic acid, nM (C16:1)
D
Palmitoleoyl-CoA, nM (C16:1-CoA)
E
Stearic acid, nM (C18:0)
F
Stearyl-CoA, nM (C18:0-CoA)
G
Oleic acid, nM (C18:1)
H
Oleoyl-CoA, nM (C18:1-CoA)

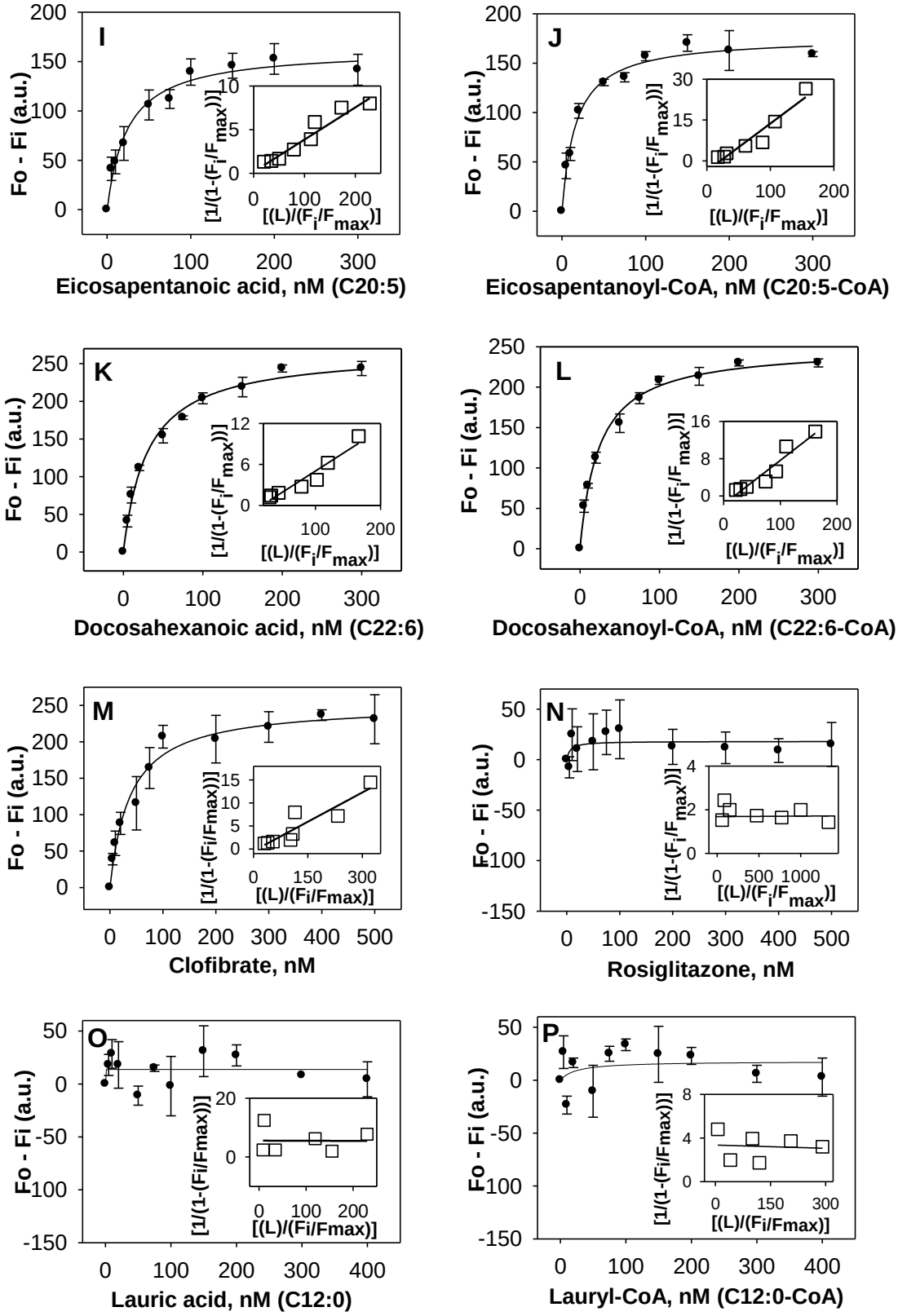
I
Fo - Fi (a.u.)
Eicosapentanoic acid, nM (C20:5)
[1/(1-(Fi/Fmax))]
[(L)/(Fi/Fmax)]
J
Eicosapentanoyl-CoA, nM (C20:5-CoA)
K
Docosahexanoic acid, nM (C22:6)
L
Docosahexanoyl-CoA, nM (C22:6-CoA)
M
Clofibrate, nM
[(L)/(Fi/Fmax)]
N
Rosiglitazone, nM
O
Lauric acid, nM (C12:0)
P
Lauryl-CoA, nM (C12:0-CoA)

**Fig. 12.** Interaction of naturally-occurring fatty acids and fatty acyl-CoA with mPPARα. Direct binding assay based on quenching of mPPARα aromatic amino acid fluorescence emission when titrated with the following ligands: (A) palmitic acid, (B) palmitoyl-CoA, (C) palmitoleic acid, (D) palmitoleoyl-CoA (E) stearic acid (F) stearoyl-CoA, (G) oleic acid, (H) oleoyl-CoA, (I) eicosapentaenoic acid, (J) eicosapentaenoyl-CoA, (K) docosahexanoic acid (L) docosahexanoyl-CoA, (M) clofibrate, (N) rosiglitazone (O) lauric acid and (P) lauryl-CoA. Data are presented as the change in fluorescence intensity ($F_0$- $F_i$) plotted as a function of ligand concentration. Insets represent linear plots of the binding curve from each panel. All values represent mean ± S.E., $n \geq 3$.

**Table II**. Affinity of mPPARα for non-fluorescent ligands determined by quenching of mPPARα aromatic amino acid fluorescence and by displacement of mPPARα-bound BODIPY C16-CoA.

| Ligand | Chain length: double bonds (position) | $K_d$ (nM) Fatty acid | $K_d$ (nM) Fatty acyl-CoA | $K_i$ (nM) Fatty acid | *Ki* (nM) Fatty acyl-CoA |
|---|---|---|---|---|---|
| Lauric acid/CoA | C12:0 | ND | ND | ND | ND |
| Palmitic acid/CoA | C16:0 | 92±13 | 14±2 | 135±13 | 23±4 |
| Palmitoleic acid/CoA | C16:1 (n-7) | 32±3 | 24±5 | 35±3 | 31±4 |
| Stearic acid/CoA | C18:0 | 81±15 | 28±5 | 134±30 | 37±5 |
| Oleic acid/CoA | C18:1 (n-9) | 22±5 | 37±5 | 37±4 | 38±6 |
| Eicosapentanoic acid/CoA | C20:5 (n-3) | 24±6 | 17±3 | 33±5 | 21±3 |
| Docosahexanoic acid/CoA | C22:6 (n-3) | 31±2 | 24±2 | 34±3 | 13±3 |
| Clofibrate | | 39±6 | | 46±3 | |
| Rosiglitazone | | ND | | ND | |

Values represent the mean ± S.E. (n ≥ 3). ND, not determined.

*Effect of endogenous fatty acids and fatty acyl-CoAs on hPPARα secondary structure:* Ligand-activated receptors, such as PPARα, undergo conformational changes upon ligand binding, which allows for altered co-factor interactions (*10, 117, 182*). Circular dichroism was used to examine whether the binding of LCFA or LCFA-CoA altered the hPPARα secondary structure. The far UV circular dichroic spectrum of hPPARα suggested the presence of substantial α-helical content, exhibiting a large positive peak at 192 nm and two negative peaks at 207 and 222 nm (Fig. 13A-K, filled circles). Quantitative analyses of the circular dichroic spectra confirmed that hPPARα was composed of approximately 32 % α-helix, 18 % β-sheets, 21 % β-turns and 29 % unordered structures (Table III).

Since most of the examined ligands were shown to bind at a single binding site, ligand effects were measured at a molar concentration equivalent to that of hPPARα. The addition of high-affinity LCFA and LCFA-CoA ligands resulted in alterations in molar ellipticity at 192, 207, and 222 nm (Fig. 13B-J), demonstrating hPPARα conformational changes. Although both increases and decreases of the 192 nm peak were noted, most of the examined LCFA and LCFA-CoA resulted in less negative peaks at 207 and 222 nm (Fig. 13B-J), suggestive of decreased α-helical content. Quantitative analyses confirmed that most high-affinity LCFA and LCFA-CoA ligands significantly decreased the estimated fraction of α-helical content and concomitantly increased the estimated fraction of β-sheets (Table III). However, lauric acid and its CoA thioester, which showed no binding, resulted in only minor, non-significant changes to the hPPARα secondary structure (Fig. 13A, Table III). Contrary to previously published mPPARα data (*116, 117*), the strongest conformational changes

were noted with palmitic acid, stearic acid, eicosapentaenoic acid, and docosahexaenoic acid (Fig. 13, Table III). These changes in spectra and percent composition were stronger than those observed with the addition of clofibrate (Fig. 13K, open circles, Table III), and no changes were observed with the addition of rosiglitazone (Fig. 13K, filled triangles, Table III), consistent with the decreased affinity of hPPARα for these compounds.

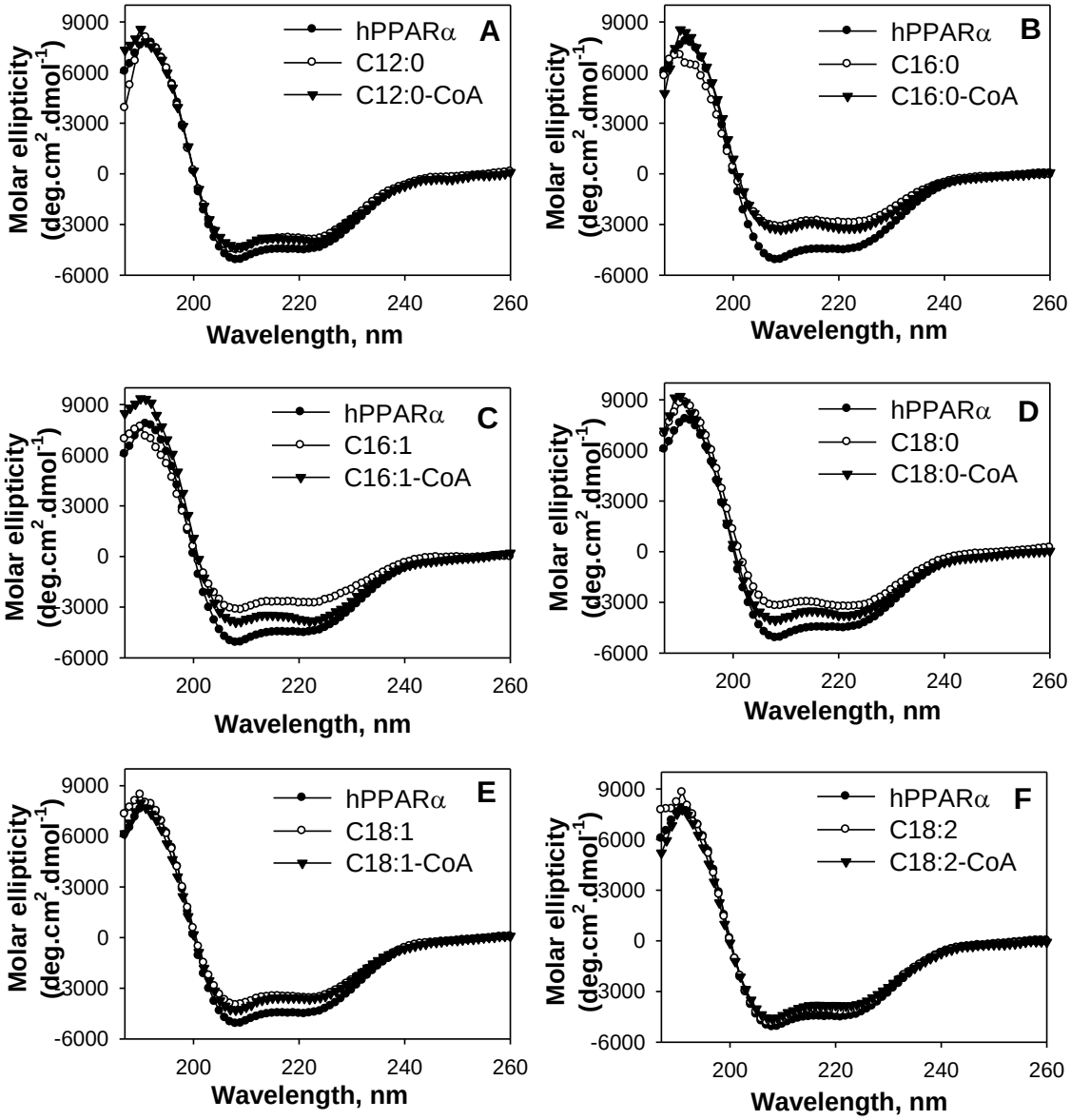
A
hPPARα
C12:0
C12:0-CoA
B
hPPARα
C16:0
C16:0-CoA
C
hPPARα
C16:1
C16:1-CoA
D
hPPARα
C18:0
C18:0-CoA
E
hPPARα
C18:1
C18:1-CoA
F
hPPARα
C18:2
C18:2-CoA
Molar ellipticity (deg.cm2.dmol-1)
Wavelength, nm
9000
6000
3000
0
-3000
-6000
200
220
240
260

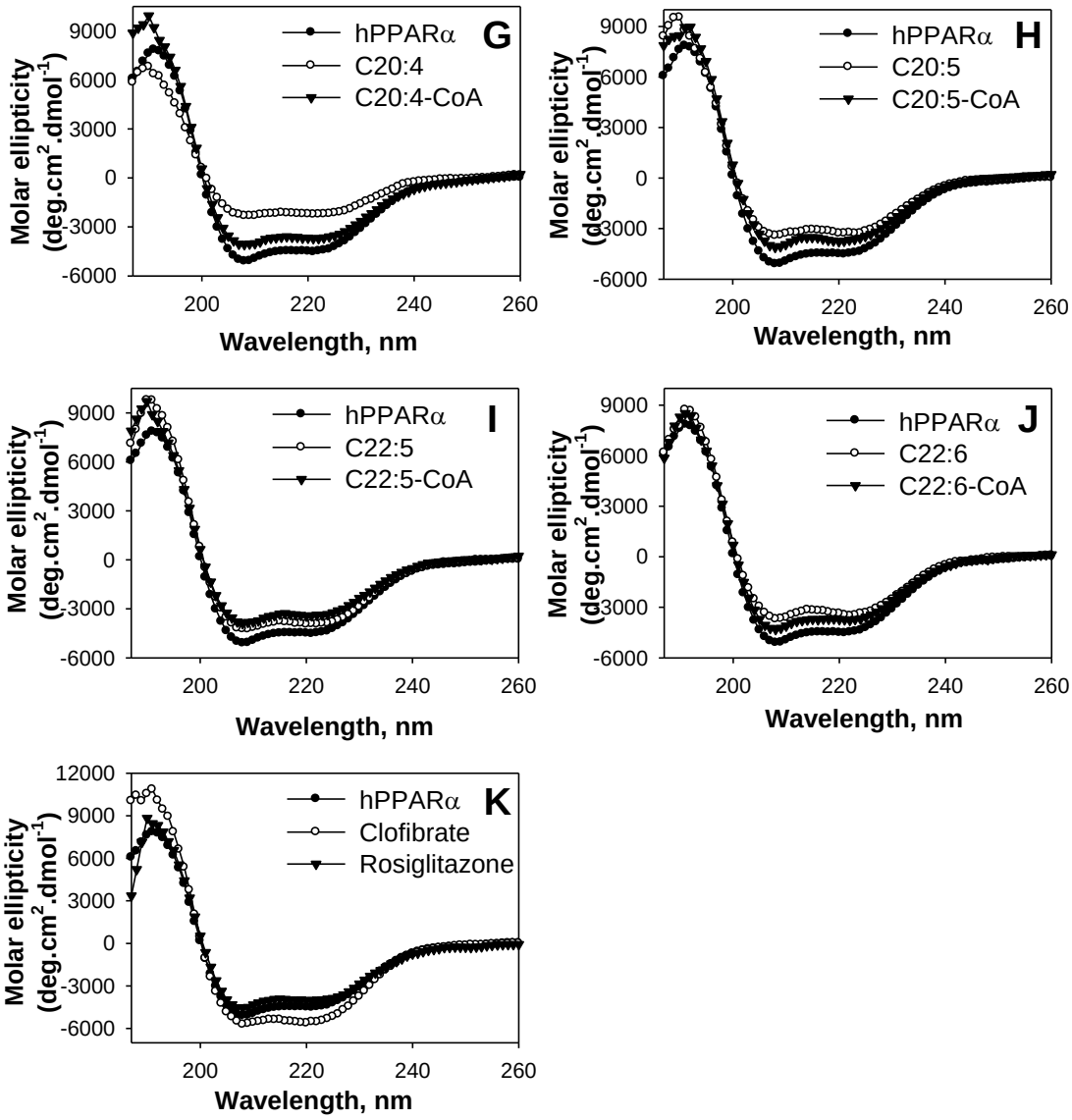
G
hPPARα
C20:4
C20:4-CoA
H
hPPARα
C20:5
C20:5-CoA
I
hPPARα
C22:5
C22:5-CoA
J
hPPARα
C22:6
C22:6-CoA
K
hPPARα
Clofibrate
Rosiglitazone
Molar ellipticity (deg.cm2.dmol-1)
Wavelength, nm
9000
6000
3000
0
-3000
-6000
12000
200
220
240
260

**Fig. 13.** Far UV circular dichroic (CD) spectra of hPPARα in the absence (filled circles) and presence of added ligand: (A) lauric acid (open circles) or lauryl-CoA (filled triangles); (B) palmitic acid (open circles) or palmitoyl-CoA (filled triangles); (C) palmitoleic acid (open circles) or palmitoleoyl-CoA (filled triangles); (D) stearic acid (open circles) or stearoyl-CoA (filled triangles); (E) oleic acid (open circles) or oleoyl-CoA (filled triangles); (F) linoleic acid (open circles) or linoleoyl-CoA (filled triangles); (G) arachidonic acid (open circles) or arachidonoyl-CoA (filled triangles); (H) eicosapentaenoic acid (open circles) or eicosapentaenoyl-CoA (filled triangles); (I) docosapentanoic acid (open circles) or docosapentanoyl-CoA (filled triangles); (J) docosahexanoic acid (open circles) or docosahexanoyl-CoA (filled triangles); and (K), clofibrate (open circles) or rosiglitzone (filled triangles). Each spectrum represents an average of 5 scans for a given representative spectrum from at least three replicates.

**Table III.** Effect of ligands on the relative proportion of hPPARα secondary structure determined by CD. These structures were as follows: total helices (H; a sum of regular α-helices and distorted α-helices), total sheets (S; a sum of regular β-sheets and distorted β-sheets), turns (Trn; *β*-turns), and unordered (Unrd) structures.

| **Average** | **Total H ± S.E.** | **Total S ± S.E.** | **Trn ± S.E.** | **Unrd ± S.E.** |
|---|---|---|---|---|
| hPPARα | 32±1 | 19±1 | 21.3±0.3 | 29.3±0.5 |
| hPPARα + lauric acid | 30±1 | 20±2 | 21.8±0.4 | 28.7±0.3 |
| hPPARα + lauryl-CoA | 31±3 | 18.2±0.2 | 20±1 | 29±1 |
| hPPARα + palmitic acid | 16±3** | 32±2** | 21.7±0.4 | 30±1 |
| hPPARα + palmitoyl-CoA | 13±3** | 34±2** | 22.5±0.2 | 30±1 |
| hPPARα + palmitoleic acid | 22±4* | 28±3* | 21±1 | 28±1 |
| hPPARα + palmitoleoyl-CoA | 24±5# | 27±3* | 21±1 | 29±1 |
| hPPARα + stearic acid | 14±3** | 33±2** | 22.0±0.2 | 31±2 |
| hPPARα + stearyl-CoA | 24±4# | 27±2* | 21±1 | 29±1 |
| hPPARα + oleic acid | 18±2** | 31±2** | 22±1 | 29±1 |
| hPPARα + oleoyl-CoA | 26±3 | 25±2# | 21±1 | 28.3±0.3 |
| hPPARα + linoleic acid | 27±6 | 28±2* | 19±2* | 26±3 |
| hPPARα + linoleoyl-CoA | 24±3# | 26±2* | 21±1 | 28.8±0.1 |
| hPPARα + arachidonic acid | 19±1* | 30±1** | 21.8±0.3 | 28.9±0.1 |
| hPPARα + arachidonoyl-CoA | 30±1 | 23.4±0.4 | 19.4±0.5# | 26.9±0.4 |
| hPPARα + EPA | 14±7** | 24±6 | 23±2 | 33±5 |
| hPPARα + EPA-CoA | 21±1* | 29±1* | 21.6±0.3 | 29±1 |
| hPPARα + DPA | 17±4** | 32±3** | 21.9±0.1 | 30±1 |
| hPPARα + DPA-CoA | 20±1* | 30±1** | 21±1 | 29.6±0.2 |
| hPPARα + DHA | 12±3** | 38±4** | 21±1 | 30±1 |
| hPPARα + DHA-CoA | 20±2* | 29±2* | 22±1 | 28.9±0.2 |
| hPPARα + Clofibrate | 33±1 | 15±1* | 22±1 | 30±1 |
| hPPARα + Rosiglitazone | 29±1 | 22±2 | 20±1 | 28±1 |

Asterisks represent significant differences between hPPARα only and hPPARα in the presence of added ligand (* $P < 0.05$, ** $P < 0.001$ and # $P = 0.07$).

*Effect of endogenous fatty acids and fatty acyl-CoAs on mPPARα secondary structure:* Consistent with hPPARα the far UV circular dichroic spectrum of mPPARα suggested the presence of substantial α-helical content, exhibiting a large positive peak at 192 nm and two negative peaks at 207 and 222 nm (Fig. 14A-K, filled circles). Quantitative analyses of the circular dichroic spectra confirmed that mPPARα was composed of approximately 30 % α-helix, 19 % β-sheets, 22 % β-turns, and 29 % unordered structures (Table IV), similar to hPPARα (Table III). With the exception of lauric acid and lauryl-CoA (Fig. 14A), the addition of fatty acids (Fig. 14B-J, open circles) and fatty acyl-CoA (Fig. 14B-J, filled triangles) resulted in mPPARα conformational changes consistent with decreased molar ellipticity at 192 nm and increased molar ellipticity at 207 and 222 nm. Addition of clofibrate resulted in the strongest changes to the mPPARα spectrum, but consistent with binding data, no changes were seen with the addition of rosiglitazone (Fig. 14K). Quantitative analyses of multiple replicates indicated that LCFA and LCFA-CoA significantly decreased the mPPARα estimated α-helical content and concomitantly increased the estimated percentage of α-sheets (Table IV), a trend similar to that seen with hPPARα. However, for several ligands the magnitude of the change was different between the two proteins. While palmitic acid and stearic acid resulted in some of the strongest changes to the hPPARα structure, addition of these same ligands resulted in some of the weakest changes seen to the mPPARα structure. Moreover, clofibrate had the strongest effect on mPPARα secondary structure and a very small effect on hPPARα secondary structure. The changes in circular dichroic spectra and estimated percentage composition were consistent with the affinity of mPPARα for each ligand. These data

further suggest that species differences in ligand specificity and affinity exist between mouse and human PPARα.

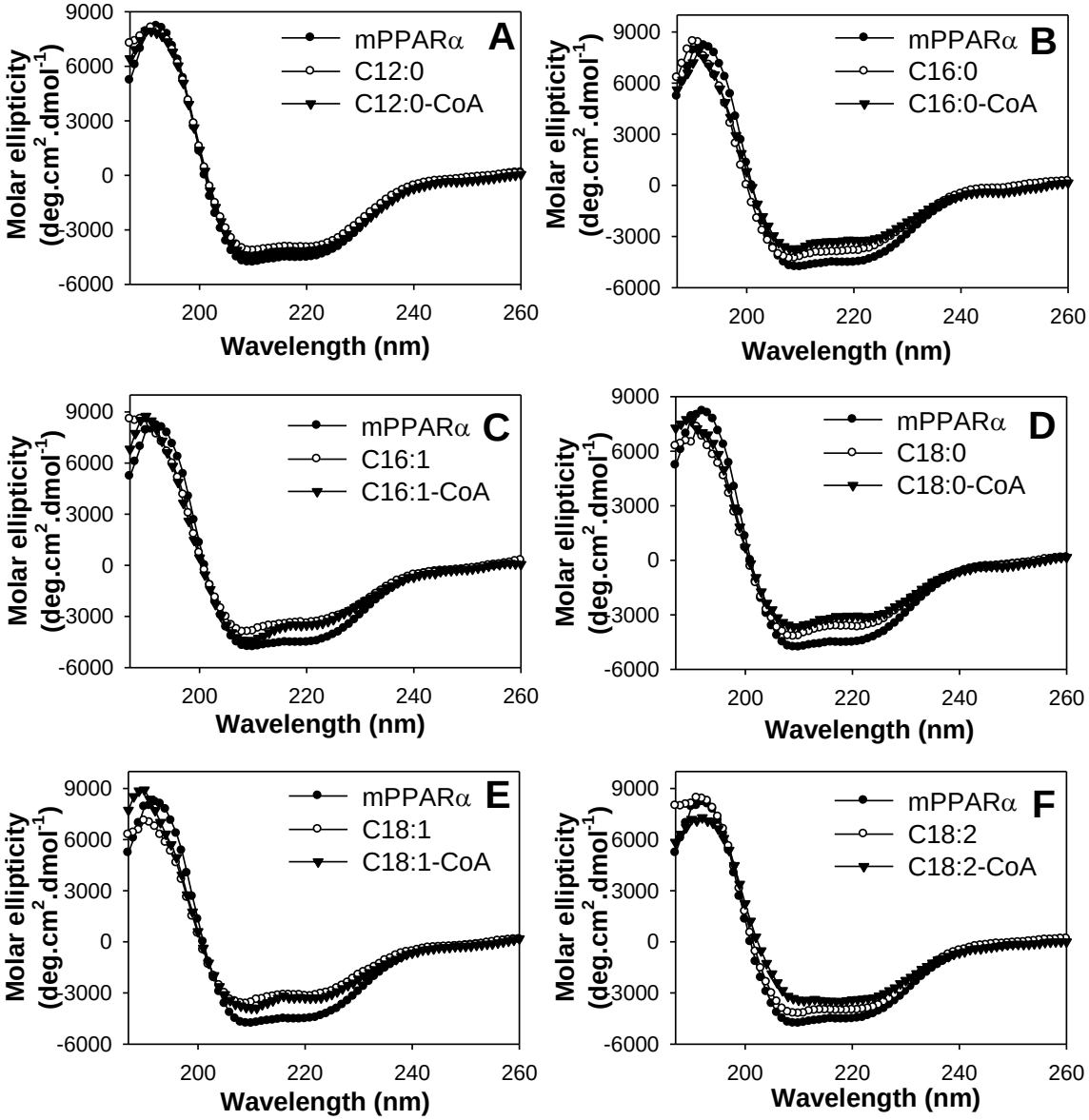
A
mPPARα
C12:0
C12:0-CoA
B
mPPARα
C16:0
C16:0-CoA
C
mPPARα
C16:1
C16:1-CoA
D
mPPARα
C18:0
C18:0-CoA
E
mPPARα
C18:1
C18:1-CoA
F
mPPARα
C18:2
C18:2-CoA
Molar ellipticity (deg.cm2.dmol-1)
Wavelength (nm)
9000
6000
3000
0
-3000
-6000
200
220
240
260

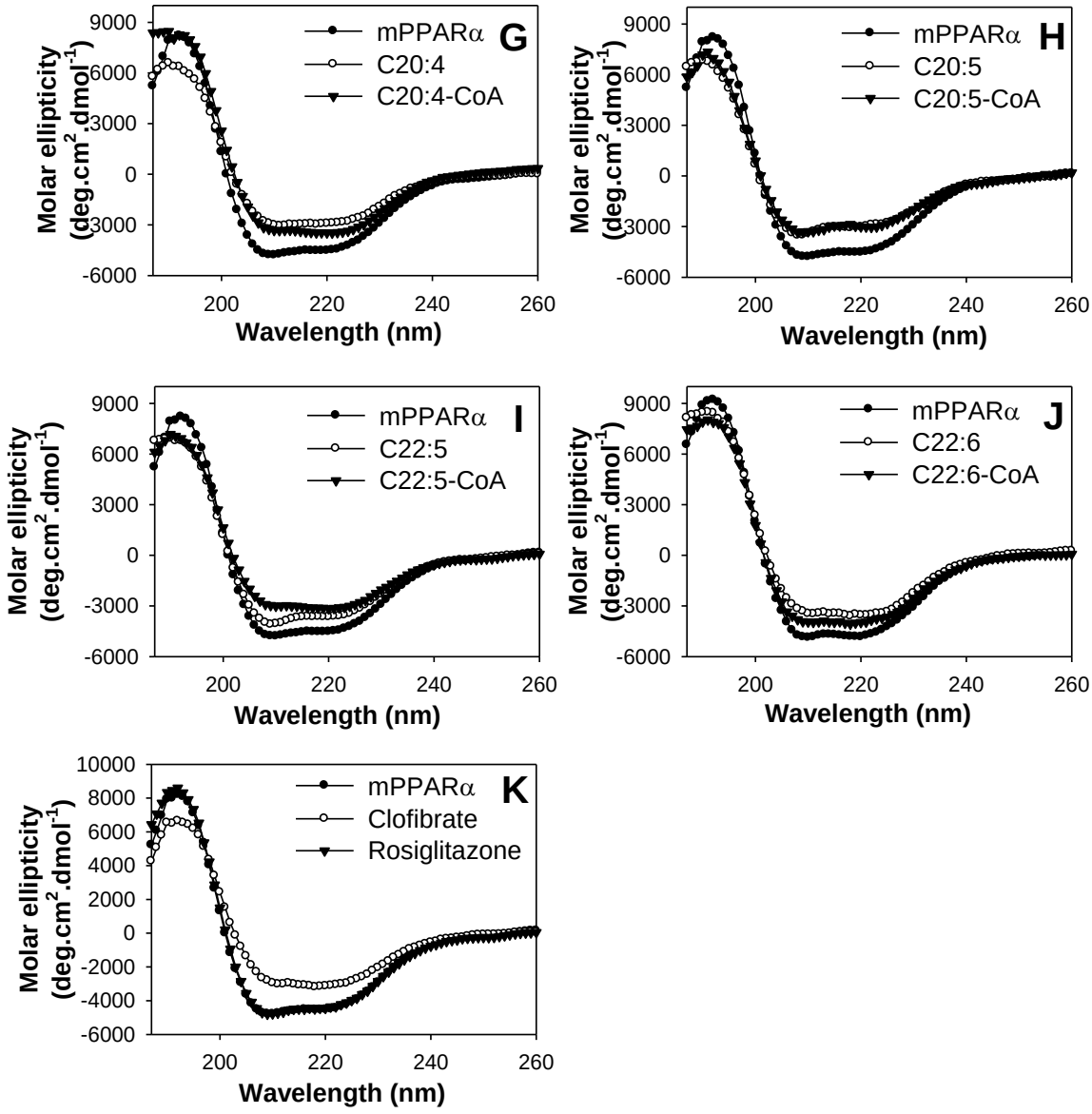
G
mPPARα
C20:4
C20:4-CoA
H
mPPARα
C20:5
C20:5-CoA
I
mPPARα
C22:5
C22:5-CoA
J
mPPARα
C22:6
C22:6-CoA
K
mPPARα
Clofibrate
Rosiglitazone
Molar ellipticity (deg.cm2.dmol-1)
Wavelength (nm)

**Fig. 14.** Far UV circular dichroic (CD) spectra of mPPARα in the absence (filled circles) and presence of added ligand: (A) lauric acid (open circles) or lauryl-CoA (filled triangles); (B) palmitic acid (open circles) or palmitoyl-CoA (filled triangles); (C) palmitoleic acid (open circles) or palmitoleoyl-CoA (filled triangles); (D) stearic acid (open circles) or stearoyl-CoA (filled triangles); (E) oleic acid (open circles) or oleoyl-CoA (filled triangles); (F) linoleic acid (open circles) or linoleoyl-CoA (filled triangles); (G) arachidonic acid (open circles) or arachidonoyl-CoA (filled triangles); (H) eicosapentaenoic acid (open circles) or eicosapentaenoyl-CoA (filled triangles); (I) docosapentanoic acid (open circles) or docosapentanoyl-CoA (filled triangles); (J) docosahexanoic acid (open circles) or docosahexanoyl-CoA (filled triangles); and (K), clofibrate (open circles) or rosiglitzone (filled triangles). Each spectrum represents an average of 10 scans for a given representative spectrum from at least three replicates.

**Table IV.** Effect of ligands on the relative proportion of mPPARα secondary structure determined by CD. These structures were as follows: total helices (H; a sum of regular α-helices and distorted α-helices), total sheets (S; a sum of regular β-sheets and distorted β-sheets), turns (Trn; *β*-turns), and unordered (Unrd) structures.

| **Average** | **Total H ± S.E.** | **Total S ± S.E.** | **Trn ± S.E.** | **Unrd ± S.E.** |
|---|---|---|---|---|
| mPPARα | 30±1 | 19±2 | 22±1 | 29±1 |
| mPPARα + lauric acid | 29±1 | 20±1 | 22±1 | 28.8±0.1 |
| mPPARα + lauryl-CoA | 27±3 | 23±3 | 22.1±0.1 | 28.9±0.1 |
| mPPARα + palmitic acid | 23±3* | 23±2 | 21±2 | 30±2 |
| mPPARα + palmitoyl-CoA | 16±1** | 32±1** | 23±1 | 29.2±0.2 |
| mPPARα + palmitoleic acid | 14±1** | 29±1* | 23±1 | 34±5 |
| mPPARα + palmitoleoyl-CoA | 19±1* | 34±5** | 21±1 | 28±1 |
| mPPARα + stearic acid | 21.8±0.5* | 28±0.5* | 21.2±0.1 | 28.6±0.2 |
| mPPARα + stearyl-CoA | 21±2* | 30±4* | 21±1 | 29.7±0.3 |
| mPPARα + oleic acid | 10±4** | 36±3** | 23±2 | 31±1 |
| mPPARα + oleoyl-CoA | 22±4* | 28±2* | 20±1 | 29±1 |
| mPPARα + linoleic acid | 21±1* | 30±1* | 22±1 | 28.5±0.3 |
| mPPARα + linoleoyl-CoA | 17±2** | 33±2** | 22.0±0.5 | 28.7±0.1 |
| mPPARα + arachidonic acid | 18±1** | 31±1* | 22.5±0.5 | 28.7±0.2 |
| mPPARα + arachidonoyl-CoA | 22±3* | 28±3* | 21.7±0.1 | 28±1 |
| mPPARα + EPA | 15±2** | 31±3* | 21±1 | 30±1 |
| mPPARα + EPA-CoA | 22.5±1.5* | 28±2* | 20.1±0.3 | 30±1 |
| mPPARα + DPA | 20±1* | 29±1* | 22±1 | 29.1±0.3 |
| mPPARα + DPA-CoA | 16±3** | 34±3** | 22.1±0.2 | 27.9±0.5 |
| mPPARα + DHA | 16±5** | 30±4* | 21±1 | 30±2 |
| mPPARα + DHA-CoA | 9.5±0.5** | 37±1** | 21.9±0.2 | 31.8±0.2 |
| mPPARα + Clofibrate | 13±3** | 34±3** | 22.4±0.1 | 31±1 |
| mPPARα + Rosiglitazone | 27±2 | 24±3 | 25.5±3.5 | 23±2 |

Asterisks represent significant differences between mPPARα only and mPPARα in the presence of added ligand (* $P < 0.05$, ** $P < 0.001$).

*Effect of fatty acids and fatty acyl-CoA on transactivation of PPARα-RXRα heterodimers:* Since PPARα heterodimerizes with RXRα to induce transactivation (*7*), COS-7 cells were cotransfected with pSG5 empty vector, PPARα alone, RXRα alone, or PPARα with RXRα and analyzed for transactivation of an acyl-CoA oxidase PPRE-luciferase reporter construct in the absence or presence of ligands (Fig. 15). Transactivation was measured as percent firefly luciferase activity normalized to *Renilla* luciferase (internal control). In comparison to cells overexpressing RXRα alone (extremely low transactivation; Fig. 15A, 15B), cells overexpressing PPARα alone (Fig 15A, 15B) had significant transactivation even in the absence of ligands. While these findings could be a result of some basal endogenous levels of RXRα, they also suggest that transactivation is indeed mediated by PPARα. In cells overexpressing only hPPARα (Fig. 15A) or mPPARα (Fig. 15B), docosahexaenoic acid and clofibrate significantly increased transactivation. Although normalized activity was extremely low in hRXRα (Fig. 14A) and mRXRα (Fig. 15B) over-expressing cells, docosahexaenoic acid significantly increased transactivation in both, suggesting that this ligand (or its metabolite) is a strong activator of endogenous PPARα. While cells over-expressing hPPARα and hRXRα (Fig. 15A) or mPPARα and mRXRα (Fig. 15B) both showed increased activity, even in the absence of ligand, differences were noted in their ligand-induced effects. For cells over-expressing hPPARα and hRXRα, addition of palmitic acid, palmitoleic acid, stearic acid, oleic acid, eicosapentaenoic acid, and docosahexaenoic acid resulted in similar effects on transactivation as the PPARα agonist, clofibrate (Fig. 15A). These data further validated LCFA or their metabolites as endogenous ligands of hPPARα needed to induce PPARα activity. However,

addition of only the examined unsaturated LCFA and clofibrate significantly increased activity levels in COS-7 cells overexpressing mPPARα and mRXRα (Fig. 15B). The addition of the palmitic acid and stearic acid resulted in no significant changes in activity (Fig. 15B), consistent with the weak binding affinity of mPPARα for these ligands. In addition to suggesting that LCFA and LCFA-CoA represent high-affinity ligands for mPPARα, these data also suggested that differences in binding affinity for saturated LCFA could significantly affect the activity of PPARα.

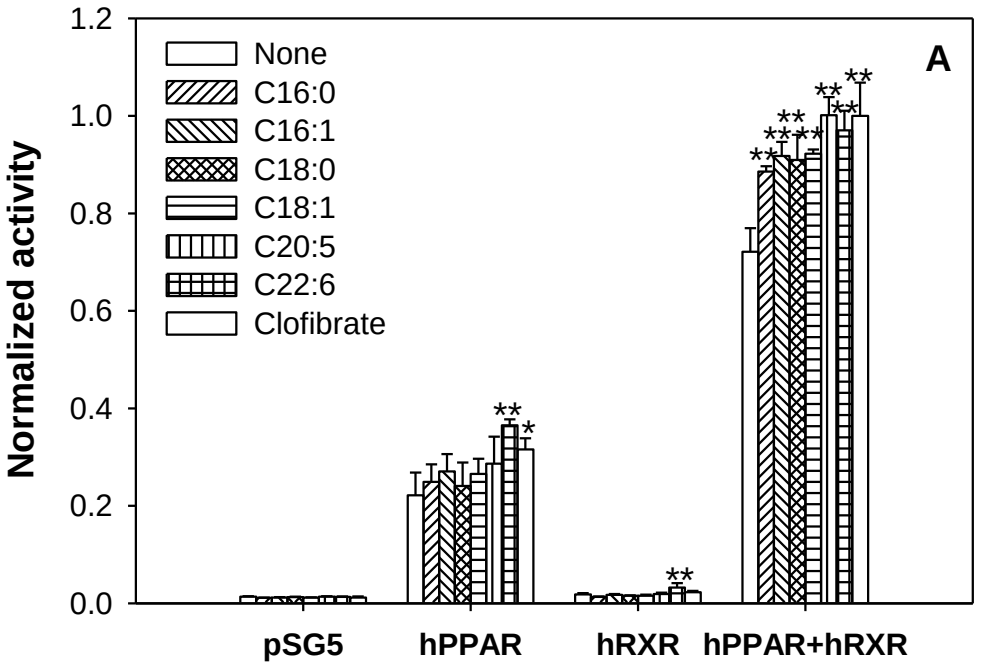
A
Normalized activity
1.2
1.0
0.8
0.6
0.4
0.2
0.0
None
C16:0
C16:1
C18:0
C18:1
C20:5
C22:6
Clofibrate
pSG5
hPPAR
hRXR
hPPAR+hRXR

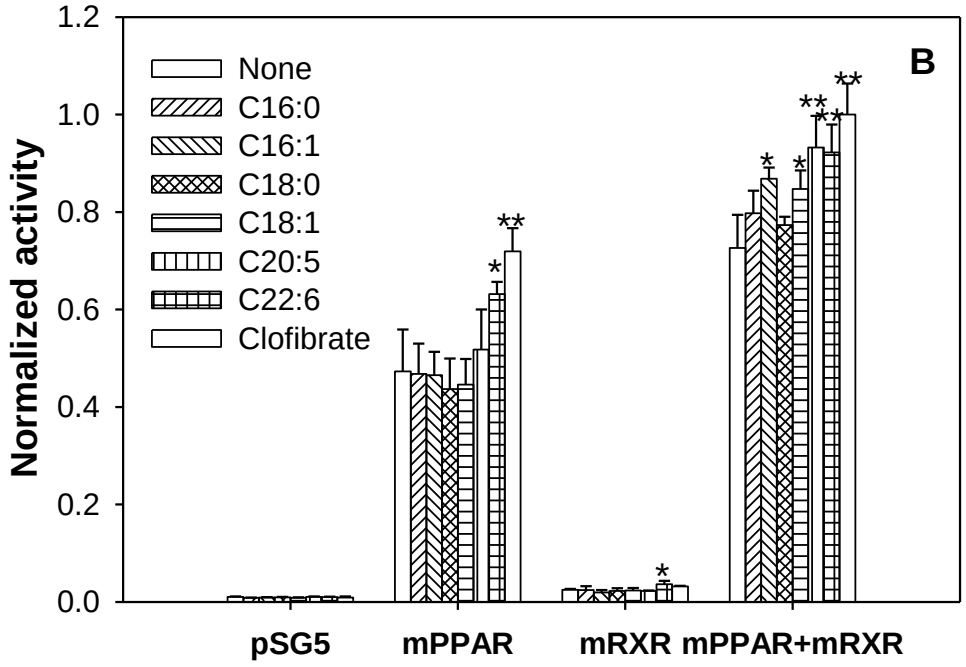
B
Normalized activity
1.2
1.0
0.8
0.6
0.4
0.2
0.0
None
C16:0
C16:1
C18:0
C18:1
C20:5
C22:6
Clofibrate
pSG5
mPPAR
mRXR
mPPAR+mRXR

**Fig. 15.** PPARα ligands alter PPARα transactivation. COS-7 cells transfected with pSG5 empty vector, PPARα, RXRα, and both PPARα and RXRα were analyzed for transactivation of the acyl-CoA oxidase-PPRE-luciferase reporter construct in the presence of vehicle (*open bars*), 1 μM palmitic acid (*diagonally upward bars*), 1 μM palmitoleic acid (*diagonally downward bars*), 1 μM stearic acid (*cross-hatched bars*), 1 μM oleic acid (*horizontal lined bars*), 1 μM eicosapentaenoic acid (*vertically lined bars*), 1 μM docosahexanoic acid (*hatched bars*), and 1 μM clofibrate (*open bars*). For comparison between human and mouse effects, COS-7 cells were transfected with human versions of these proteins (A) or mouse versions of these proteins (B). The *y-axis* represents values for firefly luciferase activity that have been normalized to *Renilla* luciferase (internal control), where PPARα and RXRα overexpressing cells in the presence of 1 μM clofibrate were arbitrarily set to 1. The bar graph represents the mean values ($n \geq 3$) ± standard error. * $P < 0.05$, ** $P < 0.01$.

## 5. Discussion

Although lipids have been shown to be endogenous ligands of PPARα from several species, including mouse, studies with hPPARα have focused on exogenous ligands. Since an increasing number of studies suggest species differences exist for ligand specificity and affinity (*102, 161-163*), this study focused on LCFA and/or LCFA-CoA as putative endogenous ligands of hPPARα. These data are the first to demonstrate full-length hPPARα binding to LCFA and LCFA-CoA at physiologically relevant concentrations. Human PPARα displayed high affinity binding for saturated, monounsaturated, and polyunsaturated LCFA and LCFA-CoA ($K_d$ = 11-40 nM), consistent with previously reported nuclear concentrations (3-68 nM) of LCFA and LCFA-CoA (*88, 120*). These high affinity ligands significantly altered the secondary structure of hPPARα, while ligands that did not bind hPPARα (lauric acid, lauryl-CoA, and rosiglitazone) did not demonstrate any significant change in the structure of the protein. LCFA that bound to hPPARα *in vitro* transactivated the ACOX PPRE-luciferase reporter in a PPARα dependent manner in COS-7 cells, further suggesting that LCFA and LCFA-CoA are endogenous ligands of hPPARα. These data are consistent with experiments using peroxisomal ACOX and/or PPARα knockout mice which also suggest that LCFA and their thioester derivatives serve as natural ligands for PPARα *in vivo* (*145, 146, 183*).

Apart from identifying LCFA and LCFA-CoA as physiologically relevant endogenous ligands for hPPARα, these data highlight important species differences with respect to ligand specificity and affinity. While affinities for LCFA-CoA and unsaturated LCFA were similar between full-length human and murine PPARα,

mPPARα only weakly bound the saturated palmitic acid and stearic acid, yet hPPARα strongly bound both. Similarly, some of the strongest changes in hPPARα secondary structure occurred with the addition of saturated and polyunsaturated LCFA, whereas saturated LCFA had only minor effects on mPPARα secondary structure. Consistent with these data, COS-7 cells overexpressing mPPARα and mRXRα treated with these saturated LCFA did not transactivate the ACOX-PPRE-luciferase reporter at the examined concentrations, while unsaturated LCFA did. Taken together, these data suggested that the human and mouse PPARα proteins bind and respond differently to specific ligands.

Given the high evolutionary rate exhibited by PPARα (*184*), it is not surprising to see such differences between hPPARα and mPPARα. In addition, strong physiological differences exist between human and rodent PPARα activation. Long-term administration of PPARα agonists are associated with hepatic carcinomas in rodents, but "humanized" PPARα mice are resistant to PPARα agonist induced hepatocellular adenomas and carcinomas (*102, 150*). The potency and efficacy of many hypolipidemic agents and phthalate monoesters on the activation of human and mouse PPARα are also different (*161-163*). As previous microarray experiments have demonstrated a strong divergence between PPARα regulated genes in mouse and human hepatocytes (*163*), it is likely that a combination of ligand binding differences and target gene differences are responsible for the overall physiological variations. Other factors, including differences in ligand uptake and ligand metabolism between cell types, may account for some of these differences as well. However, this same study showed a high conservation in PPARα regulation of genes involved in lipid

metabolism (*163*), suggesting that differences in these processes must be due to another mechanism – not just variation in target genes. Since a single mutation in the mouse PPARα ligand binding domain (E282G) results in altered activity but displays similar DNA binding capacity, protein levels, and protein localization (*164*), it suggests that individual amino acid differences in the ligand binding domain can affect activity through ligand binding. Such differences in specificity of mouse and human PPARα for specific nutrients could reflect an adaptation to different physiological and/or nutritional patterns of the species.

Additionally, these data suggest that differences exist in the binding affinity of full-length versus truncated PPARα. Data presented herein indicate that both full-length hPPARα and mPPARα bound polyunsaturated LCFA with strong affinity. This data challenges previously published data indicating that mouse PPARα does not bind saturated LCFA in the physiological range, and only weakly interacts with PUFA (*115-117*). While such differences may exist due to variations in protein preparation, ligand binding techniques, or changes in the protein's secondary structure, it should be noted that the previously published data was generated using a truncated mouse PPARα protein that lacked the N-terminus (mPPARΔAB). Therefore, it is possible that the N-terminal domain of PPARα influences ligand binding. This hypothesis is supported in the case of PPARα, where it was shown that mutation of specific residues within the N-terminal A/B domain affects the binding affinity of a synthetic PPARα agonist (*34*).

In summary, LCFA and LCFA-CoA function as endogenous hPPARα ligands; binding with high affinity, altering PPARα secondary structure, and affecting transactivation. Although LCFA-CoA similarly bound both hPPARα and mPPARα,

several ligands (including fluorescent LCFA/LCFA-CoA analogues, saturated LCFA, PUFA, and clofibrate) resulted in significant species differences. These data suggest that even though there is overlap in the endogenous ligands for mouse and human PPARα, significant species differences exist, and these differences may affect downstream gene regulation. These findings corroborate the importance of PPARα in allosteric regulation of fatty acid metabolism, where PPARα acts as a sensor to monitor the levels of fatty acids and their metabolites, then transcriptionally activates enzymes involved their metabolism.

# CHAPTER II

## A SINGLE AMINO ACID CHANGE HUMANIZES LONG-CHAIN FATTY ACID BINDING AND ACTIVATION OF MOUSE PEROXISOME PROLIFERATOR-ACTIVATED RECEPTOR α

## 1. Abstract

Peroxisome proliferator-activated receptor α (PPARα) is an important regulator of hepatic lipid metabolism which functions through ligand binding. Despite high amino acid sequence identity (>90%), marked differences in PPARα ligand binding, activation and gene regulation have been noted across species. Similar to previous observations with synthetic agonists, we have recently reported differences in ligand affinities and extent of activation between human PPARα (hPPARα) and mouse PPARα (mPPARα) in response to long chain fatty acids (LCFA). The present study was aimed to determine if structural alterations could account for these differences. The binding of PPARα to LCFA was examined through *in silico* molecular modeling and docking simulations. Modeling suggested that variances at amino acid position 272 are likely to be responsible for differences in saturated LCFA binding to hPPARα and mPPARα. To confirm these results experimentally, LCFA binding, circular dichroism, and transactivation studies were performed using a F272I mutant form of mPPARα. Experimental data correlated with *in silico* docking simulations, further confirming the importance of amino acid 272 in LCFA binding. Although the driving force for evolution of species differences at this position are yet unidentified, this study enhances our understanding of ligand-induced regulation by PPARα and demonstrates the efficacy of molecular modeling and docking simulations (*185*).

## 2. Introduction

Peroxisome proliferator-activated receptor alpha (PPARα) belongs to the nuclear hormone receptor superfamily of ligand-dependent transcription factors and has emerged as one of the central regulators of nutrient-gene interactions. Structurally similar to other members of the nuclear hormone receptor family, the PPARα protein structure consists of an N-terminal ligand-independent transactivation function (AF-1), a highly conserved DNA binding domain (DBD), a hinge region and the C-terminal ligand binding domain (LBD) containing a ligand-dependent transactivation function (AF-2). The LBD of PPARα constitutes a large hydrophobic ligand-binding pocket (1300-1400 $Å^3$) that allows interaction with a broad range of natural and synthetic ligands (*25, 26*). PPARα interacts with a variety of endogenous ligands, including fatty acids and fatty acid metabolites, as well as synthetic compounds such as hypolipidemic fibrate drugs, to regulate cellular processes related to fatty acid metabolism, glucose metabolism, inflammation, differentiation and proliferation (*83, 108, 113, 186*).

While long-chain fatty acids (LCFA) serve as major metabolic fuels and important components of biological membranes, they also play a significant role as signaling molecules and gene regulators in response to food intake and nutritional changes. Recently, we have demonstrated that LCFA and their thioesters (long-chain fatty acyl-CoA; LCFA-CoA) constitute high-affinity endogenous ligands of human PPARα (hPPARα) and mouse PPARα (mPPARα). Such ligand binding induces PPARα conformational changes and increases transactivation, consistent with expectations for an endogenous ligand of a ligand-activated nuclear receptor (*165*). Thus, PPARα in conjunction with LCFA and their metabolites could serve to regulate metabolic pathways

governing fuel utilization, storage, transport and mobilization. However, we also reported differences in binding affinities and the extent of ligand-induced transactivation between mPPARα and hPPARα in response to saturated LCFA (*165*).

Species differences in PPARα-mediated downstream regulation of target genes have been noted previously (*163, 187*). Human and mouse PPARα proteins promote transcription to a different extent in response to certain hypolipidemic agents and pthalate monoesters (*161, 162*). Furthermore, it is well established that long-term administration of PPARα agonists result in hepatic cancer in rats and mice – an effect that is not seen in guinea pigs, canines, non-human primates, or even humans (*102*). While a single cause for the existence of such differences is highly unlikely, possible explanations include: differences in expression levels of PPARα or differences in PPARα target genes, alternatively spliced or mutant forms of PPARα protein, mutations or polymorphisms in target gene response elements, increased expression of oncogenes and/or inhibition of apoptosis (*102, 103, 188, 189*). However, transgenic mice that express human PPARα mainly in the liver do not exhibit hepatocarcinogenesis upon administration of PPARα agonists (*149, 150*). This observation suggests that structural differences in the PPARα protein could be the underlying cause of such species variation.

Comparison of the PPARα amino acid sequence across species, particularly of the LBD, resulted in >90% homology (*18*). However it should be noted that a single amino acid change can result in marked alterations in ligand selectivity of nuclear receptors. For example, a single amino acid change in the mouse PPARα-LBD (E282) results in altered activity of the protein (*164*), and a valine to methionine substitution in human PPARα (V444M) produced PPARδ ligand binding characteristics, resulting in loss of fibrate

responsiveness (*52*). While we have reported differences in mPPARα and hPPARα in response to saturated LCFA (*165*), the goal of this study was to explore the mechanisms underlying such divergence. We have used methods including: molecular modeling and *in silico* docking, mutagenesis, spectrofluorometry, circular dichroism spectroscopy and transactivation studies to identify a single amino acid change at position 272 that is largely responsible for the altered saturated LCFA binding.

## 3. Material and Method

*Molecular modeling simulations:* The crystal structure of the ligand binding domain (LBD) of hPPARα complexed with a synthetic agonist (GW409544) was retrieved from RCSB Protein Data Bank (PDB identifier 1K7L) (*26*). The apo form of hPPARα-LBD was generated by extracting the ligand (GW409544) from the 1K7L model (using Swiss PDB Viewer, http://www.expasy.org/spdbv/). This structural model was used in all docking simulations. Since the structure of mPPARα has not been crystallized, a homology modeling approach was used to generate the mPPARα-LBD structure. We compared the amino acid sequence of hPPARα to mPPARα and substituted all amino acid residues that were different in the hPPAR-LBD crystal structure. In total, 23 amino acid residues in the hPPARα-LBD were replaced with the corresponding mPPARα residues, followed by energy minimization of the resulting model. This model was used as an initial structure of mPPARα-LBD for all docking simulations. All energy computations were done in vacuo using GROMOS96 43B1 parameters without reaction field, implemented in Swiss PDB Viewer (*190*). An energy minimized model of the F272I mPPARα-LBD was also generated using the Swiss PDB Viewer (http://www.expasy.org/spdbv/).

*Molecular docking simulations: In silico* docking studies were performed using both AutoDock Vina 1.1.2 (*191*) and the FlexiDock™ module available on SYBYL®-X 2.0 (Tripos, St. Louis, MO). While AutoDock Vina 1.1.2 allows only the ligand to have flexible/rotatable bonds, the FlexiDock™ module on SYBYL®-X 2.0 permits both protein (sidechains) and ligands to carry flexible/rotatable bonds. For docking with both AutoDock Vina 1.1.2 and FlexiDock™, a search space or putative binding site was

defined in a restricted region of the protein. In the present study, the ligand binding pocket was defined based on the experimentally obtained structure of the GW409544 ligand bound to hPPARα-LBD (*26*). Once the hPPARα and mPPARα models were energy minimized, docking simulations were carried out using both AutoDock Vina 1.1.2 and FlexiDock™. Docking simulations were first validated using the GW409544 ligand by comparing the x-ray crystal structure 1K7L (hPPARα-LBD + GW409544) with that of the docking output generated using apo-hPPARα with GW409544 ligand. Both AutoDock Vina 1.1.2 and FlexiDock™ generated multiple docking poses (differentiated by RMSD's relative to the best pose) that were subjected to careful visualization and only the most energetically favorable conformation was chosen for further analysis.

Docking of LCFA was carried out using both AutoDock Vina 1.1.2 and FlexiDock™. For each binding conformation, the binding energies were calculated using the FlexiDock scoring function based on the Tripos Force Field, as implemented by FlexiDock. The resulting docking conformations were visualized using the PyMOL Molecular Graphics System (Version 1.5.0.4 Schrödinger, LLC) and the program LIGPLOT (*192*). Further, in order to determine the volumes of the ligand binding pockets of PPARα, we took advantage of the POVME algorithm (*193*). Based on the occupancy of GW409544 within the hPPARα ligand binding pocket we defined the ligand binding pocket using 37 overlapping inclusion spheres. This pocket was visualized using the Visual Molecular Dynamics (VMD) program (*194*), and volume-grid points near the protein atoms were systematically deleted with a padding variable of 1.09 (radius of a hydrogen atom) or 0.5 (half of a carbon-hydrogen bond length) using POVME (*193*). This was followed by volume measurement of each resultant binding pocket.

*Chemicals:* Fluorescent fatty acid (BODIPY-C16) was purchased from Molecular Probes, Inc. (Eugene, OR). Docosahexaenoyl-CoA and BODIPY C16-CoA were synthesized and purified by HPLC as previously described (in Chapter I and (*117*, *171*)), and found to be >99% unhydrolyzed. All other fatty acid ligands and clofibrate were from Sigma-Aldrich (St. Louis, MO). Rosiglitazone (LKT labs) was a kind gift from Dr Khalid Elased and bovine serum albumin (lipid-free) was obtained from Gemini Bioproducts (Sacramento, CA).

*Purification of Recombinant F272I mutant mPPARα protein:* The cloning and purification of wild-type 6xHis-GST-mPPARα has already been described in (*165*) and in chapter I of this dissertation. A mutant form of full-length mPPARα (amino acids 1-468) in which the phenylalanine residue at 272 in helix 3 was replaced by isoleucine (F272I; to mimic hPPARα) was used for all experiments presented herein. The bacterial expression plasmid for full-length F272I mutant mPPARα (6xhis-GST-F272I mPPARα) was produced by Dr. S. Dean Rider, Jr. (Wright State University). The full-length recombinant mutant F272I mPPARα protein was expressed in Rosetta$^{TM}$2 cells (Novagen, Gibbstown, NJ) and purified as described previously in chapter I and (*165*) for the wild-type. The protein purity was verified using SDS-PAGE with Coomassie blue staining and immunoblotting. Protein concentrations were estimated by Bradford Assay (Bio-Rad Laboratories, Hercules, CA) and by absorbance spectroscopy using the molar extinction coefficient for the protein.

*Fluorescence based Ligand Binding Assays:* The binding affinity of F272I mPPARα to a fluorescent 16 carbon fatty acid analogue (BODIPY C16) or its CoA thioester (BODIPY C16-CoA) was determined as described previously for wild-type mPPARα and

hPPARα in chapter I and (*165*). Based on the binding affinities obtained herein, displacement assays were performed in the presence of BODIPY C16-CoA (110 nM) using non-fluorescent LCFA and LCFA-CoA as described in chapter I and (*165*). The maximal fluorescence intensity was measured, and the effect of increasing concentrations of naturally-occurring non-fluorescent ligands was measured as a decrease in fluorescence. The direct binding of F272I mPPARα to non-fluorescent ligands was also determined by quenching of intrinsic PPARα aromatic amino acid fluorescence as described in chapter I of this dissertation for wild-type mPPARα and hPPARα (*165, 173*). For all measurements, emission spectra were corrected for background and inner-filter effects were avoided. Changes in fluorescence intensity were used to calculate the dissociation constant ($K_d$), inhibition constant ($K_i$) and the number of binding sites ($n$) as described in chapter 1 of this dissertation.

*Circular Dichroism*: Circular dichroic spectra of F272I mPPARα (0.6 μM in 600 μM HEPES pH 8.0, 24 μM dithiothreitol, 6 μM EDTA, 6mM KCl and 0.6 % glycerol) were recorded in the presence and absence of LCFA and LCFA-CoA (0.6 μM) with a J-815 spectropolarimeter (Jasco Inc., Easton, MD) as previously described in chapter I for the wild-type mPPARα and hPPARα (*165*). Spectra were recorded from 260 to 187 nm with a bandwidth of 2.0 nm, sensitivity of 10 millidegrees, scan rate of 50 nm/min and a time constant of 1 s. Ten scans per replicate were averaged, and the average spectrum was used to determine the percent composition of α-helices, β-strands, turns and unordered structures with the CONTIN/LL program of the software package CDpro (*117, 179*).

*Mammalian Expression Plasmids:* The pSG5-hPPARα, pSG5mPPARα, pSG5-hRXRα and pSG5-mRXRα plasmids have been described in chapter I of this dissertation

(*165*). The F272I mutant mPPARα was amplified from 6xhis-GST-F272I mPPARα using the following primers: 5'-cggatccaccATGGTGGACACAGAGAGCCC-3' and ctcctcgagTCAGTACATGTCTCTGTAGA-3'. In these primers, lowercase represents nucleotides outside of the PPARα open reading frame and restriction sites are underlined. The PCR product was cloned into the pGEM®-T easy vector (Promega Corp., Madison, WI). A *Bam* HI / end-filled *Xho* I F272I mutant mPPARα fragment was subcloned into the *Bam* HI / end-filled *Bgl* II multiple cloning site of pSG5 (Stratagene, La Jolla, CA) to produce pSG5-F272I mPPARα. The reporter construct, PPRE×3 TK LUC was a kind gift of Dr. Bruce Spiegelman (Addgene plasmid # 1015) and contained three copies of the acyl-CoA oxidase (ACOX) peroxisome proliferator response element (PPRE) (*180*).

*Cell culture and Transactivation assay:* COS-7 cells (ATCC, Manassas, VA) were grown in DMEM supplemented with 10 % fetal bovine serum (Invitrogen, Grand Island, NY), at 37°C with 5% $CO_2$ in a humidified chamber. Cells were seeded onto 24-well culture plates and transfected with Lipofectamine™ 2000 (Invitrogen, Grand Island, NY) and 0.4 μg of each full-length mammalian expression vector (pSG5-hPPARα and pSG5-hRXRα, pSG5-mPPARα and pSG5-mRXRα, pSG5- F272I mPPARα and pSG5-mRXRα,) or empty plasmid (pSG5), 0.4 μg of the PPRE×3 TK LUC reporter construct, and 0.04 μg of the internal transfection control plasmid pRL-CMV (Promega Corp., Madison, WI) as previously described in chapter 1. Following transfection incubation, medium was replaced with serum-free medium for 2 h, ligands (1μM) were added, and the cells were grown for an additional 20 h. Fatty acids were added as a complex with bovine serum albumin (BSA) as described (*117, 195*). Firefly luciferase activity, normalized to *Renilla* luciferase (for transfection efficiency), was determined with the

dual luciferase reporter assays system (Promega Corp., Madison, WI) and measured with a SAFIRE$^2$ microtiter plate reader (Tecan Systems, Inc. San Jose, CA). The clofibrate treated samples in each case, overexpressing both PPARα and RXRα, were arbitrarily set to 1.

*Statistical Analysis:* Data were analyzed using a one-way ANOVA to evaluate overall significance (SigmaPlot™, Systat Software, San Jose, CA). A Fisher Least Significant Difference (LSD) post-hoc test was used to identify individual group differences. The results are presented as mean ± SEM. The confidence limit of $p < 0.05$ was considered statistically significant.

## 4. Results and Discussion

Since its discovery and cloning, PPARα has been shown to be activated by structurally diverse ligands, including the fibrate class of drugs, some herbicides, phthalate monoesters, fatty acids and fatty acid derivatives (*83, 108, 113, 117, 186*). However, a vast array of studies have highlighted species differences not just with respect to gene regulation (*163, 187*), but also in binding or activation of PPARα (*102, 161, 162*). For example, mouse and human PPARα display differences in ligand binding, activation and physiological responses upon administration of certain hypolipidemic agonists, phthalate monoesters and LCFA (*161, 162, 165*). The present study examines structural differences in the PPARα proteins, which could be an underlying cause of species differences in ligand binding.

*Molecular modeling simulations of hPPARα-LBD and mPPARα-LBD:* The X-ray crystal structure of hPPARα is composed of a helical sandwich and a four-stranded β-sheet. The Y-shaped PPARα ligand binding pocket (≈ 1400 $Å^3$) spans between the C-terminal helix 12 (containing the AF-2) and the 4 stranded β-sheet, splitting into 2 arms roughly parallel to helix 3 (*26*). In order to investigate the mechanisms underlying differential binding and activation of mouse and human PPARα in response to LCFA, the amino acid sequences of mPPARα and hPPARα were compared. While human and mouse PPARα proteins (468 amino acids) bear approximately 92% sequence identity, there are 35 amino acid differences (Fig. 16).

**Fig. 16**. Primary amino acid sequence of human and mouse PPARα. The N-terminal domain in depicted in black, DNA binding domain in red, hinge region in green and ligand binding domain in blue. The different amino acids between human and mouse PPARα are highlighted in yellow.

| Human PPARα | | | | | |
|---|---|---|---|---|---|
| 1 | MVDTESPLCP | LSPLEAGDLE | SPLSEEFLQE | MGNIQEISQS | IGEDSSGSFG |
| 51 | FTEYQYLGSC | PGSDGSVITD | TLSPASSPSS | VTYPVVPGSV | DESPSGALNI |
| 101 | ECRICGDKAS | GYHYGVHACE | GCKGFFRRTI | RLKLVYDKCD | RSCKIQKKNR |
| 151 | NKCQYCRFHK | CLSVGMSHNA | IRFGRMPRSE | KAKLKAEILT | CEHDIEDSET |
| 201 | ADLKSLAKRI | YEAYLKNFNM | NKVKARVILS | GKASNNPPFV | IHDMETLCMA |
| 251 | EKTLVAKLVA | NGIQNKEAEV | RIFHCCQCTS | VETVTELTEF | AKAIPGFANL |
| 301 | DLNDQVTLLK | YGVYEAIFAM | LSSVMNKDGM | LVAYGNGFIT | REFLKSLRKP |
| 351 | FCDIMEPKFD | FAMKFNALEL | DDSDISLFVA | AIICCGDRPG | LLNVGHIEKM |
| 401 | QEGIVHVLRL | HLQSNHPDDI | FLFPKLLQKM | ADLRQLVTEH | AQLVQIIKKT |
| 451 | ESDAALHPLL | QEIYRDMY | | | |
| Mouse PPARα | | | | | |
| 1 | MVDTESPICP | LSPLEADDLE | SPLSEEFLQE | MGNIQEISQS | IGEESSGSFG |
| 51 | FADYQYLGSC | PGSEGSVITD | TLSPASSPSS | VSCPVIPAST | DESPGSALNI |
| 101 | ECRICGDKAS | GYHYGVHACE | GCKGFFRRTI | RLKLVYDKCD | RSCKIQKKNR |
| 151 | NKCQYCRFHK | CLSVGMSHNA | IRFGRMPRSE | KAKLKAEILT | CEHDLKDSET |
| 201 | ADLKSLGKRI | HEAYLKNFNM | NKVKARVILA | GKTSNNPPFV | IHDMETLCMA |
| 251 | EKTLVAKMVA | NGVEDKEAEV | RFFHCCQCMS | VETVTELTEF | AKAIPGFANL |
| 301 | DLNDQVTLLK | YGVYEAIFTM | LSSLMNKDGM | LIAYGNGFIT | REFLKNLRKP |
| 351 | FCDIMEPKFD | FAMKFNALEL | DDSDISLFVA | AIICCGDRPG | LLNIGYIEKL |
| 401 | QEGIVHVLKL | HLQSNHPDDT | FLFPKLLQKM | VDLRQLVTEH | AQLVQVIKKT |
| 451 | ESDAALHPLL | QEIYRDMY | | | |

In the X-ray crystal structure of hPPARα-LBD employed in this study (1K7L; 267 amino acids), 23 amino acids are different between the hPPARα-LBD and the modeled structure of the mPPARα-LBD. Regardless of this difference in amino acids, when we compared the energy minimized apo forms of hPPARα-LBD and mPPARα-LBD using Swiss PDB Viewer or the PyMOL Molecular Graphics System, there was no significant 3 dimensional structural difference between the two proteins (Cα atoms RMSD < 0.05 $Å^3$; Fig. 17). Similarly, no differences were noted in the Ramachandran plots of the two proteins (data not shown). This was consistent with circular dichroism spectroscopy data from chapter I that demonstrated no significant differences in the secondary structural content of hPPARα and mPPARα (*165*).

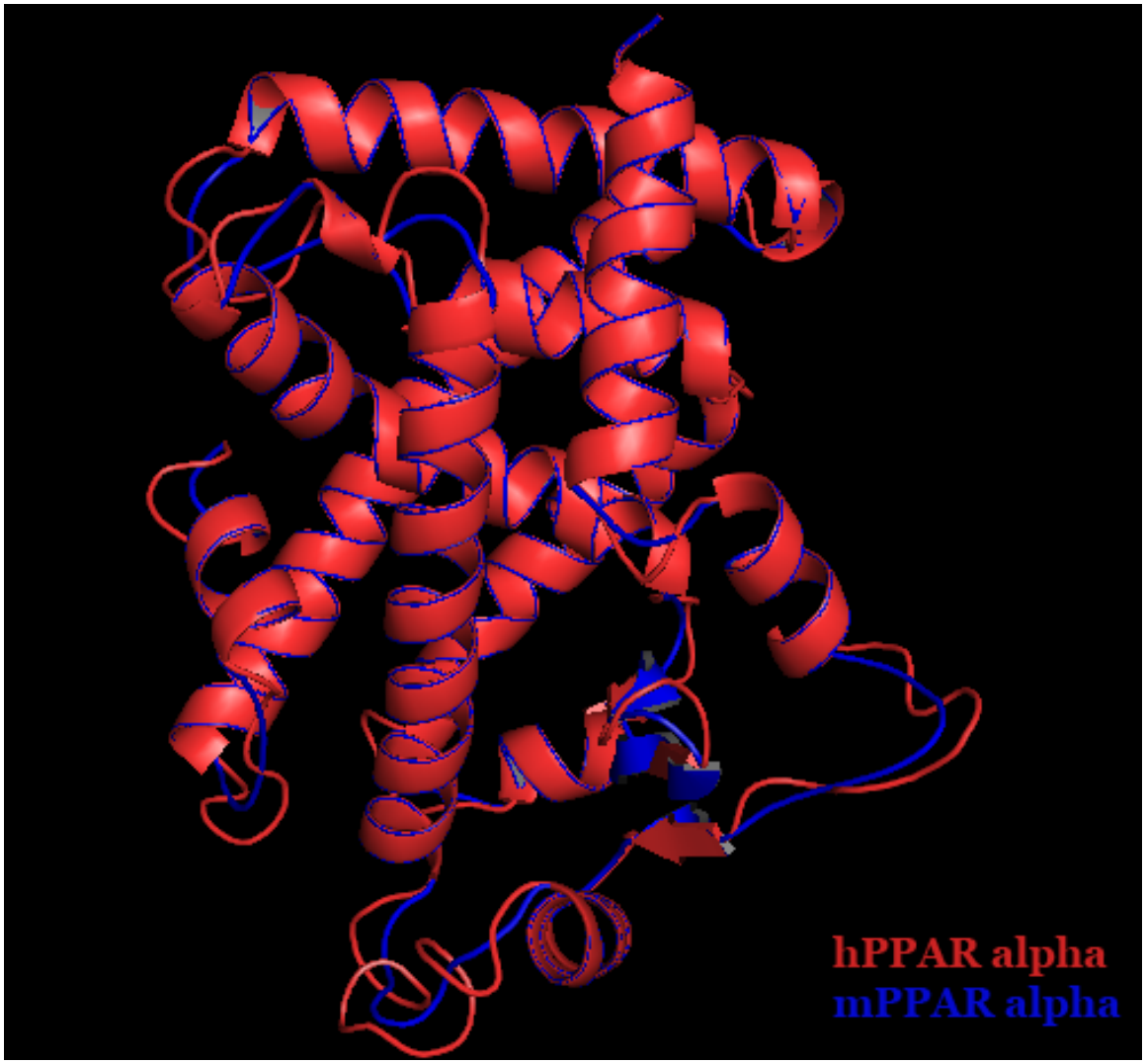


**Fig. 17.** An overlay of the energy minimized structures of hPPARα-LBD (red; adopted from PDB code: 1K7L) and mPPARα-LBD (blue; modeled using 1K7L). No significant structural difference was observed between the two proteins (Cα atoms RMSD < 0.05 $Å^3$).

*Molecular docking simulations with hPPARα-LBD and mPPARα-LBD:* For all docking simulations we utilized both AutoDock Vina (*191*) and the FlexiDock™ module available on SYBYL®-X 2.0. In order to validate our docking simulations, we compared the energy minimized structure of hPPARα-LBD + GW409544 obtained using our docking approaches to the experimentally obtained X-ray crystal structure of the same (*26*). There was no significant difference between the two structures (Cα RMSD < 0.01 $Å^3$). Furthermore, the orientation of GW409544, as well as the amino acids participating in the interaction between GW409544 and the protein, were quite comparable in the two structures (Fig. 18A and 18B). Thus, this docking protocol was considered suitable for subsequent docking runs. We next simulated the docking of GW409544 to our energy minimized model of mPPARα-LBD. Although there was no significant difference between the RMSD value for the Cα atoms (RMSD < 0.05 Å), the orientation of GW409544 was remarkably different in the hPPARα-LBD and mPPARα-LBD (Fig. 18C and 18D). This was consistent with previous molecular modeling data which reported similar variations in the orientation and position of GW409544 within the ligand binding pockets of mPPARα-LBD and hPPARα-LBD (*159*). It was proposed that part of these variances could be attributed to the bulky phenylalanine residue at 272 in mPPARα-LBD (Isoleucine in hPPARα-LBD), and that this may cause a large shift in the phenyloxazol arm of GW409544 (Fig. 18D).

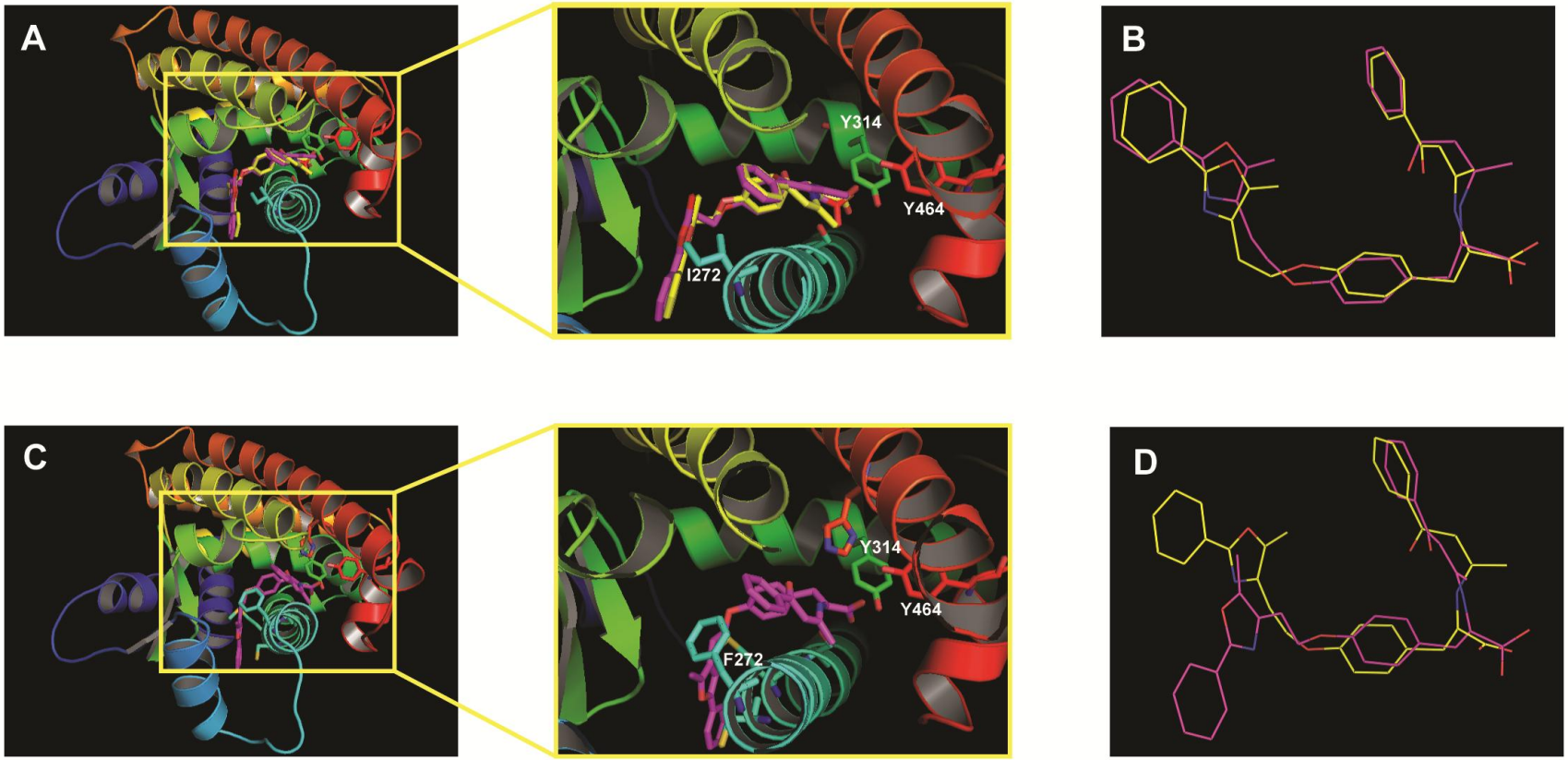
A
Y314
Y464
I272
B
C
Y314
Y464
F272
D

**Fig. 18.** (A) An overlay of the optimized structure of hPPARα-LBD in complex with GW409544 (magenta) along with its crystal structure (PDB code: 1K7L; GW409544 shown in yellow). The right-hand figure is a close-up of the panel on the left, with key amino acids Tyr-314, Tyr-464 and Ile-272 labeled. (B) An overlay of GW409544 in the hPPARα-LBD generated using our docking approach (magenta) and/or obtained from PBD code 1K7L (yellow). (C) The binding pose for the energy minimized structure of mPPARα-LBD in complex with GW409544 with a close-up view around the ligand (magenta). (D) An overlay of GW409544 conformations from docking poses generated using hPPARα-LBD (yellow) and mPPARα-LBD (magenta).

Upon validation of the docking parameters, the docking of LCFA to hPPARα-LBD and mPPARα-LBD were examined. Docking of saturated LCFA (palmitic and stearic acid) were preferentially examined, because mPPARα and hPPARα have been shown to bind with different affinities to such LCFA (*165*). Based on reported crystal structures and structure-activity relationships, most PPARα agonists bind to PPARα with the acidic head group forming hydrogen bonds with Y314 on helix 5 and Y464 on the AF-2 of helix 12. The hydrophobic tails of these ligands are stabilized by numerous hydrophobic interactions extending upward or downward in the 2 arms of the PPARα pocket (*26*). Based on these observations and the fact that LCFA serve to activate PPARα, we expected the carboxylic acid group of the LCFA to form a specific hydrogen bonding network with Y314 and Y464 to stabilize the AF-2 helix, permitting PPARα activation.

The binding mode of palmitic acid to hPPARα-LBD demonstrated striking resemblance to that of other PPARα agonists – stabilized by a combination of hydrogen bonds and hydrophobic interactions. The carboxylic acid group of palmitic acid was oriented towards the AF-2 helix forming hydrogen bonds with Y314 and Y464, and its hydrophobic tail was stabilized by numerous hydrophobic interactions in the core PPARα pocket (Fig. 19A, Fig. 19B). Similar docking poses were generated for another saturated (stearic acid; C18:0; Fig. 20A), monounsaturated (palmitoleic acid; C16:1; Fig. 20B) and polyunsaturated (docosohexaenoic acid; C22:6; Fig. 20C) LCFA. The binding energies estimated by the docking software are presented in Table V. Although both AutoDock Vina and the SYBYL®-X 2.0 gave consistent and similar output for the docking modes, the FlexiDock™ module on SYBYL®-X 2.0 was used to obtain binding energies

associated with this docking. The FlexiDock™ module on SYBYL® - X 2.0 was chosen because 1) it permits both protein (sidechains) and ligands to carry flexible/rotatable bonds, and 2) the FlexiDock™ energy evaluation function is based on the Tripos Force Field and estimates the binding energy of ligand, the receptor binding pocket, as well as the interaction between them. These results demonstrated that LCFA are bound in a similar manner as other PPARα ligands and further support previous observations that suggest LCFA are high affinity endogenous ligands of hPPARα (*108, 117, 165*).

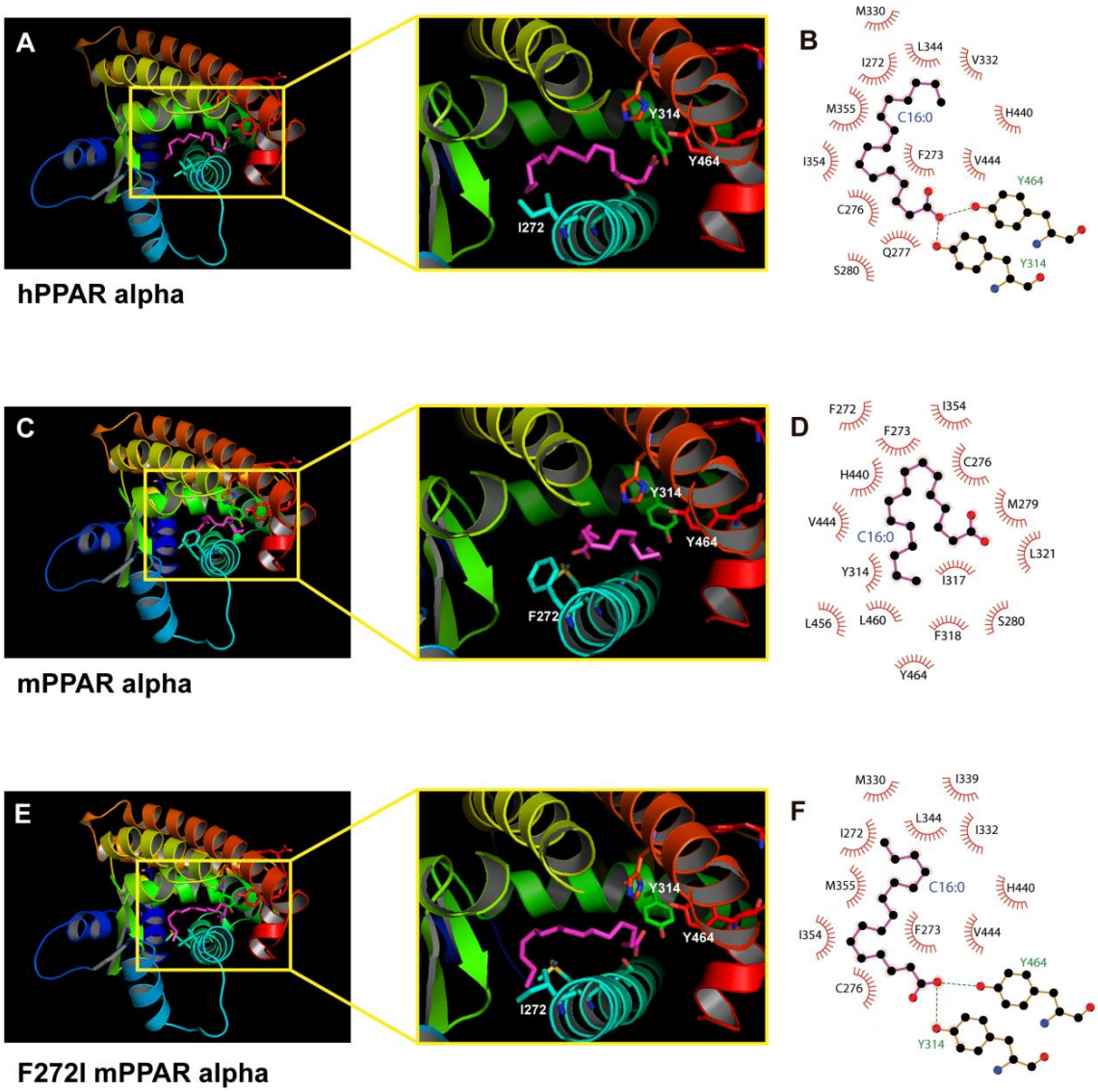
A
Y314
Y464
I272
hPPAR alpha
B
M330
L344
I272
V332
M355
C16:0
H440
I354
F273
V444
Y464
C276
Q277
Y314
S280
C
Y314
Y464
F272
mPPAR alpha
D
F272
I354
F273
C276
H440
M279
V444
C16:0
L321
Y314
I317
L456
L460
F318
S280
Y464
E
Y314
Y464
I272
F272I mPPAR alpha
F
M330
I339
L344
I272
I332
M355
C16:0
H440
I354
F273
V444
Y464
C276
Y314

**Fig. 19.** Comparison of the binding modes of C16:0 complexed with (A) hPPARα LBD, (C) mPPARα LBD and (E) F272I mPPARα LBD. All docking poses presented here were generated using the FlexiDock™ module available on SYBYL® - X 2.0 and are comparable to those generated using AutoDock Vina. In the left-hand figures AF2 helix 12, helix 3 and helix 5 are depicted in red, cyan and green respectively. The right-hand figures are close-up views of respective panels from the left. The ligand is colored in magenta and the amino-acids Tyr 314, Tyr 464 and Ile-272 or Phe-272 are labeled. Two-dimensional representations of key hydrogen bonding (green dotted lines) and hydrophobic interactions (red dashed lines) between C16:0 and hPPARα LBD (B) or mPPARα LBD (D) or F272I mPPARα LBD (F) were produced using LIGPLOT (*192*).

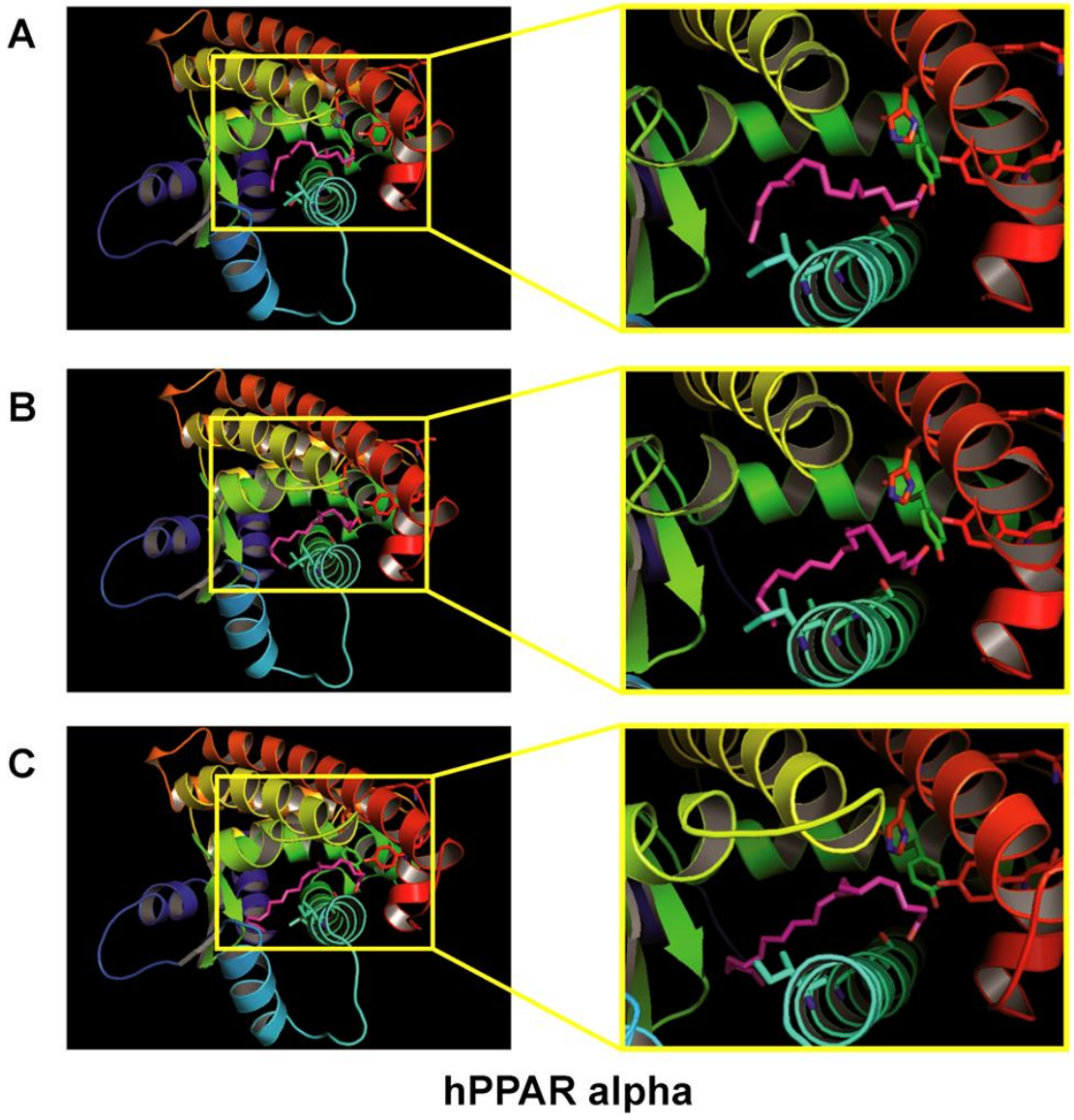


**Fig. 20.** Energy minimized structures of hPPARα-LBD in complex with (A) palmitoleic acid, (B) stearic acid and (C) docosahexaenoic acid. The figures in the right panels are close-up views of respective panels on the left. All docking poses presented here were generated using the FlexiDock™ module available on SYBYL® - X 2.0 and are comparable to those generated using AutoDock Vina.

**Table V.** Comparison of binding energies (kcal/mol) for mouse and human PPARα LBD complexed with LCFA ligands.

| Ligand | Chain length: double bonds (position) | hPPARα kcal/mol | mPPARα kcal/mol | F272I mPPARα kcal/mol |
|---|---|---|---|---|
| Palmitic acid | C16:0 | -1150 | -284 | -1089 |
| Palmitoleic acid | C16:1 (n-7) | -1149 | -1143 | -1149 |
| Stearic acid | C18:0 | -1153 | -298 | -1112 |
| Docosahexanoic acid | C22:6 (n-3) | -1187 | -932 | -1039 |

Binding energies were derived using the FlexiDock™ module available on SYBYL® - X 2.0 (Tripos, St. Louis, MO).

While experimental results have shown that mPPARα binds with strong affinity to monounsaturated and polyunsaturated LCFA, it binds only weakly to saturated LCFA (*165*). Consistent with these observations, our docking simulations demonstrated that, with the exception of saturated LCFA, the binding modes and energies generated for the mPPARα-LBD in complex with monounsaturated (C16:1; Fig. 21A) and polyunsaturated (C22:6; Fig. 21C) LCFA are quite comparable to that of hPPARα-LBD. However, the conformation and position of saturated palmitic (Fig. 19C, 19D) and stearic acid (Fig. 21B) in the mPPARα-LBD are remarkably different, demonstrating 4-fold higher binding energies (weaker binding) when compared to the docking poses in hPPARα-LBD (Table V).

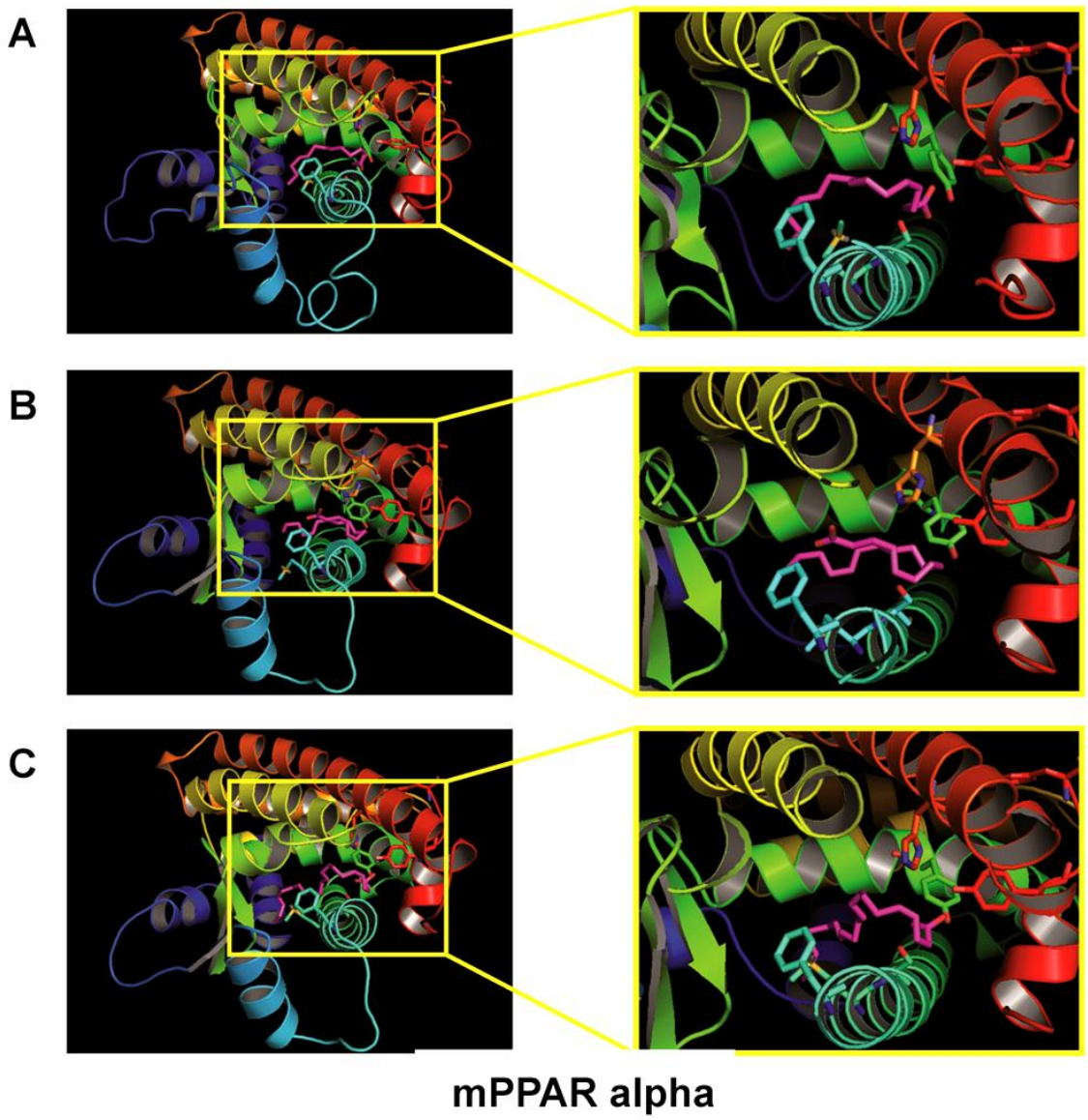


**Fig. 21.** Energy minimized structures of mPPARα-LBD in complex with (A) palmitoleic acid, (B) stearic acid and (C) docosahexaenoic acid. The figures in the right panels are close-up views of respective panels on the left. All docking poses presented here were generated using the FlexiDock™ module available on SYBYL® - X 2.0 and are comparable to those generated using AutoDock Vina.

Two striking features were noted between the binding orientation of palmitic acid and stearic acid to mPPARα-LBD compared to hPPARα-LBD. Although multiple docking poses were generated, suggesting several possible conformations of the palmitic (or stearic) acid within the binding pocket, these characteristics were consistently seen in all poses for the mPPARα-LBD. First, the carboxylic acid group does not form hydrogen bonds with the C terminal amino acids - possibly raising the binding energy (less negative or less favorable). Second, the alkyl chain is not fully extended in the mPPARα-LBD pocket (Fig. 19C, 19D), and the fatty acid was unable to orient along the same axis as seen with the hPPARα-LBD. This may raise the binding energy, resulting in weaker binding affinity of saturated LCFA to mPPARα-LBD. It is known that saturated alkyl chains normally prefer a fully extended conformation (*196*). These results were consistent with the weaker binding affinities of saturated LCFA reported for mPPARα (*165*).

While the computational and experimental binding trends are similar, it is noteworthy that binding energies obtained in this study do not necessarily convert into the same nanomolar binding affinities reported experimentally. Such differences between computational binding energies and experimental binding affinities could in part be explained by parameters that are not taken into consideration in the docking simulations, including the contribution of entropy, effects of solvation and the dynamic nature of proteins in solution. It is worth noting that in the human and mouse PPARα comparison of LCFA binding, solvation by itself is not likely to be of paramount importance. This is because the solvation energy of palmitic or stearic acid are about the same regardless of the protein to which they bind (*197*). We anticipate that the hydration of the binding pocket is also similar given the similar polarity of the amino acid substitutions at 272 and

270 (F272I and T279M). However, the overall protein flexibility and the role of water in this process is of particular importance. While these possibilities were not tested in this study, another factor that may play a crucial role in explaining such differences is the use of full-length PPARα protein in experimental ligand binding studies as compared to the use of PPARα-LBD in computational docking simulations.

Comparison of the amino acid sequences from the human and mouse PPARα-LBD, especially in helices 3, 5, 7 and 12 which form the central core of the ligand binding pocket, exhibit two major differences in helix 3, which occur at amino acid 272 (isoleucine to phenylalanine) and 279 (threonine to methionine). While both of these substitutions are fairly conservative, the amino acid at 272 in hPPARα is an isoleucine with a small isobutyl group, whereas in mPPARα this residue is a phenylalanine with a bulkier benzyl side chain. We speculated that the electron rich bulkier benzyl group of F272 in mPPARα might cause steric hindrance and change the shape and volume of the mPPARα ligand binding pocket. In order to test this hypothesis, we substituted the phenylalanine residue at 272 in the mPPARα-LBD structure with an isoleucine (F272I mPPARα-LBD). The binding modes and energies generated using such an energy minimized model of F272I mPPARα-LBD in complex with palmitic acid (Fig. 18E, 18F), as well as palmitoleic, stearic and docosahexaenoic acids (Fig. 22A, 22B, 22C) were similar to that obtained using the hPPARα-LBD structure (Table V). These results suggest that the amino acid residue at position 272 of helix 3 plays a critical role in determining species specificity and selectivity of PPARα ligands.

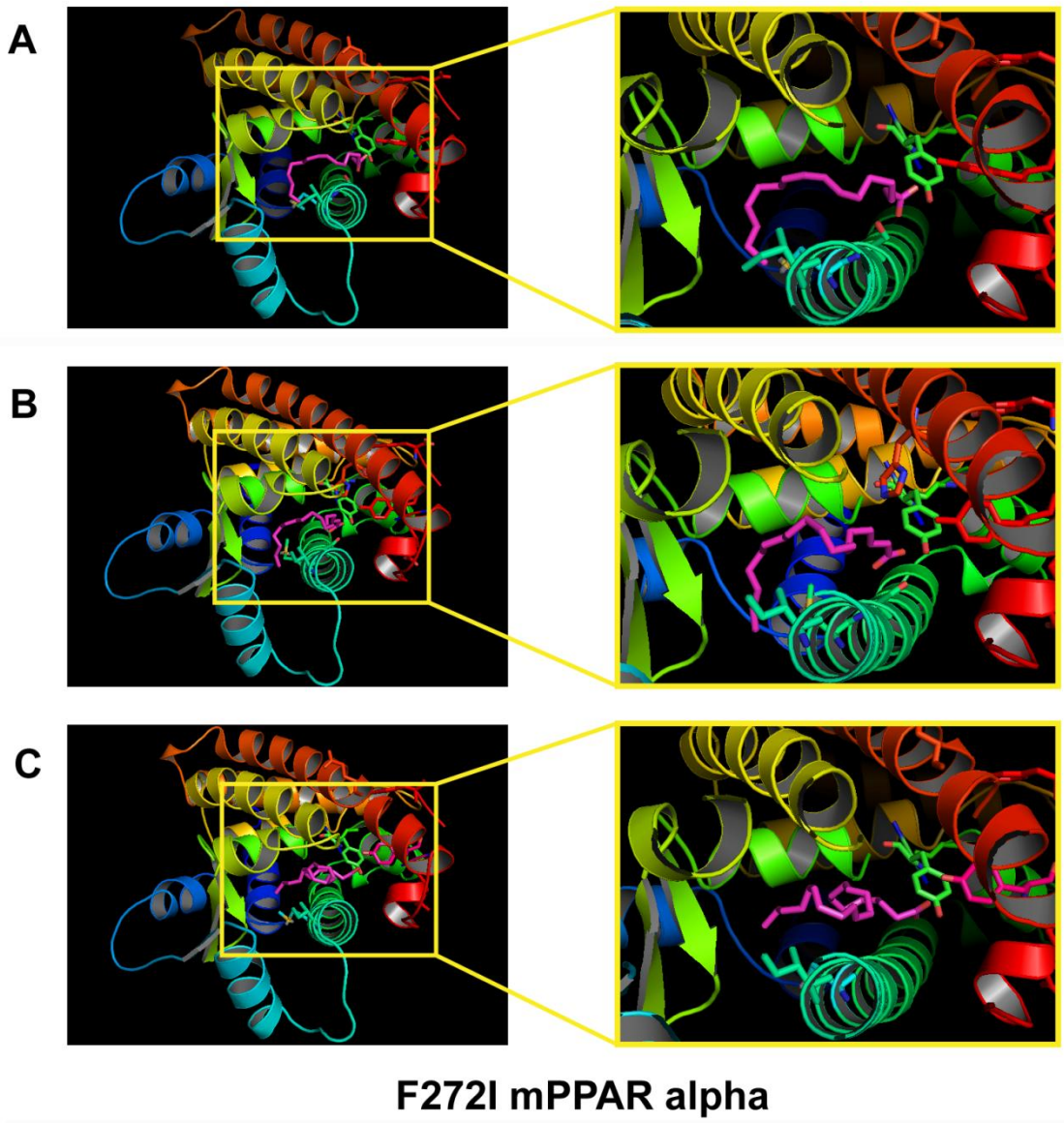


**Fig. 22.** Structural determinants of endogenous LCFA selectivity for mouse and human PPARα. Energy minimized structures of F272I mPPARα-LBD in complex with (A) palmitoleic acid, (B) stearic acid and (C) docosahexaenoic acid. The figures in the right panels are close-up views of respective panels on the left. All docking poses presented here were generated using the FlexiDock™ module available on SYBYL® - X 2.0 and are comparable to those generated using AutoDock Vina.

In order to confirm the importance of the amino acid residue at position 272, docking simulations were also performed with an energy minimized point mutant model of I272F hPPARα-LBD in the presence of palmitic or stearic acid (Fig. 23). Although such binding/docking displayed weaker binding affinity (higher binding energies; -866 kcal/mol, C16:0 and -745 kcal/mol, C18:0) than the wild-type hPPARα (Table V), it was not as weak as the F272I mPPARα (-284 kcal/mol, C16:0 and -298 kcal/mol, C18:0). The differences in the binding energy between I272F hPPARα-LBD and F272I mPPARα-LBD complexed with C16:0 or C18:0 may be attributed to the manner in which the ligands orient around the amino acid at 279 (threonine in hPPARα and methionine in mPPARα) (Fig. 23). For example, if the threonine 279 in I272F hPPARα-LBD is mutated to methionine (like in F272I mPPARα-LBD) the binding mode/energy generated with palmitic or stearic acid mimics that of F272I mPPARα-LBD.

Similarly, the orientation of the ligand around the amino acid residue at 279 also explains the slight difference in binding energies seen between human and mouse PPARα for C22:6 (Table V). This T279M substitution has previously been reported to cause differences in the activation of human and mouse PPARα in response to synthetic PPARα agonists (*160*). A schematic explaining the significance of these amino acids in relation to saturated LCFA binding is presented below (Fig. 23). Depending on the chemistry of the ligand both amino acid residues at 272 as well as 279 could be crucial determinants of PPARα ligand specificity. However for LCFA binding to mPPARα-LBD, the amino acid residue at 272 plays an important role in imparting ligand specificity.

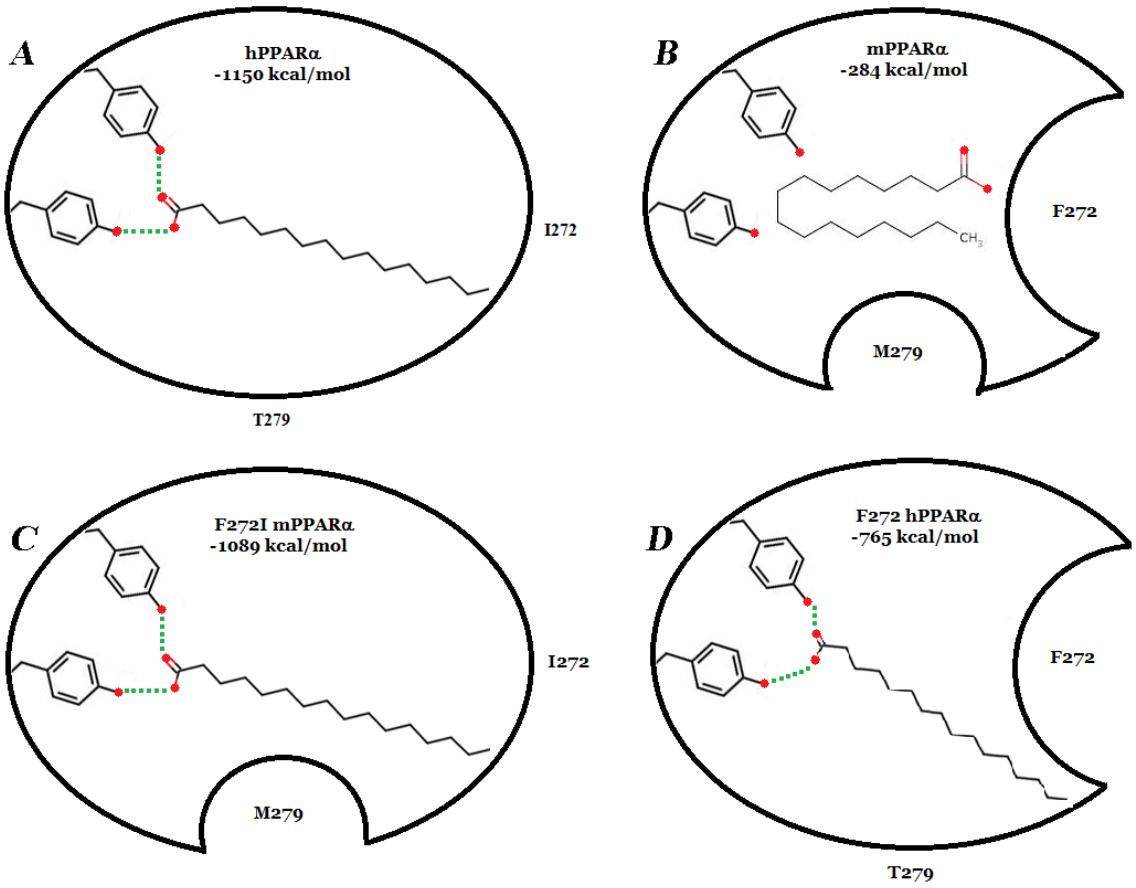


**Fig. 23.** Illustration of saturated LCFA binding to human and mouse PPARα – Importance of amino acid residues at position 272 and 279. A) Human PPARα binds saturated fatty acids with high affinity. B) Owing to stearic hindrance due to phenylalanine at 272 (F272) mPPARα binds this ligand relatively weakly. C) Reversal of phenylalanine at 272 to isoleucine (F272I) in mPPARα results in high affinity binding of saturated LCFA. D) Mutation of isoleucine at 272 to phenylalanine in hPPARα (I272F) results in weaker binding of the saturated fatty acids but it is not as weak as F272I mPPARα in C. These differences are a result of how the ligand orients around T279 (in hPPARα) such that mutation of both amino acids (I272F and T279M) results in binding mode similar to B.

In order to determine the contribution of these amino acids to the PPARα ligand binding pocket, we evaluated binding pocket volume calculations using the POVME algorithm. Based on the occupancy of the GW409544 ligand (in 1K7L) and a padding variable set to 0.5 (deduced based in a carbon-hydrogen bond length of 1.09 Å) the ligand binding pocket of hPPARα-LBD was 1177 $Å^3$ (Fig. 24A) In contrast, owing to I272F and T279M substitutions, the binding pocket of mPPARα-LBD was 1073 $Å^3$(Fig. 24B). A single mutation of F272I or two mutations including both F272I and M279I in mPPARα-LBD resulted in binding pocket volumes of 1130 $Å^3$ (Fig. 24C) and 1161 $Å^3$ (Fig. 24D) respectively. It is apparent from these results that the amino acid differences at residues 272 and 279 do alter the size of the pocket. However, as the average volume of a fatty acid (e.g. palmitic acid) is < 300 $Å^3$, there is plenty of space within each of these pockets for fatty acid binding. This suggests that favorable interactions with the AF-2 domain (which are based on the orientation of the ligand) are more important for determining PPARα ligand specificity, with regards to LCFA, than the total volume available within the pocket.

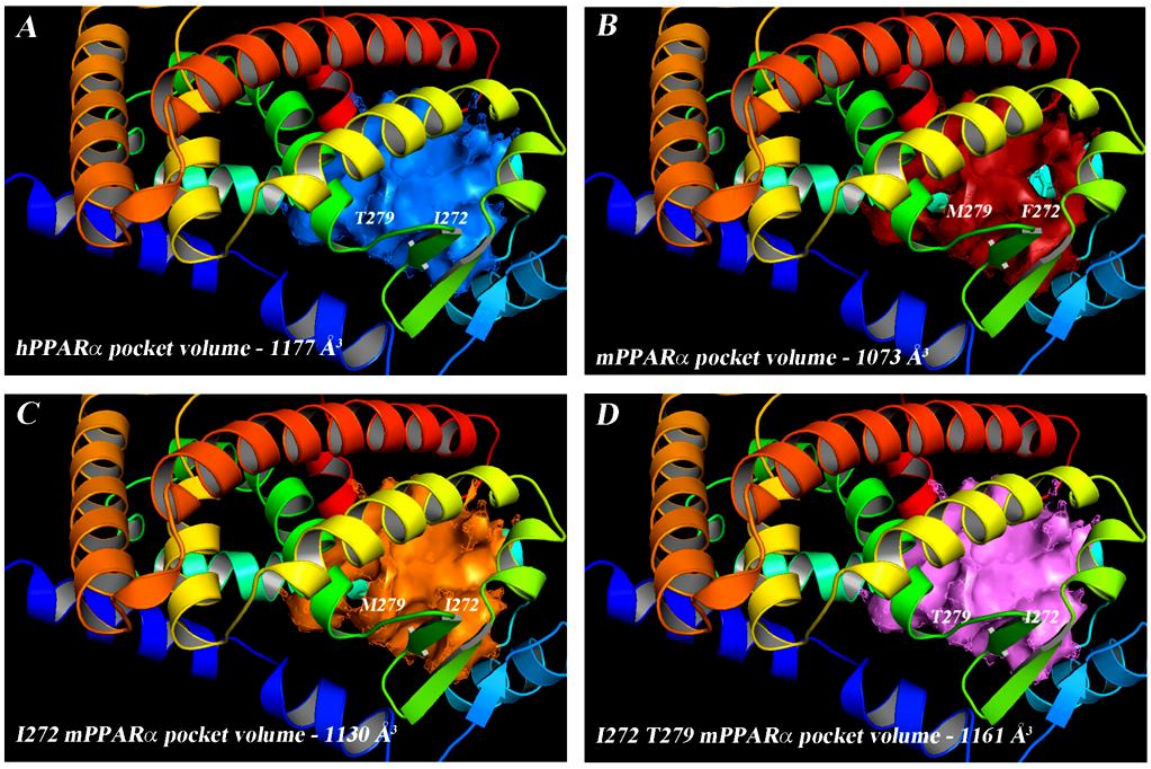


**Fig. 24.** Ligand binding pocket volumes for (A) hPPARα-LBD, (B) mPPARα-LBD, (C) F272I mPPARα-LBD and (D) F272I, M279T mPPARα-LBD determined using the POVME algorithm (*193*).

*Purification of full-length recombinant F272I mPPARα:* In order to experimentally determine the effect of a phenylalanine to isoleucine substitution at amino acid 272 of mPPARα, full-length recombinant F272I mPPARα protein was expressed and purified as described for full-length mPPARα and hPPARα (*165*). SDS-PAGE and Coomassie blue staining indicated a predominant band of 52kDa corresponding to the expected size of full-length F272I mPPARα (>85% purity; Fig. 25B), with similar purity as mPPARα (Fig. 25A). The low intensity band at 75 kDa represents a small fraction of un-cut/tagged protein (< 10%).

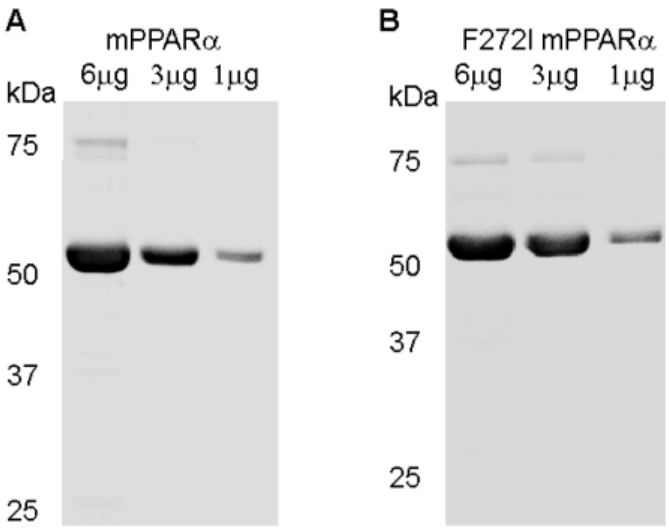


**Fig. 25.** SDS-PAGE and Coomassie blue staining of 1 μg, 3 μg and 6 μg of purified recombinant (A) mPPARα (left) and (B) F272I mPPARα showing relative purity of the protein. The prominent band at 52 kDa represent full-length, untagged recombinant mPPARα and F272I mPPARα.

*Binding of fluorescent fatty acids and fatty acyl-CoAs to F272I mPPARα.* While BODIPY fluorescence was low for each examined fluorophore in the absence of protein, titration of F272I mPPARα with BODIPY C16-CoA resulted in increased fluorescence which approached saturation near 200 nM. (Fig. 26A, 26B). This data transformed into a linear double reciprocal plot (Fig. 26B, inset), consistent with a single binding site ($R^2$ > 0.90). Binding of BODIPY C16 fatty acid was also strongly saturable at a single binding site (Fig. 26C). Multiple replicates yielded $K_d$ values of 55 ± 4 nM and 18 ± 3 nM for BODIPY C16-CoA and BODIPY C16 fatty acid, respectively, indicating high-affinity binding. These results were consistent with previously reported binding affinities of wild-type mPPARα (*165*), suggesting that this amino acid change did not disrupt or alter the binding of these ligands.

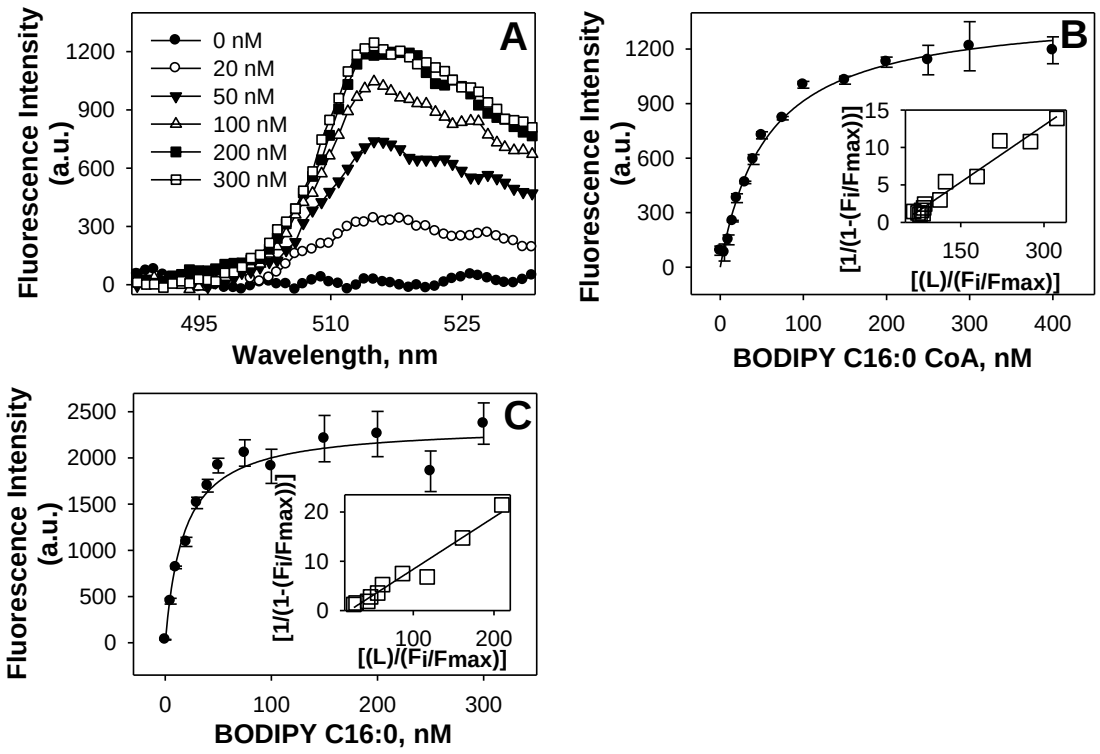


**Fig. 26.** (A) Corrected fluorescence emission spectra of 0.1 μM F272I mPPARα titrated with 0 (filled circles), 20 (open circles), 50 (filled triangles), 100 (open triangles), 200 (filled squares) and 300 nM (open squares) of BODIPY C16-CoA upon excitation at 465 nm. These results demonstrate increased fluorescence intensity upon binding to F272I mPPARα. Plot of F272I mPPARα fluorescence emission at 515 nm (excitation 465 nm) as a function of BODIPY C16:0-CoA (B) and BODIPY C16:0 FA (C). Insets represent double reciprocal plots of the binding curve from each panel. All values represent the mean ± S.E., $n \geq 3$.

*Binding of endogenous LCFA and LCFA-CoA to F272I mPPARα:* In order to experimentally test the hypothesis that the F272I substitution could explain the differences in binding affinity of human and mouse PPARα for saturated LCFA, the ligand specificity of F272I mPPARα for naturally-occurring, endogenous LCFA and LCFA-CoA was examined. The binding affinities for naturally-occurring LCFA and LCFA-CoA were estimated by monitoring their ability to compete and displace BODIPY C16-CoA from F272I mPPARα, which was observed as decreased BODIPY fluorescence. With the exception of lauric acid and lauroyl-CoA (Fig. 27K, 27L), titration with the fatty acids and fatty acyl-CoA examined here resulted in significantly decreased BODIPY fluorescence (Fig. 27A-H). Quantitative analyses of these data suggested strong binding ($K_i$ = 17-29 nM, Table VI). By comparison, the synthetic PPARα agonist clofibrate showed slightly weaker binding affinity (Fig. 27I; $K_i$ = 51 nM), and the synthetic PPARγ agonist rosiglitazone did not displace BODIPY C16-CoA (Fig. 27J, Table VI).

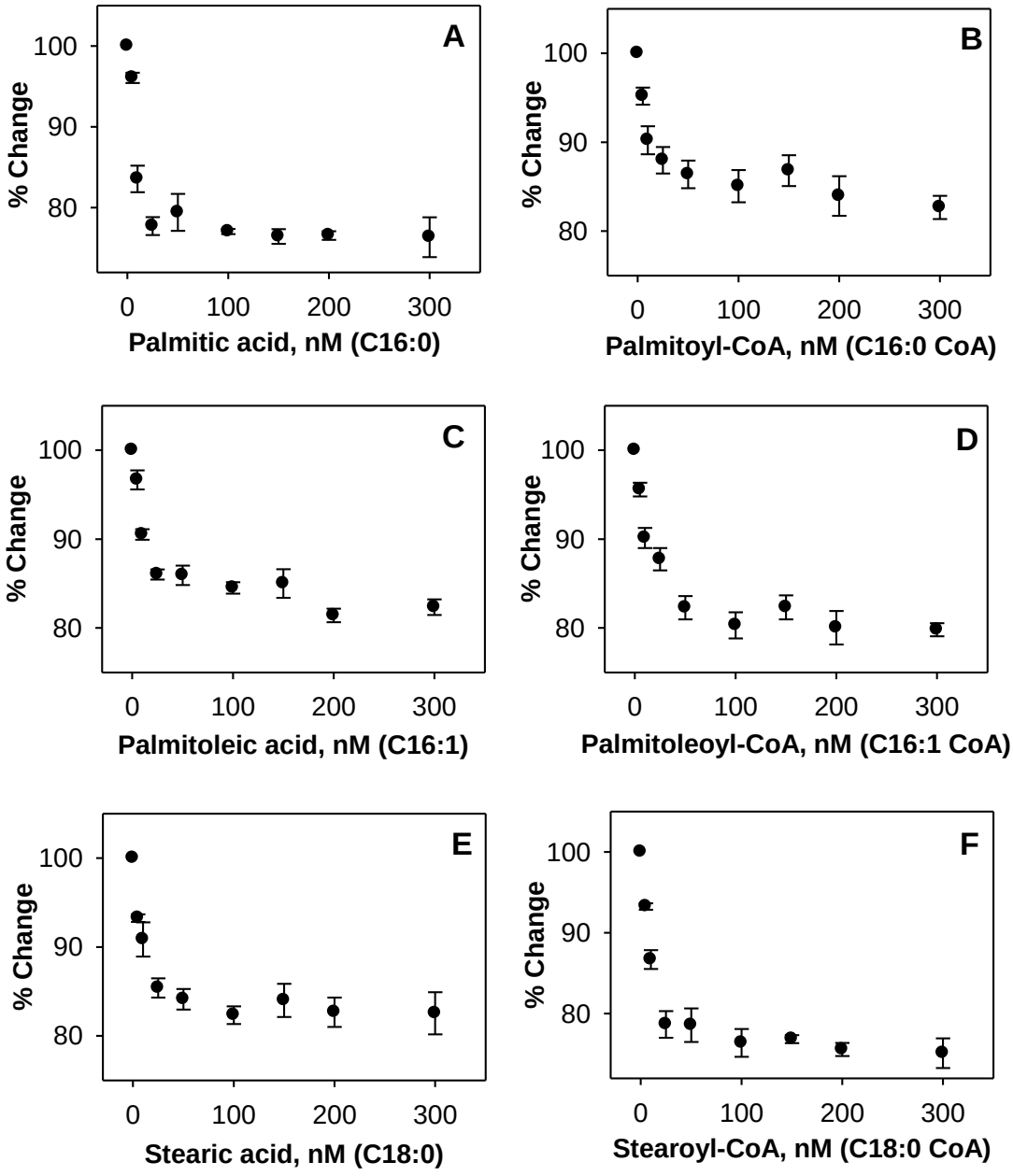
A
% Change
100
90
80
0
100
200
300
Palmitic acid, nM (C16:0)
B
% Change
100
90
80
0
100
200
300
Palmitoyl-CoA, nM (C16:0 CoA)
C
% Change
100
90
80
0
100
200
300
Palmitoleic acid, nM (C16:1)
D
% Change
100
90
80
0
100
200
300
Palmitoleoyl-CoA, nM (C16:1 CoA)
E
% Change
100
90
80
0
100
200
300
Stearic acid, nM (C18:0)
F
% Change
100
90
80
0
100
200
300
Stearoyl-CoA, nM (C18:0 CoA)

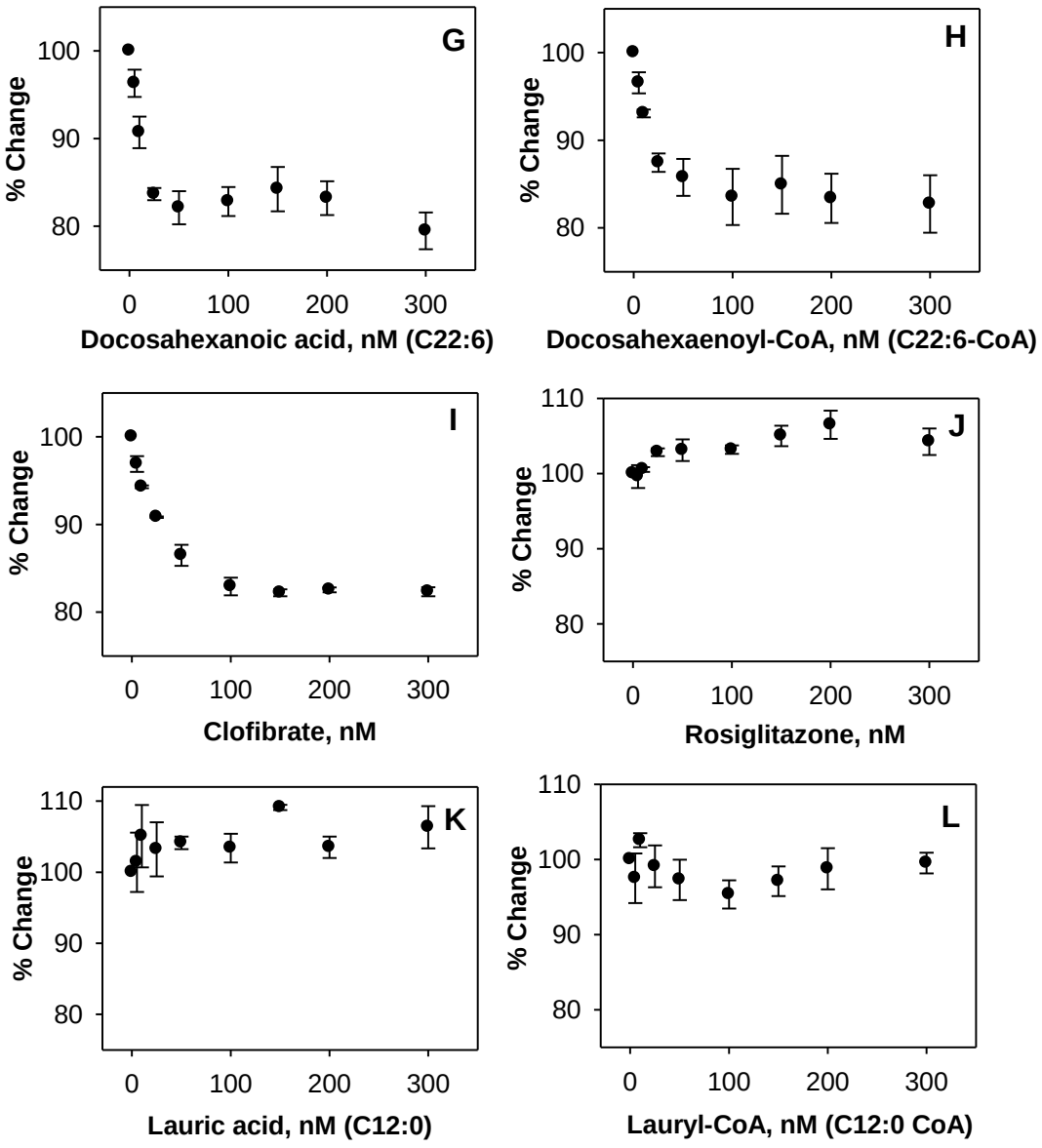
G
% Change
100
90
80
0
100
200
300
Docosahexanoic acid, nM (C22:6)
H
% Change
100
90
80
0
100
200
300
Docosahexaenoyl-CoA, nM (C22:6-CoA)
I
% Change
100
90
80
0
100
200
300
Clofibrate, nM
J
% Change
110
100
90
80
0
100
200
300
Rosiglitazone, nM
K
% Change
110
100
90
80
0
100
200
300
Lauric acid, nM (C12:0)
L
% Change
110
100
90
80
0
100
200
300
Lauryl-CoA, nM (C12:0 CoA)

**Fig. 27.** Interaction of naturally-occurring fatty acids and fatty acyl-CoA with F272I mPPARα based on displacement of BODIPY C16-CoA. F272I mPPARα complexed with BODIPY C16-CoA was titrated with the following ligands: (A) palmitic acid, (B) palmitoyl-CoA, (C) palmitoleic acid, (D) palmitoleoyl-CoA, (E) stearic acid, (F) stearoyl-CoA, (G) docosahexaenoic acid, (H) docosahexaenoyl-CoA, (I) clofibrate, (J) rosiglitazone, (K) lauric acid and (L) lauroyl-CoA. The maximal fluorescence emission of BODIPY C16-CoA was measured at 515 nm (excitation at 465 nm). Data are presented as percent change of initial fluorescence plotted as a function of ligand concentration. All values represent mean ± S.E., $n \geq 3$.

To confirm the ligand binding specificity of F272I mPPARα, the binding affinity of LCFA and LCFA-CoA was also measured by spectroscopically monitoring the quenching of F272I mPPARα aromatic amino acid emission. Titration of F272I mPPARα with both palmitic (Fig. 28A) and stearic (Fig. 28E) acid (saturated LCFA) effectively quenched F272I mPPARα fluorescence, yielding a sharp saturation curve with a maximal change at 100 nM. These data transformed into linear reciprocal plots (Fig. 28A, 28E insets), indicating high affinity binding at a single binding site ($K_d$ of 20 nM and 11 nM for palmitic and stearic acids, respectively). With the exception of lauric acid (Fig. 28K) and lauryl-CoA (Fig. 28L), similar results were obtained for all examined fatty acids and fatty acyl-CoA (Fig. 28A-H), with single site binding affinities in the 11-27 nM range (Table VI). The PPARα agonist clofibrate strongly quenched F272I mPPARα fluorescence (Fig. 28I), but displayed weaker affinity than the LCFA (Table VI), while the PPARγ agonist rosiglitazone showed no binding (Fig. 28J, Table VI).

While the binding affinities obtained for F272I mPPARα with saturated LCFA were comparable to those obtained with hPPARα ($K_d$ = 14-22 nM), they are significantly different (4-5 fold) from those obtained using wild-type mPPARα ($K_d$ = 81-135 nM) (*165*). These data further corroborate the importance of amino acid residue 272 in determining species selectivity for endogenous PPARα ligands. LCFA-CoA binding was similar to previous reports for both mPPARα and hPPARα (*165*), suggesting that amino acid 272 is not as important for the orientation of these ligands within the pocket.

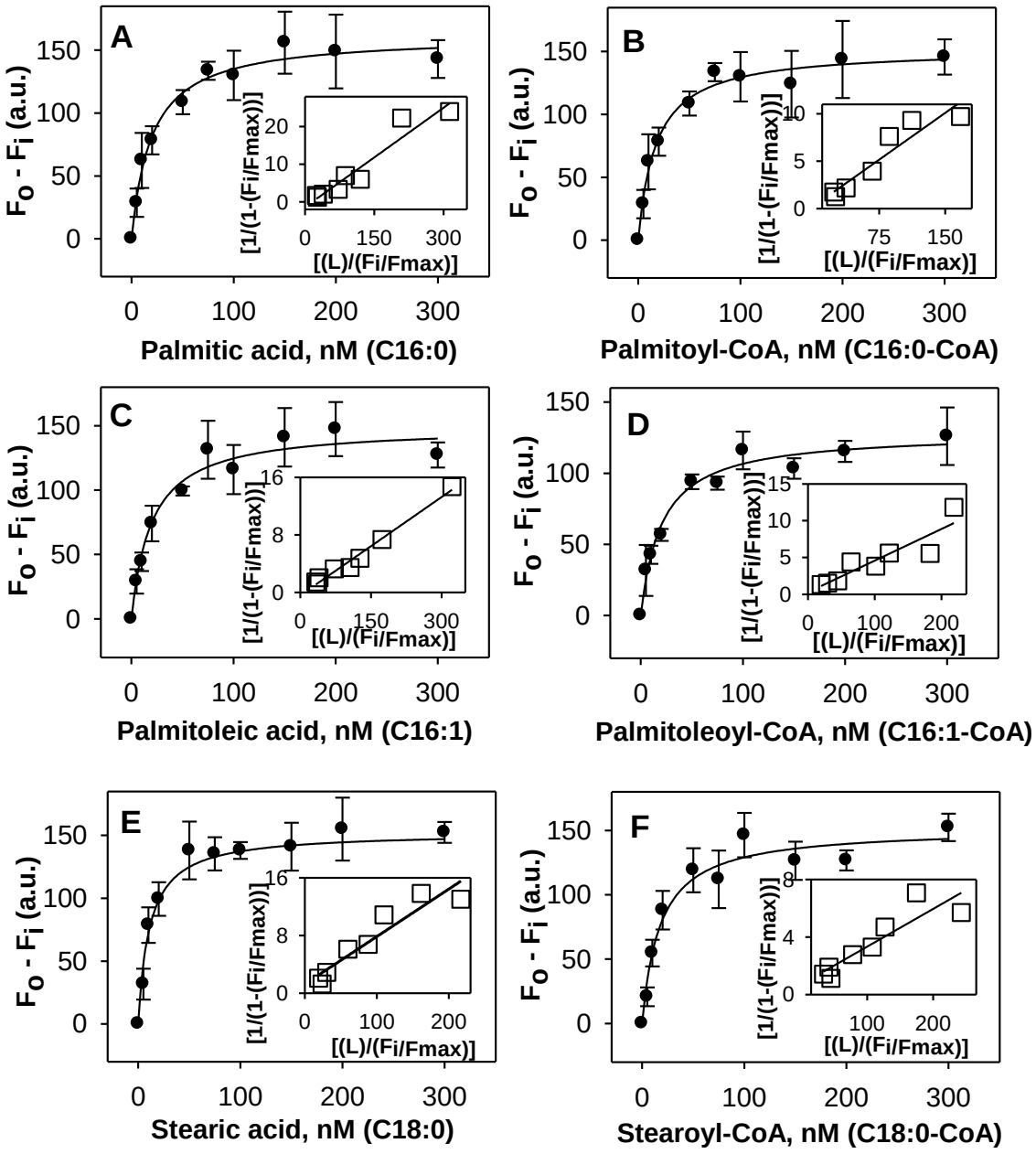
A
B
C
D
E
F
$F_O$ - $F_i$ (a.u.)
[1/(1-(Fi/Fmax))]
[(L)/(Fi/Fmax)]
Palmitic acid, nM (C16:0)
Palmitoyl-CoA, nM (C16:0-CoA)
Palmitoleic acid, nM (C16:1)
Palmitoleoyl-CoA, nM (C16:1-CoA)
Stearic acid, nM (C18:0)
Stearoyl-CoA, nM (C18:0-CoA)

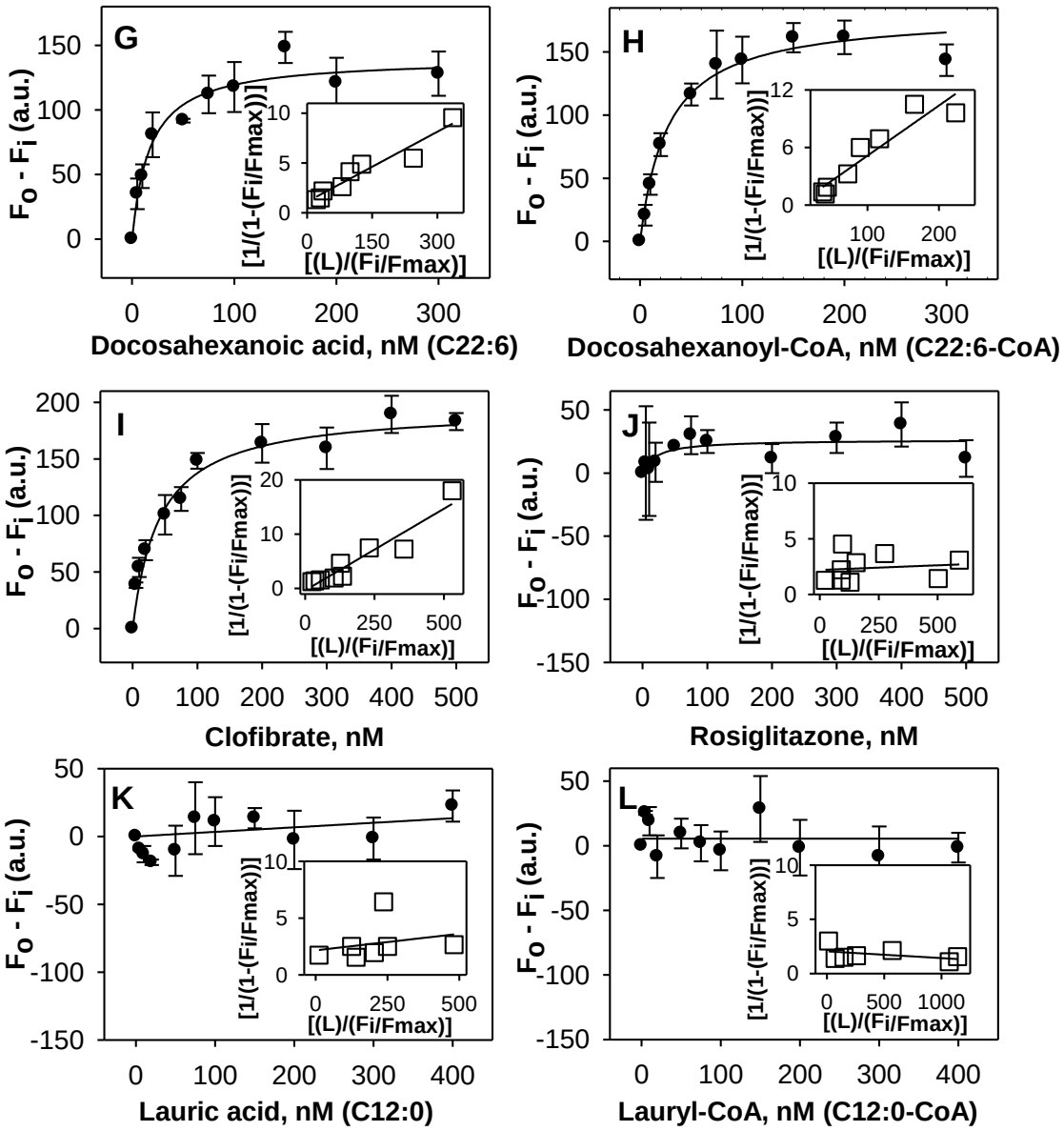
G
H
I
J
K
L
Fo - Fi (a.u.)
[1/(1-(Fi/Fmax))]
[(L)/(Fi/Fmax)]
Docosahexanoic acid, nM (C22:6)
Docosahexanoyl-CoA, nM (C22:6-CoA)
Clofibrate, nM
Rosiglitazone, nM
Lauric acid, nM (C12:0)
Lauryl-CoA, nM (C12:0-CoA)

**Fig. 28.** Interaction of naturally-occurring fatty acids and fatty acyl-CoA with F272I mPPARα. Direct binding assay based on quenching of F272I mPPARα aromatic amino acid fluorescence emission (excitation = 280 nm and emission = 300-400 nm) when titrated with the following ligands: (A) palmitic acid, (B) palmitoyl-CoA, (C) palmitoleic acid, (D) palmitoleoyl-CoA, (E) stearic acid, (F) stearoyl-CoA, (G) docosahexaenoic acid, (H) docosahexaenoyl-CoA, (I) clofibrate, (J) rosiglitazone, (K) lauric acid and (L) lauroyl-CoA. Data are presented as the change in fluorescence intensity ($F_0$- $F_i$) plotted as a function of ligand concentration. Insets represent linear plots of the binding curve from each panel. All values represent mean ± S.E., $n \geq 3$.

**Table VI.** Affinity of F272I mPPARα for non-fluorescent ligands determined by quenching of hPPARα aromatic amino acid fluorescence and by displacement of F272I mPPARα-bound BODIPY C16-CoA.

| Ligand | Chain length: double bonds (position) | $K_d$ (nM) Fatty acid | $K_d$ (nM) Fatty acyl-CoA | $K_i$ (nM) Fatty acid | *Ki* (nM) Fatty acyl-CoA |
|---|---|---|---|---|---|
| Lauric acid/CoA | C12:0 | ND | ND | ND | ND |
| Palmitic acid/CoA | C16:0 | 20±3 | 17±2 | 19±2 | 18±2 |
| Palmitoleic acid/CoA | C16:1 (n-7) | 19±3 | 21±2 | 22±3 | 28±3 |
| Stearic acid/CoA | C18:0 | 11±2 | 18±2 | 15±1 | 19±2 |
| Docosahexanoic acid/CoA | C22:6 (n-3) | 17±3 | 27±3 | 17±2 | 29±3 |
| Clofibrate | | 42±6 | | 51±3 | |
| Rosiglitazone | | ND | | ND | |

Values represent the mean ± S.E. (n ≥ 3). ND, not determined.

*Effect of endogenous fatty acids and fatty acyl-CoAs on F272I mPPARα secondary structure.* Circular dichroism (CD) was used to examine whether the binding of LCFA or LCFA-CoA altered the F272I mPPARα secondary structure. The far UV CD spectrum of F272I mPPARα suggested the presence of substantial α-helical content, exhibiting a large positive peak at 192 nm and two negative peaks at 207 and 222 nm (Fig. 30A-E, filled circles). Quantitative analyses confirmed that F272I mPPARα was composed of approximately 30 % α-helix, 18 % β-sheets, 22 % β-turns and 29 % unordered structures (Table VII). A comparison of the CD spectra (Fig. 29) and relative proportions of the secondary structures for wild-type hPPARα, mPPARα and F272I mPPARα suggested no significant differences in the structure of these proteins - a finding consistent with our observations from the modeling data. This suggested that the F272I mutation in mPPARα does not disrupt the secondary structure or folding of the protein.

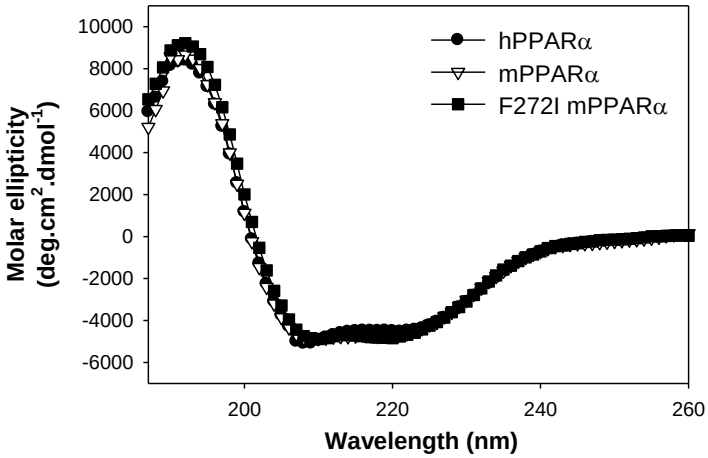


**Fig. 29.** An overlay of the far UV circular dichroic (CD) spectra of hPPARα (filled circles), mPPARα (open triangles) and F272I mPPARα (filled squares) in the absence of any ligands. Each spectrum represents an average of 10 scans for a given representative spectrum from at least three replicates.

The addition of high-affinity ligands to F272I mPPARα resulted in conformational changes demonstrated by alterations in the molar ellipticity at 192, 207, and 222 nm (Fig. 30B-E), indicative of ligand binding. Conversely, no changes were observed with the addition of lauric acid (Fig. 30A), lauroyl-CoA (Fig. 30A) or rosiglitazone (Fig. 30F), consistent with the lack of binding of F272I mPPARα to these ligands. While saturated LCFA do not induce secondary structural changes to mPPARα (*165*), there was a significant decrease in the fraction of α-helical content and a concomitant increase in the fraction of β-sheets for F272I mPPARα (Table VII), similar to those reported for hPPARα (Table III) (*165*). Similar helix-sheet transitions have been previously reported with other nuclear receptors and transmembrane proteins (*117, 177, 198*). Most of the examined LCFA and LCFA-CoA resulted in F272I mPPARα structural changes (Table VII) similar to those previously reported for hPPARα (Table III) (*165*), further indicating the importance of residue 272 in LCFA binding. However, palmitoyl-CoA and docosahexaenoic acid changes (Table VII) were more similar to those reported for mPPARα (Table IV) (*165*), suggesting that ligand structure may also be important in determining ligand orientation and binding.

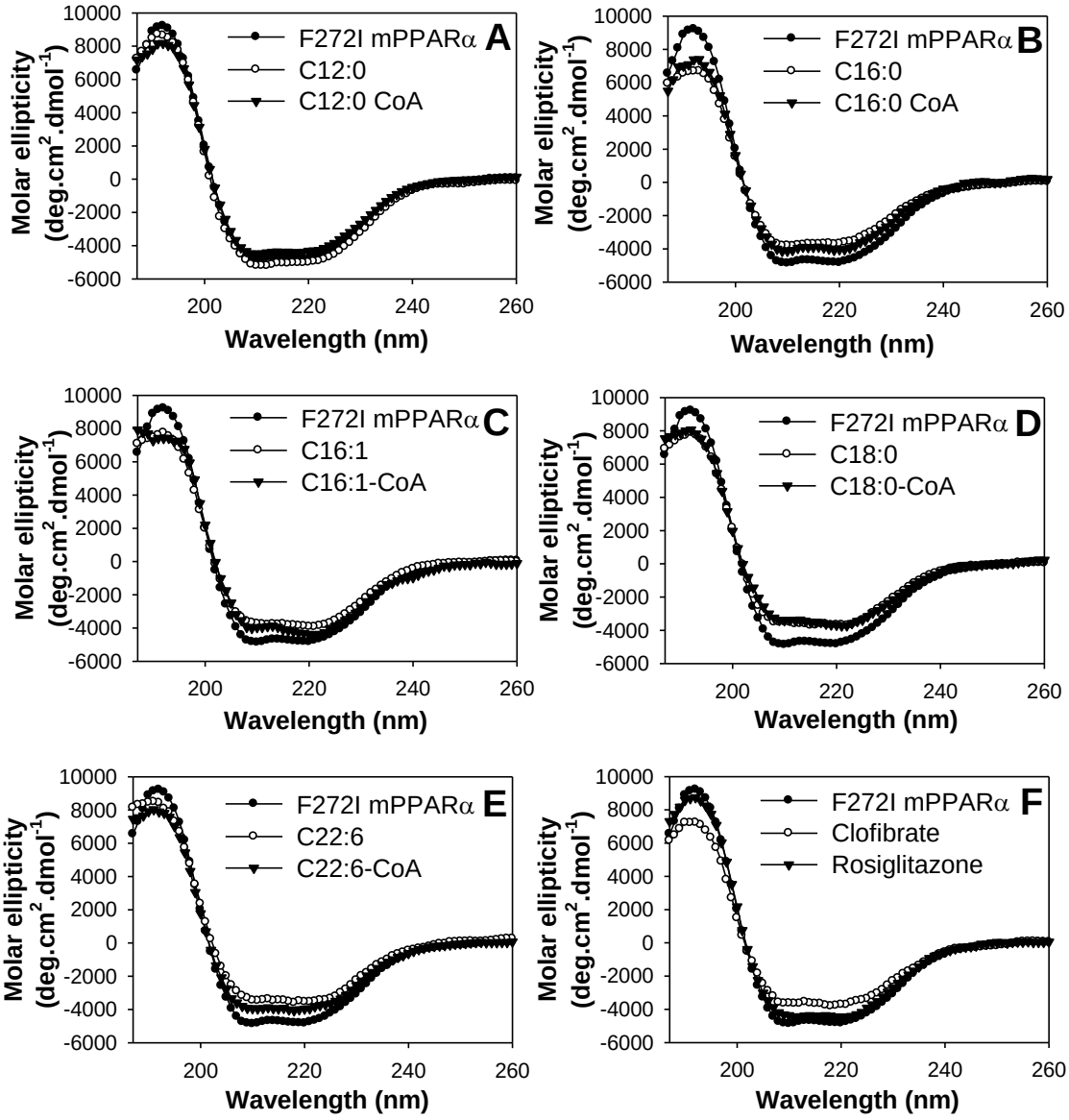
A
F272I mPPARα
C12:0
C12:0 CoA
B
F272I mPPARα
C16:0
C16:0 CoA
C
F272I mPPARα
C16:1
C16:1-CoA
D
F272I mPPARα
C18:0
C18:0-CoA
E
F272I mPPARα
C22:6
C22:6-CoA
F
F272I mPPARα
Clofibrate
Rosiglitazone
Molar ellipticity (deg.cm².dmol⁻¹)
Wavelength (nm)
10000
8000
6000
4000
2000
0
-2000
-4000
-6000
200
220
240
260

**Fig. 30.** Far UV circular dichroic (CD) spectra of F272I mPPARα in the absence (filled circles) and presence of added ligand: A, Lauric acid (open circles) or Lauryl CoA (filled triangles); B, palmitic acid (open circles) or palmitoyl CoA (filled triangles); C, palmitoleic acid (open circles) or palmitoleoyl-CoA (filled triangles); D, stearic acid (open circles) or stearoyl-CoA (filled triangles); E, docosahexanoic acid (open circles) or docosahexaenoyl-CoA (filled triangles); and F, clofibrate (open circles) or rosiglitzone (filled triangles). Each spectrum represents an average of 10 scans for a given representative spectrum from at least three replicates.

**Table VII.** Effect of ligands on the relative proportion of F272I mPPARα secondary structure determined by CD. These structures were as follows: total helices (H; a sum of regular α-helices and distorted α-helices), total sheets (S; a sum of regular β-sheets and distorted β-sheets), turns (Trn; *β*-turns), and unordered (Unrd) structures.

| **Average** | **Total H ± S.E.** | **Total S ± S.E.** | **Trn ± S.E.** | **Unrd ± S.E.** |
|---|---|---|---|---|
| F272I mPPARα | 30 ± 2 | 18.3 ± 2.3 | 21.8 ± 0.2 | 28.8 ± 0.2 |
| F272I mPPARα + C12:0 | 29 ± 1 | 21 ± 2 | 21.8 ± 0.1 | 28.9 ± 0.2 |
| F272I mPPARα + C12:0-CoA | 30 ± 1 | 20 ± 1 | 21.7 ± 0.3 | 29.1 ± 0.1 |
| F272I mPPARα + C16:0 | 18.1 ± 0.2** | 31.5 ± 0.5** | 22 ± 0.1 | 28.6 ± 0.3 |
| F272I mPPARα + C16:0-CoA | 21 ± 2* | 29 ± 1* | 22.1 ± 0.3 | 29.1 ± 0.2 |
| F272I mPPARα + C16:1 | 20 ± 1# | 30 ± 1# | 21.7 ± 0.1 | 28.7 ± 0.2 |
| F272I mPPARα + C16:1-CoA | 22 ± 2* | 28 ± 1* | 21.4 ± 0.2 | 28.5 ± 0.5 |
| F272I mPPARα + C18:0 | 18.3 ± 0.1** | 31.1 ± 0.1** | 21.9 ± 0.1 | 28.5 ± 0.1 |
| F272I mPPARα + C18:0-CoA | 20 ± 1* | 29 ± 1* | 21.5 ± 0.2 | 28.7 ± 0.3 |
| F272I mPPARα + C22:6 | 19 ± 1** | 30.8 ± 0.3** | 21.5 ± 0.1 | 28.7 ± 0.1 |
| F272I mPPARα + C22:6-CoA | 19.1 ± 0.1# | 30.6 ± 0.3** | 22 ± 1 | 28.6 ± 0.1 |
| F272I mPPARα + Clofibrate | 17.1 ± 0.1** | 31.9 ± 0.3** | 22 ± 1 | 29.0 ± 0.2 |
| F272I mPPARα + Rosiglitazone | 31 ± 1 | 19 ± 1 | 21.9 ± 0.1 | 28.6 ± 0.1 |

Asterisks represent significant differences between F272I mPPARα only and F272I mPPARα in the presence of added ligand (* $P < 0.05$, ** $P < 0.001$ and # $P = 0.001$).

*Effect of fatty acids on transactivation of PPARα-RXRα heterodimers.* In order to determine whether residue 272 is also responsible for variances observed between mPPARα and hPPARα transactivation in response to saturated LCFA (*165*), luciferase reporter assays utilizing hPPARα, mPPARα and F272I mPPARα were performed. Since PPARα heterodimerizes with RXRα to induce transactivation, COS-7 cells were cotransfected with either pSG5 empty vector or a combination of hPPARα and hRXRα, mPPARα and mRXRα or F272I mPPARα and mRXRα. The transactivation of a PPRE×3 TK LUC reporter construct was analyzed in the absence or presence of ligands (Fig. 31). Transactivation was measured as percent firefly luciferase activity normalized to *Renilla* luciferase (internal control).

Cells overexpressing hPPARα and hRXRα demonstrated significantly increased transactivation of the PPRE×3 TK LUC reporter in response to high-affinity ligands of hPPARα (Fig. 31). In contrast, for cells overexpressing mPPARα and mRXRα, only the examined unsaturated LCFA and clofibrate significantly increased transactivation. Consistent with the weak binding affinity of saturated LCFA for mPPARα, addition of these ligands did not affect the activity in COS-7 cells. However, in cells overexpressing F272I mPPARα and mRXRα the addition of saturated LCFA (palmitic and stearic acid), as well as unsaturated LCFA (palmitoleic, and docosahexaenoic acid) resulted in significantly increased transactivation similar to clofibrate treated cells (Fig. 31). This was consistent with the high-affinity binding of these ligands to F272I mPPARα. In all treatments the addition of lauric acid, which consistently did not bind to hPPARα, mPPARα or F272I mPPARα, had no significant effect on activity. These findings suggested that only high-affinity endogenous ligands increase PPARα activity and, more

importantly, the amino acid at 272 could be responsible for the differences in saturated LCFA-mediated transactivation of the PPRE×3 TK LUC reporter in cells overexpressing hPPARα and mPPARα.

These results are consistent with previous transactivation studies and gene expression studies which demonstrate species differences in the activity of human and mouse PPARα in response to synthetic agonists such as 5, 8, 11, 14-eicosatetraynoic acid (ETYA), WY-14,643 and 2-ethylphenylpropanoic acid derivative (KCL), among others (*158, 160-163, 187, 199*). While an I272F substitution diminished the agonistic activity of KCL, a T279M substitution increased the agonistic activity of WY-14,643 in hPPARα (*158*). Our studies with endogenous LCFA ligands suggested that, to a large extent, only amino acid 272 plays an important role in determining species differences, particularly for saturated LCFA. We speculate that based on the structure of ligands and their potential orientation and interactions within the PPARα pocket, both amino acids at 272 and 279 are crucial determinants of species differences exhibited by PPARα across species.

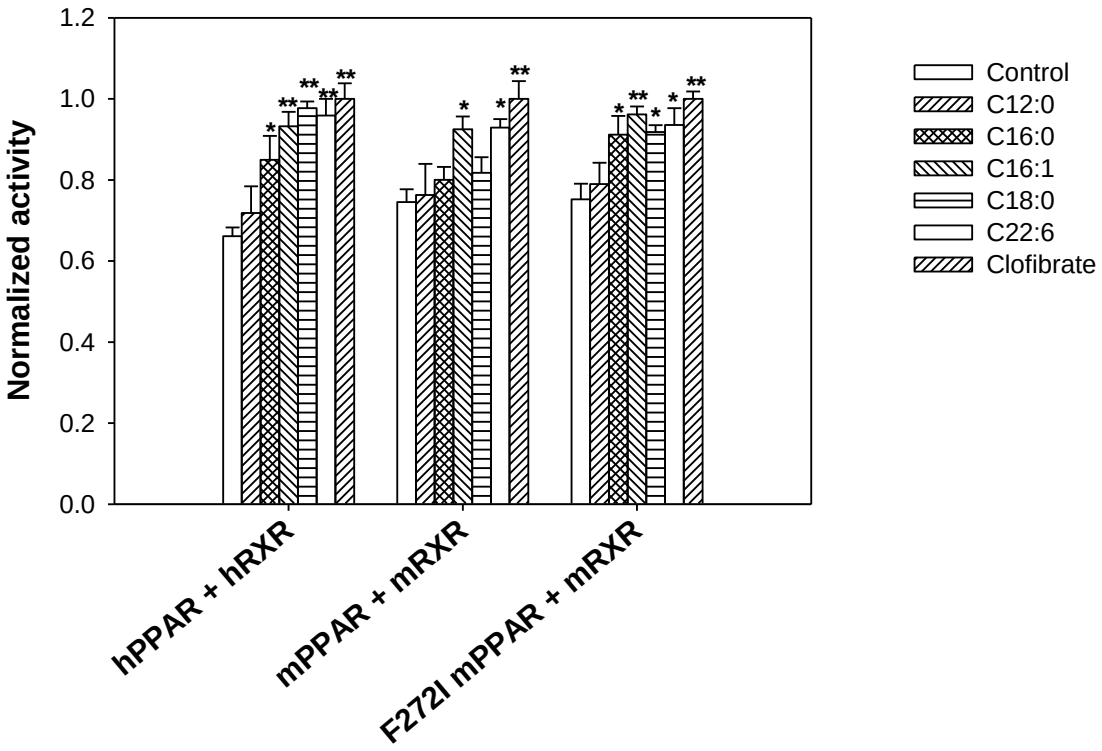


**Fig. 31.** Fatty acids mediate species-selective transactivation of PPARα-RXRα heterodimers. Cos7 cells transfected with either both hPPARα and hRXRα, both mPPARα and mRXRα, or both F272I mPPARα and mRXRα analyzed for transactivation of the acyl-CoA oxidase reporter construct in presence of vehicle (*open bars*), 1 μM lauric acid (*diagonally upward bars*), 1 μM palmitic acid (*hatched bars*), 1 μM palmitoleic acid (*diagonally downward bars*), 1 μM stearic acid (*horizontally lined bars*), 1 μM docosahexanoic acid (*open bars*) and 1 μM clofibrate (*diagonally upward bars*). The *y-axis* represents values for firefly luciferase activity that have been normalized to *Renilla* luciferase (internal control) as well as controls for cells transfected with empty pSG5 vector. The bar graph represents the mean values ($n \geq 3$) ± standard error. * $P < 0.01$, ** $P < 0.001$.

Computational and experimental data support the notion that amino acid substitutions could be responsible for differences in binding affinity and activation observed between human and mouse PPARα. It is believed that during the course of evolution, emerging nuclear receptors acquired the ligand-binding capacities and further refined their specificities for a particular biologically signficiant ligand (*184, 200, 201*). Among 117 vertebrate PPARα protein coding sequences identified by BLAST, isoleucine 272 is conserved from bony fish to primates, with the exception of mouse (*Mus musculus*), rat (*Rattus norvegicus*) and two unrelated rodents: the naked mole rat (*Heterocephalus glaber*) and the thirteen-lined ground squirrel (*Ictidomys tridecemlineatus*). The distribution of these species suggests that the substitution of isoleucine for phenylalanine has evolved at least three times. A simple transversion (A to T) in the first position of the codon is enough to convert an isoleucine to a phenylalanine codon. However, given the high evolutionary rate of PPARα (*184, 200, 201*), the conservation of isoleucine in this position implies that there are functional and evolutionary consequences associated with this change (e.g. it is under purifying selection).

Consistent with this, our results indicated that compared to humans, the I272F amino acid change seen in mouse represents a partial loss of function mutation (hypomorphic) with respect to LCFA binding. Whether this change is responsible for the increased sensitivity of mouse to peroxisome proliferation or hepatic cancer remains to be determined, but the single F272I substitution in mPPARα recapitulates the human-like LCFA binding and trans-activation functions. Other amino acid positions examined that were not predicted to alter LCFA binding energies (such as position 279) displayed much

greater variation among species, suggesting more relaxed functional and evolutionary constraints at those positions. One could speculate that PPARα underwent strong selective pressure that was directly affected by dietary changes and that this eventually provided crucial structural and functional changes like I272F in mouse. However, there is no clear dietary or metabolic relationship uniquely shared among the four species that harbor the I272F amino acid change, and compensatory mechanisms that may allow this mutation to persist within these species are not clearly established. Therefore, the important question that still remains unsolved is why such differences in PPARα structure would exist.

Nonetheless, we demonstrated for the first time that differences in amino acids in the LBD of PPARα contribute to species selectivity and specificity for endogenous PPARα ligands. The importance of PPARα in human disease is validated by the lipid lowering effects of synthetic PPARα agonists. The data presented herein enhances our understanding of dietary effects on PPARα and may aid in the development of more targeted therapeutics. Moreover, these data demonstrate the efficacy of molecular modeling and docking simulations for examining the effect of structural variations on ligand binding.

**Summary and Conclusions:**

The importance of dietary fat has been acknowledged ever since Burr and Burr (1929) examined the effects of fat-free diets in rats (*202*). They noticed that, as compared to rats on normal diet, rats on fat-free diets (with same calories via proteins and vitamins) failed to thrive and developed various physiological problems including skin disorders and kidney problems (*202*). Further, these rats were reverted to good health when dietary fats were added to their food (*202*). It is known today that dietary fatty acids are ubiquitous molecules that serve as major metabolic fuels, important components of biological membranes and signaling molecules, and play significant roles as gene regulators. The regulation of lipid metabolism is thus crucial for whole-body energy homeostasis. Since the amount of available nutrients do not always match their energetic demands, it is important that living organisms continuously adapt their metabolism to their nutritional status, such that energy intake and expenditure remain adjusted. Unfortunately, the rate of fat oxidation is not necessarily determined by the amount of fat intake, but rather by the energy gap resulting post carbohydrate metabolism (*203*). Therefore the regulation of lipid metabolism in mammals is complex in nature. It consists of a short/rapid component involving rapid modulation of protein activity/stability (by allosteric means or post-translational modifications) and a long-term component involving transcription factors.

PPARα is a ligand-activated nuclear transcription factor that plays an important regulatory role in cellular processes such as fatty acid metabolism, glucose metabolism, inflammation, differentiation and proliferation (*7-10*). In 2015 we will be celebrating the $25^{th}$ year anniversary of the PPARα discovery. Initially isolated as a receptor that serves

as a target for a diverse class of peroxisome proliferators in rodents, today it is regarded as a lipid sensor that regulates the expression of several proteins/enzymes involved in fatty acid metabolism. Although fatty acids and their derivatives has been shown to activate PPARα of several species including mouse PPARα (mPPARα) (*8, 108, 110, 113-117*), the identity of high-affinity endogenous ligands for human PPARα (hPPARα) have been more elusive. In order to understand the molecular role of dietary LCFA in human PPARα mediated regulation of energy homeostasis we set out with two main goals for this dissertation: 1) to determine whether LCFA and LCFA-CoA constitute high-affinity endogenous ligands for full-length hPPARα and 2) to investigate whether there exist differences in such affinity between hPPARα and mPPARα. The main outcomes and conclusions of this dissertation are discussed below:

*LCFA and their thioesters serve as high affinity physiological ligands for PPARα –metacrine signaling and transcriptional control.* For the first time we demonstrated that LCFA and LCFA-CoA represent high affinity ligands for full-length recombinant hPPARα. Such binding occured at physiologically relevant concentrations ($K_d$ = 11-40 nM) and was associated with strong secondary structural changes in the protein (hallmarks of nuclear receptor ligand binding). Ligand binding also resulted in a PPARα-dependent transactivation of the ACOX PPRE-luciferase reporter in COS-7 cells, suggesting that these ligands could in fact activate PPARα *in vivo*. While it is acknowledged that PPARα has evolved as a lipoid sensor that regulates the expression of target genes involved in lipid metabolism (*111, 114, 121*), the identification of LCFA and LCFA-CoA as ligands for PPARα further substantiates our knowledge on PPARα function. Such a link between nutrient/metabolite and transcriptional regulation has been

long appreciated in bacteria. For example, the *lac* repressor in bacteria binds a lactose metabolite (allolactose) and coordinates the synthesis of the enzymes required for the breakdown/catabolism of lactose or its metabolites (*204*). It is possible that such allosteric regulation is in place in higher organism as well. For example, LCFA or their metabolites bind PPARα and induce feed-forward activation or feedback inhibition in the expression of genes involved in their metabolism. The first evidence or proof for such theory came from genetically engineered mouse models. For example, in ACOX knock-out mice (ACOX-/-; first enzyme involved in β-oxidation) there is accumulation of PPARα ligands (LCFA and LCFA-CoA) and hyperactivity of PPARα because these ligands cannot enter the β-oxidation pathway (*121*). Also, peroxisomal bifunctional enzyme (second enzyme involved in β-oxidation) knockout mice have up-regulated PPARα target genes because intermediates of peroxisomal β-oxidation serve as PPARα ligands (*205*). Liver-specific fatty acid synthase (FAS; first enzyme involved in fatty acid biosynthesis) knockout mice on a zero-fat diet exhibit severe hypoglycemia and fatty liver similar to the PPARα knockout mice phenotype (*206*). These effects were reversed upon administration of either dietary fat or a PPARα agonist (*206*). All these findings along with our results further confirm the role of PPARα as a lipid sensor.

While in most studies, LCFA and LCFA-CoA activate PPARα, Murakami *et al.* suggested that LCFA-CoA interact with PPARα and have an inhibitory effect on PPARα activity (*84*). Assuming that this is the case, it is possible that metabolites such as LCFA-CoA could increase or decrease PPARα activity depending on the target gene or the effect desired. For example, LCFA are rapidly converted to LCFA-CoA by an enzyme called long chain acyl-CoA synthase 1 (ACSL1) - a PPARα target. It is possible that

while LCFA induces the expression of ACSL1 (through a PPRE in its promoter), depending on the relative ratio of LCFA/LCFA-CoA, LCFA-CoA may repress ACSL1 by a negative feedback mechanism. Although this possibility has not been tested in this dissertation, it will be interesting to test this angle of nutrient mediated PPARα regulation of target genes. It is necessary to mention that the inhibitory activities of LCFA-CoA reported by Murakami *et al.* were derived on the basis of their inability to recruit a coactivator peptide of SRC-1 to the hPPARα-LBD. Since only one coactivator peptide was tested for binding to hPPARα-LBD in response to LCFA-CoA binding (no full-length coactivator or protein), the significance of these findings are not clear. It is possible that LCFA-CoA bound PPARα recruits SRC-1 to the coactivator binding motif on the A/B domain (PPARα-LBD used in these studies) as discussed in the introduction of this dissertation. Alternatively, LCFA-CoA bound PPARα may selectively recruit other coactivators other than SRC-1.

Although our *in vitro* experiments using multiple fluorescence-based approaches and CD spectroscopy demonstrated binding of both LCFA and LCFA-CoA to hPPARα, data from our transactivation assays did not differentiate the effects of LCFA on hPPARα activity from that of LCFA-CoA. One way to do this would be to use cells that do not express long chain acyl-CoA synthase (ACSL) - the cellular enzyme that converts LCFA to LCFA-CoA. However, there are 5 isoforms of ACSL numbered as 1, 3, 4, 5 and 6 that belong to a much larger family of acyl-CoA synthases (26 members including ACSLs) (*207*, *208*). Owing to the many isoforms of this protein, it will be challenging to knock-down the activity of this enzyme. Another way to approach this problem is to pharmacologically inhibit ACSL activity in the cell by using inhibitors such as triascin C

(*209*). Such experiments involving the use of triascin C attempted in our lab as well as by others, resulted in significant cell death (unpublished data Ms. Jeanette Loyer, Hostetler lab and (*210*)). Another way that one might address this issue is to treat cells with non-metabolizable forms of LCFA (e.g. bromopalmitic acid) and LCFA-CoA (e.g. S-hexadecyl-CoA) and determine the expression of PPARα target genes such as ACSL1. While this approach has not been tested in this dissertation, it will be interesting to determine 1) whether these ligands bind with equivalent affinity as the natural ligands and 2) whether these ligands exhibit any difference in PPARα mediated transactivation (using the ACOX PPRE×3 reporter construct) or gene expression.

It is essential to mention that all ligand binding studies in this dissertation were carried out using recombinant full-length forms of human and mouse PPARα. These proteins were expressed in bacteria and subsequently purified using affinity chromatography. That being said, an important consideration must be given to the fact that since these proteins were expressed in bacteria, they may lack post-translational modifications that are commonly seen in eukaryotic organisms. PPARα undergoes post-translational modifications in the form of phosphorylation (*211*), ubiquitination (*212*) and SUMOylation (*213*). While it is not clear whether post translational modifications have any observable effects on ligand binding, such modifications definitely have an impact on the activity of PPARα. For example, phosphorylation increases the ligand-induced transcriptional activity of PPARα, whereas SUMOylation decreases it. However, post-translational modifications mainly influence PPARα activity through preferential recruitment of cofactors (coactivators or corepressors) (*211, 213*). Likewise ligand binding also influences the occurances of post translational modifications. For example

ligand binding decreases PPARα ubiquination and SUMOylation (*214*). Recombinant proteins have been widely used to study various aspects of PPARα function for a long time. Although we cannot rule out the effect of post-translational modifications on ligand binding, data from transactivation assays done in COS-7 cells (where post-translational modifications could occur) corroborate and confirm ligand mediated activation of PPARα.

We utilized the ACOX PPRE×3 reporter construct in all our transactivation assays. Although this reporter has been widely used to test the PPARα activity, it represents an artificial reporter system where three copies of the ACOX PPRE along with the thymidine kinase (TK) minimal promoter have been cloned upstream of a firefly luciferase gene (*39, 180*). Such reporter assays essentially determine whether a nuclear receptor (PPARα) can activate or repress gene transcription (in response to ligands) when it binds to its response element (PPRE) (*215*). Since sequences around the PPRE could be a determinant in PPARα specificity (*29, 43*), it will be interesting to see how LCFA ligands affect the transcription of the luciferase gene driven by a much larger promoter of a PPARα target gene. Alternatively, it would also be interesting to determine the actual transcript or protein levels of PPARα target genes upon administration of such ligands.

*LCFA and their thioesters serve as high affinity physiological ligands for PPARα – binding affinity number considerations.* In addition to demonstrating the binding of LCFA and LCFA-CoA to hPPARα, we also report binding affinities for such ligands. The interaction of ligands with their binding site on the receptor is characterized in terms of binding affinity. Higher binding affinity means that a lower concentration of ligand is sufficient to maximally occupy all the binding sites. Binding affinity is represented in

terms of a dissociation constant or $K_d$ – the concentration of the ligand at which 50% of the receptor binding sites are occupied (*178*). Binding affinity numbers reported here for LCFA and LCFA-CoA interaction with full-length PPARα are consistent with the physiological concentrations of these ligands in the cell (*88, 95, 117, 118, 120, 152*). This comparison of receptor-ligand binding affinity and physiological concentration of the ligands serves as a guideline to confirm the relevance of the ligand for receptor function. For example, vitamin D receptor (VDR) binds vitamin D at nanomolar concentrations (consistent with cellular concentrations), but it is also activated by bile acids at much higher concentrations (*216*). It is possible that bile acids either do not represent true ligands for VDR (or bring about VDR activation indirectly) or VDR may have some other functions in the gut where the concentration of bile acids could be considerably higher than other organs (*216*). In a similar manner, LCFA and LCFA-CoA may activate PPARα in tissues with high involvement in fat metabolism and/or nanomolar concentrations of these ligands (such as liver, muscle, heart, adipose) but they may not play a role in other tissues which are not as dependent on fat metabolism, such as the brain (*152*, *217*).

In the case of drug molecules, binding affinity numbers are indicative of drug specificity and efficacy, and it helps determine the effective dose of the drug. Along with structure-activity relationship, binding affinity numbers help design better drugs with selective affinity to the targeted receptor and lesser side-effects. Knowing the binding affinities for different fatty acids and their derivatives will help determine the kind of competition a synthetic agonist or a therapeutic drug may encounter. The degree of PPARα activation *in vivo* may not result from its interactions with a single high affinity

fatty acid ligand but may instead arise from the pool of fatty acids and/or its metabolites. Thus when a drug is administered (example, a PPARα agonist such as clofibrate) it has to compete with this pool of endogenous ligands. Since the nutritional status of each individual varies greatly owing to dietary parameters and physiological/disease state, the anticipated therapeutic response may not be achieved in each and every individual. For example, clinically it is observed that fibrate treatment improves the lipid profile for the majority of the patients but there is always a fraction of patients, who do not respond to such therapy (*218*). Similarly differences in responses are also observed with mice strain variations. It is possible that in addition to genotype, diet-drug interactions could also result in such differences in responses to therapeutic treatments. Thus, better knowledge of these affinity numbers along with the metabolic/nutritional status of a patient will allow for careful dose adjustments for effective therapeutic treatments.

*There exist differences in activation of human and mouse PPARα in response to saturated LCFA – species differences considerations.* One of the most important outcomes of this dissertation is the species differences in the ligand binding specificity and affinity between the full-length forms of hPPARα and mPPARα. Species differences in the binding of endogenous ligands for other nuclear receptors such as the estrogen receptors have also been observed (*219*). Before going into depths comparing the two full-length proteins, it is essential to compare our LCFA binding data from full-length mPPARα to that of truncated mPPARαΔAB (lacking the N-terminal A/B domain). In contrast to our study with full-length mPPARα, previous studies with mPPARαΔAB indicate very weak binding to saturated and polyunsaturated LCFA (but strong binding to their thioester derivatives) (*115-117*). While these differences could arise from

differences in the protein preparation or techniques used, it should also be noted that one of the main differences lies in the fact that these data were generated using truncated form of PPARα (*115-117*). The N-terminal A/B domain of PPARα not only contributes to transcriptional activity of PPARα (*30, 31*) but also determines DNA binding (*31*) and ligand specificity (*34*). Mutations of residues in the A/B domain (particularly S112) altered ligand binding and activity (function of E/F domain) of PPARγ (*34*). Berbaum *et al.* also reported differences in coactivator recruitment and fibrate-induced transcriptional activation between the full-length and LBD forms of PPARα (*153*). These results provide evidence to the interdomain communications between the various domains structures of the protein.

We have reported significant differences in the ligand binding affinities and activity of hPPARα and mPPARα in response to saturated LCFA. A careful examination of the existing literature demonstrated that: 1) species differences in the activity of human and mouse PPARα in response to synthetic agonists such as WY-14,643 have been observed by others researchers (*158, 160-163, 187, 199*) and 2) differences in the target gene profiles and activity of human and mouse PPARα have also been reported (*158, 160-163, 187, 199*). Since the discovery of peroxisomal proliferators, it has been established that long-term administration of PPARα agonists result in hepatic cancer only in rodents (*102*). Further, transgenic mice that express human PPARα mainly in the liver do not exhibit liver tumors upon administration of PPARα agonists (*149, 150*). All these observations suggest that structural differences in the PPARα protein could be one possible underlying cause of such species variation. Owing to the use of the rodent models for toxicological evaluation of therapeutics, and the importance of PPARα as a

pharmaceutical target, we decided to focus on the structural aspects of the human and the mouse protein to explain possible mechanisms of such differences.

Comparison of the primary sequence of PPARα from more than 100 vertebrate species demonstrated that they harbor the same amino acids at 314 and 464 (tyrosine) that participate in direct hydrogen bonding interactions with synthetic agonists as well as LCFA ligands. Despite these similarities, there were differences in the binding affinities as well as binding energies for interaction of human and mouse PPARα with saturated LCFA (palmitic and stearic acids). This suggested that other amino acid residues may also play a role in ligand specificity. Using the strategies of molecular modeling, docking, pocket volume estimations and mutagenesis, we were able to narrow down two amino acid residues at 272 and 279 as crucial determinants of such ligand specificity. The amino acid residue at 272 (isoleucine in human and phenylalanine in mouse) was especially critical for determining ligand specificity for saturated LCFA. These findings were consistent with other researchers who have also demonstrated similar species differences with PPARα (*158, 160-163, 187, 199*).

While it is still not clear is why such differences would exist, one hypothesis includes the nuclear receptor evolution of ligand binding capacity. It is speculated that nuclear receptors evolved from a common ancesteral orphan receptor (no ligand) (*184, 200, 201*). During the course of evolution, emerging nuclear receptors acquired ligand-binding capacities and underwent very subtle changes (typically due to just a few mutations) resulting in further refining their specificities for a given ligand (*184, 200, 201*). Except for rats and mice, the isoleucine at 272 in hPPARα is highly conserved across more than 100 vertebrate species. Owing to the high evolutionary rate of PPARα

(*184, 200, 201*), one could speculate that the receptor underwent evolutionary adaptations by mutations in response to a different range of ligands in different species. While it is not obvious what could have been the source of such adaptation, dietary changes have also been proposed to be one of the strong driving forces for such adaptation (*220*). For example, the persistence of lactase expression in populations with a long history of milk consumption (*220*). It is tempting to speculate that genes that were directly affected by dietary changes came under strong selective pressures which eventually lead to crucial structural and functional changes (example I272F).

With that being said, the bigger question that one needs to address is whether the rodent model is ideal for studying proteins with such species diversity. Mice as a model system have several advantages. For example, 1) their genome is fairly similar to the human genome, 2) their small size facilitates high through-put studies in a cost effective manner and 3) the availability of genetically engineered mice (such as the PPARα -/- mice) provides a wealth of information on disease processes (and functional aspects of the PPARα protein). However, there are also drawbacks – they are not humans (*221*). In addition to structural and functional differences in the mouse and human forms of PPARα, long-term administration of PPARα agonists results in rodent specific hepatocarcinogenesis (*102*). Since amino acid residues at 272 and 279 in the PPARα ligand binding domain are crucial determinants of ligand specificity, quantitative structure activity relationship must be utilized extensively to screen potential PPARα drug candidates that are more specific for the human form of the protein. Further, in order to carry out pharmacological and toxicological evaluation of potential PPARα drug

candidates, other model organisms (which do not display such diversity) or humanized mouse models of PPARα should be employed.

In conclusion, fatty acids are essential dietary components that serve as metacrine signals transducing metabolic parameters into regulatory events. Elevated levels of triglycerides or fatty acids are a major component of obesity and its co-morbidities including the metabolic syndrome. PPARα serves to sense the total flux of fatty acids and regulate various metabolic pathways associated with fatty acid metabolism. The importance of PPARα in human disease is validated by the lipid lowering effects of synthetic PPARα agonists. Our data suggests that LCFA serve as high affinity ligands for PPARα and thus help regulate lipid homeostasis. However special consideration must be given to differences in ligand binding specificity and affinity between mouse and human PPARα. Our results, along with others, call for careful interpretation and extrapolation of data that use mouse as a model for studying this protein. Further, they emphasize on the need to develop drugs that have greater specificity for human versus rodent PPARα.

## References


1. Reaven, G. M. (1988) Banting lecture 1988. Role of insulin resistance in human disease, Diabetes 37, 1595-1607.
2. Grundy, S. M., Brewer, H. B., Jr., Cleeman, J. I., Smith, S. C., Jr., and Lenfant, C. (2004) Definition of metabolic syndrome: Report of the National Heart, Lung, and Blood Institute/American Heart Association conference on scientific issues related to definition, Circulation 109, 433-438.
3. Ervin, R. B. (2009) Prevalence of metabolic syndrome among adults 20 years of age and over, by sex, age, race and ethnicity, and body mass index: United States, 2003-2006, Natl Health Stat Report, 1-7.
4. Ogden, C. L., and Carroll, M. D. (2010) Prevalence of Obesity Among Children and Adolescents: United States, Trends 1963-1965 Through 2007-2008, Center for Disease Control and Prevention, Division of Health and Nutrition Examination Surveys, NCHS Health E-Stat.
5. Ogden, C. L., Carroll, M. D., Kit, B. K., and Flegal, K. M. (2012) Prevalence of obesity in the United States, 2009-2010, NCHS Data Brief, 1-8.
6. Cawley, J., and Meyerhoefer, C. (2012) The medical care costs of obesity: an instrumental variables approach, J Health Econ 31, 219-230.
7. Kersten, S., Desvergne, B., and Wahli, W. (2000) Roles of PPARs in health and disease, Nature 405, 421-424.
8. Pyper, S. R., Viswakarma, N., Yu, S., and Reddy, J. K. (2010) PPARalpha: energy combustion, hypolipidemia, inflammation and cancer, Nucl Recept Signal 8, e002.

9. Vincent Laudet, H. G. (2002) PPAR, Academic Press.

10. Escher, P., and Wahli, W. (2000) Peroxisome proliferator-activated receptors: insight into multiple cellular functions, Mutat Res 448, 121-138.

11. Reddy, J. K., Azarnoff, D. L., and Hignite, C. E. (1980) Hypolipidaemic hepatic peroxisome proliferators form a novel class of chemical carcinogens, Nature 283, 397-398.

12. Lalwani, N. D., Reddy, M. K., Qureshi, S. A., Sirtori, C. R., Abiko, Y., and Reddy, J. K. (1983) Evaluation of selected hypolipidemic agents for the induction of peroxisomal enzymes and peroxisome proliferation in the rat liver, Hum Toxicol 2, 27-48.

13. Lalwani, N. D., Fahl, W. E., and Reddy, J. K. (1983) Detection of a nafenopin-binding protein in rat liver cytosol associated with the induction of peroxisome proliferation by hypolipidemic compounds, Biochem Biophys Res Commun 116, 388-393.

14. Lalwani, N. D., Alvares, K., Reddy, M. K., Reddy, M. N., Parikh, I., and Reddy, J. K. (1987) Peroxisome proliferator-binding protein: identification and partial characterization of nafenopin-, clofibric acid-, and ciprofibrate-binding proteins from rat liver, Proc Natl Acad Sci U S A 84, 5242-5246.

15. Issemann, I., and Green, S. (1990) Activation of a member of the steroid hormone receptor superfamily by peroxisome proliferators, Nature 347, 645-650.

16. Kliewer, S. A., Forman, B. M., Blumberg, B., Ong, E. S., Borgmeyer, U., Mangelsdorf, D. J., Umesono, K., and Evans, R. M. (1994) Differential

expression and activation of a family of murine peroxisome proliferator-activated receptors, Proc Natl Acad Sci U S A 91, 7355-7359.

17. Dreyer, C., Krey, G., Keller, H., Givel, F., Helftenbein, G., and Wahli, W. (1992) Control of the peroxisomal beta-oxidation pathway by a novel family of nuclear hormone receptors, Cell 68, 879-887.

18. Sher, T., Yi, H. F., McBride, O. W., and Gonzalez, F. J. (1993) cDNA cloning, chromosomal mapping, and functional characterization of the human peroxisome proliferator activated receptor, Biochemistry 32, 5598-5604.

19. Schmidt, A., Endo, N., Rutledge, S. J., Vogel, R., Shinar, D., and Rodan, G. A. (1992) Identification of a new member of the steroid hormone receptor superfamily that is activated by a peroxisome proliferator and fatty acids, Mol Endocrinol 6, 1634-1641.

20. Greene, M. E., Blumberg, B., McBride, O. W., Yi, H. F., Kronquist, K., Kwan, K., Hsieh, L., Greene, G., and Nimer, S. D. (1995) Isolation of the human peroxisome proliferator activated receptor gamma cDNA: expression in hematopoietic cells and chromosomal mapping, Gene Expr 4, 281-299.

21. Fajas, L., Auboeuf, D., Raspe, E., Schoonjans, K., Lefebvre, A. M., Saladin, R., Najib, J., Laville, M., Fruchart, J. C., Deeb, S., Vidal-Puig, A., Flier, J., Briggs, M. R., Staels, B., Vidal, H., and Auwerx, J. (1997) The organization, promoter analysis, and expression of the human PPARgamma gene, J Biol Chem 272, 18779-18789.

22. Gervois, P., Torra, I. P., Chinetti, G., Grotzinger, T., Dubois, G., Fruchart, J. C., Fruchart-Najib, J., Leitersdorf, E., and Staels, B. (1999) A truncated human

peroxisome proliferator-activated receptor alpha splice variant with dominant negative activity, Mol Endocrinol 13, 1535-1549.

23. Choi, Y. J., Roberts, B. K., Wang, X., Geaney, J. C., Naim, S., Wojnoonski, K., Karpf, D. B., and Krauss, R. M. (2012) Effects of the PPAR-delta agonist MBX-8025 on atherogenic dyslipidemia, Atherosclerosis 220, 470-476.

24. Ooi, E. M., Watts, G. F., Sprecher, D. L., Chan, D. C., and Barrett, P. H. (2011) Mechanism of action of a peroxisome proliferator-activated receptor (PPAR)-delta agonist on lipoprotein metabolism in dyslipidemic subjects with central obesity, J Clin Endocrinol Metab 96, E1568-1576.

25. Desvergne, B., and Wahli, W. (1999) Peroxisome proliferator-activated receptors: nuclear control of metabolism, Endocr Rev 20, 649-688.

26. Xu, H. E., Lambert, M. H., Montana, V. G., Plunket, K. D., Moore, L. B., Collins, J. B., Oplinger, J. A., Kliewer, S. A., Gampe, R. T., McKee, D. D., Moore, J. T., and Willson, T. M. (2001) Structural determinants of ligand binding selectivity between the peroxisome proliferator-activated receptors, Proc Natl Acad Sci USA 98, 13919-13924.

27. Dahlman-Wright, K., Baumann, H., McEwan, I. J., Almlof, T., Wright, A. P., Gustafsson, J. A., and Hard, T. (1995) Structural characterization of a minimal functional transactivation domain from the human glucocorticoid receptor, Proc Natl Acad Sci U S A 92, 1699-1703.

28. Warnmark, A., Wikstrom, A., Wright, A. P., Gustafsson, J. A., and Hard, T. (2001) The N-terminal regions of estrogen receptor alpha and beta are

unstructured in vitro and show different TBP binding properties, J Biol Chem 276, 45939-45944.

29. Chandra, V., Huang, P., Hamuro, Y., Raghuram, S., Wang, Y., Burris, T. P., and Rastinejad, F. (2008) Structure of the intact PPAR-gamma-RXR- nuclear receptor complex on DNA, Nature 456, 350-356.

30. Hi, R., Osada, S., Yumoto, N., and Osumi, T. (1999) Characterization of the amino-terminal activation domain of peroxisome proliferator-activated receptor alpha. Importance of alpha-helical structure in the transactivating function, J Biol Chem 274, 35152-35158.

31. Hsu, M. H., Palmer, C. N., Song, W., Griffin, K. J., and Johnson, E. F. (1998) A carboxyl-terminal extension of the zinc finger domain contributes to the specificity and polarity of peroxisome proliferator-activated receptor DNA binding, J Biol Chem 273, 27988-27997.

32. Bugge, A., Grontved, L., Aagaard, M. M., Borup, R., and Mandrup, S. (2009) The PPARgamma2 A/B-domain plays a gene-specific role in transactivation and cofactor recruitment, Mol Endocrinol 23, 794-808.

33. Castillo, G., Brun, R. P., Rosenfield, J. K., Hauser, S., Park, C. W., Troy, A. E., Wright, M. E., and Spiegelman, B. M. (1999) An adipogenic cofactor bound by the differentiation domain of PPARgamma, EMBO J 18, 3676-3687.

34. Shao, D., Rangwala, S. M., Bailey, S. T., Krakow, S. L., Reginato, M. J., and Lazar, M. A. (1998) Interdomain communication regulating ligand binding by PPAR-gamma, Nature 396, 377-380.

35. Glass, C. K. (1994) Differential recognition of target genes by nuclear receptor monomers, dimers, and heterodimers, Endocr Rev 15, 391-407.

36. Dreyer, C., Keller, H., Mahfoudi, A., Laudet, V., Krey, G., and Wahli, W. (1993) Positive regulation of the peroxisomal beta-oxidation pathway by fatty acids through activation of peroxisome proliferator-activated receptors (PPAR), Biol Cell 77, 67-76.

37. Schwabe, J. W., Chapman, L., Finch, J. T., and Rhodes, D. (1993) The crystal structure of the estrogen receptor DNA-binding domain bound to DNA: how receptors discriminate between their response elements, Cell 75, 567-578.

38. Rastinejad, F., Perlmann, T., Evans, R. M., and Sigler, P. B. (1995) Structural determinants of nuclear receptor assembly on DNA direct repeats, Nature 375, 203-211.

39. Kliewer, S. A., Umesono, K., Noonan, D. J., Heyman, R. A., and Evans, R. M. (1992) Convergence of 9-cis retinoic acid and peroxisome proliferator signalling pathways through heterodimer formation of their receptors, Nature 358, 771-774.

40. Tugwood, J. D., Issemann, I., Anderson, R. G., Bundell, K. R., McPheat, W. L., and Green, S. (1992) The mouse peroxisome proliferator activated receptor recognizes a response element in the 5' flanking sequence of the rat acyl CoA oxidase gene, EMBO J 11, 433-439.

41. van der Meer, D. L., Degenhardt, T., Vaisanen, S., de Groot, P. J., Heinaniemi, M., de Vries, S. C., Muller, M., Carlberg, C., and Kersten, S. (2010) Profiling of promoter occupancy by PPARalpha in human hepatoma cells via ChIP-chip analysis, Nucleic Acids Res 38, 2839-2850.

42. Palmer, C. N., Hsu, M. H., Griffin, H. J., and Johnson, E. F. (1995) Novel sequence determinants in peroxisome proliferator signaling, J Biol Chem 270, 16114-16121.

43. Juge-Aubry, C., Pernin, A., Favez, T., Burger, A. G., Wahli, W., Meier, C. A., and Desvergne, B. (1997) DNA binding properties of peroxisome proliferator-activated receptor subtypes on various natural peroxisome proliferator response elements. Importance of the 5'-flanking region, J Biol Chem 272, 25252-25259.

44. A, I. J., Jeannin, E., Wahli, W., and Desvergne, B. (1997) Polarity and specific sequence requirements of peroxisome proliferator-activated receptor (PPAR)/retinoid X receptor heterodimer binding to DNA. A functional analysis of the malic enzyme gene PPAR response element, J Biol Chem 272, 20108-20117.

45. Aranda, A., and Pascual, A. (2001) Nuclear hormone receptors and gene expression, Physiol Rev 81, 1269-1304.

46. Vincent Laudet, H. G. (2002) General organization of nuclear receptors.

47. Mangelsdorf, D. J., Thummel, C., Beato, M., Herrlich, P., Schutz, G., Umesono, K., Blumberg, B., Kastner, P., Mark, M., Chambon, P., and Evans, R. M. (1995) The nuclear receptor superfamily: the second decade, Cell 83, 835-839.

48. Egea, P. F., Mitschler, A., and Moras, D. (2002) Molecular recognition of agonist ligands by RXRs, Mol Endocrinol 16, 987-997.

49. Nolte, R. T., Wisely, G. B., Westin, S., Cobb, J. E., Lambert, M. H., Kurokawa, R., Rosenfeld, M. G., Willson, T. M., Glass, C. K., and Milburn, M. V. (1998) Ligand binding and co-activator assembly of the peroxisome proliferator-activated receptor-gamma, Nature 395, 137-143.

50. Xu, H. E., Lambert, M. H., Montana, V. G., Parks, D. J., Blanchard, S. G., Brown, P. J., Sternbach, D. D., Lehmann, J. M., Wisely, G. B., Willson, T. M., Kliewer, S. A., and Milburn, M. V. (1999) Molecular recognition of fatty acids by peroxisome proliferator-activated receptors, Mol Cell 3, 397-403.

51. Xu, H. E., Stanley, T. B., Montana, V. G., Lambert, M. H., Shearer, B. G., Cobb, J. E., McKee, D. D., Galardi, C. M., Plunket, K. D., Nolte, R. T., Parks, D. J., Moore, J. T., Kliewer, S. A., Willson, T. M., and Stimmel, J. B. (2002) Structural basis for antagonist-mediated recruitment of nuclear co-repressors by PPARalpha, Nature 415, 813-817.

52. Takada, I., Yu, R. T., Xu, H. E., Lambert, M. H., Montana, V. G., Kliewer, S. A., Evans, R. M., and Umesono, K. (2000) Alteration of a single amino acid in peroxisome proliferator-activated receptor-alpha (PPAR alpha) generates a PPAR delta phenotype, Mol Endocrinol 14, 733-740.

53. Dowell, P., Peterson, V. J., Zabriskie, T. M., and Leid, M. (1997) Ligand-induced peroxisome proliferator-activated receptor alpha conformational change, J Biol Chem 272, 2013-2020.

54. Juge-Aubry, C. E., Gorla-Bajszczak, A., Pernin, A., Lemberger, T., Wahli, W., Burger, A. G., and Meier, C. A. (1995) Peroxisome proliferator-activated receptor mediates cross-talk with thyroid hormone receptor by competition for retinoid X receptor. Possible role of a leucine zipper-like heptad repeat, J Biol Chem 270, 18117-18122.

55. Huang, P., Chandra, V., and Rastinejad, F. (2010) Structural overview of the nuclear receptor superfamily: insights into physiology and therapeutics, Annu Rev Physiol 72, 247-272.

56. Jin, L., and Li, Y. Structural and functional insights into nuclear receptor signaling, Adv Drug Deliv Rev 62, 1218-1226.

57. Bourguet, W., Ruff, M., Chambon, P., Gronemeyer, H., and Moras, D. (1995) Crystal structure of the ligand-binding domain of the human nuclear receptor RXR-alpha, Nature 375, 377-382.

58. Wurtz, J. M., Bourguet, W., Renaud, J. P., Vivat, V., Chambon, P., Moras, D., and Gronemeyer, H. (1996) A canonical structure for the ligand-binding domain of nuclear receptors, Nat Struct Biol 3, 87-94.

59. Renaud, J. P., Rochel, N., Ruff, M., Vivat, V., Chambon, P., Gronemeyer, H., and Moras, D. (1995) Crystal structure of the RAR-gamma ligand-binding domain bound to all-trans retinoic acid, Nature 378, 681-689.

60. Pissios, P., Tzameli, I., Kushner, P., and Moore, D. D. (2000) Dynamic stabilization of nuclear receptor ligand binding domains by hormone or corepressor binding, Mol Cell 6, 245-253.

61. Nagy, L., and Schwabe, J. W. (2004) Mechanism of the nuclear receptor molecular switch, Trends Biochem Sci 29, 317-324.

62. Wang, Z., Benoit, G., Liu, J., Prasad, S., Aarnisalo, P., Liu, X., Xu, H., Walker, N. P., and Perlmann, T. (2003) Structure and function of Nurr1 identifies a class of ligand-independent nuclear receptors, Nature 423, 555-560.

63. Johnson, B. A., Wilson, E. M., Li, Y., Moller, D. E., Smith, R. G., and Zhou, G. (2000) Ligand-induced stabilization of PPARgamma monitored by NMR spectroscopy: implications for nuclear receptor activation, J Mol Biol 298, 187-194.

64. Keidel, S., LeMotte, P., and Apfel, C. (1994) Different agonist- and antagonist-induced conformational changes in retinoic acid receptors analyzed by protease mapping, Mol Cell Biol 14, 287-298.

65. Leng, X., Tsai, S. Y., O'Malley, B. W., and Tsai, M. J. (1993) Ligand-dependent conformational changes in thyroid hormone and retinoic acid receptors are potentially enhanced by heterodimerization with retinoic X receptor, J Steroid Biochem Mol Biol 46, 643-661.

66. Kallenberger, B. C., Love, J. D., Chatterjee, V. K., and Schwabe, J. W. (2003) A dynamic mechanism of nuclear receptor activation and its perturbation in a human disease, Nat Struct Biol 10, 136-140.

67. Raghuram, S., Stayrook, K. R., Huang, P., Rogers, P. M., Nosie, A. K., McClure, D. B., Burris, L. L., Khorasanizadeh, S., Burris, T. P., and Rastinejad, F. (2007) Identification of heme as the ligand for the orphan nuclear receptors REV-ERBalpha and REV-ERBbeta, Nat Struct Mol Biol 14, 1207-1213.

68. Horwitz, K. B., Jackson, T. A., Bain, D. L., Richer, J. K., Takimoto, G. S., and Tung, L. (1996) Nuclear receptor coactivators and corepressors, Mol Endocrinol 10, 1167-1177.

69. Glass, C. K., Rose, D. W., and Rosenfeld, M. G. (1997) Nuclear receptor coactivators, Curr Opin Cell Biol 9, 222-232.

70. Vincent Laudet, H. G. (2002) Molecular mechanisms of transcriptional regulation.

71. Sadowski, I., Ma, J., Triezenberg, S., and Ptashne, M. (1988) GAL4-VP16 is an unusually potent transcriptional activator, Nature 335, 563-564.

72. Onate, S. A., Tsai, S. Y., Tsai, M. J., and O'Malley, B. W. (1995) Sequence and characterization of a coactivator for the steroid hormone receptor superfamily, Science 270, 1354-1357.

73. Alen, P., Claessens, F., Schoenmakers, E., Swinnen, J. V., Verhoeven, G., Rombauts, W., and Peeters, B. (1999) Interaction of the putative androgen receptor-specific coactivator ARA70/ELE1alpha with multiple steroid receptors and identification of an internally deleted ELE1beta isoform, Mol Endocrinol 13, 117-128.

74. Onate, S. A., Boonyaratanakornkit, V., Spencer, T. E., Tsai, S. Y., Tsai, M. J., Edwards, D. P., and O'Malley, B. W. (1998) The steroid receptor coactivator-1 contains multiple receptor interacting and activation domains that cooperatively enhance the activation function 1 (AF1) and AF2 domains of steroid receptors, J Biol Chem 273, 12101-12108.

75. Glass, C. K., and Rosenfeld, M. G. (2000) The coregulator exchange in transcriptional functions of nuclear receptors, Genes Dev 14, 121-141.

76. Chen, J. D., and Evans, R. M. (1995) A transcriptional co-repressor that interacts with nuclear hormone receptors, Nature 377, 454-457.

77. Dowell, P., Ishmael, J. E., Avram, D., Peterson, V. J., Nevrivy, D. J., and Leid, M. (1999) Identification of nuclear receptor corepressor as a peroxisome

proliferator-activated receptor alpha interacting protein, J Biol Chem 274, 15901-15907.

78. Hu, X., and Lazar, M. A. (1999) The CoRNR motif controls the recruitment of corepressors by nuclear hormone receptors, Nature 402, 93-96.

79. Perissi, V., Staszewski, L. M., McInerney, E. M., Kurokawa, R., Krones, A., Rose, D. W., Lambert, M. H., Milburn, M. V., Glass, C. K., and Rosenfeld, M. G. (1999) Molecular determinants of nuclear receptor-corepressor interaction, Genes & Development 13, 3198-3208.

80. Lonard, D. M., and O'Malley, B. W. (2006) The expanding cosmos of nuclear receptor coactivators, Cell 125, 411-414.

81. Puigserver, P., Wu, Z., Park, C. W., Graves, R., Wright, M., and Spiegelman, B. M. (1998) A cold-inducible coactivator of nuclear receptors linked to adaptive thermogenesis, Cell 92, 829-839.

82. Misiti, S., Schomburg, L., Yen, P. M., and Chin, W. W. (1998) Expression and hormonal regulation of coactivator and corepressor genes, Endocrinology 139, 2493-2500.

83. Krey, G., Braissant, O., L'Horset, F., Kalkhoven, E., Perroud, M., Parker, M. G., and Wahli, W. (1997) Fatty acids, eicosanoids, and hypolipidemic agents identified as ligands of peroxisome proliferator-activated receptors by coactivator-dependent receptor ligand assay, Mol Endocrinol 11, 779-791.

84. Murakami, K., Ide, T., Nakazawa, T., Okazaki, T., Mochizuki, T., and Kadowaki, T. (2001) Fatty-acyl-CoA thioesters inhibit recruitment of steroid receptor co-

activator 1 to alpha and gamma isoforms of peroxisome-proliferator-activated receptors by competing with agonists, Biochem J 353, 231-238.

85. Guiochon-Mantel, A., Delabre, K., Lescop, P., and Milgrom, E. (1994) Nuclear localization signals also mediate the outward movement of proteins from the nucleus, Proc Natl Acad Sci U S A 91, 7179-7183.

86. Guiochon-Mantel, A., Delabre, K., Lescop, P., Perrot-Applanat, M., and Milgrom, E. (1994) Cytoplasmic-nuclear trafficking of progesterone receptor. In vivo study of the mechanism of action of antiprogestins, Biochem Pharmacol 47, 21-24.

87. Kumar, S., Saradhi, M., Chaturvedi, N. K., and Tyagi, R. K. (2006) Intracellular localization and nucleocytoplasmic trafficking of steroid receptors: an overview, Mol Cell Endocrinol 246, 147-156.

88. Huang, H., Starodub, O., McIntosh, A., Atshaves, B. P., Woldegiorgis, G., Kier, A. B., and Schroeder, F. (2004) Liver fatty acid-binding protein colocalizes with peroxisome proliferator activated receptor alpha and enhances ligand distribution to nuclei of living cells, Biochemistry 43, 2484-2500.

89. Hostetler, H. A., McIntosh, A. L., Atshaves, B. P., Storey, S. M., Payne, H. R., Kier, A. B., and Schroeder, F. (2009) L-FABP directly interacts with PPARalpha in cultured primary hepatocytes, J Lipid Res 50, 1663-1675.

90. Wolfrum, C., Borrmann, C. M., Borchers, T., and Spener, F. (2001) Fatty acids and hypolipidemic drugs regulate peroxisome proliferator-activated receptors alpha - and gamma-mediated gene expression via liver fatty acid binding protein: a signaling path to the nucleus, Proc Natl Acad Sci U S A 98, 2323-2328.

91. Akiyama, T. E., Baumann, C. T., Sakai, S., Hager, G. L., and Gonzalez, F. J. (2002) Selective intranuclear redistribution of PPAR isoforms by RXR alpha, Mol Endocrinol 16, 707-721.

92. Feige, J. N., Gelman, L., Tudor, C., Engelborghs, Y., Wahli, W., and Desvergne, B. (2005) Fluorescence imaging reveals the nuclear behavior of peroxisome proliferator-activated receptor/retinoid X receptor heterodimers in the absence and presence of ligand, J Biol Chem 280, 17880-17890.

93. Umemoto, T., and Fujiki, Y. (2012) Ligand-dependent nucleo-cytoplasmic shuttling of peroxisome proliferator-activated receptors, PPARalpha and PPARgamma, Genes Cells 17, 576-596.

94. Iwamoto, F., Umemoto, T., Motojima, K., and Fujiki, Y. (2010) Nuclear transport of peroxisome-proliferator activated receptor &alpha, J Biochem 149, 311-319.

95. McIntosh, A. L., Atshaves, B. P., Hostetler, H. A., Huang, H., Davis, J., Lyuksyutova, O. I., Landrock, D., Kier, A. B., and Schroeder, F. (2009) Liver type fatty acid binding protein (L-FABP) gene ablation reduces nuclear ligand distribution and peroxisome proliferator-activated receptor-alpha activity in cultured primary hepatocytes, Arch Biochem Biophys 485, 160-173.

96. Brazda, P., Krieger, J., Daniel, B., Jonas, D., Szekeres, T., Langowski, J., Toth, K., Nagy, L., and Vamosi, G. (2014) Ligand binding shifts highly mobile retinoid x receptor to the chromatin-bound state in a coactivator-dependent manner, as revealed by single-cell imaging, Mol Cell Biol 34, 1234-1245.

97. Voss, T. C., and Hager, G. L. (2014) Dynamic regulation of transcriptional states by chromatin and transcription factors, Nat Rev Genet 15, 69-81.

98. Metivier, R., Reid, G., and Gannon, F. (2006) Transcription in four dimensions: nuclear receptor-directed initiation of gene expression, EMBO Rep 7, 161-167.

99. Kuenzli, S., and Saurat, J. H. (2003) Peroxisome proliferator-activated receptors in cutaneous biology, British Journal of Dermatology 149, 229-236.

100. Foxworthy, P. S., White, S. L., Hoover, D. M., and Eacho, P. I. (1990) Effect of ciprofibrate, bezafibrate, and LY171883 on peroxisomal beta-oxidation in cultured rat, dog, and rhesus monkey hepatocytes, Toxicol Appl Pharmacol 104, 386-394.

101. Bell, A. R., Savory, R., Horley, N. J., Choudhury, A. I., Dickins, M., Gray, T. J., Salter, A. M., and Bell, D. R. (1998) Molecular basis of non-responsiveness to peroxisome proliferators: the guinea-pig PPARalpha is functional and mediates peroxisome proliferator-induced hypolipidaemia, Biochem J 332 ( Pt 3), 689-693.

102. Gonzalez, F. J., and Shah, Y. M. (2008) PPARalpha: mechanism of species differences and hepatocarcinogenesis of peroxisome proliferators, Toxicology 246, 2-8.

103. Klaunig, J. E., Babich, M. A., Baetcke, K. P., Cook, J. C., Corton, J. C., David, R. M., DeLuca, J. G., Lai, D. Y., McKee, R. H., Peters, J. M., Roberts, R. A., and Fenner-Crisp, P. A. (2003) PPARalpha agonist-induced rodent tumors: modes of action and human relevance, Crit Rev Toxicol 33, 655-780.

104. Blaauboer, B. J., van Holsteijn, C. W., Bleumink, R., Mennes, W. C., van Pelt, F. N., Yap, S. H., van Pelt, J. F., van Iersel, A. A., Timmerman, A., and Schmid, B. P. (1990) The effect of beclobric acid and clofibric acid on peroxisomal beta-

oxidation and peroxisome proliferation in primary cultures of rat, monkey and human hepatocytes, Biochem Pharmacol 40, 521-528.

105. Rubins, H. B., Robins, S. J., Collins, D., Fye, C. L., Anderson, J. W., Elam, M. B., Faas, F. H., Linares, E., Schaefer, E. J., Schectman, G., Wilt, T. J., and Wittes, J. (1999) Gemfibrozil for the secondary prevention of coronary heart disease in men with low levels of high-density lipoprotein cholesterol. Veterans Affairs High-Density Lipoprotein Cholesterol Intervention Trial Study Group, N Engl J Med 341, 410-418.

106. Frick, M. H., Elo, O., Haapa, K., Heinonen, O. P., Heinsalmi, P., Helo, P., Huttunen, J. K., Kaitaniemi, P., Koskinen, P., Manninen, V., and et al. (1987) Helsinki Heart Study: primary-prevention trial with gemfibrozil in middle-aged men with dyslipidemia. Safety of treatment, changes in risk factors, and incidence of coronary heart disease, N Engl J Med 317, 1237-1245.

107. Manninen, V., Elo, M. O., Frick, M. H., Haapa, K., Heinonen, O. P., Heinsalmi, P., Helo, P., Huttunen, J. K., Kaitaniemi, P., Koskinen, P., and et al. (1988) Lipid alterations and decline in the incidence of coronary heart disease in the Helsinki Heart Study, JAMA 260, 641-651.

108. Kliewer, S. A., Sundseth, S. S., Jones, S. A., Brown, P. J., Wisely, G. B., Koble, C. S., Devchand, P., Wahli, W., Willson, T. M., Lenhard, J. M., and Lehmann, J. M. (1997) Fatty acids and eicosanoids regulate gene expression through direct interactions with peroxisome proliferator-activated receptors alpha and gamma, Proc Natl Acad Sci U S A 94, 4318-4323.

109. Keller, H., Dreyer, C., Medin, J., Mahfoudi, A., Ozato, K., and Wahli, W. (1993) Fatty acids and retinoids control lipid metabolism through activation of peroxisome proliferator-activated receptor-retinoid X receptor heterodimers, Proc Natl Acad Sci U S A 90, 2160-2164.

110. Gottlicher, M., Widmark, E., Li, Q., and Gustafsson, J. A. (1992) Fatty acids activate a chimera of the clofibric acid-activated receptor and the glucocorticoid receptor, Proc Natl Acad Sci U S A 89, 4653-4657.

111. Devchand, P. R., Keller, H., Peters, J. M., Vazquez, M., Gonzalez, F. J., and Wahli, W. (1996) The PPARalpha-leukotriene B4 pathway to inflammation control, Nature 384, 39-43.

112. Yu, K., Bayona, W., Kallen, C. B., Harding, H. P., Ravera, C. P., McMahon, G., Brown, M., and Lazar, M. A. (1995) Differential activation of peroxisome proliferator-activated receptors by eicosanoids, J Biol Chem 270, 23975-23983.

113. Forman, B. M., Chen, J., and Evans, R. M. (1997) Hypolipidemic drugs, polyunsaturated fatty acids, and eicosanoids are ligands for peroxisome proliferator-activated receptors alpha and delta, Proc Natl Acad Sci U S A 94, 4312-4317.

114. Ellinghaus, P., Wolfrum, C., Assmann, G., Spener, F., and Seedorf, U. (1999) Phytanic acid activates the peroxisome proliferator-activated receptor alpha (PPARalpha) in sterol carrier protein 2-/ sterol carrier protein x-deficient mice, J Biol Chem 274, 2766-2772.

115. Lin, Q., Ruuska, S. E., Shaw, N. S., Dong, D., and Noy, N. (1999) Ligand selectivity of the peroxisome proliferator-activated receptor alpha, Biochemistry 38, 185-190.

116. Hostetler, H. A., Kier, A. B., and Schroeder, F. (2006) Very-long-chain and branched-chain fatty acyl-CoAs are high affinity ligands for the peroxisome proliferator-activated receptor alpha (PPAR alpha), Biochemistry 45, 7669-7681.

117. Hostetler, H. A., Petrescu, A. D., Kier, A. B., and Schroeder, F. (2005) Peroxisome proliferator-activated receptor alpha interacts with high affinity and is conformationally responsive to endogenous ligands, J. Biol. Chem. 280, 18667-18682.

118. Schroeder, F., Petrescu, A. D., Huang, H., Atshaves, B. P., McIntosh, A. L., Martin, G. G., Hostetler, H. A., Vespa, A., Landrock, D., Landrock, K. K., Payne, H. R., and Kier, A. B. (2008) Role of fatty acid binding proteins and long chain fatty acids in modulating nuclear receptors and gene transcription, Lipids 43, 1-17.

119. Hostetler, H. A., Lupas, D., Tan, Y., Dai, J., Kelzer, M. S., Martin, G. G., Woldegiorgis, G., Kier, A. B., and Schroeder, F. (2011) Acyl-CoA binding proteins interact with the acyl-CoA binding domain of mitochondrial carnitine palmitoyl transferase I, Mol Cell Biochem 355, 135-148.

120. Huang, H., Starodub, O., McIntosh, A., Kier, A. B., and Schroeder, F. (2002) Liver fatty acid-binding protein targets fatty acids to the nucleus. Real time confocal and multiphoton fluorescence imaging in living cells, J Biol Chem 277, 29139-29151.

121. Fan, C. Y., Pan, J., Chu, R., Lee, D., Kluckman, K. D., Usuda, N., Singh, I., Yeldandi, A. V., Rao, M. S., Maeda, N., and Reddy, J. K. (1996) Hepatocellular and hepatic peroxisomal alterations in mice with a disrupted peroxisomal fatty acyl-coenzyme A oxidase gene, J Biol Chem 271, 24698-24710.

122. Issemann, I., Prince, R., Tugwood, J., and Green, S. (1992) A role for fatty acids and liver fatty acid binding protein in peroxisome proliferation?, Biochem Soc Trans 20, 824-827.

123. Frohnert, B. I., Hui, T. Y., and Bernlohr, D. A. (1999) Identification of a functional peroxisome proliferator-responsive element in the murine fatty acid transport protein gene, J Biol Chem 274, 3970-3977.

124. Wolfrum, C., Ellinghaus, P., Fobker, M., Seedorf, U., Assmann, G., Borchers, T., and Spener, F. (1999) Phytanic acid is ligand and transcriptional activator of murine liver fatty acid binding protein, J Lipid Res 40, 708-714.

125. Brandt, J. M., Djouadi, F., and Kelly, D. P. (1998) Fatty acids activate transcription of the muscle carnitine palmitoyltransferase I gene in cardiac myocytes via the peroxisome proliferator-activated receptor alpha, J Biol Chem 273, 23786-23792.

126. Schoonjans, K., Watanabe, M., Suzuki, H., Mahfoudi, A., Krey, G., Wahli, W., Grimaldi, P., Staels, B., Yamamoto, T., and Auwerx, J. (1995) Induction of the acyl-coenzyme A synthetase gene by fibrates and fatty acids is mediated by a peroxisome proliferator response element in the C promoter, J Biol Chem 270, 19269-19276.

127. Varanasi, U., Chu, R., Huang, Q., Castellon, R., Yeldandi, A. V., and Reddy, J. K. (1996) Identification of a peroxisome proliferator-responsive element upstream of the human peroxisomal fatty acyl coenzyme A oxidase gene, J Biol Chem 271, 2147-2155.

128. Gulick, T., Cresci, S., Caira, T., Moore, D. D., and Kelly, D. P. (1994) The peroxisome proliferator-activated receptor regulates mitochondrial fatty acid oxidative enzyme gene expression, Proc Natl Acad Sci U S A 91, 11012-11016.

129. Muerhoff, A. S., Griffin, K. J., and Johnson, E. F. (1992) The peroxisome proliferator-activated receptor mediates the induction of CYP4A6, a cytochrome P450 fatty acid omega-hydroxylase, by clofibric acid, J Biol Chem 267, 19051-19053.

130. Aldridge, T. C., Tugwood, J. D., and Green, S. (1995) Identification and characterization of DNA elements implicated in the regulation of CYP4A1 transcription, Biochem J 306 ( Pt 2), 473-479.

131. Hebbachi, A. M., Knight, B. L., Wiggins, D., Patel, D. D., and Gibbons, G. F. (2008) Peroxisome proliferator-activated receptor alpha deficiency abolishes the response of lipogenic gene expression to re-feeding: restoration of the normal response by activation of liver X receptor alpha, J Biol Chem 283, 4866-4876.

132. Fernandez-Alvarez, A., Alvarez, M. S., Gonzalez, R., Cucarella, C., Muntane, J., and Casado, M. (2011) Human SREBP1c expression in liver is directly regulated by peroxisome proliferator-activated receptor alpha (PPARalpha), J Biol Chem 286, 21466-21477.

133. Horton, J. D., Goldstein, J. L., and Brown, M. S. (2002) SREBPs: transcriptional mediators of lipid homeostasis, Cold Spring Harb Symp Quant Biol 67, 491-498.

134. Tobin, K. A., Steineger, H. H., Alberti, S., Spydevold, O., Auwerx, J., Gustafsson, J. A., and Nebb, H. I. (2000) Cross-talk between fatty acid and cholesterol metabolism mediated by liver X receptor-alpha, Mol Endocrinol 14, 741-752.

135. Schoonjans, K., Peinado-Onsurbe, J., Lefebvre, A. M., Heyman, R. A., Briggs, M., Deeb, S., Staels, B., and Auwerx, J. (1996) PPARalpha and PPARgamma activators direct a distinct tissue-specific transcriptional response via a PPRE in the lipoprotein lipase gene, EMBO J 15, 5336-5348.

136. Staels, B., Vu-Dac, N., Kosykh, V. A., Saladin, R., Fruchart, J. C., Dallongeville, J., and Auwerx, J. (1995) Fibrates downregulate apolipoprotein C-III expression independent of induction of peroxisomal acyl coenzyme A oxidase. A potential mechanism for the hypolipidemic action of fibrates, J Clin Invest 95, 705-712.

137. Hertz, R., Bishara-Shieban, J., and Bar-Tana, J. (1995) Mode of action of peroxisome proliferators as hypolipidemic drugs. Suppression of apolipoprotein C-III, J Biol Chem 270, 13470-13475.

138. Vu-Dac, N., Schoonjans, K., Kosykh, V., Dallongeville, J., Fruchart, J. C., Staels, B., and Auwerx, J. (1995) Fibrates increase human apolipoprotein A-II expression through activation of the peroxisome proliferator-activated receptor, J Clin Invest 96, 741-750.

139. Vu-Dac, N., Chopin-Delannoy, S., Gervois, P., Bonnelye, E., Martin, G., Fruchart, J. C., Laudet, V., and Staels, B. (1998) The nuclear receptors peroxisome proliferator-activated receptor alpha and Rev-erbalpha mediate the

species-specific regulation of apolipoprotein A-I expression by fibrates, J Biol Chem 273, 25713-25720.

140. Chinetti, G., Lestavel, S., Bocher, V., Remaley, A. T., Neve, B., Torra, I. P., Teissier, E., Minnich, A., Jaye, M., Duverger, N., Brewer, H. B., Fruchart, J. C., Clavey, V., and Staels, B. (2001) PPAR-alpha and PPAR-gamma activators induce cholesterol removal from human macrophage foam cells through stimulation of the ABCA1 pathway, Nat Med 7, 53-58.

141. Chiang, J. Y., Kimmel, R., and Stroup, D. (2001) Regulation of cholesterol 7alpha-hydroxylase gene (CYP7A1) transcription by the liver orphan receptor (LXRalpha), Gene 262, 257-265.

142. Ramanan, S., Kooshki, M., Zhao, W., Hsu, F. C., and Robbins, M. E. (2008) PPARalpha ligands inhibit radiation-induced microglial inflammatory responses by negatively regulating NF-kappaB and AP-1 pathways, Free Radic Biol Med 45, 1695-1704.

143. Staels, B., Koenig, W., Habib, A., Merval, R., Lebret, M., Torra, I. P., Delerive, P., Fadel, A., Chinetti, G., Fruchart, J. C., Najib, J., Maclouf, J., and Tedgui, A. (1998) Activation of human aortic smooth-muscle cells is inhibited by PPARalpha but not by PPARgamma activators, Nature 393, 790-793.

144. Shashkin, P., Dragulev, B., and Ley, K. (2005) Macrophage differentiation to foam cells, Curr Pharm Des 11, 3061-3072.

145. Lee, S. S., Pineau, T., Drago, J., Lee, E. J., Owens, J. W., Kroetz, D. L., Fernandez-Salguero, P. M., Westphal, H., and Gonzalez, F. J. (1995) Targeted disruption of the alpha isoform of the peroxisome proliferator-activated receptor

gene in mice results in abolishment of the pleiotropic effects of peroxisome proliferators, Mol Cell Biol 15, 3012-3022.

146. Aoyama, T., Peters, J. M., Iritani, N., Nakajima, T., Furihata, K., Hashimoto, T., and Gonzalez, F. J. (1998) Altered constitutive expression of fatty acid-metabolizing enzymes in mice lacking the peroxisome proliferator-activated receptor alpha (PPARalpha), J Biol Chem 273, 5678-5684.

147. Peters, J. M., Hennuyer, N., Staels, B., Fruchart, J. C., Fievet, C., Gonzalez, F. J., and Auwerx, J. (1997) Alterations in lipoprotein metabolism in peroxisome proliferator-activated receptor alpha-deficient mice, J Biol Chem 272, 27307-27312.

148. Costet, P., Legendre, C., More, J., Edgar, A., Galtier, P., and Pineau, T. (1998) Peroxisome proliferator-activated receptor alpha-isoform deficiency leads to progressive dyslipidemia with sexually dimorphic obesity and steatosis, J Biol Chem 273, 29577-29585.

149. Cheung, C., Akiyama, T. E., Ward, J. M., Nicol, C. J., Feigenbaum, L., Vinson, C., and Gonzalez, F. J. (2004) Diminished hepatocellular proliferation in mice humanized for the nuclear receptor peroxisome proliferator-activated receptor alpha, Cancer Res 64, 3849-3854.

150. Morimura, K., Cheung, C., Ward, J. M., Reddy, J. K., and Gonzalez, F. J. (2006) Differential susceptibility of mice humanized for peroxisome proliferator-activated receptor alpha to Wy-14,643-induced liver tumorigenesis, Carcinogenesis 27, 1074-1080.

151. Bosworth, N., and Towers, P. (1989) Scintillation proximity assay, Nature 341, 167-168.

152. Ves-Losada, A., Mate, S. M., and Brenner, R. R. (2001) Incorporation and distribution of saturated and unsaturated fatty acids into nuclear lipids of hepatic cells, Lipids 36, 273-282.

153. Berbaum, J., and Harrison, R. K. (2005) Comparison of full-length versus ligand binding domain constructs in cell-free and cell-based peroxisome proliferator-activated receptor alpha assays, Anal Biochem 339, 121-128.

154. Petrescu, A. D., Hertz, R., Bar-Tana, J., Schroeder, F., and Kier, A. B. (2005) Role of regulatory F-domain in hepatocyte nuclear factor-4alpha ligand specificity, J Biol Chem 280, 16714-16727.

155. Lefstin, J. A., Thomas, J. R., and Yamamoto, K. R. (1994) Influence of a steroid receptor DNA-binding domain on transcriptional regulatory functions, Genes Dev 8, 2842-2856.

156. Lefstin, J. A., and Yamamoto, K. R. (1998) Allosteric effects of DNA on transcriptional regulators, Nature 392, 885-888.

157. Helsen, C., Dubois, V., Verfaillie, A., Young, J., Trekels, M., Vancraenenbroeck, R., De Maeyer, M., and Claessens, F. (2012) Evidence for DNA-binding domain--ligand-binding domain communications in the androgen receptor, Mol Cell Biol 32, 3033-3043.

158. Nagasawa, M., Ide, T., Suzuki, M., Tsunoda, M., Akasaka, Y., Okazaki, T., Mochizuki, T., and Murakami, K. (2004) Pharmacological characterization of a

human-specific peroxisome proliferater-activated receptor alpha (PPARalpha) agonist in dogs, Biochem Pharmacol 67, 2057-2069.

159. Nakagawa, T., Kurita, N., Kozakai, S., Iwabuchi, S., Yamaguchi, Y., Hayakawa, M., Ito, Y., Aoyama, T., and Nakajima, T. (2008) Molecular mechanics and molecular orbital simulations on specific interactions between peroxisome proliferator-activated receptor PPARalpha and plasticizer, J Mol Graph Model 27, 45-58.

160. Miyachi, H., and Uchiki, H. (2003) Analysis of the critical structural determinant(s) of species-selective peroxisome proliferator-activated receptor alpha (PPAR alpha)-activation by phenylpropanoic acid-type PPAR alpha agonists, Bioorg Med Chem Lett 13, 3145-3149.

161. Keller, H., Devchand, P. R., Perroud, M., and Wahli, W. (1997) PPAR alpha structure-function relationships derived from species-specific differences in responsiveness to hypolipidemic agents, Biol Chem 378, 651-655.

162. Bility, M. T., Thompson, J. T., McKee, R. H., David, R. M., Butala, J. H., Vanden Heuvel, J. P., and Peters, J. M. (2004) Activation of mouse and human peroxisome proliferator-activated receptors (PPARs) by phthalate monoesters, Toxicol Sci 82, 170-182.

163. Rakhshandehroo, M., Hooiveld, G., Muller, M., and Kersten, S. (2009) Comparative analysis of gene regulation by the transcription factor PPARalpha between mouse and human, PLoS One 4, e6796.

164. Hsu, M. H., Palmer, C. N., Griffin, K. J., and Johnson, E. F. (1995) A single amino acid change in the mouse peroxisome proliferator-activated receptor alpha

alters transcriptional responses to peroxisome proliferators, Mol Pharmacol 48, 559-567.

165. Oswal, D. P., Balanarasimha, M., Loyer, J. K., Bedi, S., Soman, F. L., Rider, S. D., Jr., and Hostetler, H. A. (2013) Divergence between human and murine peroxisome proliferator-activated receptor alpha ligand specificities, J Lipid Res 54, 2354-2365.

166. Reddy, J. K., and Hashimoto, T. (2001) Peroxisomal beta-oxidation and peroxisome proliferator-activated receptor alpha: an adaptive metabolic system, Annu Rev Nutr 21, 193-230.

167. Mangelsdorf, D. J., and Evans, R. M. (1995) The RXR heterodimers and orphan receptors, Cell 83, 841-850.

168. Desvergne, B., Michalik, L., and Wahli, W. (2004) Be fit or be sick: peroxisome proliferator-activated receptors are down the road, Mol Endocrinol 18, 1321-1332.

169. Frederiksen, K. S., Wulf, E. M., Wassermann, K., Sauerberg, P., and Fleckner, J. (2003) Identification of hepatic transcriptional changes in insulin-resistant rats treated with peroxisome proliferator activated receptor-alpha agonists, J Mol Endocrinol 30, 317-329.

170. Maloney, E. K., and Waxman, D. J. (1999) trans-Activation of PPARalpha and PPARgamma by structurally diverse environmental chemicals, Toxicol Appl Pharmacol 161, 209-218.

171. Hubbell, T., Behnke, W. D., Woodford, J. K., and Schroeder, F. (1994) Recombinant liver fatty acid binding protein interacts with fatty acyl-coenzyme A, Biochemistry 33, 3327-3334.

172. Balanarasimha, M. (2011) Structural and functional alteration of full length PPARα and LXRα by fatty acids and their thioesters, in Biochemistry and Molecular biology, Wright State University, Dayton.

173. Hostetler, H. A., Huang, H., Kier, A. B., and Schroeder, F. (2008) Glucose directly links to lipid metabolism through high affinity interaction with peroxisome proliferator-activated receptor alpha, J Biol Chem 283, 2246-2254.

174. Hostetler H. A., M. A. L., Petrescu A. D., Huang H., Atshaves B. P., Murphy E. J., Kier A. B., Schroeder F. (2010) Flourescence methods to assess the impact of lipid binding proteins on ligand mediated activation of gene expression, in Lipid-mediated signalling (Murphy E. J., R. T. A., Ed.), pp 299-348, CRC Press.

175. Mukerjee Pasupati, K. M. (1971) Critical micelle concentrations of aqueous surfactant systems, (United States Department of Commerce, N. B. o. S., Ed.), Washington D.C.

176. Smith, R. H., and Powell, G. L. (1986) The critical micelle concentration of some physiologically important fatty acyl-coenzyme A's as a function of chain length, Arch Biochem Biophys 244, 357-360.

177. Petrescu, A. D., Hertz, R., Bar-Tana, J., Schroeder, F., and Kier, A. B. (2002) Ligand specificity and conformational dependence of the hepatic nuclear factor-4alpha (HNF-4alpha ), J Biol Chem 277, 23988-23999.

178. Michaelis, L., Menten, M. L., Johnson, K. A., and Goody, R. S. (2011) The original Michaelis constant: translation of the 1913 Michaelis-Menten paper, Biochemistry 50, 8264-8269.

179. Sreerama, N., and Woody, R. W. (2000) Estimation of protein secondary structure from circular dichroism spectra: comparison of CONTIN, SELCON, and CDSSTR methods with an expanded reference set, Anal Biochem 287, 252-260.

180. Kim, J. B., Wright, H. M., Wright, M., and Spiegelman, B. M. (1998) ADD1/SREBP1 activates PPARgamma through the production of endogenous ligand, Proc Natl Acad Sci U S A 95, 4333-4337.

181. Spector, A. A. (1969) Influence of pH of the medium on free fatty acid utilization by isolated mammalian cells, J Lipid Res 10, 207-215.

182. Francis, G. A., Fayard, E., Picard, F., and Auwerx, J. (2003) Nuclear receptors and the control of metabolism, Annu Rev Physiol 65, 261-311.

183. Hashimoto, T., Fujita, T., Usuda, N., Cook, W., Qi, C., Peters, J. M., Gonzalez, F. J., Yeldandi, A. V., Rao, M. S., and Reddy, J. K. (1999) Peroxisomal and mitochondrial fatty acid beta-oxidation in mice nullizygous for both peroxisome proliferator-activated receptor alpha and peroxisomal fatty acyl-CoA oxidase. Genotype correlation with fatty liver phenotype, J Biol Chem 274, 19228-19236.

184. Laudet, V. (1997) Evolution of the nuclear receptor superfamily: early diversification from an ancestral orphan receptor, J Mol Endocrinol 19, 207-226.

185. Oswal, D. P., Alter, G. M. R., S. D., and Hostetler, H. A. (2014) A single amino acid change humanizes long-chain fatty acid binding and activation of mouse

peroxisome proliferator-activated receptor α, Journal of Molecular Graphics and Modelling 51, 27-36.

186. Rakhshandehroo, M., Knoch, B., Muller, M., and Kersten, S. (2010) Peroxisome proliferator-activated receptor alpha target genes, PPAR Res 2010.

187. Guo, Y., Jolly, R. A., Halstead, B. W., Baker, T. K., Stutz, J. P., Huffman, M., Calley, J. N., West, A., Gao, H., Searfoss, G. H., Li, S., Irizarry, A. R., Qian, H. R., Stevens, J. L., and Ryan, T. P. (2007) Underlying mechanisms of pharmacology and toxicity of a novel PPAR agonist revealed using rodent and canine hepatocytes, Toxicol Sci 96, 294-309.

188. Shah, Y. M., Morimura, K., Yang, Q., Tanabe, T., Takagi, M., and Gonzalez, F. J. (2007) Peroxisome proliferator-activated receptor alpha regulates a microRNA-mediated signaling cascade responsible for hepatocellular proliferation, Mol Cell Biol 27, 4238-4247.

189. Bosgra, S., Mennes, W., and Seinen, W. (2005) Proceedings in uncovering the mechanism behind peroxisome proliferator-induced hepatocarcinogenesis, Toxicology 206, 309-323.

190. van Gunsteren W. F., B. S. R., Eising A. A., Hünenberger P. H., Krüger P., Mark A. E., Scott, W. R. P., Tironi I. G. (1996) Biomolecular Simulation: The GROMOS96 Manual and User Guide, Vdf Hochschulverlag AG an der ETH Zürich, Zürich, Switzerland.

191. Trott, O., and Olson, A. J. (2010) AutoDock Vina: improving the speed and accuracy of docking with a new scoring function, efficient optimization, and multithreading, J Comput Chem 31, 455-461.

192. Wallace, A. C., Laskowski, R. A., and Thornton, J. M. (1995) LIGPLOT: a program to generate schematic diagrams of protein-ligand interactions, Protein Eng 8, 127-134.

193. Durrant, J. D., de Oliveira, C. A., and McCammon, J. A. (2011) POVME: an algorithm for measuring binding-pocket volumes, J Mol Graph Model 29, 773-776.

194. Humphrey, W., Dalke, A., and Schulten, K. (1996) VMD: visual molecular dynamics, J Mol Graph 14, 33-38, 27-38.

195. Spector, A. A., and Hoak, J. C. (1969) An improved method for the addition of long-chain free fatty acid to protein solutions, Anal Biochem 32, 297-302.

196. Reginald H. Garrett, C. M. G. (2013) Biochemistry, 5th ed., Brooks/Cole, Cengage Learning.

197. Tanford, C. (1979) The hydrophobic effect: Formation of micelles and bioogical membranes, 2nd ed., John Wiley and Sons, Inc., New York.

198. Yassine, W., Taib, N., Federman, S., Milochau, A., Castano, S., Sbi, W., Manigand, C., Laguerre, M., Desbat, B., Oda, R., and Lang, J. (2009) Reversible transition between alpha-helix and beta-sheet conformation of a transmembrane domain, Biochim Biophys Acta 1788, 1722-1730.

199. Uchiki, H., and Miyachi, H. (2004) Molecular modeling study of species-selective peroxisome proliferator-activated receptor (PPAR) alpha agonist; possible mechanism(s) of human PPARalpha selectivity of an alpha-substituted phenylpropanoic acid derivative (KCL), Chem Pharm Bull (Tokyo) 52, 365-367.

200. Escriva, H., Delaunay, F., and Laudet, V. (2000) Ligand binding and nuclear receptor evolution, Bioessays 22, 717-727.

201. Escriva, H., Safi, R., Hanni, C., Langlois, M. C., Saumitou-Laprade, P., Stehelin, D., Capron, A., Pierce, R., and Laudet, V. (1997) Ligand binding was acquired during evolution of nuclear receptors, Proc Natl Acad Sci U S A 94, 6803-6808.

202. Burr, G. O., and Burr, M. M. (1929) A new deficiency disease produced by the rigid exclusion of fat from the diet, J. Biol. Chem. 82, 345-367.

203. Flatt, J. P. (1995) Use and storage of carbohydrate and fat, Am. J. Clin. Nutr. 61, S952-S959.

204. Jobe, A., and Bourgeois, S. (1972) The lac repressor-operator interaction. VII. A repressor with unique binding properties: the X86 repressor, J Mol Biol 72, 139-152.

205. Jia, Y., Qi, C., Zhang, Z., Hashimoto, T., Rao, M. S., Huyghe, S., Suzuki, Y., Van Veldhoven, P. P., Baes, M., and Reddy, J. K. (2003) Overexpression of peroxisome proliferator-activated receptor-alpha (PPARalpha)-regulated genes in liver in the absence of peroxisome proliferation in mice deficient in both L- and D-forms of enoyl-CoA hydratase/dehydrogenase enzymes of peroxisomal beta-oxidation system, J Biol Chem 278, 47232-47239.

206. Chakravarthy, M. V., Pan, Z., Zhu, Y., Tordjman, K., Schneider, J. G., Coleman, T., Turk, J., and Semenkovich, C. F. (2005) "New" hepatic fat activates PPARalpha to maintain glucose, lipid, and cholesterol homeostasis, Cell Metab 1, 309-322.

207. Mashek, D. G., Bornfeldt, K. E., Coleman, R. A., Berger, J., Bernlohr, D. A., Black, P., DiRusso, C. C., Farber, S. A., Guo, W., Hashimoto, N., Khodiyar, V., Kuypers, F. A., Maltais, L. J., Nebert, D. W., Renieri, A., Schaffer, J. E., Stahl, A., Watkins, P. A., Vasiliou, V., and Yamamoto, T. T. (2004) Revised nomenclature for the mammalian long-chain acyl-CoA synthetase gene family, J Lipid Res 45, 1958-1961.

208. Watkins, P. A., Maiguel, D., Jia, Z., and Pevsner, J. (2007) Evidence for 26 distinct acyl-coenzyme A synthetase genes in the human genome, J Lipid Res 48, 2736-2750.

209. Vessey, D. A., Kelley, M., and Warren, R. S. (2004) Characterization of triacsin C inhibition of short-, medium-, and long-chain fatty acid: CoA ligases of human liver, J Biochem Mol Toxicol 18, 100-106.

210. Mashima, T., Sato, S., Okabe, S., Miyata, S., Matsuura, M., Sugimoto, Y., Tsuruo, T., and Seimiya, H. (2009) Acyl-CoA synthetase as a cancer survival factor: its inhibition enhances the efficacy of etoposide, Cancer Sci 100, 1556-1562.

211. Shalev, A., Siegrist-Kaiser, C. A., Yen, P. M., Wahli, W., Burger, A. G., Chin, W. W., and Meier, C. A. (1996) The peroxisome proliferator-activated receptor alpha is a phosphoprotein: regulation by insulin, Endocrinology 137, 4499-4502.

212. Blanquart, C., Barbier, O., Fruchart, J. C., Staels, B., and Glineur, C. (2002) Peroxisome proliferator-activated receptor alpha (PPARalpha ) turnover by the ubiquitin-proteasome system controls the ligand-induced expression level of its target genes, J Biol Chem 277, 37254-37259.

213. Pourcet, B., Pineda-Torra, I., Derudas, B., Staels, B., and Glineur, C. (2010) SUMOylation of human peroxisome proliferator-activated receptor alpha inhibits its trans-activity through the recruitment of the nuclear corepressor NCoR, J Biol Chem 285, 5983-5992.

214. Wadosky, K. M., and Willis, M. S. (2012) The story so far: post-translational regulation of peroxisome proliferator-activated receptors by ubiquitination and SUMOylation, Am J Physiol Heart Circ Physiol 302, H515-526.

215. Sladek R., G. V. (1999) Nuclear Receptors A practical approach, Oxford University Press, New York.

216. Makishima, M., Lu, T. T., Xie, W., Whitfield, G. K., Domoto, H., Evans, R. M., Haussler, M. R., and Mangelsdorf, D. J. (2002) Vitamin D receptor as an intestinal bile acid sensor, Science 296, 1313-1316.

217. Noy, N. (2007) Ligand specificity of nuclear hormone receptors: sifting through promiscuity, Biochemistry 46, 13461-13467.

218. Chandler, H. A., and Batchelor, A. J. (1994) Ciprofibrate and lipid profile, Lancet 344, 128-129.

219. Matthews, J., Celius, T., Halgren, R., and Zacharewski, T. (2000) Differential estrogen receptor binding of estrogenic substances: a species comparison, J Steroid Biochem Mol Biol 74, 223-234.

220. Babbitt, C. C., Warner, L. R., Fedrigo, O., Wall, C. E., and Wray, G. A. (2010) Genomic signatures of diet-related shifts during human origins, Proc Biol Sci 278, 961-969.

221. Thyagarajan, T., Totey, S., Danton, M. J., and Kulkarni, A. B. (2003) Genetically altered mouse models: the good, the bad, and the ugly, Crit Rev Oral Biol Med 14, 154-174.

# APPENDIX

# REGULATION OF ADIPONECTIN BY LIGAND-ACTIVATED PEROXISOME PROLIFERATOR-ACTIVATED RECEPTOR ALPHA

**Abstract**

Adiponectin is an adipocyte-secreted adipokine that has attracted much attention due to its salutary effects on obesity related cardiovascular complications. Adiponectin plays a large role in maintaining energy homeostasis by interacting with its receptors to increase fatty acid oxidation, glucose uptake and decrease gluconeogenesis. Recent studies have reported adiponectin expression from other tissues such as heart, liver and muscle, where it is believed to act in a local manner to regulate homeostasis. In addition, numerous studies have reported decreased expression of adiponectin associated with cardiovascular and metabolic complications. Clinical and preclinical studies have suggested regulation of adiponectin by PPAR α and γ agonists. While PPARγ agonists are thought to act by mediating adipogenesis and transactivating adiponectin, the role of PPARα and its underlying mechanisms in regulating the expression of adiponectin is not clear. PPARα binds endogenous ligands (long chain fatty acids (LCFA)) as well as exogenous ligands (fibrates) to regulate the transcription of genes involved in fatty acid oxidation. The goal of this study was to determine whether ligand-activated human PPARα regulates the expression of adiponectin in cultured human hepatoma cells (HepG2). Although not convincing, data from electrophoretic mobility shift assays (EMSA) and transactivation assays suggest that PPARα may bind PPRE sequences in the adiponectin promoter and may contribute towards regulation of the adiponectin gene (either directly or indirectly). Since we were not able to detect the expression of adiponectin in HepG2 cells, future studies investigating the role of PPARα in adiponectin regulation must be carried out in a cell line that constitutively expresses adiponectin.

## Introduction

Obesity is defined as an increased mass of adipose tissue and is a major risk factor for coronary heart disease, hypertension, atherosclerosis, dyslipidemia and diabetes (*1*). The prevalence of obesity is associated with a surge in the metabolic syndrome in industrialized or developing countries (*2, 3*). For this reason, there has been a great scientific interest in studying the physiology of the adipose tissue. The adipose tissue has been traditionally considered as a site of triglyceride (TG) storage and free fatty acid release in response to increased energy demands (*1, 4*). However in the past decade, adipose tissue has been recognized to have endocrine functions regulating energy homeostasis and inflammation by releasing a number of biologically active peptides. The term adipokine or adipocytokine was coined to describe these signaling messengers that are secreted by the adipose tissue, some of which include leptin (*5*), resistin (*6*), tumor necrosis factor α (TNFα) (*7*) and adiponectin (*8-11*).

Adiponectin was originally reported independently by four groups using different approaches and is also referred to as AdipoQ (*11*), Acrp30 (30 kDa adipocyte complement related protein) (*8*), apM1 (adipose most abundant gene transcript) (*9*) and gelatin binding protein of 28 kDa (GBP28) (*10*). Today, the most widely accepted name is adiponectin, which will therefore be used hereafter. The human adiponectin is a 30 kDa and 247 amino acid protein that consists of an N-terminal signal sequence/peptide (SS), a hypervariable region (VR), a collagenous domain and a C-terminal globular domain (*11, 12*) (Fig. 32). The collagenous domain consists of 22 Gly-X-Y repeats (where X and Y are any amino acid) along with prolines and lysine residues that are subjected to post-translational modifications including glycosylation and hydroxylations (*11*). The

carboxy-terminal globular domain on the other hand is similar to complement factor C1q, VIII and X and also bears structural homology (but no amino acid sequence homology) with TNFα (*12*).

The human adiponectin gene spans a length of 17 kb and is localized to chromosome 3q27, a region highlighted as a genetic susceptibility locus for type 2 diabetes and metabolic syndrome (*13*). Its transcript is most abundantly found in adipocytes and consists of three exons and two introns (*14*). It exists abundantly in human blood (5-30 μg/ml) forming about 0.05 % of all plasma proteins and the molar concentration of 5 μg/ml adiponectin in human plasma corresponds to approximately 3 nM (*8-11*). Adiponectin circulates in the blood predominantly in three different oligomeric forms – trimer, hexamer and high molecular weight oligomer (12-18 protomers; Fig. 32). Three adiponectin monomers come together via hydrophobic interactions in the globular domain to form a trimer, which is also referred to as the low molecular weight adiponectin (LMW). Two trimers then associate to form hexamers (medium molecular weight; MMW) and high molecular weight oligomers comprised of 12-18 protomers/monomers (high molecular weight; HMW) (*8-11*). The disulfide bridges formed by cysteine residues at position 39 are responsible for the oligomerization of adiponectin and mutation of this residue (C39S) abolishes the formation of such oligomers (*15*). Post-translational modifications in the collagenous domain are also required for the assembly of the HMW oligomers (*16*).

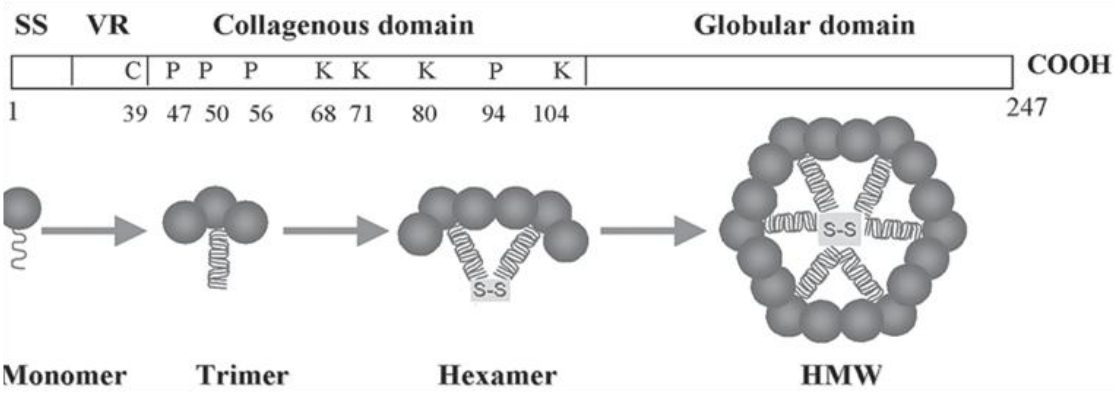


**Fig. 32** - Primary structure of adiponectin consisting of signal sequence (SS), hypervariable region (VR) collagen-like domain prolines (P) and lysines (K) and C-terminal globular domain. Multimer formation of adiponectin where monomer forms trimer (hydrophobic interactions) and trimers come together to form hexamers and high molecular weight oligomers (disulphide bonds via C39). Figure modified from (*17*)

While it is speculated that different forms of adiponectin (monomeric, trimeric, oligomeric) have distinct tissue specific levels biological activities, many of these results are controversial and not clear at this stage. For example, several studies indicate that the HMW form of adiponectin is the most bioactive form of adiponectin (*18-20*). Kadowaki *at al.* have reported that populations with rare mutations in the adiponectin gene (G90S, G84R) have lower levels of HMW adiponectin and are associated with insulin resistance and type 2 diabetes (*18*). While these findings suggest that HMW may be the most bioactive form of adiponectin, mutant recombinant adiponectin (G90S, G84R) expressed in NIH-3T3 fibroblasts fail form the HMW multimers (*18*). Thus lower levels of HMW oligomers in these populations could just be a result of impaired multimerization. Besides, other researchers have suggested that monomeric or trimeric forms of adiponectin may be important in mediating the pleotropic effects of adiponectin in skeletal muscles (*19, 21-23*). Since the significance of the different oligomeric forms of adiponectin are not clear, the total plasma adiponectin measurements are the most commonly reported (*24*).

Irrespective of their oligomeric state, adiponectin exerts its effects by binding to two isoforms of adiponectin receptors (AdipoR) – AdipoR1 and AdipoR2. While the AdipoR1 gene encodes a 42.4 kDa and 375 amino acid protein, the AdipoR2 gene encodes a 311 amino acid protein of 35.4 kDa (*25*). These proteins bear about 67% sequence homology and they also share about ~95 % homology between mice and humans. As far as the expression of these receptors is concerned, they are ubiquitously expressed, with the expression of AdipoR1 highest in skeletal muscle and AdipoR2 highest in the liver (*25, 26*). Structurally, both AdipoR1 and AdipoR2 contain seven

transmembrane domains but are distinct from G protein coupled receptors (GPCR) in structure and function. Unlike GPCRs, adipoR1 and adipoR2 have inverted membrane topologies with an extracellular C-terminal domain and an intracellular N-terminal domain (*25*). The expression of the adiponectin receptors is speculated to be regulated by various factors including the presence of adiponectin, insulin (*27*), and nuclear receptors such as PPARα and PPARγ (*28-31*). However, the cause/effect relationship of such regulation is largely unknown. For example, the increase in levels of adiponectin receptors observed with a PPARγ agonist could be result of increased expression of adiponectin or vice versa (*31*).

In the past decade, adiponectin has attracted much attention due to its beneficial effects on obesity-related cardiovascular and metabolic complications. Upon binding to its receptors, adiponectin mediates a cascade of intracellular signaling events, including the activation of adenosine monophosphate (AMP)-activated protein kinase (AMPK) – a key enzyme involed in maintaining cellular energy homeostasis. AMPK is activated under conditions of reduced cellular ATP or increased levels of AMP (*32*). Activation of AMPK on one hand stimulates ATP generating processes such as fatty acid oxidation and glycolysis, it also shuts down ATP consuming processes such as lipogenesis (*32*). For example, under conditions of starvation/fasting fatty acids are mobilized from the adipose tissue along with activation of AMPK in the liver and skeletal muscles – resulting in ATP generation from fatty acid oxidation (*32*). These effects are very similar to the pleotrophic effects caused by PPARα agonists. It is tempting to speculate that PPARα, in addition to its role in lipid metabolism, may also upregulate adiponectin and cause additive effects on fatty acid oxidation and inflammation pathways (via adiponectin).

Recently, it was suggested that an adaptor protein containing a pleckstrin homology domain, a phosphotyrosine domain and a leucine zipper motif (APPL1) mediates the intracellular signaling events that occur following binding of adiponectin to its receptors (*33, 34*). APPL1 binds to the intracellular N-terminal part of adiponectin bound AdipoR and mediates the activation of AMPK (*33, 34*). The net result of AMPK activation includes increased fatty acid oxidation (due to increased activity of carnitine palmitoyl transferase), glucose uptake (increased activity of insulin receptor substrate and GLUT4 glucose transporter), production of nitric oxide (activation of nitric oxide synthase) and decreased gluconeogenesis (suppression of gluconeogenic enzymes) and diminished activity of nuclear factor κ B (NfκB; due to activation of inhibitory κ B) (*26, 32, 33*).

Indeed adiponectin exhibits cardioprotective, antidiabetic, antiatherosclerotic and anti-inflammatory effects (*26, 33, 35, 36*) and this is further supported by decreased circulating levels of adiponectin observed in patients with obesity (*37, 38*), cardiovascular diseases (*39-42*), hypertension (*26, 40, 43*), type 2 diabetes (*38, 44*) and metabolic syndrome (*26, 36, 45*). Conversely, it has been observed that increased plasma adiponectin levels are associated with a lowered risk for obesity related co-morbidities (*46, 47*). Consistent with clinical observations, adiponectin deficient mice are prone to atherosclerosis, hypertension, hyperglycemia, insulin resistance and also show delayed clearance of free fatty acids from plasma (*35, 43, 48, 49*). The levels of adiponectin are also downregulated in mice models of obesity and type 2 diabetes (*48, 50-52*). Further, administration of recombinant adiponectin in these mice improves insulin sensitivity,

glucose tolerance, increases fatty acid oxidation, glucose uptake and decreases gluconeogenesis (*48, 53*).

Consistent with the association of hypoadiponectinemia with obesity and its co-morbidities, several single nucleotide polymorphisms (SNPs) in the adiponectin gene are also associated with aspects of metabolic disorders (*54*). The most commonly identified SNPs in the adiponectin gene locus include T → G transversions at codon 45 and 276 (*55, 56*). These SNPs are associated with obesity, insulin resistance, type 2 diabetes, altered blood pressure, coronary artery disease and dyslipidemia (*54-56*). Owing to all these experimental and clinical investigations, adiponectin has emerged as a potential pharmaceutical target and/or a biomarker in the context of a spectrum of metabolic disorders. Administration of recombinant adiponectin in preclinical models has resulted in improved metabolic parameters that combat insulin resistance, obesity related disorders and inflammation (*48, 53*). However, production of recombinant adiponectin on a large scale, along with its short half-life (1 hour in mice and 2 hours in humans (*57*)) and high circulation levels, makes it difficult to obtain high levels of the protein at a reasonable price (*24*). Thus, strategies that would improve/increase the expression of adiponectin (or its signaling) or prevent its down-regulation could result in improvements in insulin sensitivity, decrease cardiovascular risk and reduction in many parameters of obesity-linked disorders.

**Development of hypothesis**

Based on the clinical and preclinical evidence from above and numerous other epidemiological studies (*58*), hypoadiponectinemia is an independent risk factor for obesity-related disorders including cardiovascular diseases, atherosclerosis, dyslipidemia and type 2 diabetes – most of which are coupled with metabolic imbalances with respect to fatty acid metabolism. For example, elevated fatty acids are associated with metabolic and cardiovascular complications that also foresee decreased expression of adiponectin. Thus "factors" regulating fatty acid metabolism may play an important role in the regulation of adiponectin. The adiponectin gene contains several putative transcription factor binding sites and is thus speculated to be under complex regulation by various upstream signals (*59*). Amongst binding sites for other transcription factors such as CCAAT/enhancer binding protein (C/EBP) (*59*), adipocyte determination and differentiation-dependent factor 1/Sterol regulatory element-binding protein 1c (ADD/SREBP1-c) (*60*) and cAMP response element binding protein (*61*), the adiponectin promoter also contains binding site for the peroxisome proliferator-activated receptors (*59*).

As discussed in the earlier portions of this dissertation, the peroxisome proliferator activated receptors (PPAR; α, β/δ and γ) are a class of ligand dependent nuclear transcription factors that play crucial roles in the transcriptional regulation of energy metabolism and homeostasis (*62-65*). While PPARα (expressed predominantly in liver, heart, muscle) and PPARβ/δ (expressed predominantly in intestines and keratinocytes) are potent activators of genes involved in fatty acid oxidation, PPARγ (expressed predominantly in adipose tissue) activates genes involved in lipogenesis and

adipocyte differentiation (*62-65*). A substantial body of evidence has suggested that PPAR α and γ agonists increase the expression of adiponectin (*52, 66-73*). While the mechanism by which PPARγ agonists induce the expression of adiponectin mainly includes adipogenesis and transactivation of adiponectin gene (*67, 74*), the role of PPARα and its underlying mechanisms in regulating adiponectin is unclear.

A direct role of PPARγ in adipogenesis was suggested based in two main forms of evidences: 1) the expression of PPARγ was very low in preadipocytes cell lines (such as 3T3-L1) but its expression surges when these cell lines undergo differentiation (even before other differentiation markers such as activating protein 2; aP2) (*75*) and 2) PPARγ agonists such as thiazolidinidiones were able to promote the differentiation of preadipocytes to adipocytes (*76*). The secretion of adipocytokines from the adipose tissue is a function of the adipocyte state/size (*74*). While smaller adipocytes secrete insulin sensitizing and anti-inflammatory molecules such as adiponectin, larger hypertrophied adipocytes secrete inflammatory molecules such as TNFα (*74*). As potent inducers of adipogenesis, PPARγ agonists are capable of promoting the secretion of adiponectin. In addition, Iwaki *et al.* demonstrated that PPARγ may also transactivate the adiponectin gene and thereby induce the expression of this protein (*67*).

There is very little information regarding the role and involvement of PPARα in the expression of adiponectin. Clinical and preclinical studies have demonstrated that administration of PPARα specific agonists (fibrates) results in pleotropic increases in the expression of adiponectin (*69-71, 73, 77*). Such an effect was not observed in PPARα deficient adipocytes or PPARα knockout mice (PPARα-/-) (*73*). In fact, even the basal expression of adiponectin in PPAR-/- mice and diet-induced obese mice was significantly

lower when compared to age matched wild-type littermates (*52, 57, 78*). Administration of PPARα agonists promotes revascularization in response to ischemia in an AMPK/endothelial nitric oxide synthase (eNOS) dependent manner (downstream effectors of adiponectin) – an effect that was abrogated in adiponectin knockout mice (*71*). Further, Hiuge *et al.* demonstrated that the fibrates (PPARα agonists) induce the expression of adiponectin in white adipose tissue of mice and that this effect was abolished in PPARα -/- mice (*73*). All these findings suggest that PPARα plays a direct role in the regulation of adiponectin expression, particularly in pathological states such as diabetes, obesity and dyslipidemia.

While the adipose tissue serves as a primary source of adiponectin, Maddineni et. al. demonstrated that in chickens, the pituitary gland, liver, skeletal muscle, kidney, ovary and spleen can also secrete adiponectin (*79*). Similar to these observations, in humans and rodents its expression was also found in tissues other than the adipocytes. These include the bone marrow (*80*), osteoblasts (*81*), fetal tissue (*82*), skeletal muscle (*83*), cardiomyocytes (*84-87*), salivary glands (*88*) and the liver (*89, 90*). These findings suggest an autocrine or paracrine role of adiponectin in these tissues. In fact, cardiac adiponectin is demonstrated to act in an autocrine/paracrine manner (independent of serum levels) to regulate cardiac metabolism and functionality, and that deregulation of this could be a determinant in the development of various cardiac pathologies (*84, 87, 91*). For example, cardiac adiponectin has been shown to protect against myocardial ischemia-reperfusion injury and hypertrophy (*87, 91*). In addition, Skurk *et. al.* have further demonstrated that cardiac adiponectin is downregulated independent of its serum levels in diabetic cardiomyopathy (*84*). There is compelling evidence which supports the

role of PPARα and adiponectin as regulators of energy homeostasis. However, the regulation of a local adiponectin system at the level of the liver has not been explored yet. Kaser *et al.* reported no correlation between circulating adiponectin levels and liver adiponectin expression in patients with steatohepatitis (*89*). Considering the predominant expression of PPARα in the liver and its important role in lipid homeostasis (*62-65*), it may play a significant role in the possible regulation of adiponectin at the level of the liver.

Elevated long chain fatty acids (LCFA) are associated with metabolic and cardiovascular complications that also foresee decreased expression of adiponectin. The fact that LCFA have been suggested to be ligands for PPARα (*92, 93*), implicates an important role of ligand-activated PPARα in the regulation of adiponectin. *We thus hypothesize that LCFA that serve as ligands for hPPARα regulate the expression of adiponectin in HepG2 cells (human hepatoma cells).* Therefore, the main goal of this part of the dissertation was to determine whether ligand-activated hPPARα directly regulates the expression of adiponectin in HepG2 cells. It is likely that endogenous ligands found in Chapter I of this dissertation could have a profound effect on the expression of adiponectin. The outcome of this research could help explain the importance of dietary nutrients and their correlation to differential transcription, expression or activity of proteins involved in the pathophysiology of the metabolic syndrome.

**Materials and Methods**

*Chemicals:* While fatty acid ligands and clofibrate were purchased from Sigma-Aldrich (St. Louis, MO), bovine serum albumin (lipid-free) was obtained from Gemini Bioproducts (Sacramento, CA). Rosiglitazone (LKT labs) was a kind gift from Dr Khalid Elased.

*Electrophoretic mobility shift assays (EMSAs):* Promoter analysis for adiponectin revealed two putative PPRE at -2345/-2358 (PPRE1) and -335/-368 (PPRE2) base pairs upstream of the transcription start site. Gel-shift assays were performed to measure the DNA-binding ability of hPPARα-hRXRα heterodimers in the presence and absence of ligands using *in vitro* reactions. Purified recombinant hPPARα was purified as described in chapter I of this dissertation. The bacterial expression plasmid for full-length hRXRα (6xhis-GST-hRXRα) was produced by Dr. S. Dean Rider, Jr. (Wright State University) and the recombinant hRXRα protein purification was conducted by Ms. Frances Soman (Hostetler Lab). Double-stranded oligonucleotides spanning from -2337/-2366 and -327/-376 were obtained from the adiponectin promoter. Additional mutant oligonucleotides were also be generated to confirm the binding of the heterodimeric complex to the putative PPRE tested. Double-stranded oligonucleotides of the following sequences were used: wild-type adiponectin PPRE 1, 5' – CAGACTCCTGACCTCAAGTGATCTGCCCG-3 and wild-type adiponectin PPRE 2, 5' -TGTGGTTTTGACTTTTGCCCCATCTTCTG-3; mutant adiponectin PPRE 1, 5' – CAGACTCCCTTAATGGTCTGATCTGCCCG – 3 and mutant adiponectin PPRE 2, 5' – TGTGGTTTCATATATGTCGACATCTTCTG – 3'. *In vitro* reactions containing 39 nM of each recombinant protein (hPPARα and hRXRα) along with 2.1 pmol of double

stranded oligonucleotides (wild-type or mutant) in 13 mM Tris pH 8.0, 40mM KCl, 35 mM NaCl, 1 mM dithiothreitol, 0.1 mM EDTA, 0.05 % nonidet P-40 and 8 % glycerol were incubated at room temperature for 20 minutes, cross-linked and loaded onto 7% nondenaturing polyacrylamide gels. The gels containing separated DNA, protein or both were stained using an EMSA kit (Molecular Probes, Eugene OR) containing two fluorescent dyes for detection, SYBR Green EMSA stain (DNA) and SYPRO Ruby EMSA stain (Protein). The bands were visualized on the Fujifilm LAS 4000 and quantified densitometrically using Image J.

*Cell culture and treatments:* HepG2 cells (ATCC, Manassas, VA) cultured in Eagle's minimum essential medium (EMEM) with 10% fetal bovine serum (FBS) at 37°C with 5% $CO_2$ in a humidified chamber were used in this study. Cell were seeded onto 6-well culture plates and upon reaching 70-80% confluency, media was replaced with serum-free media followed by incubation for 2 hours. Next, confirmed hPPARα ligands (stearic acid, C18:0; oleic acid, C18:1; docosahexanoic acid, C22:6; from chapter I) were added to the media and the cells were allowed to grow for 22-24 hours. Fatty acids were added to the cells as a complex with BSA (as described in chapter I of this dissertation) and clofibrate and rosiglitazone (controls; solubilized in DMSO) were added directly to the media. Although each ligand was examined at 10 µM, a dose of 100 µM was also tested initially. This was followed by determination of adiponectin mRNA and protein levels by qRT-PCR and Western blotting.

*RNA isolation and qRT-PCR:* Total RNA was extracted using the Taqman® Cells-to-$C_T$ kit (Ambion, Grand Island, NY) and reverse transcribed at 37°C for 60 minutes followed by 95°C for 5 minutes on a Multigene thermocycler (Labnet International Inc.,

Edison NJ). The expression of adiponectin, PPARα (control) and 18S rRNA (internal control) was determined using the Taqman® Gene Expression Assays On Demand™ designed for these specific genes (human adiponectin, Hs00605917_m1 FAM ;hPPARα, Hs00947536_m1 FAM; 18S, Hs99999901_s1 FAM). Briefly, 4 µl of each reverse transcribed product served as a template in a 20 µl PCR containing 16 µl of a gene specific mastermix (10 µl Taqman® Master Mix, 1 µl of respective Taqman® Gene Expression Assays On Demand™ and 5 µl of nuclease-free water). The PCR was carried out on a MicroAmp 96-well plate (Applied Biosystems, Grand Island, NY) and the amplification was a carried using a StepOnePlus thermocycler (Applied BioSystems, Grand Island, NY). The amplification conditions included 50°C for 4 minutes, 95°C for 10 minutes, followed by 40 cycles of 15 seconds at 95°C and 1 minute at 60°C. Cycle threshold (Ct values) thus obtained, were used to calculate the $\Delta\Delta Ct$ and the fold change for each gene and treatment condition as described previously (*94*).

*Western Blotting Analysis:* HepG2 cells treated with ligands as indicated above were lysed by sonication in a buffer containing 5 mM HEPES, 0.4% triton X, 100 mM $Na_3VO_4$, (sodium orthovanadate) 2 U of apritinin/ml, 5 U of Leupeptin/ml and 2 U of pepstatin/ml. Whole-cell lysates were denatured by boiling in sodium dodecyl sulfate (SDS) sample buffer and dithiothreitol and resolved on a 12% SDS-PAGE gel followed by electrophoretic transfer to a nitrocellulose membrane. Proteins were detected using specific antibodies against adiponectin (Abcam, ab22554), PPARα (Santacruz, sc-9000) and β-actin (Sigma, A5316) followed by incubation in respective secondary antibody (Sigma, St. Louis, MO) prior to visualization by enhanced chemiluminescence on the Fujifilm LAS 4000 (Fujifilm Medical Systems USA Inc., Stamford, CT). The relative

amount of a given protein for each condition was examined by densitometry (ImageJ) and compared to controls.

*Plasmids:* Mammalian expression plasmids for the overexpression of hPPARα (pSG5-hPPARα) and hRXRα (pSG5-hRXRα) have already been described in chapter I of this dissertation. In order to generate luciferase constructs with the adiponectin promoter, a 2.4 kb fragment of the adiponectin promoter containing both putative PPRE and the minimal transcriptional machinery was amplified from cDNA derived from HepG2 cells with the following primers: 5'- cggtaccTTCACCATCTTCGTCAGGCT-3' and 5'- cgagctcAGACTGCAGTCAGAATGGAA -3'. In these and subsequent primers, lowercase represents nucleotides outside of the open reading frame with restriction sites underlined. This PCR product was cloned into the pGEM®-T easy vector (Promega Corp., Madison, WI), sequenced to confirm amplification and subsequently cloned into the *Kpn I* and *Sac I* sites of the pGL4.17 luciferase construct (Promega Corp., Madison, WI) to produce pHH 83

In order to test selective PPARα activation by one or the other response element (PPRE1 or PPRE2), mutant luciferase constructs for adiponectin promoters were also generated with either one or both PPRE abolished. In order to mutate PPRE1, pHH 83 was amplified using 5'–cggtaccTCAGACTCCTTTAAAGGTCTGATCTGCCCGCCTCAG–3' and 5'-cgagctcAGACTGCAGTCAGAATGGAA such that the PCR product had the mutated/scrambled nucleotides in place of the PPRE (marked in the primer). This PCR product was cloned into the pGEM®-T easy vector (Promega Corp., Madison, WI), sequenced to confirm amplification and subsequently cloned into the *Kpn I* and *Sac I*

sites of the pGL4.17 luciferase construct (Promega Corp., Madison, WI) to produce pHH 145. In order to mutate PPRE 2, pHH 83 was used to amplify 2 PCR products using the following primers: 5'- cggtaccTTCACCATCTTCGTCAGGCT-3' and 5' – TGTCGACATATATGAAACCACAGCAGGAAAACAAGA – 3' (giving a ~2.0 kb fragment with mutated/scrambled PPRE 2) and 5' – GGTCGACATCTTCTGTTGCTGTTGTAGGAG – 3' and 5' – CgagctcAGACTGCAGTCAGAATGGAA – 3' (giving a ~300 bp fragment with a mutated/scrambled half of the PPRE 2). Both these fragments were individually cloned into the pGEM®-T easy vector (Promega Corp., Madison, WI) followed by sequencing to confirm amplification. These two fragments - *Kpn I/Sal I* fragment (~2.0 kb) and *Sal I/Sac I* fragment (~300 bp), were subsequently directionally cloned into the *Kpn I* and *Sac I* sites of the pGL4.17 luciferase construct (Promega Corp., Madison, WI) to produce pHH 142. To mutate both PPRE 1 and PPRE 2, pHH 142 was used to amplify a PCR product using the following primers: 5'–cggtaccTCAGACTCCTTTAAAGGTCTGATCTGCCCGCCTCAG–3' (containing mutated/scrambled PPRE 1) and 5'- cgagctcAGACTGCAGTCAGAATGGAA. The PCR product with both PPRE's mutated/scrambled and was cloned into the pGEM®-T easy vector (Promega Corp., Madison, WI), sequenced to confirm amplification and sub-cloned into the *Kpn I* and *Sac I* sites of the pGL4.17 luciferase construct (Promega Corp., Madison, WI) to produce pHH 146.

*Transactivation assays:* COS-7 cells are derived from CV-1 cells (African green monkey kidney cells) and have classically been used in transactivation experiments for nuclear receptors such as the PPARs (*95*). In addition to having the

basal transcriptional machinery, they have low basal expression of PPARs and have relatively high transfection efficiencies (*96*). COS-7 cells (ATCC, Manassas, VA) were grown in DMEM supplemented with 10 % fetal bovine serum (Invitrogen, Grand Island, NY) at 37°C with 5% $CO_2$ in a humidified chamber. Cells were seeded onto 24-well culture plates and transfected with Lipofectamine™ 2000 (Invitrogen, Grand Island, NY) and 0.4 µg of each full-length mammalian expression vector (pSG5-hPPARα, pSG5-hRXRα or both) or empty plasmid (pSG5), 0.4 µg of each luciferase reporter construct (pHH 83, pHH 142, pHH 143, pHH 146) and 0.04 µg of the internal transfection control plasmid pRL-CMV (Promega Corp., Madison, WI) as previously described (*92*, *97*). Following transfection incubation, medium was replaced with serum-free medium for 2 h, ligands (1µM) were added, and the cells were grown for an additional 20-24 h. Fatty acids were added as a complex with bovine serum albumin (BSA) as described (*98*). Clofibrate and rosiglitazone (solubilized in DMSO) were added directly to the media. Firefly luciferase activity, normalized to Renilla luciferase (for transfection efficiency), was determined with the dual luciferase reporter assays system (Promega, Madison, WI) and measured with a SAFIRE$^2$ microtiter plate reader (Tecan Systems, Inc. San Jose, CA). No treatment samples overexpressing both PPARα and RXRα were arbitrarily set to 1.

**Results and Discussion**

Since the discovery of PPARα, it has been postulated that one of its main functions is to sense LCFA and/or their metabolic intermediates as ligands and induce downstream genes that are either directly or indirectly involved in fatty acid metabolism (*62-65*). Adiponectin also functions to regulate energy homeostasis by promoting fatty acid oxidation, glucose uptake and decreasing gluconeogenesis (*26, 33*). Studies also suggest that PPARα agonists (*69-71, 73, 77*) and polyunsaturated fatty acids (PUFA) (*66, 72, 99*) could induce the expression of adiponectin. Given all the background on the lipid-sensing role of PPARα, we anticipated that hPPARα plays an important role in ligand dependent regulation of adiponectin.

*Electrophoretic mobility shift assays (EMSAs): PPARα-RXRα heterodimers bind to human adiponectin PPREs.* Since adiponectin promoter analysis revealed two putative PPRE (PPRE 1, -2345/-2358 and PPRE 2, -335/-368), EMSA were performed to confirm the binding of PPARα-RXRα heterodimers to each of the identified PPRE. While hPPARα alone or hRXRα alone did not bind to either adiponectin PPRE, hPPARα-hRXRα incubated together with either PPRE 1 or PPRE 2 resulted in retarded movement of the DNA – suggesting binding of hPPARα-hRXRα to these PPRE (Fig. 33A). The signal of such band was diminished by 40-50 % when hPPARα-hRXRα were incubated with mutant forms of these PPRE (Figure 33B and 33C). According to the classical mode of action for nuclear receptors, ligand binding induces specific conformational changes that promote heterodimerization and DNA binding (*62-65, 100, 101*). Previous mobility shift assays have not only demonstrated the binding hPPARα-hRXRα heterodimers to DNA in absence of ligand, but have also shown that such binding was enhanced in the

presence of synthetic agonists such as Wy-14,643 (*100, 101*). Thus we anticipated differences in DNA binding in the presence of hPPARα ligands. However, the addition of hPPARα ligands such as stearic acid (C18:0), oleic acid (C18:1), eicosapentanoic acid (EPA) or clofibrate did not cause any significant differences in DNA binding or hPPARα-hRXRα-DNA band intensities (Figure 33B and 33C). Based on the outcome of these experiments, three points specifically need to be addressed here. These include 1) binding of unliganded hPPARα-hRXRα to PPRE, 2) no significant changes in ligand induced DNA binding and 3) only 25-45% reduction in DNA binding with the use of mutated or disrupted PPRE.

Firstly, *in vitro* binding of hPPARα-hRXRα to PPRE sequences even in the absence of a ligand has been demonstrated by a large number of studies (almost 2 decades ago) (*100, 101*). While such binding of unliganded receptors to specific DNA sequences has been attributed to the independent function of the DNA binding domain (DBD) in the nuclear receptors, Brazda *et. al.* recently demonstrated that nuclear receptors are in continuous motion, such that they rapidly bind and unbind DNA. The addition of a ligand by and large only increases their residual time on the DNA (*102*). These findings help explain the binding of nuclear receptors (hPPARα-hRXRα) to DNA sequences (PPRE sequences) even in absence of a ligand. Secondly, addition of ligands to the *in vitro* reactions did not alter DNA binding. Balanarasimha *et al.* also demonstrate similar findings where the binding of hPPARα-hRXRα heterodimers to the ACOX PPRE (classical PPARα responsive gene) is not affected by ligand binding (*103*). It is likely that hPPARα-hRXRα heterodimers by themselves bind very well to the PPRE (*in vitro*) such that no difference in DNA binding is seen in the presence of hPPARα ligands. Van der

Meer *et. al*. utilized chromatin immunoprecipitation with genomic sequencing (ChIP-seq) and transcriptomics to demonstrate that, of all the genomic binding sites for PPARα (corresponding to about 2875 genes) about 82% of the genes are bound by PPARα equally well in the presence or absence of ligand (*104*). Since transactivation/transrepression is also a function of promoter occupancy and cofactor binding to the nuclear receptor dimeric complex, DNA binding may not be representative of the amount of ligand induced activation/repression seen *in vivo* (*62-65, 102*).

Lastly, we have demonstrated specific binding of hPPARα-hRXRα to both PPRE1 and PPRE2 (Fig. 33A). However, we were able to achieve only 25-45% reduction in DNA/PPRE binding with the use of mutant PPREs (as opposed to complete ablation of such binding). Such binding of hPPARα-hRXRα to mutated PPRE1 and PPRE2 could be a result of some non-specific binding to the DNA. Such non-specific interactions on a gel-shift assay have also been observed with other transcription factors and could be attributed to the conditions used in such assays or even the degeneracy of the oligonucleotides (*67, 105*). The PPRE motif belongs to the direct repeat 1 category (DR-1) and consists of two repeats of a hexameric core motif, separated by one nucleotide (*62-65*). Since DR-1 motifs (constituting the PPRE) are quite degenerate in nature (*62-65*), other factors may determine nuclear receptor specificity to the DR-1 such as the 5' flanking extension (to DR1), spacing nucleotide or assisted binding to the response elements (via other proteins or DNA sequences) (*106-108*). Competition based mobility shift assays have shown that mutated unlabelled PPRE sequences also reduce the signal of PPAR-RXR binding to wild-type labeled PPRE sequences (although not as dramatically as wild-type unlabelled PPRE) (*67*). Similarly, Van der Meer *et al.* reported

the binding of nuclear receptors to DNA even the absence of a consensus DR-1 motif (in ChIP-chip studies) (*104*). These occurrences may be a result of the degeneracy of the core motif, indirect protein-protein interactions and DNA looping (in case of ChIP-chip studies), assisted binding to the DR-1 core motif as a result of the other nuclear receptor partner (in our case either PPARα or RXRα) or due to aberrant binding due to structural and electrostatic end-effects (*105*). However, having tested only one mutant per PPRE, it is difficult to rule out the possibility of some non-specific binding of hPPARα-hRXRα to the PPRE.

Albeit the many drawbacks, our data suggests that hPPARα-hRXRα heterodimers may be capable of binding the two putative PPREs in the human adiponectin promoter. One of these PPREs (PPRE 2, -335/-368) has also been previously reported to bind PPARγ-RXRα heterodimers (*67*). It is possible that based on the cell-type/organ system and the concentrations of PPARα versus PPARγ, adiponectin may be regulated by both these nuclear receptors. Nonetheless, the effects of hPPARα ligands on adiponectin transactivation/transrepression still remain elusive. It will be interesting to 1) see the outcome of competitive inhibition of hPPARα-hRXRα heterodimer binding to these PPREs and 2) to obtain PPARα promoter occupancy data from human heptoma cells (HepG2 cells; from van der Meer *et al.* (*104*)) particularly to determine PPARα binding sites in the adiponectin promoter.

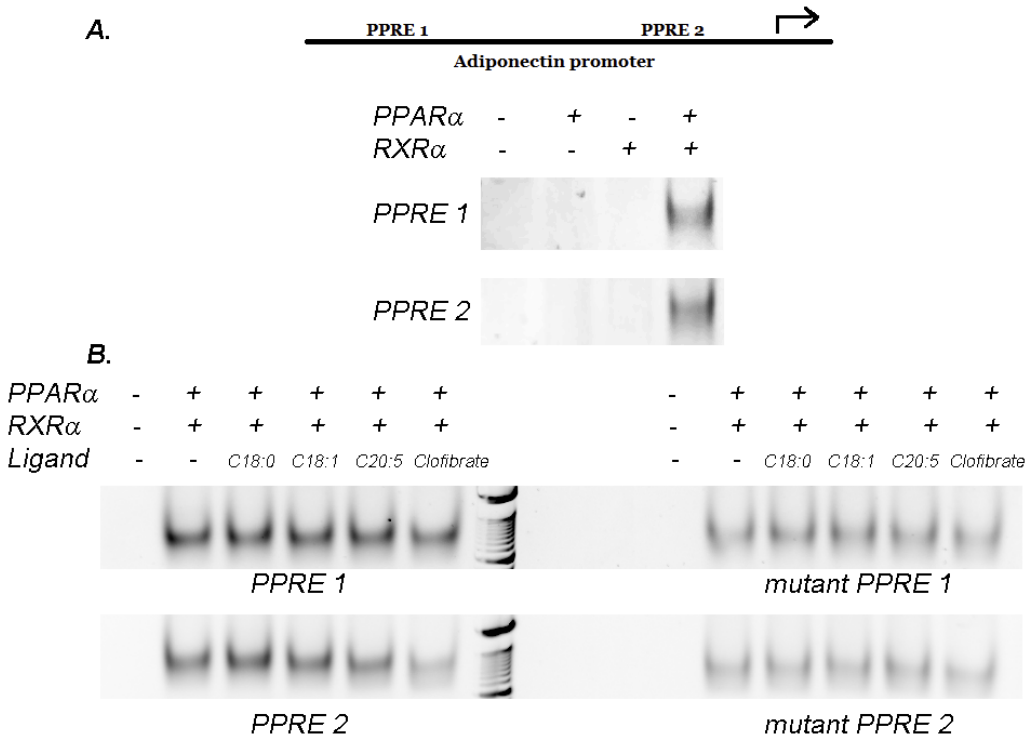
A.
PPRE 1
PPRE 2
Adiponectin promoter
PPARα - + - +
RXRα - - + +
PPRE 1
PPRE 2
B.
PPARα - + + + + + - + + + + +
RXRα - + + + + + - + + + + +
Ligand - - C18:0 C18:1 C20:5 Clofibrate - - C18:0 C18:1 C20:5 Clofibrate
PPRE 1
mutant PPRE 1
PPRE 2
mutant PPRE 2

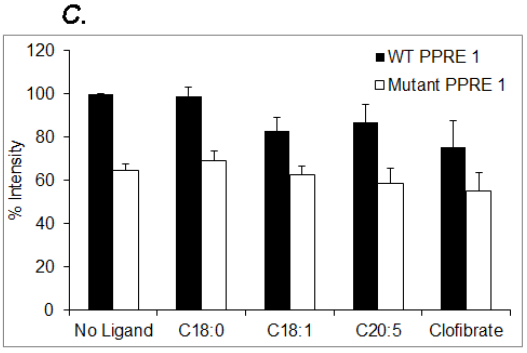
C.
WT PPRE 1
Mutant PPRE 1
% Intensity
120
100
80
60
40
20
0
No Ligand
C18:0
C18:1
C20:5
Clofibrate

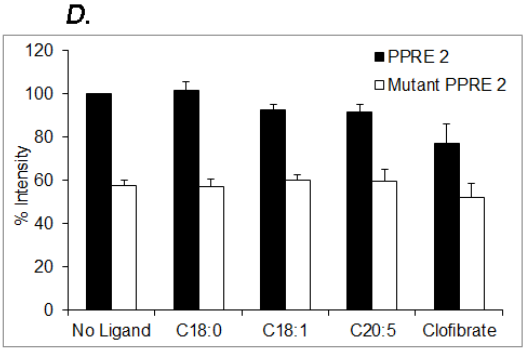
D.
PPRE 2
Mutant PPRE 2
% Intensity
120
100
80
60
40
20
0
No Ligand
C18:0
C18:1
C20:5
Clofibrate

**Fig. 33.** Electrophoretic mobility shift assays (EMSAs): Oligonucleotides containing putative PPRE from the human adiponectin promoter (PPRE 1 or PPRE 2) were incubated with recombinant hPPARα and hRXRα in the presence or absence of ligands. The position shifted hPPARα/hRXRα-oligonucleotide complex was labeled with SYBR Green EMSA stain (DNA) and SYPRO Ruby EMSA stain (Protein). A) SYBR green staining of the two PPREs incubated in the presence of hPPARα alone, hRXRα alone or both hPPARα/hRXRα (absence of any ligands). B) SYBR green staining of the position shifted hPPARα/hRXRα-oligonucleotide complex in the presence or absence of hPPARα ligands. Ligands tested include stearic acid (C18:0), oleic acid (C18:1), eicosapentanoic acid (C20:5) and clofibrate. C) SYBR green band intensities resulting from the hPPARα/hRXRα-oligonucleotide complex in the presence or absence of hPPARα ligands measured using ImageJ software, and plotted as relative mean bound DNA ± SEM, $n \geq 7$.

*Adiponectin expression in HepG2 cells and its regulation by hPPARα ligands:* Fewer studies have demonstrated hepatic expression of adiponectin in humans as well as mice (*89, 90, 109-111*). Therefore cultured human heptoma cells (HepG2) which represent the most widely used cellular model for human liver cells (*104*), were used to study the effect of hPPARα ligands on the mRNA and protein expression of adiponectin. While we were not able to detect adiponectin mRNA using Taqman® Gene Expression Assays specific for human adiponectin (qPCR), western blotting using a specific antibody for adiponectin demonstrated the presence of adiponectin protein in the cell lysates from all treatments (Fig. 34A). Adiponectin mRNA remained undetectable under different conditions such as overexpression of PPARα-RXRα and/or treatment with various hPPARα ligands.

Although we did not test any positive controls validating the Taqman® Gene Expression Assays used to detect human adiponectin, these probes have been commonly used for detection of adiponectin mRNA in other tissues (*112-114*). The lack of detection of adiponectin mRNA in HepG2 cells was unexpected, especially because we were able to detect adiponectin protein using specific antibodies in western blotting (Fig. 34A). It was later determined that adiponectin was present in the fetal-bovine serum (FBS) present in the EMEM media used to grow HepG2 cells. Thus, detection of adiponectin in the western blots from cell lysates could be an artifact resulting from contamination of media with bovine adiponectin (from FBS; Fig. 34B).

The lack of detection of adiponectin in cultured liver cells (HepG2) in our hands was surprising and contrary to some studies in the literature (*89, 90, 109-111*). However, upon careful review of the literature, we found that our results were also in agreement

with some other reports (*115, 116*). Immunohistochemistry based studies done in human and mouse livers revealed that adiponectin expression in the liver tissue was primarily localized to the endothelial cells of portal vessels and/or liver sinusoids and hepatic stellate cells (*115, 116*). It was also suggested that this staining could be a result of some "contamination" from circulating plasma adiponectin (*115, 116*). Similarly, Knotts *et al.* (using the same Taqman® Gene Expression Assay as our study) were also not able to detect the expression of adiponectin mRNA in HepG2 cells (*114*).

One major cause of such differences in results for hepatic expression of adiponectin could be due to the physiological/pathophysiological state of the patient/mice/HepG2 cells. For example, morbidly obese patients with steatosis (*90*) or mice treated with carbon tetrachloride (model for hepatic fibrosis) (*117*) or infected with hepatitis B virus express adiponectin in the liver (*110*). Similarly, adiponectin was also detected in HepG2 cells infected with hepatitis B virus (*111*) or stimulated with an inflammatory cytokine such as interleukin-6 (IL-6) (*117*). In these experiments, the levels of adiponectin in wild-type or control HepG2 cells were either very low (*111*) or not detectable (*117*). Based on these observations, it is possible that adiponectin secretion from HepG2 cells occurs only under situations that are far from normal homeostatic conditions. Yoda-Murakami *et al.* demonstrated that treatment of mice with carbon tetrachloride (to induce liver injury/fibrosis) resulted in a gradual increase in the adiponectin mRNA with time (*117*). It is speculated that as the liver damage progresses, there is increased production of inflammatory cytokines such as IL-6 which in turn trigger the production of anti-inflammatory adiponectin locally in the liver. Thus under conditions that were used in our experiments, we were not able to gather convincing data

on the detection of adiponectin. Therefore it is difficult to predict the effect of PPARα ligands on the expression of adiponectin in these cell lines/culture conditions/treatments.

The other possibility that needs to be considered is that the HepG2 cells do not express adiponectin. Assuming that all the data showing adiponectin protein expression in human or mouse livers and HepG2 cells was biased due to "contamination" from the circulating forms of adiponectin or "contamination" from cell media, the question that still remains unexplained is the detection of adiponectin mRNA in liver samples (humans/mice). The human liver is composed of primarily hepatocytes (more than 60%) (*118*). However, it also consists of other cell types such as the kupffer cells (20%) and liver sinusoidal endothelial cells (15%) (*118*). Since immunohistochemistry based staining of adiponectin was localized to these cells in certain studies (*115, 116*), it is possible that adiponectin mRNA in the liver tissue arises from these cells (and not hepatycytes).

To answer all these questions/concerns, it is important to test our hypothesis in HepG2 cells under stimulation/stress (proinflammatory cytokines) or in a different cell line that constitutively expresses adiponectin such as adipose tissue. PPARγ is predominantly found in the adipose tissue where it plays a major role in adipogenesis. Considering the PPARγ involvement in the regulation of adiponectin, it will be challenging to test PPARα-mediated regulation of adiponectin in these cells. Several groups have reported expression of PPARα in the adipose tissue (*73, 119*), where it plays major role in lipolysis and fatty acid oxidation (*119*). Hiuge *et al.* also demonstrated that PPARα agonists directly regulate the expression of adiponectin in white adipose tissue in mice as well as mouse primary adipocytes and 3T3-L1 cultured adipocytes (*73*). This

effect was not seen in PPARα knockout mice or cells where PPARα expression was knocked down (*73*). It will be interesting to study the effects of PPARα ligands in PPARγ knockdown adipocytes.

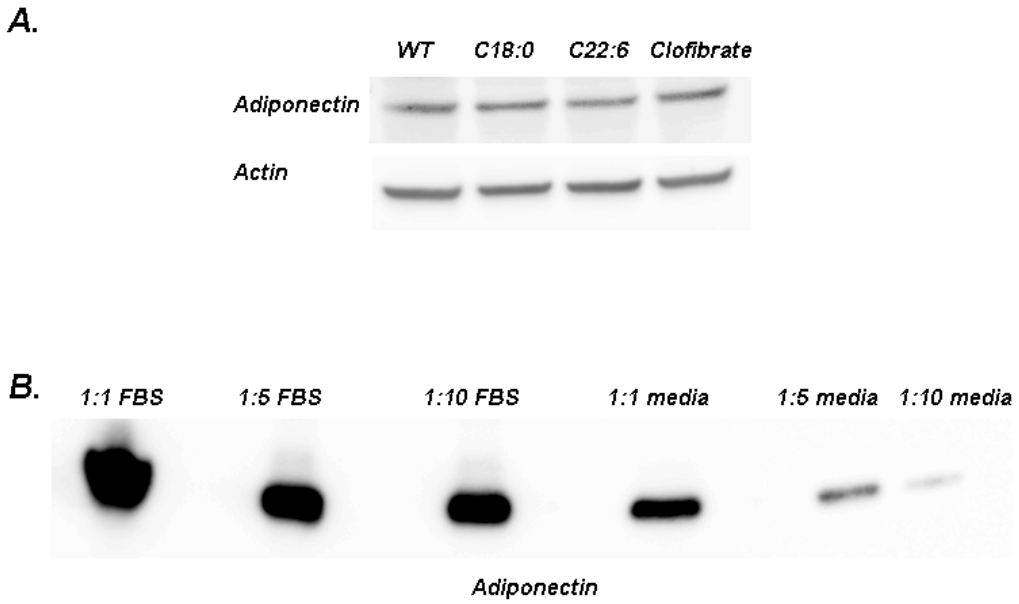


**Fig. 34.** *Adiponectin expression in HepG2 cells and its regulation by hPPARα ligands.* A) HepG2 cells treated with 10 µM of the indicated ligand and incubated for 18-20 hours following which whole cell extracts were analyzed by SDS PAGE and probed with indicated antibodies. B) Serially diluted fetal bovine serum (FBS) and EMEM media (containing 10% FBS) were by SDS PAGE and probed for adiponectin.

*Transactivation assays:* To examine whether PPARα is directly involved in transactivation/transrepression of the adiponectin promoter, COS-7 cells were transfected with mutant or wild-type adiponectin luciferase reporter constructs along with mammalian expression plasmids for hPPARα alone, hRXRα alone, both hPPARα and hRXRα and/or empty vector (pSG5). Transactivation was measured as percent firefly luciferase activity normalized to *Renilla* luciferase (internal transfection control) is depicted in figure 35. When compared to cells overexpressing empty vector (pSG5; Fig 35.D), PPARα alone (Fig. 35B) or RXRα alone (Fig. 35C), the basal transactivation for the wild-type adiponectin promoter was significantly increased in cells overexpressing both PPARα and RXRα (Fig. 35A). These findings are consistent with findings from transactivation assays using PPRE×3 TK LUC reporter construct (Chapter I), suggesting that both PPARα and RXRα work as heterodimeric partners to regulate gene expression. Compared to the transactivation seen for the wild-type adiponectin promoter in cells overexpressing both PPARα and RXRα, about 60 ± 9 % transactivation was even observed in cells overexpressing RXRα alone (Fig. 35C) – suggesting that in addition to the PPARα-RXRα heterodimers, other factors (possibly RXRα dependent/driven) may also play a role in the regulation of the adiponectin promoter.

In cells overexpressing both PPARα and RXRα, mutating PPRE 1 versus PPRE 2 makes a considerable difference in the basal promoter activity (Fig. 35A). Mutating both PPRE 1 and PPRE 2 in the adiponectin promoter caused a considerable decrease in transactivation when compared to the wild-type promoter construct (50 ± 1%; Fig. 33A). While such decrease in transactivation was also observed when only PPRE 2 was mutated, no decrease in transactivation was seen when PPRE 1 was mutated

(transactivation similar to wild-type). These findings, although in contrast with our data from mobility shift assays, suggest that only one PPRE (PPRE 2) may be responsive to PPARα activation (Fig. 35A). There were no differences in the DNA binding ability of hPPARα-RXRα (to PPRE1 vs. PPRE2) in mobility shift assays. However, transactivation/transrepression is also a function of cofactor binding to the hPPARα-hRXRα complex (*62-65, 102*), and DNA binding reflected in our mobility shift assays does not take this factor into consideration. Thus DNA binding in our mobility shift assays may not be representative of the amount of ligand induced activation/repression seen in reporter assays.

PPRE 2 is the same response element that has also been shown to be regulated by PPARγ (*67*). Over the years, scientists have suggested sharing of response elements between nuclear receptors. In fact genomic profiling of transcription factor binding sites has revealed a lot of degeneracy and overlaps of binding sites (*104, 105, 120*). Boergenes *et al.* have further demonstrated that there is substantial overlap between liver X receptor (LXR) and PPARα binding sites. They further suggest that PPARα may bind to the particular site in one cell type, whereas LXR may predominate such binding in another cell type (*120*). Similarly, since PPARα and PPARγ share the same degenerate PPRE motif in the adiponectin promoter (PPRE 2), it is likely based on the cell-type/tissue-type each PPAR subtype plays a differential role in the regulation of adiponectin. This can be extended to the physiological role of the tissue (example, liver vs. adipose tissue) and the specific function of adiponectin desired (example, fatty acid oxidation, gluconeogenesis, glucose uptake or anti-inflammatory function).

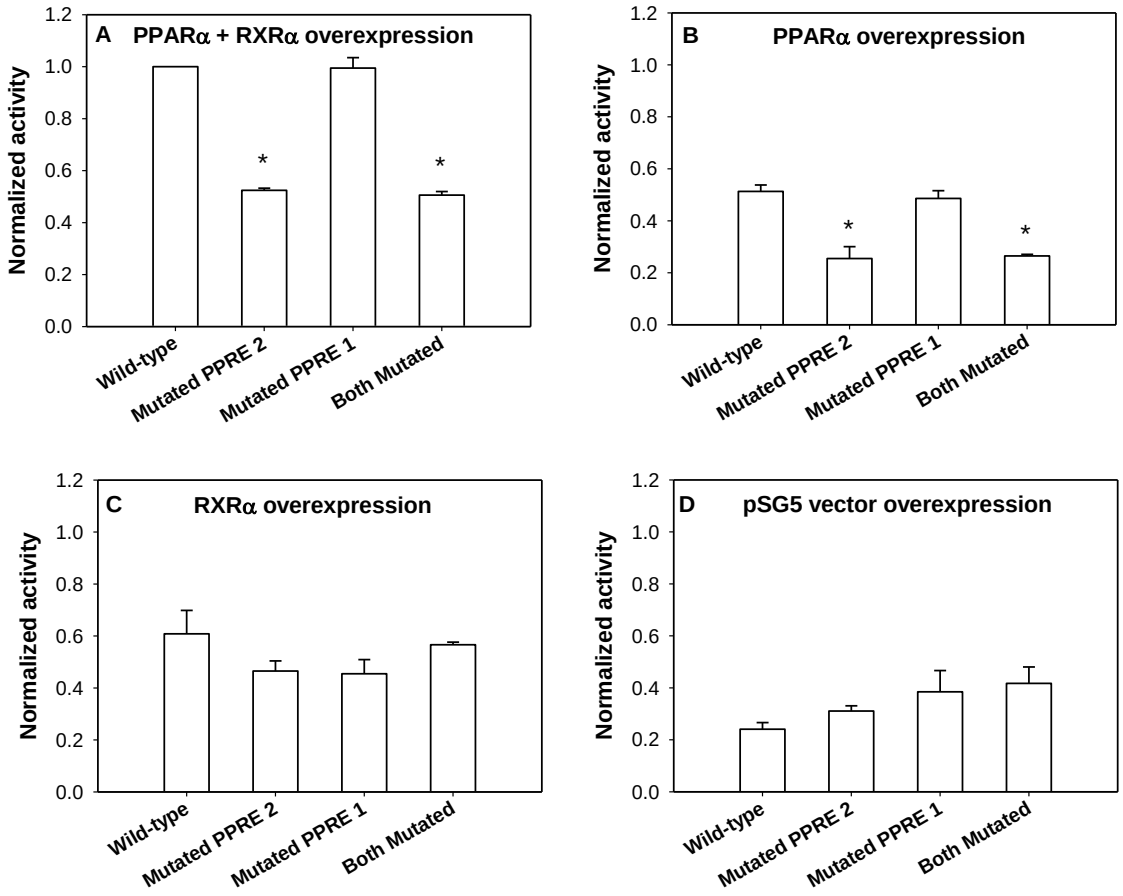


**Fig. 35.** The transactivation of the adiponectin promoter-luciferase construct or mutants where one or both of the putative PPRE were disrupted was measured in COS-7 cells transfected with A) both PPARα and RXRα, B) PPARα alone, C) RXRα alone or D) pSG5 empty vector. The *y-axis* represents values for firefly luciferase activity that have been normalized to *Renilla* luciferase (internal control) The PPARα and RXRα overexpressing cells with wild-type adiponectin promoter-luciferase construct was arbitrarily set to 1 and the bar graph represents the mean values (n $\geq$ 3) $\pm$ standard error. * $P < 0.001$.

Compared to the basal transactivation of the adiponectin promoter (Fig. 35), it is not clear whether hPPARα ligands have any effect on the adiponectin promoter activity (Fig. 36). While PPARα ligands such as stearic acid and clofibrate did cause any significant changes in transactivation of the wild-type adiponectin promoter, the addition docosahexanoic acid resulted in a significant decrease in such transactivation (Fig. 36A). Since PPARγ has previously been shown to transactivate adiponectin (*67*), cells were also treated with a synthetic PPARγ agonist (rosiglitazone) to account for the possible PPARγ involvement in such regulation. Similar to docosahexanoic acid, the addition of rosiglitazone also resulted in a significant decrease in transactivation of the adiponectin promoter (Fig. 36A). Such decrease in transactivation (with C22:6 or rosiglitazone) was seen consistently in all transfections, including mutant adiponectin promoter constructs or cells overexpressing both PPARα and RXRα (Fig. 36A), PPARα alone (Fig. 36B), RXRα alone (Fig. 36C) or pSG5 vector (Fig. 36D). This suggests that the resultant decrease in transactivation could be resulting from indirect effects or effects that are independent of the peroxisome proliferator-activated receptor response elements.

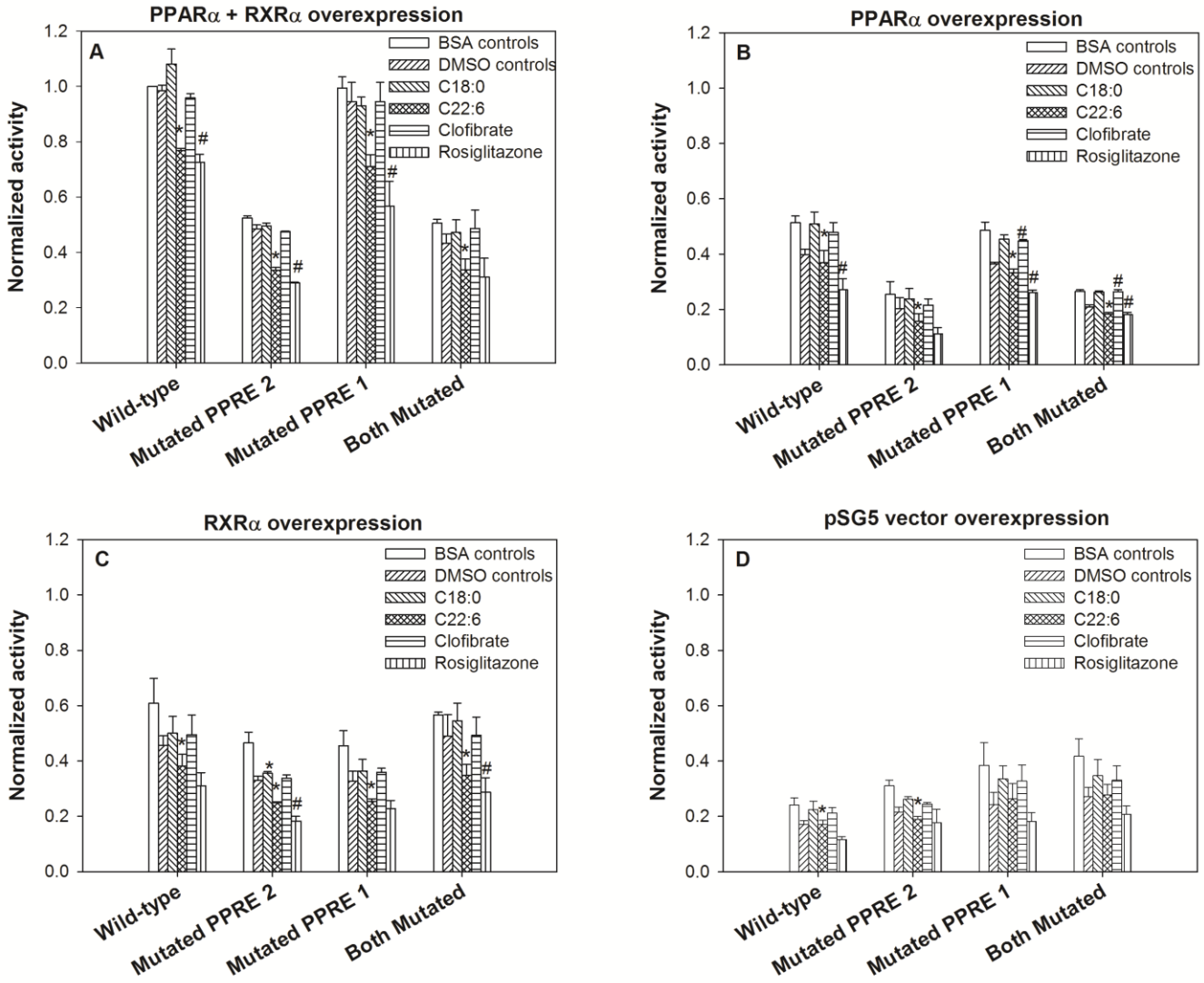
PPARα + RXRα overexpression
A
BSA controls
DMSO controls
C18:0
C22:6
Clofibrate
Rosiglitazone
Normalized activity
0.0
0.2
0.4
0.6
0.8
1.0
1.2
Wild-type
Mutated PPRE 2
Mutated PPRE 1
Both Mutated
PPARα overexpression
B
RXRα overexpression
C
pSG5 vector overexpression
D

**Fig. 36.** Effect of PPARα ligands on the transactivation of adiponectin promoter. COS-7 cells transfected with A) both PPARα and RXRα, B) PPARα alone, C) RXRα alone or D) pSG5 empty vector were analyzed for transactivation of the adiponectin promoter-luciferase construct in the presence of bovine serum albumin (BSA) based vehicle (controls for fatty acid ligands; *open bars*), dimethyl sulfoxide (DMSO) based vehicle (controls for drugs; *diagonally upward bars*), 10 µM BSA linked-stearic acid (C18:0; *diagonally downward bars*), 10 µM BSA-docosahexanoic acid (*cross-hatched bars*), 10 µM clofibrate (PPARα agonist solubilized in DMSO; *horizontal lined bars*), and 10 µM rosiglitazone (PPARγ agonist solubilized in DMSO; *vertically lined bars*). The *y-axis* represents values for firefly luciferase activity that have been normalized to *Renilla* luciferase (internal control), where PPARα and RXRα overexpressing cells in the presence of BSA vehicle controls were arbitrarily set to 1. The bar graph represents the mean values ($n \geq 3$) ± standard error. * $P < 0.05$ in comparison to BSA controls and # $P < 0.05$ in comparison to DMSO controls.

Apart from PPARγ and the possible involvement of PPARα, the adiponectin gene has been shown to be regulated by multiple transcription factors. Some of these transcription factors include transcriptional activators such as CCAAT/enhancer binding protein (C/EBP) (*121, 122*), nuclear factor Y (NF-Y) (*121*), adipocyte determination and differentiation-dependent factor 1/Sterol regulatory element-binding protein 1c (ADD/SREBP1-c) (*60*), and transcriptional repressors like activating transcription factor (ATF3) (*123*), cAMP response element binding protein (*61*), nuclear factor of activated T cells (NFAT) (*123*). Although these transcription factors are reported to regulate the expression of adiponectin, the significance of some of these results are not clear. For example, subjects with insulin resistance, obesity or metabolic syndrome (with low levels of adiponectin) do not have any changes in their levels or activity of C/EBP (a positive regulator of adiponectin (*124*). Nonetheless, the regulation by multiple transcription factors suggests the transcription of adiponectin is under intricate regulation by various upstream signals.

Upon manually analyzing the adiponectin promoter constructs in our experiments, it was found that the putative binding sites for all of these transcription factors are located in the region of the adiponectin promoter that was cloned upstream of the luciferase gene. Thus, the possible involvement of these transcription factors could not be ruled out. Alternatively, since increased transactivation is only seen when both PPARα and RXRα are overexpressed (and not when PPARα ligands are added or PPARα alone or RXRα alone are overexpressed), it is also possible that these effects are mediated indirectly by PPARα-RXRα heterodimers – via regulation/cross-talk of other transcription factors. For

example, human SREPB-1c (positive regulator of adiponectin) is also under regulation of PPARα through a PPRE in its promoter (*125*).

Genomic profiling of transcription factor binding sites has revealed a lot of degeneracy and overlaps of binding sites (*105, 120, 126*). Thus it has been suggested that there might be clustering of transcription factors and/or other accessory proteins to the regulatory regions of genes resulting in stabilization of protein-protein interactions such that, they function as a complex (*105, 120, 126*). Profiling of PPAR binding sites has revealed that genes that are activated by the PPARs are enriched in specific transcription factor binding sites other than the PPARs (*104, 127*). For example, genes containing a PPRE-like motif are likely to have a C/EBP binding element, TATA binding protein binding motif and signal transducer of transcription (STAT) binding motifs in their vicinity (*104, 127*). Such clustering has also been demonstrated for estrogen receptor with C/EBP and octamer transcription factor 1 (Oct1) binding elements in its vicinity (*128*). It is possible that PPARα-RXRα heterodimers are a part of a cluster of transcription factors that aid in transactivation of the adiponectin gene such that, activation is not achieved by PPARα ligands but rather by just the presence of the PPAR-RXR heterodimer.

**Future Directions**

Owing to the drawbacks of our study, it is not clear whether PPARα has any role in the regulation of adiponectin. Clinical and preclinical evidences strongly suggest that PPARα agonists induce the expression of adiponectin. However, it is not clear whether its involvement in such regulation is a direct or an indirect effect of PPARα activation. In addition, adiponectin is speculated to be under complex regulation by a number of transcription factors and upstream signals (*59*). Thus it is challenging to tease apart the involvement of PPARα in such regulation. Some of the drawbacks of this study include lack of competition based gel-shift assays, lack of a cell line that constitutively expresses adiponectin and lack of consideration of other transcription factor involvement in the regulation of adiponectin. Future studies should address some of these concerns and lay emphasis on the kind techniques used (example, avoid use of media/FBS containing adiponectin) and cell lines used. Considering the involvement of PPARγ and the presence of a common PPRE in the adiponectin promoter it is essential to tease apart the effects of PPARγ versus PPARα. One way of doing this it to make use of a cell line that lacks either PPARα or PPARγ.

Another aspect of adiponectin regulation that has not been approached in this study is the involvement of adiponectin receptors (AdipoR1 and AdipoR2). The expression of these receptors is speculated to be under complex regulation by adiponectin itself, insulin/feeding/fasting conditions as well as nuclear receptors such as PPARα and PPARγ (*27-31*). While the expression of AdipoR's was downregulated in obese patients with coronary artery disease (*129*), livers of obese mice (*51, 52*) and in hyperglycemia (*130*), their levels were upregulated upon fasting (*51*) and upon treatment with a PPARα

agonist (*52*). These observations warrant further study mainly because the cause/effect relationship of such regulation is largely unknown. For example, decreases in levels of AdipoRs could be a result of low circulating levels of adiponectin (auto-regulation) and increases in levels of adiponectin receptors due to a PPARα or PPARγ agonists could be the result of increased expression of adiponectin or vice versa (*31*). Since strategies that would either increase the expression of adiponectin or its signaling (via its AdipoR) could improve a number of parameters associated with the metabolic syndrome, it is crucial to understand the molecular mechanism of the adiponectin system.

## References


1. Kopelman, P. G. (2000) Obesity as a medical problem, Nature 404, 635-643.
2. Grundy, S. M., Brewer, H. B., Jr., Cleeman, J. I., Smith, S. C., Jr., and Lenfant, C. (2004) Definition of metabolic syndrome: Report of the National Heart, Lung, and Blood Institute/American Heart Association conference on scientific issues related to definition, Circulation 109, 433-438.
3. Ervin, R. B. (2009) Prevalence of metabolic syndrome among adults 20 years of age and over, by sex, age, race and ethnicity, and body mass index: United States, 2003-2006, Natl Health Stat Report, 1-7.
4. Spiegelman, B. M., and Flier, J. S. (1996) Adipogenesis and obesity: Rounding out the big picture, Cell 87, 377-389.
5. Friedman, J. M. (2000) Obesity in the new millennium, Nature 404, 632-634.
6. Steppan, C. M., Bailey, S. T., Bhat, S., Brown, E. J., Banerjee, R. R., Wright, C. M., Patel, H. R., Ahima, R. S., and Lazar, M. A. (2001) The hormone resistin links obesity to diabetes, Nature 409, 307-312.
7. Hotamisligil, G. S. (1999) The role of TNF alpha and TNF receptors in obesity and insulin resistance, Journal of Internal Medicine 245, 621-625.
8. Scherer, P. E., Williams, S., Fogliano, M., Baldini, G., and Lodish, H. F. (1995) A novel serum protein similar to C1q, produced exclusively in adipocytes, J Biol Chem 270, 26746-26749.
9. Maeda, K., Okubo, K., Shimomura, I., Funahashi, T., Matsuzawa, Y., and Matsubara, K. (1996) cDNA cloning and expression of a novel adipose specific

collagen-like factor, apM1 (AdiPose Most abundant Gene transcript 1), Biochem Biophys Res Commun 221, 286-289.

10. Nakano, Y., Tobe, T., Choi-Miura, N. H., Mazda, T., and Tomita, M. (1996) Isolation and characterization of GBP28, a novel gelatin-binding protein purified from human plasma, J Biochem 120, 803-812.

11. Hu, E., Liang, P., and Spiegelman, B. M. (1996) AdipoQ is a novel adipose-specific gene dysregulated in obesity, J Biol Chem 271, 10697-10703.

12. Shapiro, L., and Scherer, P. E. (1998) The crystal structure of a complement-1q family protein suggests an evolutionary link to tumor necrosis factor, Curr Biol 8, 335-338.

13. Kissebah, A. H., Sonnenberg, G. E., Myklebust, J., Goldstein, M., Broman, K., James, R. G., Marks, J. A., Krakower, G. R., Jacob, H. J., Weber, J., Martin, L., Blangero, J., and Comuzzie, A. G. (2000) Quantitative trait loci on chromosomes 3 and 17 influence phenotypes of the metabolic syndrome, Proc Natl Acad Sci U S A 97, 14478-14483.

14. Takahashi, M., Arita, Y., Yamagata, K., Matsukawa, Y., Okutomi, K., Horie, M., Shimomura, I., Hotta, K., Kuriyama, H., Kihara, S., Nakamura, T., Yamashita, S., Funahashi, T., and Matsuzawa, Y. (2000) Genomic structure and mutations in adipose-specific gene, adiponectin, Int J Obes Relat Metab Disord 24, 861-868.

15. Pajvani, U. B., Du, X., Combs, T. P., Berg, A. H., Rajala, M. W., Schulthess, T., Engel, J., Brownlee, M., and Scherer, P. E. (2003) Structure-function studies of the adipocyte-secreted hormone Acrp30/adiponectin. Implications fpr metabolic regulation and bioactivity, J Biol Chem 278, 9073-9085.

16. Richards, A. A., Stephens, T., Charlton, H. K., Jones, A., Macdonald, G. A., Prins, J. B., and Whitehead, J. P. (2006) Adiponectin multimerization is dependent on conserved lysines in the collagenous domain: evidence for regulation of multimerization by alterations in posttranslational modifications, Mol Endocrinol 20, 1673-1687.

17. Aimen Xu, Y. W., and Karen S. L. Lam (2007) Adiponectin, Humana Press Inc. Totowa, NJ.

18. Waki, H., Yamauchi, T., Kamon, J., Ito, Y., Uchida, S., Kita, S., Hara, K., Hada, Y., Vasseur, F., Froguel, P., Kimura, S., Nagai, R., and Kadowaki, T. (2003) Impaired multimerization of human adiponectin mutants associated with diabetes. Molecular structure and multimer formation of adiponectin, J Biol Chem 278, 40352-40363.

19. Wang, Y., Lam, K. S., Yau, M. H., and Xu, A. (2008) Post-translational modifications of adiponectin: mechanisms and functional implications, Biochem J 409, 623-633.

20. Hara, K., Horikoshi, M., Yamauchi, T., Yago, H., Miyazaki, O., Ebinuma, H., Imai, Y., Nagai, R., and Kadowaki, T. (2006) Measurement of the high-molecular weight form of adiponectin in plasma is useful for the prediction of insulin resistance and metabolic syndrome, Diabetes Care 29, 1357-1362.

21. Ceddia, R. B., Somwar, R., Maida, A., Fang, X., Bikopoulos, G., and Sweeney, G. (2005) Globular adiponectin increases GLUT4 translocation and glucose uptake but reduces glycogen synthesis in rat skeletal muscle cells, Diabetologia 48, 132-139.

22. Liu, Y., Chewchuk, S., Lavigne, C., Brule, S., Pilon, G., Houde, V., Xu, A., Marette, A., and Sweeney, G. (2009) Functional significance of skeletal muscle adiponectin production, changes in animal models of obesity and diabetes, and regulation by rosiglitazone treatment, Am J Physiol Endocrinol Metab 297, E657-664.

23. Palanivel, R., Fang, X., Park, M., Eguchi, M., Pallan, S., De Girolamo, S., Liu, Y., Wang, Y., Xu, A., and Sweeney, G. (2007) Globular and full-length forms of adiponectin mediate specific changes in glucose and fatty acid uptake and metabolism in cardiomyocytes, Cardiovasc Res 75, 148-157.

24. Shetty, S., Kusminski, C. M., and Scherer, P. E. (2009) Adiponectin in health and disease: evaluation of adiponectin-targeted drug development strategies, Trends in Pharmacological Sciences 30, 234-239.

25. Yamauchi, T., Kamon, J., Ito, Y., Tsuchida, A., Yokomizo, T., Kita, S., Sugiyama, T., Miyagishi, M., Hara, K., Tsunoda, M., Murakami, K., Ohteki, T., Uchida, S., Takekawa, S., Waki, H., Tsuno, N. H., Shibata, Y., Terauchi, Y., Froguel, P., Tobe, K., Koyasu, S., Taira, K., Kitamura, T., Shimizu, T., Nagai, R., and Kadowaki, T. (2003) Cloning of adiponectin receptors that mediate antidiabetic metabolic effects, Nature 423, 762-769.

26. Brochu-Gaudreau, K., Rehfeldt, C., Blouin, R., Bordignon, V., Murphy, B. D., and Palin, M. F. (2010) Adiponectin action from head to toe, Endocrine 37, 11-32.

27. Sun, X., He, J., Mao, C., Han, R., Wang, Z., Liu, Y., and Chen, Y. (2008) Negative regulation of adiponectin receptor 1 promoter by insulin via a repressive nuclear inhibitory protein element, FEBS Lett 582, 3401-3407.

28. Jung, T. W., Lee, M. W., Lee, Y. J., Kim, S. M., Lee, K. T., Whang, W. K., Cheon, H. J., Jeong, Y. T., Chung, K. W., Cho, J. M., and Kim do, H. (2009) Regulation of adiponectin receptor 2 expression via PPAR-alpha in NIT-1 cells, Endocr J 56, 377-382.

29. Sun, X., Han, R., Wang, Z., and Chen, Y. (2006) Regulation of adiponectin receptors in hepatocytes by the peroxisome proliferator-activated receptor-gamma agonist rosiglitazone, Diabetologia 49, 1303-1310.

30. Chinetti, G., Zawadski, C., Fruchart, J. C., and Staels, B. (2004) Expression of adiponectin receptors in human macrophages and regulation by agonists of the nuclear receptors PPAR alpha, PPAR gamma, and LXR, Biochemical and Biophysical Research Communications 314, 151-158.

31. Kudoh, A., Satoh, H., Hirai, H., and Watanabe, T. (2011) Pioglitazone upregulates adiponectin receptor 2 in 3T3-L1 adipocytes, Life Sci 88, 1055-1062.

32. Lage, R., Dieguez, C., Vidal-Puig, A., and Lopez, M. (2008) AMPK: a metabolic gauge regulating whole-body energy homeostasis, Trends Mol Med 14, 539-549.

33. Deepa, S. S., and Dong, L. Q. (2009) APPL1: role in adiponectin signaling and beyond, Am J Physiol Endocrinol Metab 296, E22-36.

34. Mao, X., Kikani, C. K., Riojas, R. A., Langlais, P., Wang, L., Ramos, F. J., Fang, Q., Christ-Roberts, C. Y., Hong, J. Y., Kim, R. Y., Liu, F., and Dong, L. Q.

(2006) APPL1 binds to adiponectin receptors and mediates adiponectin signalling and function, Nat Cell Biol 8, 516-523.

35. Yamauchi, T., Kamon, J., Waki, H., Imai, Y., Shimozawa, N., Hioki, K., Uchida, S., Ito, Y., Takakuwa, K., Matsui, J., Takata, M., Eto, K., Terauchi, Y., Komeda, K., Tsunoda, M., Murakami, K., Ohnishi, Y., Naitoh, T., Yamamura, K., Ueyama, Y., Froguel, P., Kimura, S., Nagai, R., and Kadowaki, T. (2003) Globular adiponectin protected ob/ob mice from diabetes and ApoE-deficient mice from atherosclerosis, J. Biol. Chem. 278, 2461-2468.

36. Kadowaki, T., Yamauchi, T., Kubota, N., Hara, K., Ueki, K., and Tobe, K. (2006) Adiponectin and adiponectin receptors in insulin resistance, diabetes, and the metabolic syndrome, J Clin Invest 116, 1784-1792.

37. Arita, Y., Kihara, S., Ouchi, N., Takahashi, M., Maeda, K., Miyagawa, J., Hotta, K., Shimomura, I., Nakamura, T., Miyaoka, K., Kuriyama, H., Nishida, M., Yamashita, S., Okubo, K., Matsubara, K., Muraguchi, M., Ohmoto, Y., Funahashi, T., and Matsuzawa, Y. (1999) Paradoxical decrease of an adipose-specific protein, adiponectin, in obesity, Biochem Biophys Res Commun 257, 79-83.

38. Weyer, C., Funahashi, T., Tanaka, S., Hotta, K., Matsuzawa, Y., Pratley, R. E., and Tataranni, P. A. (2001) Hypoadiponectinemia in obesity and type 2 diabetes: close association with insulin resistance and hyperinsulinemia, J Clin Endocrinol Metab 86, 1930-1935.

39. Kumada, M., Kihara, S., Sumitsuji, S., Kawamoto, T., Matsumoto, S., Ouchi, N., Arita, Y., Okamoto, Y., Shimomura, I., Hiraoka, H., Nakamura, T., Funahashi, T.,

and Matsuzawa, Y. (2003) Association of hypoadiponectinemia with coronary artery disease in men, Arteriosclerosis Thrombosis and Vascular Biology 23, 85-89.

40. Ouchi, N., Kihara, S., Arita, Y., Maeda, K., Kuriyama, H., Okamoto, Y., Hotta, K., Nishida, M., Takahashi, M., Nakamura, T., Yamashita, S., Funahashi, T., and Matsuzawa, Y. (1999) Novel modulator for endothelial adhesion molecules: adipocyte-derived plasma protein adiponectin, Circulation 100, 2473-2476.

41. Kobayashi, H., Ouchi, N., Kihara, S., Walsh, K., Kumada, M., Abe, Y., Funahashi, T., and Matsuzawa, Y. (2004) Selective suppression of endothelial cell apoptosis by the high molecular weight form of adiponectin, Circ Res 94, e27-31.

42. Otsuka, F., Sugiyama, S., Kojima, S., Maruyoshi, H., Funahashi, T., Matsui, K., Sakamoto, T., Yoshimura, M., Kimura, K., Umemura, S., and Ogawa, H. (2006) Plasma adiponectin levels are associated with coronary lesion complexity in men with coronary artery disease, J Am Coll Cardiol 48, 1155-1162.

43. Ouchi, N., Ohishi, M., Kihara, S., Funahashi, T., Nakamura, T., Nagaretani, H., Kumada, M., Ohashi, K., Okamoto, Y., Nishizawa, H., Kishida, K., Maeda, N., Nagasawa, A., Kobayashi, H., Hiraoka, H., Komai, N., Kaibe, M., Rakugi, H., Ogihara, T., and Matsuzawa, Y. (2003) Association of hypoadiponectinemia with impaired vasoreactivity, Hypertension 42, 231-234.

44. Hotta, K., Funahashi, T., Arita, Y., Takahashi, M., Matsuda, M., Okamoto, Y., Iwahashi, H., Kuriyama, H., Ouchi, N., Maeda, K., Nishida, M., Kihara, S., Sakai, N., Nakajima, T., Hasegawa, K., Muraguchi, M., Ohmoto, Y., Nakamura, T., Yamashita, S., Hanafusa, T., and Matsuzawa, Y. (2000) Plasma concentrations of

a novel, adipose-specific protein, adiponectin, in type 2 diabetic patients, Arterioscler Thromb Vasc Biol 20, 1595-1599.

45. Trujillo, M. E., and Scherer, P. E. (2005) Adiponectin - journey from an adipocyte secretory protein to biomarker of the metabolic syndrome, Journal of Internal Medicine 257, 167-175.

46. Schulze, M. B., Shai, I., Rimm, E. B., Li, T., Rifai, N., and Hu, F. B. (2005) Adiponectin and future coronary heart disease events among men with type 2 diabetes, Diabetes 54, 534-539.

47. Pischon, T., Girman, C. J., Hotamisligil, G. S., Rifai, N., Hu, F. B., and Rimm, E. B. (2004) Plasma adiponectin levels and risk of myocardial infarction in men, JAMA 291, 1730-1737.

48. Yamauchi, T., Kamon, J., Waki, H., Terauchi, Y., Kubota, N., Hara, K., Mori, Y., Ide, T., Murakami, K., Tsuboyama-Kasaoka, N., Ezaki, O., Akanuma, Y., Gavrilova, O., Vinson, C., Reitman, M. L., Kagechika, H., Shudo, K., Yoda, M., Nakano, Y., Tobe, K., Nagai, R., Kimura, S., Tomita, M., Froguel, P., and Kadowaki, T. (2001) The fat-derived hormone adiponectin reverses insulin resistance associated with both lipoatrophy and obesity, Nat Med 7, 941-946.

49. Kubota, N., Terauchi, Y., Yamauchi, T., Kubota, T., Moroi, M., Matsui, J., Eto, K., Yamashita, T., Kamon, J., Satoh, H., Yano, W., Froguel, P., Nagai, R., Kimura, S., Kadowaki, T., and Noda, T. (2002) Disruption of adiponectin causes insulin resistance and neointimal formation, J Biol Chem 277, 25863-25866.

50. Altomonte, J., Harbaran, S., Richter, A., and Dong, H. (2003) Fat depot-specific expression of adiponectin is impaired in Zucker fatty rats, Metabolism 52, 958-963.

51. Tsuchida, A., Yamauchi, T., Ito, Y., Hada, Y., Maki, T., Takekawa, S., Kamon, J., Kobayashi, M., Suzuki, R., Hara, K., Kubota, N., Terauchi, Y., Froguel, P., Nakae, J., Kasuga, M., Accili, D., Tobe, K., Ueki, K., Nagai, R., and Kadowaki, T. (2004) Insulin/Foxo1 pathway regulates expression levels of adiponectin receptors and adiponectin sensitivity, J. Biol. Chem. 279, 30817-30822.

52. Tsuchida, A., Yamauchi, T., Takekawa, S., Hada, Y., Ito, Y., Maki, T., and Kadowaki, T. (2005) Peroxisome proliferator-activated receptor (PPAR)alpha activation increases adiponectin receptors and reduces obesity-related inflammation in adipose tissue - Comparison of activation of PPAR alpha, PPAR-gamma, and their combination, Diabetes 54, 3358-3370.

53. Berg, A. H., Combs, T. P., Du, X., Brownlee, M., and Scherer, P. E. (2001) The adipocyte-secreted protein Acrp30 enhances hepatic insulin action, Nat Med 7, 947-953.

54. Menzaghi, C., Trischitta, V., and Doria, A. (2007) Genetic influences of adiponectin on insulin resistance, type 2 diabetes, and cardiovascular disease, Diabetes 56, 1198-1209.

55. Mousavinasab, F., Tahtinen, T., Jokelainen, J., Koskela, P., Vanhala, M., Oikarinen, J., Keinanen-Kiukaanniemi, S., and Laakso, M. (2006) Common polymorphisms (single-nucleotide polymorphisms SNP+45 and SNP+276) of the

adiponectin gene regulate serum adiponectin concentrations and blood pressure in young Finnish men, Mol Genet Metab 87, 147-151.

56. Yang, W. S., Yang, Y. C., Chen, C. L., Wu, I. L., Lu, J. Y., Lu, F. H., Tai, T. Y., and Chang, C. J. (2007) Adiponectin SNP276 is associated with obesity, the metabolic syndrome, and diabetes in the elderly, Am J Clin Nutr 86, 509-513.

57. Qiao, L., Lee, B., Kinney, B., Yoo, H. S., and Shao, J. (2011) Energy intake and adiponectin gene expression, Am J Physiol Endocrinol Metab 300, E809-816.

58. Zhu, W., Cheng, K. K., Vanhoutte, P. M., Lam, K. S., and Xu, A. (2008) Vascular effects of adiponectin: molecular mechanisms and potential therapeutic intervention, Clin Sci (Lond) 114, 361-374.

59. Schaffler, A., Langmann, T., Palitzsch, K. D., Scholmerich, J., and Schmitz, G. (1998) Identification and characterization of the human adipocyte apM-1 promoter, Biochim Biophys Acta 1399, 187-197.

60. Seo, J. B., Moon, H. M., Noh, M. J., Lee, Y. S., Jeong, H. W., Yoo, E. J., Kim, W. S., Park, J., Youn, B. S., Kim, J. W., Park, S. D., and Kim, J. B. (2004) Adipocyte determination- and differentiation-dependent factor 1/sterol regulatory element-binding protein 1c regulates mouse adiponectin expression, J Biol Chem 279, 22108-22117.

61. Qi, L., Saberi, M., Zmuda, E., Wang, Y., Altarejos, J., Zhang, X., Dentin, R., Hedrick, S., Bandyopadhyay, G., Hai, T., Olefsky, J., and Montminy, M. (2009) Adipocyte CREB promotes insulin resistance in obesity, Cell Metab 9, 277-286.

62. Kersten, S., Desvergne, B., and Wahli, W. (2000) Roles of PPARs in health and disease, Nature 405, 421-424.

63. Pyper, S. R., Viswakarma, N., Yu, S., and Reddy, J. K. (2010) PPARalpha: energy combustion, hypolipidemia, inflammation and cancer, Nucl Recept Signal 8, e002.

64. Vincent Laudet, H. G. (2002) PPAR, Academic Press.

65. Escher, P., and Wahli, W. (2000) Peroxisome proliferator-activated receptors: insight into multiple cellular functions, Mutat Res 448, 121-138.

66. Johnson, C., Williams, R., Wei, J. Y., and Ranganathan, G. Regulation of Serum Response Factor and Adiponectin by PPARgamma Agonist Docosahexaenoic Acid, J Lipids 2011, 670479.

67. Iwaki, M., Matsuda, M., Maeda, N., Funahashi, T., Matsuzawa, Y., Makishima, M., and Shimomura, I. (2003) Induction of adiponectin, a fat-derived antidiabetic and antiatherogenic factor, by nuclear receptors, Diabetes 52, 1655-1663.

68. Maeda, N., Takahashi, M., Funahashi, T., Kihara, S., Nishizawa, H., Kishida, K., Nagaretani, H., Matsuda, M., Komuro, R., Ouchi, N., Kuriyama, H., Hotta, K., Nakamura, T., Shimomura, I., and Matsuzawa, Y. (2001) PPARgamma ligands increase expression and plasma concentrations of adiponectin, an adipose-derived protein, Diabetes 50, 2094-2099.

69. Koh, K. K., Han, S. H., Quon, M. J., Yeal Ahn, J., and Shin, E. K. (2005) Beneficial effects of fenofibrate to improve endothelial dysfunction and raise adiponectin levels in patients with primary hypertriglyceridemia, Diabetes Care 28, 1419-1424.

70. Choi, K. C., Ryu, O. H., Lee, K. W., Kim, H. Y., Seo, J. A., Kim, S. G., Kim, N. H., Choi, D. S., Baik, S. H., and Choi, K. M. (2005) Effect of PPAR-alpha and -

gamma agonist on the expression of visfatin, adiponectin, and TNF-alpha in visceral fat of OLETF rats, Biochem Biophys Res Commun 336, 747-753.

71. Li, P., Shibata, R., Maruyama, S., Kondo, M., Ohashi, K., Ouchi, N., and Murohara, T. Fenofibrate promotes ischemia-induced revascularization through the adiponectin-dependent pathway, Am J Physiol Endocrinol Metab 299, E560-566.

72. Banga, A., Unal, R., Tripathi, P., Pokrovskaya, I., Owens, R. J., Kern, P. A., and Ranganathan, G. (2009) Adiponectin translation is increased by the PPARgamma agonists pioglitazone and omega-3 fatty acids, Am J Physiol Endocrinol Metab 296, E480-489.

73. Hiuge, A., Tenenbaum, A., Maeda, N., Benderly, M., Kumada, M., Fisman, E. Z., Tanne, D., Matas, Z., Hibuse, T., Fujita, K., Nishizawa, H., Adler, Y., Motro, M., Kihara, S., Shimomura, I., Behar, S., and Funahashi, T. (2007) Effects of peroxisome proliferator-activated receptor ligands, bezafibrate and fenofibrate, on adiponectin level, Arterioscler Thromb Vasc Biol 27, 635-641.

74. Rajala, M. W., and Scherer, P. E. (2003) Minireview: The adipocyte--at the crossroads of energy homeostasis, inflammation, and atherosclerosis, Endocrinology 144, 3765-3773.

75. Tontonoz, P., Hu, E., and Spiegelman, B. M. (1994) Stimulation of adipogenesis in fibroblasts by PPAR gamma 2, a lipid-activated transcription factor, Cell 79, 1147-1156.

76. Sandouk, T., Reda, D., and Hofmann, C. (1993) Antidiabetic agent pioglitazone enhances adipocyte differentiation of 3T3-F442A cells, Am J Physiol 264, C1600-1608.

77. Chen, R., Liang, F., Morimoto, S., Li, Q., Moriya, J., Yamakawa, J., Takahashi, T., Iwai, K., and Kanda, T. (2010) The effects of a PPARalpha agonist on myocardial damage in obese diabetic mice with heart failure, Int Heart J 51, 199-206.

78. Bullen, J. W., Jr., Bluher, S., Kelesidis, T., and Mantzoros, C. S. (2007) Regulation of adiponectin and its receptors in response to development of diet-induced obesity in mice, Am J Physiol Endocrinol Metab 292, E1079-1086.

79. Maddineni, S., Metzger, S., Ocon, O., Hendricks, G., 3rd, and Ramachandran, R. (2005) Adiponectin gene is expressed in multiple tissues in the chicken: food deprivation influences adiponectin messenger ribonucleic acid expression, Endocrinology 146, 4250-4256.

80. Yokota, T., Meka, C. S., Medina, K. L., Igarashi, H., Comp, P. C., Takahashi, M., Nishida, M., Oritani, K., Miyagawa, J., Funahashi, T., Tomiyama, Y., Matsuzawa, Y., and Kincade, P. W. (2002) Paracrine regulation of fat cell formation in bone marrow cultures via adiponectin and prostaglandins, J Clin Invest 109, 1303-1310.

81. Berner, H. S., Lyngstadaas, S. P., Spahr, A., Monjo, M., Thommesen, L., Drevon, C. A., Syversen, U., and Reseland, J. E. (2004) Adiponectin and its receptors are expressed in bone-forming cells, Bone 35, 842-849.

82. Corbetta, S., Bulfamante, G., Cortelazzi, D., Barresi, V., Cetin, I., Mantovani, G., Bondioni, S., Beck-Peccoz, P., and Spada, A. (2005) Adiponectin expression in human fetal tissues during mid- and late gestation, J Clin Endocrinol Metab 90, 2397-2402.

83. Van Berendoncks, A. M., Garnier, A., Beckers, P., Hoymans, V. Y., Possemiers, N., Fortin, D., Martinet, W., Van Hoof, V., Vrints, C. J., Ventura-Clapier, R., and Conraads, V. M. (2010) Functional adiponectin resistance at the level of the skeletal muscle in mild to moderate chronic heart failure, Circ Heart Fail 3, 185-194.

84. Skurk, C., Wittchen, F., Suckau, L., Witt, H., Noutsias, M., Fechner, H., Schultheiss, H. P., and Poller, W. (2008) Description of a local cardiac adiponectin system and its deregulation in dilated cardiomyopathy, Eur Heart J 29, 1168-1180.

85. Pineiro, R., Iglesias, M. J., Gallego, R., Raghay, K., Eiras, S., Rubio, J., Dieguez, C., Gualillo, O., Gonzalez-Juanatey, J. R., and Lago, F. (2005) Adiponectin is synthesized and secreted by human and murine cardiomyocytes, FEBS Lett 579, 5163-5169.

86. Guo, Z., Xia, Z., Yuen, V. G., and McNeill, J. H. (2007) Cardiac expression of adiponectin and its receptors in streptozotocin-induced diabetic rats, Metabolism 56, 1363-1371.

87. Wang, Y., Lau, W. B., Gao, E., Tao, L., Yuan, Y., Li, R., Wang, X., Koch, W. J., and Ma, X. L. (2009) Cardiomyocyte-derived adiponectin is biologically active in

protecting against myocardial ischemia-reperfusion injury, Am J Physiol Endocrinol Metab 298, E663-670.

88. Katsiougiannis, S., Kapsogeorgou, E. K., Manoussakis, M. N., and Skopouli, F. N. (2006) Salivary gland epithelial cells: a new source of the immunoregulatory hormone adiponectin, Arthritis Rheum 54, 2295-2299.

89. Kaser, S., Moschen, A., Cayon, A., Kaser, A., Crespo, J., Pons-Romero, F., Ebenbichler, C. F., Patsch, J. R., and Tilg, H. (2005) Adiponectin and its receptors in non-alcoholic steatohepatitis, Gut 54, 117-121.

90. Ma, H., Gomez, V., Lu, L., Yang, X., Wu, X., and Xiao, S. Y. (2009) Expression of adiponectin and its receptors in livers of morbidly obese patients with non-alcoholic fatty liver disease, J Gastroenterol Hepatol 24, 233-237.

91. Amin, R. H., Mathews, S. T., Alli, A., and Leff, T. (2010) Endogenously produced adiponectin protects cardiomyocytes from hypertrophy by a PPARgamma-dependent autocrine mechanism, Am J Physiol Heart Circ Physiol 299, H690-698.

92. Hostetler, H. A., Petrescu, A. D., Kier, A. B., and Schroeder, F. (2005) Peroxisome proliferator-activated receptor alpha interacts with high affinity and is conformationally responsive to endogenous ligands, J. Biol. Chem. 280, 18667-18682.

93. Oswal, D. P., Balanarasimha, M., Loyer, J. K., Bedi, S., Soman, F. L., Rider, S. D., Jr., and Hostetler, H. A. (2013) Divergence between human and murine peroxisome proliferator-activated receptor alpha ligand specificities, J Lipid Res 54, 2354-2365.

94. Livak, K. J., and Schmittgen, T. D. (2001) Analysis of relative gene expression data using real-time quantitative PCR and the 2(-Delta Delta C(T)) Method, Methods 25, 402-408.

95. Gottlicher, M., Widmark, E., Li, Q., and Gustafsson, J. A. (1992) Fatty acids activate a chimera of the clofibric acid-activated receptor and the glucocorticoid receptor, Proc Natl Acad Sci U S A 89, 4653-4657.

96. Chinopoulos, C., Gerencser, A. A., Mandi, M., Mathe, K., Torocsik, B., Doczi, J., Turiak, L., Kiss, G., Konrad, C., Vajda, S., Vereczki, V., Oh, R. J., and Adam-Vizi, V. (2010) Forward operation of adenine nucleotide translocase during F0F1-ATPase reversal: critical role of matrix substrate-level phosphorylation, FASEB J 24, 2405-2416.

97. Hostetler, H. A., Huang, H., Kier, A. B., and Schroeder, F. (2008) Glucose directly links to lipid metabolism through high affinity interaction with peroxisome proliferator-activated receptor alpha, J Biol Chem 283, 2246-2254.

98. Spector, A. A. (1969) Influence of pH of the medium on free fatty acid utilization by isolated mammalian cells, J Lipid Res 10, 207-215.

99. Flachs, P., Mohamed-Ali, V., Horakova, O., Rossmeisl, M., Hosseinzadeh-Attar, M. J., Hensler, M., Ruzickova, J., and Kopecky, J. (2006) Polyunsaturated fatty acids of marine origin induce adiponectin in mice fed a high-fat diet, Diabetologia 49, 394-397.

100. Kliewer, S. A., Forman, B. M., Blumberg, B., Ong, E. S., Borgmeyer, U., Mangelsdorf, D. J., Umesono, K., and Evans, R. M. (1994) Differential

expression and activation of a family of murine peroxisome proliferator-activated receptors, Proc Natl Acad Sci U S A 91, 7355-7359.

101. Forman, B. M., Chen, J., and Evans, R. M. (1997) Hypolipidemic drugs, polyunsaturated fatty acids, and eicosanoids are ligands for peroxisome proliferator-activated receptors alpha and delta, Proc Natl Acad Sci U S A 94, 4312-4317.

102. Brazda, P., Krieger, J., Daniel, B., Jonas, D., Szekeres, T., Langowski, J., Toth, K., Nagy, L., and Vamosi, G. (2014) Ligand binding shifts highly mobile retinoid x receptor to the chromatin-bound state in a coactivator-dependent manner, as revealed by single-cell imaging, Mol Cell Biol 34, 1234-1245.

103. Balanarasimha, M., Davis, A. M., Soman, F. L., Rider, S. D., and Hostetler, H. A. (2014) Ligand regulated heterodimerization of peroxisome proliferator-activated receptor alpha with liver X receptor alpha, Biochemistry.

104. van der Meer, D. L., Degenhardt, T., Vaisanen, S., de Groot, P. J., Heinaniemi, M., de Vries, S. C., Muller, M., Carlberg, C., and Kersten, S. (2010) Profiling of promoter occupancy by PPARalpha in human hepatoma cells via ChIP-chip analysis, Nucleic Acids Res 38, 2839-2850.

105. Farnham, P. J. (2009) Insights from genomic profiling of transcription factors, Nat Rev Genet 10, 605-616.

106. A, I. J., Jeannin, E., Wahli, W., and Desvergne, B. (1997) Polarity and specific sequence requirements of peroxisome proliferator-activated receptor (PPAR)/retinoid X receptor heterodimer binding to DNA. A functional analysis of the malic enzyme gene PPAR response element, J Biol Chem 272, 20108-20117.

107. Juge-Aubry, C., Pernin, A., Favez, T., Burger, A. G., Wahli, W., Meier, C. A., and Desvergne, B. (1997) DNA binding properties of peroxisome proliferator-activated receptor subtypes on various natural peroxisome proliferator response elements. Importance of the 5'-flanking region, J Biol Chem 272, 25252-25259.

108. Palmer, C. N., Hsu, M. H., Griffin, H. J., and Johnson, E. F. (1995) Novel sequence determinants in peroxisome proliferator signaling, J Biol Chem 270, 16114-16121.

109. Chauvet, C., Vanhoutteghem, A., Duhem, C., Saint-Auret, G., Bois-Joyeux, B., Djian, P., Staels, B., and Danan, J. L. (2011) Control of gene expression by the retinoic acid-related orphan receptor alpha in HepG2 human hepatoma cells, PLoS One 6, e22545.

110. Kim, K. H., Shin, H. J., Kim, K., Choi, H. M., Rhee, S. H., Moon, H. B., Kim, H. H., Yang, U. S., Yu, D. Y., and Cheong, J. (2007) Hepatitis B virus X protein induces hepatic steatosis via transcriptional activation of SREBP1 and PPARgamma, Gastroenterology 132, 1955-1967.

111. Yoon, S., Jung, J., Kim, T., Park, S., Chwae, Y. J., Shin, H. J., and Kim, K. (2011) Adiponectin, a downstream target gene of peroxisome proliferator-activated receptor gamma, controls hepatitis B virus replication, Virology 409, 290-298.

112. Wetzig, A., Alaiya, A., Al-Alwan, M., Pradez, C. B., Pulicat, M. S., Al-Mazrou, A., Shinwari, Z., Sleiman, G. M., Ghebeh, H., Al-Humaidan, H., Gaafar, A., Kanaan, I., and Adra, C. (2013) Differential marker expression by cultures rich in mesenchymal stem cells, Bmc Cell Biology 14.

113. Matsunaga, H., Hokari, R., Kurihara, C., Okada, Y., Takebayashi, K., Okudaira, K., Watanabe, C., Komoto, S., Nakamura, M., Tsuzuki, Y., Kawaguchi, A., Nagao, S., Itoh, K., and Miura, S. (2008) Omega-3 Fatty Acids Exacerbate DSS-Induced Colitis Through Decreased Adiponectin in Colonic Subepithelial Myofibroblasts, Inflammatory Bowel Diseases 14, 1348-1357.

114. Knotts, T. A., Lee, H. W., Kim, J. B., Oort, P. J., McPherson, R., Dent, R., Tachibana, K., Doi, T., Yu, S., Reddy, J. K., Uno, K., Katagiri, H., Pasarica, M., Smith, S. R., Sears, D. D., Grino, M., and Adams, S. H. (2009) Molecular Characterization of the Tumor Suppressor Candidate 5 Gene: Regulation by PPARgamma and Identification of TUSC5 Coding Variants in Lean and Obese Humans, PPAR Res 2009, 867678.

115. Wu, D., Li, H., Xiang, G., Zhang, L., Li, L., Cao, Y., and Zhang, J. (2013) Adiponectin and its receptors in chronic hepatitis B patients with steatosis in china, Hepat Mon 13, e6065.

116. Bonnard, C., Durand, A., Vidal, H., and Rieusset, J. (2008) Changes in adiponectin, its receptors and AMPK activity in tissues of diet-induced diabetic mice, Diabetes Metab 34, 52-61.

117. Yoda-Murakami, M., Taniguchi, M., Takahashi, K., Kawamata, S., Saito, K., Choi-Miura, N. H., and Tomita, M. (2001) Change in expression of GBP28/adiponectin in carbon tetrachloride-administrated mouse liver, Biochem Biophys Res Commun 285, 372-377.

118. Malarkey, D. E., Johnson, K., Ryan, L., Boorman, G., and Maronpot, R. R. (2005) New insights into functional aspects of liver morphology, Toxicol Pathol 33, 27-34.

119. Goto, T., Lee, J. Y., Teraminami, A., Kim, Y. I., Hirai, S., Uemura, T., Inoue, H., Takahashi, N., and Kawada, T. (2011) Activation of peroxisome proliferator-activated receptor-alpha stimulates both differentiation and fatty acid oxidation in adipocytes, J Lipid Res 52, 873-884.

120. Boergesen, M., Pedersen, T. A., Gross, B., van Heeringen, S. J., Hagenbeek, D., Bindesboll, C., Caron, S., Lalloyer, F., Steffensen, K. R., Nebb, H. I., Gustafsson, J. A., Stunnenberg, H. G., Staels, B., and Mandrup, S. (2011) Genome-wide profiling of liver X receptor, retinoid X receptor, and peroxisome proliferator-activated receptor alpha in mouse liver reveals extensive sharing of binding sites, Mol Cell Biol 32, 852-867.

121. Park, S. K., Oh, S. Y., Lee, M. Y., Yoon, S., Kim, K. S., and Kim, J. W. (2004) CCAAT/enhancer binding protein and nuclear factor-Y regulate adiponectin gene expression in adipose tissue, Diabetes 53, 2757-2766.

122. Qiao, L., Maclean, P. S., Schaack, J., Orlicky, D. J., Darimont, C., Pagliassotti, M., Friedman, J. E., and Shao, J. (2005) C/EBPalpha regulates human adiponectin gene transcription through an intronic enhancer, Diabetes 54, 1744-1754.

123. Kim, H. B., Kong, M., Kim, T. M., Suh, Y. H., Kim, W. H., Lim, J. H., Song, J. H., and Jung, M. H. (2006) NFATc4 and ATF3 negatively regulate adiponectin gene expression in 3T3-L1 adipocytes, Diabetes 55, 1342-1352.

124. Dubois, S. G., Heilbronn, L. K., Smith, S. R., Albu, J. B., Kelley, D. E., and Ravussin, E. (2006) Decreased expression of adipogenic genes in obese subjects with type 2 diabetes, Obesity (Silver Spring) 14, 1543-1552.

125. Fernandez-Alvarez, A., Alvarez, M. S., Gonzalez, R., Cucarella, C., Muntane, J., and Casado, M. (2011) Human SREBP1c expression in liver is directly regulated by peroxisome proliferator-activated receptor alpha (PPARalpha), J Biol Chem 286, 21466-21477.

126. Voss, T. C., and Hager, G. L. (2014) Dynamic regulation of transcriptional states by chromatin and transcription factors, Nat Rev Genet 15, 69-81.

127. Nielsen, R., Pedersen, T. A., Hagenbeek, D., Moulos, P., Siersbaek, R., Megens, E., Denissov, S., Borgesen, M., Francoijs, K. J., Mandrup, S., and Stunnenberg, H. G. (2008) Genome-wide profiling of PPARgamma:RXR and RNA polymerase II occupancy reveals temporal activation of distinct metabolic pathways and changes in RXR dimer composition during adipogenesis, Genes Dev 22, 2953-2967.

128. Carroll, J. S., Meyer, C. A., Song, J., Li, W., Geistlinger, T. R., Eeckhoute, J., Brodsky, A. S., Keeton, E. K., Fertuck, K. C., Hall, G. F., Wang, Q., Bekiranov, S., Sementchenko, V., Fox, E. A., Silver, P. A., Gingeras, T. R., Liu, X. S., and Brown, M. (2006) Genome-wide analysis of estrogen receptor binding sites, Nat Genet 38, 1289-1297.

129. Kollias, A., Tsiotra, P. C., Ikonomidis, I., Maratou, E., Mitrou, P., Kyriazi, E., Boutati, E., Lekakis, J., Economopoulos, T., Kremastinos, D. T., Dimitriadis, G., and Raptis, S. A. Adiponectin levels and expression of adiponectin receptors in

isolated monocytes from overweight patients with coronary artery disease, Cardiovasc Diabetol 10, 14.

130. Fang, X., Palanivel, R., Zhou, X., Liu, Y., Xu, A., Wang, Y., and Sweeney, G. (2005) Hyperglycemia- and hyperinsulinemia-induced alteration of adiponectin receptor expression and adiponectin effects in L6 myoblasts, J Mol Endocrinol 35, 465-476.

## LIST OF ABREVIATIONS

| | |
|---|---|
| ABCA1 | ATP-cassette transporter A1 |
| ACBP | Acyl-CoA binding protein |
| ACC | Acetyl CoA carboxylase |
| ACOX | Acyl-CoA oxidase |
| ACOX-/- | Acyl-CoA oxidase knockout mice |
| ACS | Acyl-CoA synthetase |
| ACSL | Long chain acyl-CoA synthase |
| ADD/SREBP1-c | Adipocyte determination and differentiation-dependent factor 1/Sterol regulatory element-binding protein 1c |
| AdipoR | Adiponectin receptors |
| AdipoR1 | Adiponectin receptor 1 |
| AdipoR2 | Adiponectin receptor 2 |
| AF-1 | Ligand-independent transactivation function |
| AF-2 | Ligand-dependent transactivation function |
| AMPK (AMPK) | Adenosine monophosphate (AMP)-activated protein kinase |
| Apo | Apolipoprotein |
| APPL1 | Adaptor protein containing a pleckstrin homology domain, a phosphotyrosine domain and a leucine zipper motif |

| | |
|---|---|
| ATF-3 | Activating transcription factor |
| BSA | Bovine serum albumin |
| C/EBP | CCAAT/enhancer binding protein |
| CARLA | Coactivator-dependent receptor ligand binding assays |
| CD | Circular dichroism |
| ChIP-seq | Chromatin immunoprecipitation and sequencing |
| COX-2 | Cyclooxygenase-2 |
| CPTI | Carnitine palmitoyl transferase I |
| CTE | COOH-terminal extension |
| CVD | Cardiovascular disease |
| CYP7A | Cholesterol 7α-hydroxylase |
| DBD | DNA binding domain |
| DEHA | Di-(2-ethylhexyl)-adipate |
| DEHP | Di-(2-ethylhexyl)-phthalate |
| DMEM | Dubelco's modified Eagle's media |
| DMSO | Dimethyl sulfoxide |
| DR1 | Direct repeat 1 |
| EMEM | Eagle's minimum essential medium |
| EMSA | Electrophoretic mobility shift assays |

| | |
|---|---|
| eNOS | Indothelial nitric acid synthase |
| FABP | Fatty acid binding protein |
| FA-CoA | Fatty acyl-coenzyme A |
| FAS | Fatty acid synthase |
| FAT/CD36 | Fatty acid translocase |
| FATP | Fatty acid transport protein |
| FBS | Fetal-bovine serum |
| FCS | Fluorescence correlation spectroscopy |
| FRAP | Fluorescence recovery after photobleaching |
| HAT | Histone acetyltransferase activity |
| HDAC | Histone deacetylase activity |
| HDL | High density lipoprotein |
| HepG2 cells | Human hepatoma cells |
| HETE | Hydroxyeicosatetraenoic acid |
| HMW | High molecular weight |
| hPPARα | human peroxisome proliferator activated receptor α |
| HSP-90 | Heat-shock protein-90 |
| IL-1 | Interleukin-1 |
| IL-6 | Interleukin-6 |

| | |
|---|---|
| iNOS | Inducible nitric acid synthase |
| KCL | 2-ethylphenylpropanoic acid derivative |
| LBD | Ligand binding domain |
| LCFA | Long chain fatty acid |
| LCFA-CoA | Long chain fatty acyl-CoA |
| LDL | Low density lipoprotein |
| LIC | Ligand induced assays |
| LMW | Low molecular weight |
| LPL | Lipoprotein lipase |
| LSD | Least significant difference |
| LTB4 | Leukotriene $B_4$ |
| LXRE | LXR response element |
| LXRα | Liver X receptor alpha |
| MCAD | Medium chain acyl CoA dehydrogenase |
| MMW | Medium molecular weight |
| mPPARα | murine peroxisome proliferator activated receptor α |
| NCoR | Nuclear receptor corepressor |
| NFAT | Nuclear factor of activated T cells |
| NF-Y | Nuclear factor-Y |

| | |
|---|---|
| NfκB | Nuclear factor κ B |
| NURR1 | Nuclear receptor related protein 1 |
| P450 | Cytochrome P450 fatty acid ω-hydroxylase |
| PC | Photon counting spectrofluorometry |
| PGC-1 | PPARγ coactivator-1 |
| PPAR | Peroxisome proliferator activated receptor |
| PPARα (-/-) mice | Peroxisome proliferator activated receptor α knockout/null mice |
| PPARα | Peroxisome proliferator activated receptor alpha |
| PPARβ/δ | Peroxisome proliferator activated receptor beta/delta |
| PPARγ | Peroxisome proliferator activated receptor gamma |
| PPbP | Peroxisome proliferator-binding protein |
| PPRE | Peroxisome proliferator response element |
| PUFA | Polyunsaturated fatty acids |
| qRT-PCR | Quantitative real-time polymerase chain reaction |
| RAR | Retinoic acid receptor |
| RXR | Retinoid X receptor |
| SDS PAGE | Sodium dodecyl sulphate polyacrylamide gel electrophoresis |
| SMRT | Silencing mediator of retinoid and thyroid hormone receptors |
| SNP | Single nucleotide polymorphisms |

| | |
|---|---|
| SRC-1 | Steroid receptor coactivator |
| SREBP | Sterol regulatory element-binding protein |
| STAT | Signal transducer of transcription |
| TBP | TATA binding protein |
| TG | Triglycerides |
| TIF-2 | Transcriptional mediators/intermediary factor 2 |
| TK | Thymidine kinase |
| TNFα | Tumor necrosis factor α |
| TR | Thyroid receptor |
| UCP-1 | Uncoupling protein-1 |
| VDR | Vitamin D receptor |
| VLDL | Very low density lipoproteins |
| WHO | World health organization |